

# THE MINOR PLANET BULLETIN

BULLETIN OF THE MINOR PLANETS SECTION OF THE ASSOCIATION OF LUNAR AND PLANETARY OBSERVERS

VOLUME 49, NUMBER 1, A.D. 2022 JANUARY-MARCH

1.

## PHOTOMETRIC OBSERVATIONS OF MAIN-BELT ASTEROIDS 2229 MEZZARCO, 3648 RAFFINETTI AND 3919 MARYANNING

Charles Galdies  
Znith Observatory  
Armonic, E. Bradford Street,  
Naxxar NXR 2217, MALTA  
charles.galdies@um.edu.mt

Stephen M. Brincat  
Flarestar Observatory (MPC 171)  
Fl.5/B, George Tayar Street,  
San Gwann SGN 3160, MALTA  
stephenbrincat@gmail.com

(Received: 2021 July 25)

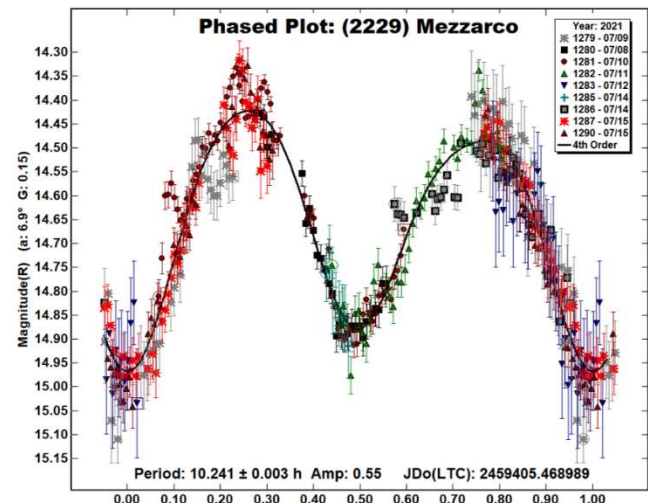
Photometric observations of three main-belt asteroids that were obtained from May through July 2021 were made from Malta in order to determine their synodic rotation periods. For 2229 Mezzarco we found a period of  $10.241 \pm 0.003$  h, amplitude  $0.55$  mag. For 3648 Raffinetti the results show a period of  $5.177 \pm 0.001$  h and  $0.47$  mag. and for 3919 Maryanning we report a period of  $7.094 \pm 0.001$  h with an amplitude of  $0.70$  mag.

Photometric observations of three main-belt asteroids were carried out from two observatories located in Malta (Europe). Observations of asteroids 2229 Mezzarco, 3648 Raffinetti and 3919 Maryanning were obtained from the following observatories that utilized the following configurations. Znith Observatory employed a 0.20-m Schmidt-Cassegrain (SCT) equipped with a Moravian G2-1600 CCD camera at  $1 \times 1$  binning, whilst Flarestar Observatory utilized the same CCD model coupled with a 0.25-m SCT telescope with the same binning configuration. All cameras were operated at sensor temperature of  $-15^\circ\text{C}$ . All images were dark subtracted and flat-fielded.

All telescopes and cameras were controlled remotely from a location near each telescope via *Sequence Generator Pro* (Main Sequence Software, 2021). Photometric reduction, light curve construction and analyses were derived through *MPO Canopus* software (Warner, 2017) where differential aperture photometry was used. The Comparison Star Selector (CSS) feature of MPO Canopus was used to select comparison stars of near-solar color. Measurements were based on the CMC-15 catalogue with magnitudes converted from J-K to BVRI.

2229 Mezzarco is a main-belt asteroid that was discovered on 1977 September 7 by Wild P. at Zimmerwald, Switzerland. This asteroid orbits the sun with a semi-major axis of 2.695 AU, eccentricity 0.265, and period of 4.42 years (JPL, 2021). The JPL Small-Bodies Database Browser (JPL, 2021) lists the diameter of this asteroid as  $8.841 \pm 0.248$  km based on an absolute magnitude  $H = 13.11$ .

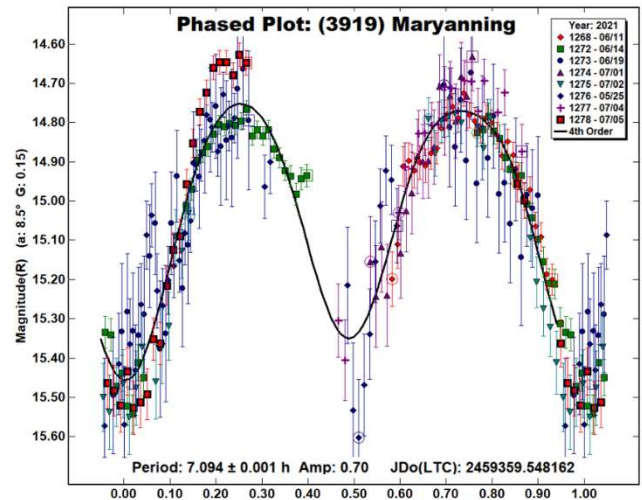
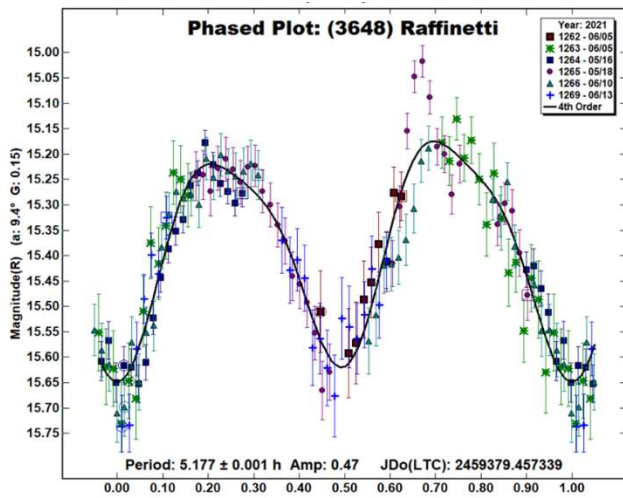
2229 Mezzarco was observed from both observatories starting on the night of 2021 July 8 until 15. Our results yielded a synodic period of  $10.241 \pm 0.003$  h and amplitude of  $0.55 \pm 0.07$  mag. The Light Curve DataBase (LCDB - Warner et al., 2009) did not contain any references of the synodic period of this asteroid.



3648 Raffinetti is a large main-belt asteroid that was discovered on 1957 April 24 at La Plata. The asteroid orbits the sun with a semi-major axis of 2.415 AU, eccentricity 0.107, and orbital period of 3.75 years (JPL, 2021). The JPL Small-Bodies Database Browser lists the diameter of 3648 Raffinetti as  $5.314 \pm 0.033$  km based on an absolute magnitude  $H = 13.33$ .

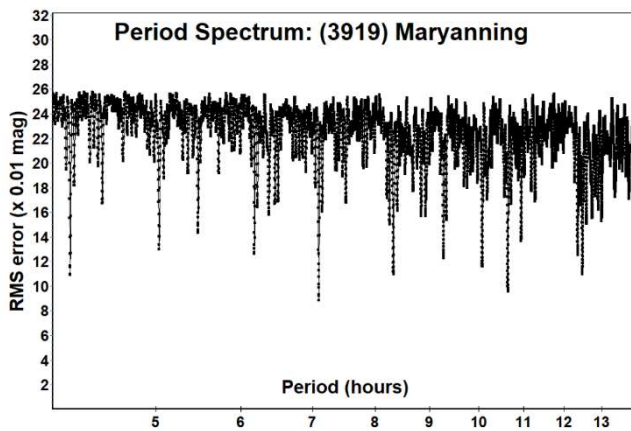
Observations were conducted from Znith Observatory and were carried out on 5 nights from 2021 May 16 to June 14. We obtained a synodic period of  $5.177 \pm 0.001$  h and amplitude of  $0.47 \pm 0.05$  mag. The Light Curve DataBase (LCDB) did not contain any references of the synodic period of this asteroid.

Our result of 3648 Raffinetti is consistent with  $5.1756$  h period and a  $0.16$  mag amplitude obtained by Matt Nowinski (2017).



**3919 Maryanning** is a main-belt asteroid that was discovered on 1984 February 23 by H Debehogne at La Silla, Chile. It has been named in memory of Mary Anning (1799-1847). This 4.784 ± 0.194 km diameter asteroid has an absolute magnitude H of 13.81 and orbits the sun with a semi-major axis of 2.218 AU. Its orbit has an eccentricity of 0.190, and a period of 3.3 years (JPL, 2021).

Observations were conducted by Znith Observatory over a period of 9 nights from 2021 May 25 to July 05. Results indicate a synodic period of  $7.094 \pm 0.001$  h and amplitude of  $0.7 \pm 0.17$  mag. The Light Curve DataBase (LCDB) did not contain any references of the synodic period of this asteroid.



#### Acknowledgements

We would like to thank Brian Warner for his work in the development of *MPO Canopus* and for his efforts in maintaining the CALL website (Warner, 2009; 2016).

This research has made use of the JPL's Small-Body Database.

#### References

- Harris, A.W.; Young, J.W.; Scaltriti, F.; Zappala, V. (1984). "Lightcurves and phase relations of the asteroids 82 Alkmene and 444 Gaptis." *Icarus* **57**, 251-258.
- JPL. (2021). Small-Body Database Browser - JPL Solar System Dynamics web site. <http://ssd.jpl.nasa.gov/sbdb.cgi> Last accessed: 11 July 2021.
- Nowinski, M. (2017). "Lightcurve Study Of V-Type Asteroids." Theses and Dissertations. 2301. <https://commons.und.edu/theses/2301>
- Sequence Generator Pro – SGP. Last accessed on 2021 October 18. <http://mainsequencesoftware.com/Products/SGPro>.
- Warner, B.D., Harris, A.W., Pravec, P. (2009). "The Asteroid Lightcurve Database." *Icarus* **202**, 134-146. Updated 2021 June. <http://www.minorplanet.info/lightcurvedatabase.html>
- Warner, B.D. (2016). Collaborative Asteroid Lightcurve Link website. <http://www.minorplanet.info/call.html> Last accessed: 26 September 2018.
- Warner, B.D. (2017). MPO Software, *MPO Canopus* version 10.7.10.0. Bdw Publishing. <http://www.minorplanetobserver.com/>

Number	Name	2021 mm/dd	Phase	L <sub>PAB</sub>	B <sub>PAB</sub>	Period(h)	P.E.	Amp	A.E.	Grp
2229	Mezzarco	07/08-07/15	7.6, 5.5	295.2	7.0	10.241	0.003	0.55	0.07	MB
3648	Raffinetti	05/16-06/13	4.6, 12.7	240.3	6.3	5.177	0.001	0.47	0.05	MB
3919	Maryanning	05/25-07/05	6.1, 20.5	251.8	5.9	7.094	0.001	0.70	0.17	MB

Table I. Observing circumstances and results. Pts is the number of data points. The phase angle is given for the first and last date. LPAB and BPAB are the approximate phase angle bisector longitude and latitude at mid-date range (see Harris et al., 1984). Grp is the asteroid family/group (Warner et al., 2009).

## A NEW SATELLITE OF 4337 ARECIBO DETECTED AND CONFIRMED BY STELLAR OCCULTATION

David Gault

Trans-Tasman Occultation Alliance: (TTOA)  
22 Booker Road, Hawkesbury Heights, 2777, Australia  
davegault@bigpond.com

Peter Nosworthy

Trans-Tasman Occultation Alliance: (TTOA)

Richard Nolthenius

Cabrillo College, Santa Cruz, CA, USA  
International Occultation Timing Association: (IOTA)

Kirk Bender

Cabrillo College, Santa Cruz, CA, USA

Dave Herald

Trans-Tasman Occultation Alliance: (TTOA)

(Received: 2021 August 3 Revised: 2021 October 16)

Two observers in Australia, at two separate sites observed asteroid 4337 Arecibo occult UCAC4 323-126197 and both observers observed a hitherto unknown satellite of the asteroid occult the same star shortly afterwards. Confirmation of the existence of the satellite occurred 20.71 days after the first observation, when two observers in California, at two separate sites observed 4337 Arecibo occult UCAC4 322-116848, and both observers observed the satellite occult the same star shortly afterwards. A third occultation, 20.78 days later, of UCAC4 323-113857 was observed at 3 sites in California however the satellite was not detected. We find the diameter of the main body is 24.4 +/- 0.6 km and the satellite is 13.0 +/- 1.5 km - assuming they are spherical. Their separations at the two occultations were: 2021 May 19.74861: 25.5 ±1.0 mas in PA 105.2° ±1.0°. 2021 June 9.45736: 32.8 ±0.7 mas in PA 94.3° ±2.7°. We find the center of mass of the system is displaced from the main body by about 14% of the distance between the two bodies. However, our observations are insufficient to fix the orbit parameters.

### Observations – Australia, 2021 May 19

D. Gault and P. Nosworthy observed 4337 Arecibo occult UCAC4 323-126197 and both observed a hitherto unknown satellite occult the same star shortly after. They observed from their home observatories located in The City of The Blue Mountains, at Hawkesbury Heights and Hazelbrook. The sites are equipped with 28 and 30 cm Schmidt Cassegrain telescopes, Watec 910BD video cameras and IOTA-VTIs that insert an accurate GPS-derived time stamp into the video stream (IOTA, 2017). The occultation occurred at an altitude of 65 degrees.

Observation circumstances and timings are shown in Table 1 and lightcurves of the target and a comparison star are in Figure 1.

For this event the recordings were closely analyzed to determine the limiting magnitude of the recording, noting that during the occultation events the lightcurve dropped to the zero-light level. The occulted star had a Gaia G-band magnitude of 13.59, and stars fainter than 15.0 were visible on the recording. The equivalent magnitude drop of at least 1.4 magnitudes for both events in each recording is much larger than the 0.75 drop that would occur if the star was a double star of equal magnitude – thereby excluding a double star as being an explanation for the event.

Observer	Longitude	Latitude	Altitude	Event	Primary Body	Satellite	
Gault	150 38 27.9	-33 39 51.90	286m	D	17:57:59.61	+/-0.08	17:58:04.73 +/-0.08
				R	17:58:01.89	+/-0.12	17:58:05.41 +/-0.12
Nosworthy	150 27 06.5	-33 42 26.60	648m	D	17:58:01.56	+/-0.16	17:58:06.92 +/-0.08
				R	17:58:03.96	+/-0.16	17:58:07.24 +/-0.08

Table 1: Observation circumstances and disappearance and reappearance times UTC of the 2021 May 19 occultations. The sites were separated by 0.7 km across the occultation path, and 18 km along the occultation path.

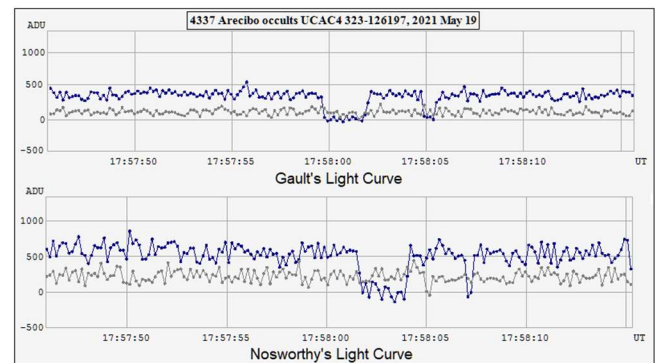


Figure 1: Lightcurves by Gault and Nosworthy of the 2021 May 19 occultations of the target star, by the asteroid main body and satellite. Light values of comparison stars are also shown.

### Observations – California, 2021 June 9

R. Nolthenius and K. Bender of Santa Cruz, CA travelled to sites approx. 4 km either side of the predicted occultation path center line, near the towns of San Ardo and Bradley CA. They observed the main body and satellite occult UCAC4 322-116848, noting that during the occultation events the light curve dropped, within error scatter, to zero light. Both observers were equipped with portable 8-inch Schmidt Cassegrain telescopes, Watec 910HX video cameras, and IOTA-VTI video time inserters (IOTA, 2017). The occultation occurred at an altitude of 20 degrees.

Observation circumstances and timings are shown in Table 2 and light curves of the target and a comparison star are shown in Figure 2.

Observer	Longitude	Latitude	Altitude	Event	Primary Body	Satellite	
Nolthenius	-120 52 22.8	35 56 13.3	158m	D	10:58:36.86	+/-0.06	10:58:41.46 +/-0.06
				R	10:58:38.90	+/-0.06	10:58:42.47 +/-0.06
Bender	-120 50 16.2	35 52 22.2	159m	D	10:58:36.64	+/-0.06	10:58:41.01 +/-0.06
				R	10:58:38.41	+/-0.06	10:58:42.12 +/-0.06

Table 2: Observation circumstances and disappearance and reappearance times UTC of the 2021 June 9 occultations. The sites were separated by 8.2 km across the occultation path, and 8.0 km along the occultation path.

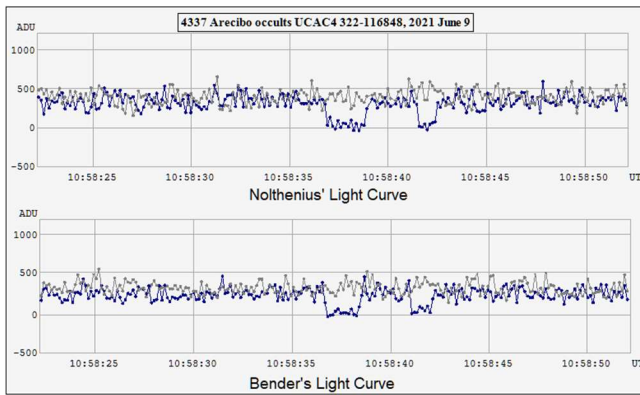


Figure 2: Lightcurves by R. Nolthenius and K. Bender of the 2021 June 9 occultations of the target star, by the asteroid main body and satellite. Light values of comparison stars are also shown.

#### Observations – California, 2021 June 30

20.78 days later, an attempt was made by observers at 15 sites across the USA to observe an occultation by 4337 Arecibo of UCAC4 323-113857, however due to challenging conditions and weather, only 5 sites made successful observations (Nolthenius, 2021). R. Nolthenius, K. Bender, and C. L. Kitting recorded occultations of the main body and did not detect the satellite, and T. Swift and H. Throop observed misses.

#### Reduction of the observations

Event times and observation circumstances were entered into Occult (Herald, 2021) and reduced for each observation and the sky-plane plots are shown on Figure 3.

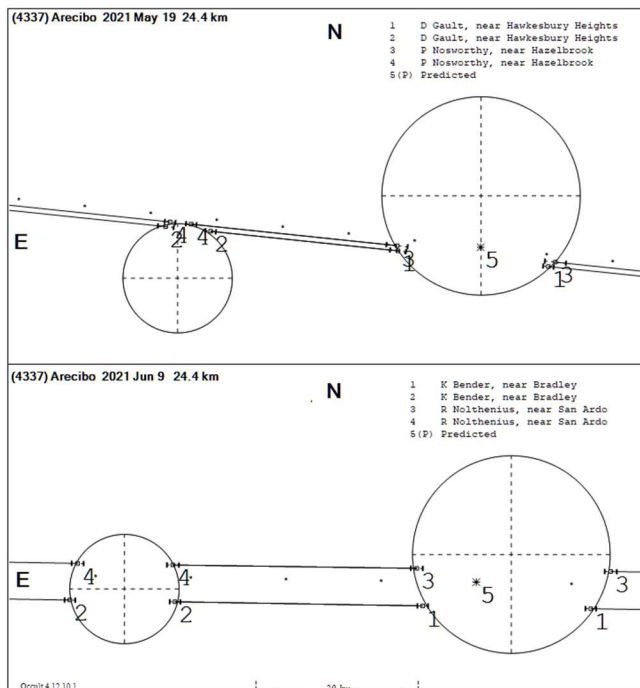


Figure 3: Reduction sky-plane plots of the 2021 May 19 and 2021 June 9 occultations, showing the asteroid and satellite for both occultation events.

The sizes of both the main body and the satellite were poorly determined by the 2021 May 19 occultation, because of the close across-path separation of the observers. Their sizes were better determined from the 2021 June 9 occultation, because the across-path separation was larger, and the chords were favorably positioned against both bodies. Regrettably the number and location of the chords, as well as their associated time uncertainties (indicated by the tick marks on the chords in Fig 3), preclude any reliable fit of an ellipse to the observations. Indeed, either body could have substantial ellipticity yet be consistent with the observed chords. Accordingly, we have determined their diameters on the basis of a fit of a circle to the chords.

The diameters determined from the 2021 June 9 occultation, using a circular fit, are:

Main body  $24.4 \pm 0.6$  km  
 Satellite  $13.0 \pm 1.5$  km

These diameters were used to then derive the position of the satellite relative to the main body for both occultations. Those positions are:

2021 May 19.74861:  $25.5 \pm 1.0$  mas in PA  $105.2^\circ \pm 1.0^\circ$   
 2021 June 9.45736:  $32.8 \pm 0.7$  mas in PA  $94.3^\circ \pm 2.7^\circ$

The fit of the three positive chords of the 2021 June 30 occultation is, within errors, consistent with a circle fit of 24 km diameter.

#### Arecibo system: center of mass and orbit

Assuming the density of the two bodies is the same, and that they are both spherical, the center of mass of the system is displaced from the main body by about 14% of the distance between the two bodies. That position is within the main body, and is separated from its center by about 60% of its radius.

The small change in satellite separation and PA between the first two events, 20.78 days apart, is suggestive this might be the approximate orbital period. However, we do not know whether this is coincidence with the orbital period being a fraction of the 20.78 days, or whether the satellite is moving very slowly. We also do not know if the satellite was on the near or far side of the sky plane for either the May 19 or June 9 events. Therefore, our observations do not fix the orbit parameters.

The apparent closeness of the satellite to the main body, and its relatively large size, suggests that mutual eclipses and occultations may presently be occurring.

We are not aware of any lightcurve measurements of this asteroid.

The observations of 2021 May 19 and 2021 June 9 were the subject of CBET 4981.

#### Acknowledgements

We acknowledge the efforts of David Dunham, Joan Dunham, Steve Preston, Hristo Pavlov, C. L. Kitting, Ted Swift, H. Throop and many others involved in the planning of the 2021 June 30 occultation observation.

## References

Herald, D. (2021). OCCULT Prediction Software  
<http://www.lunar-occultations.com/iota/occult4.htm>

IOTA (2017). IOTA-VTI Homepage  
<https://videotimers.com/home.html>

Nolthenius, R. (2021), “The June 29/30, 2021 Occultation by (4337) Arecibo. Can we Constrain the Orbit?”  
<https://www.dr-ricknolthenius.com/Apowers/PT-iota21.pdf>

## ROTATION PERIOD DETERMINATION FOR ASTEROID 663 GERLINDE

Rafael G. Farfán  
 Uraniborg Observatory (Z55)  
 Écija (Seville, Spain)  
[uraniborg16@gmail.com](mailto:uraniborg16@gmail.com)

Faustino García (J38)  
 La Vara, Valdés (Asturias, Spain)

(Received: 2021 October 15)

Photometric observations of the main-belt asteroid 663 Gerlinde were taken from the Uraniborg Observatory, in Écija (Seville, Spain), in order to determine its synodic rotation period. The results are:  $P = 10.254 \pm 0.001$  h,  $A = 0.190$  mag.

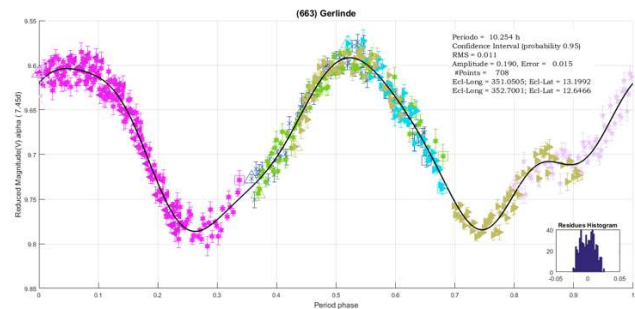
All observations were performed at the Uraniborg Observatory, (MPC-International Astronomical Union code Z55) using a 0.28-m Schmidt-Cassegrain telescope operating at  $f/6.3$ . The optical tube is mounted on NEQ6 Pro Skywatcher mount, and equipped with an ATIK 414exm CCD camera. It is a high Quantum Efficiency CCD. No filters used so as to optimize the signal-to-noise. Exposure time for all images was 90 sec. The camera was binned at  $1 \times 1$ . The image scale after  $1 \times 1$  binning was 0.78 arcsec/pixel and the field of view  $18 \times 13$  arcmin. In these fields, the asteroid and three comparison stars were measured for differential photometry.

All images were reduced in the standard manner using nightly flatfield files as well as dark-current and bias images. Photometric measurement and lightcurve analysis were performed using *FotoDif* software version 3.138 (Castellano, 2020) and *Periodos*, a script for Matlab software (Observatorio Astronómico Salvador, 2020). Besides, the light time effect was corrected. The *Cartes du Ciel* (2021) was used as the planetarium software with the most recent ephemerides downloaded from the Minor Planet Center, and *MaximDL Pro 6.0* (2021) was used for image capture.

**663 Gerlinde** (1980 DG; 1948 AB; 1952 WF; 1958 XP) is located in the main asteroid belt, with a semi-major axis of 3.072 AU, eccentricity 0.1455, inclination  $17.81^\circ$ , and an orbital period of 5.39 years. Its spectral type is X and its diameter is 107.8 km. It was discovered on June 24, 1908 by the German astronomer Augustus Kopff at the Heidelberg Observatory and named after the German female's name.

Our goal was to check if the rotation period of 663-Gerlinde has changed in recent years since the latest observations published correspond to the years 2005-2006, (Behrend, 2020) although there is only one more in 2019 according to the consulted bibliography (ALCDEF, 2020). In all these studies, the calculated period was 0.4274 days.

The asteroid phase angle was  $7.5^\circ$  when our observations started and  $9.8^\circ$  when they finished. The period analysis shows a solution for the rotational period of  $P = 10.254 \pm 0.001$  hours with an amplitude  $A = 0.190 \pm 0.015$  mag, which is very close to the previously aforementioned published results.



## References

ALCDEF (2020), Asteroid Photometry Database. <http://alcdef.org/>

Behrend, R. (2020). Observatoire de Genève website.  
<https://obswww.unige.ch/~behrend/>

Cartes du Ciel (2021). <https://www.ap-i.net/skychart/en/start>

Castellano, J. (2020). FotoDif Software.  
<http://astrosurf.com/orodeno/fotodif/index.htm>

MaximDL (2021).  
<https://diffractionlimited.com/product/maxim-dl/>

Observatorio Astronómico Salvador (2020). *Periodos* Software.  
<http://www.astrosurf.com/salvador/Programas.html>

Number	Name	20yy/mm/dd	Phase	L <sub>PAB</sub>	B <sub>PAB</sub>	Period (h)	P.E.	Amp	A.E.
663	Gerlinde	21/08/01-21/08/17	7.5, 9.8	351.9	12.9	10.254	0.001	0.190	0.015

Table I. Observing circumstances and results. Phase is the solar phase angle given at the start and end of the date range. If preceded by an asterisk, the phase angle reached an extrema during the period. L<sub>PAB</sub> and B<sub>PAB</sub> are the average phase angle bisector longitude and latitude.

## ROTATIONAL PERIOD DETERMINATION AND TAXONOMIC CLASSIFICATION FOR ASTEROID 536 MERAPI

Massimiliano Mannucci, Nico Montigiani  
Osservatorio Astronomico Margherita Hack (A57)  
Florence, ITALY  
info@astrofilifiorentini.it

(Received: 2021 July 14, Revised: 2021 August 4)

CCD photometric observations of outer main-belt asteroid 536 Merapi were obtained in order to measure the rotation period and to find the color indexes B-V and V-R. These measures were performed using the instrumentation available at the Osservatorio Astronomico Margherita Hack located on the hills near Florence (Italy).

CCD photometric observations of one main-belt asteroid was carried out in 2021 March and May at the Osservatorio Astronomico Margherita Hack (A57). We used a 0.35-m f/8,25 Smith-Cassegrain telescope, a SBIG ST10 XME CCD camera, clear filter and B, V, Rc photometric filters. The pixel scale was 1 arcsec when binned at  $2 \times 2$  pixels. Data processing and analysis were done with *MPO Canopus* (Warner, 2017). All the images were calibrated with dark and flat field frames using *Astroart* 6.0. Table I shows the observing circumstances and results.

536 Merapi was discovered by the American astronomer George Henry Peters on May 11, 1904, from Washington, D.C. It is named after Mount Merapi, one of the most active volcanos in Indonesia. We chose it from the list of lightcurve photometry opportunities on the Minor Planet Bulletin (Warner et al., 2021). 536 Merapi is an outer main-belt asteroid with a semi-major axis of 3.498 AU, eccentricity of 0.087, inclination of 19.423 deg and an orbital period of 6.54 years. Its absolute magnitude is  $H = 8.16$  (JPL, 2021; MPC, 2021). Our observations were conducted in two different steps.

The first step consisted in collecting 439 data points with clear filter in three different nights (23/3/2021, 30/3/2021 and 31/3/2021). The derived synodic period was  $P = 8.7905 \pm 0.0005$  h with an amplitude of  $A = 0.16 \pm 0.03$  mag.

Moreover, we consulted the asteroid lightcurve database (LCDB; Warner et al., 2009) and we found four previous calculated periods:  $P = 8.78 \pm 0.01$ h (Koff, 2000),  $P = 8.809 \pm 0.008$ h (Ditteon and Hawkins, 2007) and  $P = 8.79052 \pm 0.00004$ h (Ďurech et al., 2020). The period we found seems to be in good agreement with the previous mentioned periods.

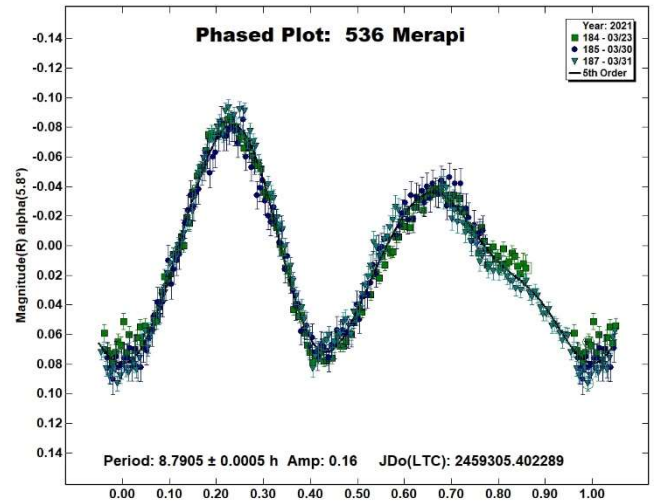


Figure 1. Phased lightcurve of 536 Merapi.

In the second step we collected further 83 data points in two different nights (08/05/2021 and 27/05/2021) using filter V, Rc and B. This allowed us to determine the color indexes  $(V-R) = 0.404 \pm 0.004$  and  $(B-V) = 0.70 \pm 0.03$ . These values are consistent with a low albedo C-type taxonomic class (Shevchenko and Lupishko, 1998) and in good accordance with the previously published results in the LCDB.

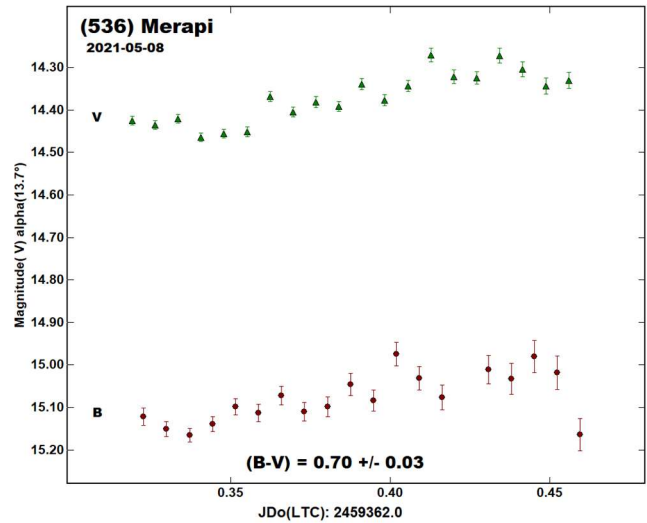


Figure 2. (B-V) raw plot of 536 Merapi.

Number	Name	2021 mm/dd	Pts	Phase	$L_{PAB}$	$B_{PAB}$	Period(h)	P.E.	Amp	A.E.	Grp
536	Merapi	23/03-31/03	436	5.81-5.04	193.1	16.9	8.7905	$\pm 0.0005$	0.16	0.03	OMB

Table I. Observing circumstances and results. Pts is the number of data points. The phase angle is given for the first and last date.  $L_{PAB}$  and  $B_{PAB}$  are the approximate phase angle bisector longitude and latitude at mid-date range (see Harris et al., 1984). Grp is the asteroid family/group (Warner et al., 2009).

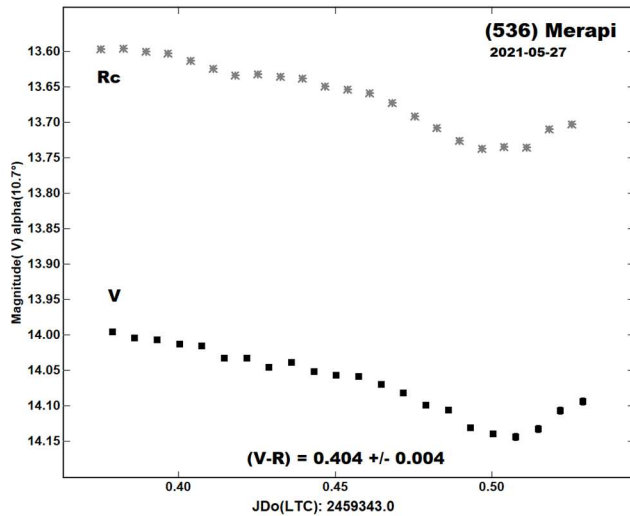


Figure 3. (V-R) raw plot of 536 Merapi.

#### References

Ditton, R.; Hawkins, S. (2007). "Asteroid Lightcurve Analysis at the Oakley Observatory - October-November 2006." *Minor Planet Bulletin* **34**, 59-64.

Đurech, J.; Tonry, J.; Erasmus, N.; Denneau, L.; Heinze, A.N.; Flewelling, H.; Vančo, R. (2020). "Asteroid models reconstructed from ATLAS photometry." *Astronomy & Astrophysics* **643**, id. A59, 5 pp.

Harris, A.W.; Young, J.W.; Scaltriti, F.; Zappala, V. (1984) "Lightcurves and phase relations of the asteroids 82 Alkeme and 444 Gytis." *Icarus* **57**, 251-258.

JPL (2021). Small-Body Database Browser.  
<http://ssd.jpl.nasa.gov/sbdb.cgi#top>

Koff, R.A. (2000). "Rotation Periods and Lightcurves of 536 Merapi and 760 Massinga." *Minor Planet Bulletin* **27**, 26-27.

MPC (2021). MPC Database.  
[http://www.minorplanetcenter.net/db\\_search/](http://www.minorplanetcenter.net/db_search/)

Shevchenko, V.G.; Lupishko, D.F. (1998) "Optical Properties of Asteroids from Photometric Data." *Solar System Research* **32**, 220.

Warner, B.D.; Harris, A.W.; Pravec, P. (2009). "The Asteroid Lightcurve Database." *Icarus* **202**, 134-146. Updated 2018 June 23.  
<http://www.minorplanet.info/lightcurvedatabase.html>

Warner, B.D. (2017). MPO Software, MPO Canopus v10.7.7.0. Bdw Publishing. <http://minorplanetobserver.com>

Warner, B.D.; Harris, A.W.; Đurech, J.; Benner, L.A.M. (2021). "Lightcurve photometry opportunities: 2021 April-June." *Minor Planet Bulletin* **4**, 194-198.

## LIGHTCURVE AND SYNODIC ROTATION PERIOD FOR 2728 YATSKIV

Vladimir Benishek  
Belgrade Astronomical Observatory  
Volgina 7, 11060 Belgrade 38, SERBIA  
[vlaben@yahoo.com](mailto:vlaben@yahoo.com)

Frederick Pilcher  
Organ Mesa Observatory  
4438 Organ Mesa Loop  
Las Cruces, NM 88011 USA

(Received: 2021 October 13)

A rotational lightcurve and a synodic rotation period were obtained for the first time on the main-belt asteroid 2728 Yatskiv from CCD photometric observations conducted over the time span 2021 June - September at two observatories widely separated in geographic longitude. As a result, a bimodal lightcurve phased to a period of  $25.069 \pm 0.006$  h was established.

Prior to our work, there were no reports on synodic rotation period and lightcurve determinations for the inner main-belt asteroid 2728 Yatskiv. As a program target within the Photometric Survey for Asynchronous Binary Asteroids (*BinAstPhot Survey*) under the leadership of Dr. Petr Pravec from the Astronomical Institute of the Czech Academy of Sciences, 2728 Yatskiv was proposed for active photometric follow-up in 2021 June.

Benishek at Sopot Astronomical Observatory (SAO) in Serbia began photometric observations on 2021 June 13, employing a 0.35-m (f/6.3) Schmidt-Cassegrain telescope (SCT) equipped with a SBIG ST-8XME CCD camera operating in 2x2 binning mode. The first dense photometric datasets obtained by the end of June indicated not only a somewhat longer rotation period, and also its pronounced near commensurability with the Earth's rotation. Due to the parallel work on many other priority targets, and as the rather long rotation period for 2728 Yatskiv became apparent, a sparse data acquisition was implemented in some Benishek's datasets by taking one data point per half an hour.

These early datasets have yielded several harmonically related solutions (various multiples of the basic monomodal solution of somewhat over 12.5 hours). None of them could have been adopted as unequivocal one due to the rather limited amount of data and the shortness of the observing runs, as well as the fact that progress in observational covering of a broader range of rotational phases from a single geographic longitude was very slow, since possible period solutions are near commensurate with the Earth's rotation.

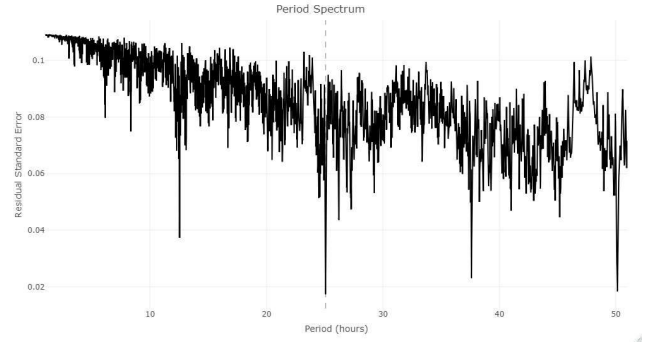
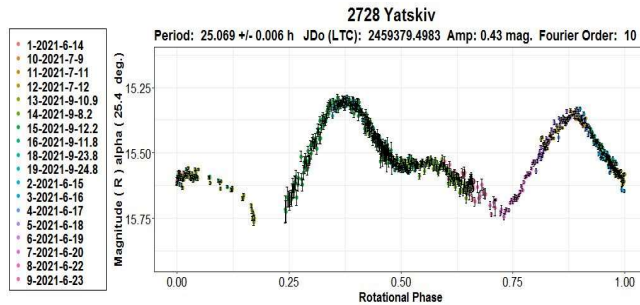
After a certain delay in the 2728 Yatskiv follow-up observations caused by a large number of other priority targets in the SAO observing schedule, Frederick Pilcher of the Organ Mesa Observatory in Las Cruces, USA was invited to contribute 2728 Yatskiv photometry from a significantly different geographic longitude to effectively resolve the existing period ambiguity. Pilcher kindly accepted the invitation and obtained his first dataset on 2021 September 08. Pilcher used a 0.35-m (f/10) SCT and a SBIG STL-1001E CCD camera. Two 2021 September long datasets by Pilcher were crucial to definitively determine a total amplitude of the combined lightcurve, which turned out to be greater than 0.4 magnitudes, and they also significantly covered a large gap in the lightcurve corresponding to a bimodal period solution of just over 25 hours.

As of 2021 September 24, when the last data were taken, a total of 19 individual datasets were obtained.

Photometric reduction and differential photometry with up to five comparison stars of near solar color ( $0.5 \leq B-V \leq 0.9$ ) was performed by both authors in *MPO Canopus* software (Warner, 2018). To ensure a high degree of uniformity of the magnitude zero points (up to a few hundreds of magnitude) both authors performed internal calibration of field comparison stars using standard Cousins R magnitudes derived from the Carlsberg Meridian Catalog 15 (VizieR, 2021) Sloan  $r'$  magnitudes by applying the formula:  $R = r' - 0.22$ .

Lightcurve construction and period analysis were performed with a custom-made program *Perfindia* developed by Benishek in the R statistical programming language (R Core Team, 2020). Among several possible period solutions, a bimodal solution of  $25.069 \pm 0.006$  hours stands out for its minimal *residual standard error*. In addition, having in mind the rather large lightcurve amplitude corresponding to this bimodal solution (0.43 mag.) over the range of relatively low solar phase angles, it could be concluded with a high degree of reliability that the derived bimodal period is the most reliable value (Harris et al., 2014). An independent period analysis conducted by Pilcher over the same combined dataset in *MPO Canopus* gives almost the same period value of 25.064 hours.

The period error shown on the lightcurve plot represents so-called 2% error, i.e. an error that would cause the last data point in a combined data set by date order to be shifted by 2% (Warner, 2012) and represented by  $\Delta P = (0.02 \cdot P^2) / T$ , where P and T are the rotational period and the total time span of observations expressed in the same units, respectively.



## Acknowledgements

Observational work at Sopot Astronomical Observatory is supported by a 2018 Gene Shoemaker NEO Grant from The Planetary Society.

## References

Harris, A.W.; Pravec, P.; Galad, A.; Skiff, B.A.; Warner, B.D.; Vilagi, J.; Gajdos, S.; Carbognani, A.; Hornoch, K.; Kusnirak, P.; Cooney, W.R.; Gross, J.; Terrell, D.; Higgins, D.; Bowell, E.; Koehn, B.W. (2014). "On the maximum amplitude of harmonics on an asteroid lightcurve." *Icarus* **235**, 55-59.

R Core Team (2020). R: A language and environment for statistical computing. R Foundation for Statistical Computing. Vienna, Austria. <https://www.R-project.org/>

VizieR (2021). <http://vizier.u-strasbg.fr/viz-bin/VizieR>

Warner, B.D.; Harris, A.W.; Pravec, P. (2009). "The Asteroid Lightcurve Database." *Icarus* **202**, 134-146. Updated 2021 June. <http://www.minorplanet.info/lightcurvedatabase.html>

Warner, B.D. (2012). The MPO Users Guide: A Companion Guide to the MPO Canopus/PhotoRed Reference Manuals. BDW Publishing, Colorado Springs, CO.

Warner, B.D. (2018). MPO Canopus software, version 10.7.11.3. <http://www.bdwpublishing.com>

Number	Name	20yy/mm/dd	Phase	$L_{PAB}$	$B_{PAB}$	Period (h)	P.E.	Amp	A.E.	Grp
2728	Yatskiv	21/06/13-21/09/24	*25.4, 20.9	318	4	25.069	0.006	0.43	0.02	MB-I

Table 1. Observing circumstances and results. Phase is the solar phase angle given at the start and end of the date range. If preceded by an asterisk, the phase angle reached an extrema during the period.  $L_{PAB}$  and  $B_{PAB}$  are the average phase angle bisector longitude and latitude. Grp is the asteroid family/group (Warner et al., 2009): MB-I = main-belt inner.

**LIGHTCURVES AND ROTATION PERIODS OF  
57 MNEMOSYNE AND 58 CONCORDIA**

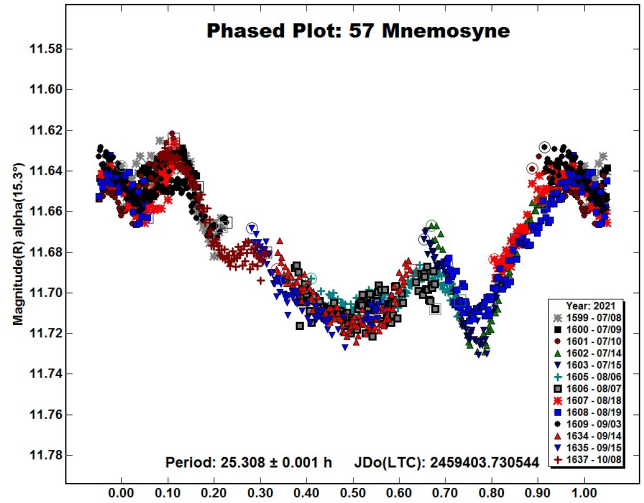
Frederick Pilcher  
Organ Mesa Observatory (G50)  
4438 Organ Mesa Loop  
Las Cruces, NM 88011 USA  
fpilcher35@gmail.com

(Received: 2021 October 8)

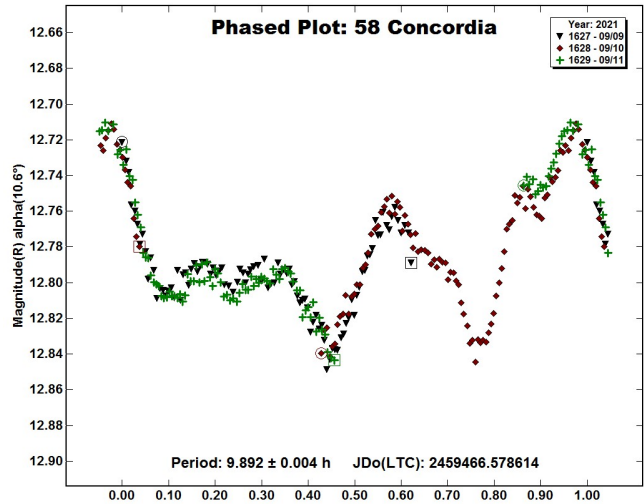
Synodic rotation periods and amplitudes are found for  
57 Mnemosyne: 25.308 +/- 0.001 h, 0.08 +/- 0.01 mag;  
58 Concordia: 9.892 +/- 0.004 h, 0.12 +/- 0.01 mag.

Observations to produce the results reported in this paper were made at the Organ Mesa Observatory with a Meade 35 cm LX200 GPS Schmidt-Cassegrain, SBIG STL-1001E CCD, 30 second exposures for 57 Mnemosyne, 60 second exposures for 58 Concordia, unguided, clear filter. Image measurement and lightcurve construction were with *MPO Canopus* software with all calibration star magnitudes from the CMC15 catalog reduced to the Cousins R band. Zero-point adjustments of a few  $\times$  0.01 magnitude were made for best fit. To reduce the number of data points on the lightcurves and make them easier to read, data points have been binned in sets of 3 with maximum time difference 5 minutes.

57 Mnemosyne. Earlier published periods are by Harris et al. (1992), 12.463 hours; Ditteon and Hawkins (2007), 12.66 hours; Behrend (2016web), 12.92 hours. This author (Pilcher, 2019b) was unable to fit a lightcurve to a period near 12.5 hours and found a synodic period 25.324 hours with one maximum and minimum per cycle near celestial longitude 197 degrees. Pilcher (2020) obtained another set of observations near celestial longitude 258 degrees, finding a synodic period 25.281 hours with a complex lightcurve. New observations on 13 nights 2021 July 8 - Oct. 8 near celestial longitude 331 degrees provide a good fit to a lightcurve with synodic period  $25.308 \pm 0.001$  hours, amplitude  $0.08 \pm 0.01$  magnitudes, again with a complex shape. Misfits in the lightcurve can be attributed to the relevant segments being sampled at greatly different phase angles ranging from  $-15.3^\circ$  to  $5.9^\circ$  to  $15.0^\circ$  during the three-month observation campaign. The observations in years 2019, 2020, and 2021, respectively, indicate consistent rotation periods but very different lightcurve shapes. The differing shapes indicate that the observations were made at different astero-centric latitudes and should be helpful toward future LI modeling.



58 Concordia. Previously published periods are by Gil-Hutton (1993), >16. hours; Wang (2002), 9.89 hours; Behrend (2006web), 9.9 hours; Behrend (2010web), 9.905 hours; Behrend (2011web), 9.904 hours; Stephens (2006), 9.895 hours; Pilcher (2016), 9.895 hours; Pilcher (2019a), 9.895 hours, Pilcher (2020), 9.899 hours. New observations on 3 nights 2021 Sept. 9 - 11 provide a good fit to an irregular lightcurve with period  $9.892 \pm 0.004$  hours, amplitude  $0.12 \pm 0.01$  magnitudes, consistent with most of the previously published values.



Number	Name	2021/mm/dd	Phase	LPAB	BPAB	Period(h)	P.E	Amp	A.E.
57	Mnemosyne	07/08-10/08	* 15.3, 15.0	331	14	25.308	0.001	0.08	0.01
58	Concordia	09/09-09/11	10.6, 11.3	321	1	9.892	0.004	0.12	0.01

Table I. Observing circumstances and results. Pts is the number of data points. The phase angle is given for the first and last date, unless a minimum (second value) was reached. LPAB and BPAB are the approximate phase angle bisector longitude and latitude at mid-date range (see Harris et al., 1984).

## References

- Behrend, R. (2006web, 2010web, 2011web, 2016web). Observatoire de Geneve web site.  
[http://obswww.unige.ch/~behrend/page\\_cou.html](http://obswww.unige.ch/~behrend/page_cou.html).
- Ditteon, R.; Hawkins, S. (2007). "Asteroid lightcurve analysis at the Oakley Observatory - November 2006." *Minor Planet Bull.* **34**, 59-64
- Gil-Hutton, R. (1993). "Photoelectric photometry of asteroids 58 Concordia, 122 Gerda, 326 Tamara, and 441 Bathilde." *Rev. Mexicana Astron. Astrof.* **25**, 75-77.
- Harris, A.W.; Young, J.W.; Scaltriti, F.; Zappala, V. (1984). "Lightcurves and phase relations of the asteroids 82 Alkmea and 444 Ggyptis." *Icarus* **57**, 251-258.
- Harris, A.W.; Young, J.W.; Dockweiler, T.; Gibson, J.; Poutanen, M.; Bowell, E. (1992). "Asteroid lightcurve observations from 1981." *Icarus* **95**, 115-147.
- Pilcher, F. (2016). "Rotation period determinations for 50 Virginia, 58 Concordia, 307 Nike, and 339 Dorothea." *Minor Planet Bull.* **43**, 304-306.
- Pilcher, F. (2019a). "Rotation period determinations for 58 Concordia, 384 Burdigala, 464 Megaira, 488 Kreusa, and 491 Carina." *Minor Planet Bull.* **46**, 360-363.
- Pilcher, F. (2019b). "New lightcurves of 50 Virginia, 57 Mnemosyne, 59 Elpis, 444 Ggyptis, and 997 Priska." *Minor Planet Bull.* **46**, 445-448.
- Pilcher, F. (2020). "Lightcurves and rotation periods of 50 Virginia, 57 Mnemosyne, 58 Concordia, 59 Elpis, 78 Diana, and 529 Preziosa." *Minor Planet Bull.* **47**, 344-346.
- Stephens, R. D. (2006). "Asteroid lightcurve photometry from Santana and GMARS observatories - winter and spring 2006." *Minor Planet Bull.* **33**, 100-101.
- Wang, X.-B. (2002). "CCD photometry of asteroids (58) Concordia, (360) Carlova, and (405) Thia." *Earth, Moon, and Planets* **91**, 25-30
- Warner, B.D., Harris, A.W., Pravec, P. (2009). "The Asteroid Lightcurve Database." *Icarus* **202**, 134-146. Updated 2021 June.  
<https://minplanobs.org/MPIInfo/php/lcdb.php>

**ROTATION PERIOD DETERMINATION FOR ASTEROIDS  
2232 ALTAJ, 3699 MILBOURN, 4101 RUIKOU,  
(6787) 1991 PF15 AND 8416 OKADA**

Alessandro Marchini, Leonardo Cavaglioni,  
Chiara Angelica Privitera  
Astronomical Observatory, DSFTA - University of Siena (K54)  
Via Roma 56, 53100 - Siena, ITALY  
marchini@unisi.it

Riccardo Papini, Fabio Salvaggio  
Wild Boar Remote Observatory (K49)  
San Casciano in Val di Pesa (FI), ITALY

(Received: 2021 October 15)

Photometric observations of five main-belt asteroids were conducted in order to determine their synodic rotation periods. For 2232 Altaj we found  $P = 8.089 \pm 0.001$  h,  $A = 0.30 \pm 0.02$  mag; for 3699 Milbourn we found  $P = 3.816 \pm 0.002$  h,  $A = 0.20 \pm 0.02$  mag; for 4101 Ruikou we found  $P = 8.098 \pm 0.009$  h,  $A = 0.07 \pm 0.03$  mag; for (6787) 1991 PF15 we found  $P = 4.645 \pm 0.001$  h,  $A = 0.80 \pm 0.01$  mag; for 8416 Okada we found  $P = 2.646 \pm 0.001$  h,  $A = 0.04 \pm 0.02$  mag.

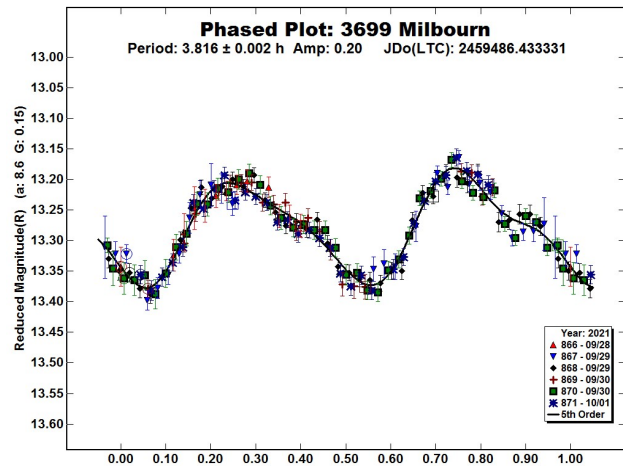
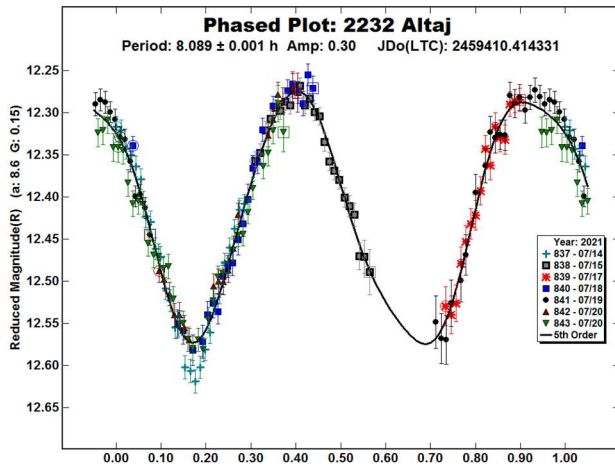
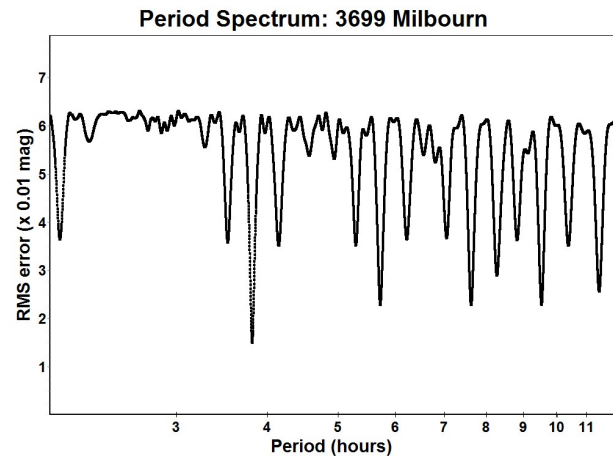
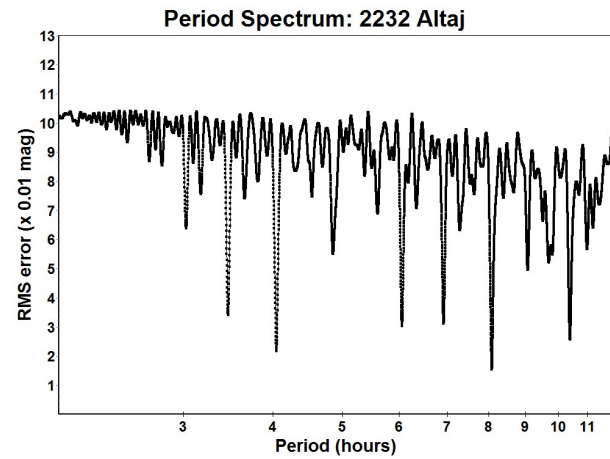
CCD photometric observations of five main-belt asteroids were carried out in 2021 July - October at the Astronomical Observatory of the University of Siena (K54), a facility inside the Department of Physical Sciences, Earth and Environment (DSFTA, 2021). We used a 0.30-m  $f/5.6$  Maksutov-Cassegrain telescope, SBIG STL-6303E NABG CCD camera, and clear filter; the pixel scale was 2.30 arcsec when binned at  $2 \times 2$  pixels and all exposures were 300 seconds.

Data processing and analysis were done with *MPO Canopus* (Warner, 2018). All images were calibrated with dark and flat-field frames and the instrumental magnitudes converted to R magnitudes using solar-colored field stars from a version of the CMC-15 catalogue distributed with *MPO Canopus*. Table I shows the observing circumstances and results.

A search through the asteroid lightcurve database (LCDB; Warner *et al.*, 2009) indicates that our results may be the first reported lightcurve observations and results for these asteroids. For 2232 Altaj we found in literature a previously published period in good agreement with our solution.

2232 Altaj (1969 RD2) was discovered on 1969 September 15 by B. A. Burnasheva at the Crimean Astrophysical Observatory and named after the place of residence of the discoverer's mother, Elena Andreevna Vasil'eva. [Ref: *Minor Planet Circ.* 5850] It is a main-belt asteroid with a semi-major axis of 2.668 AU, eccentricity 0.143, inclination  $3.693^\circ$ , and an orbital period of 4.36 years. Its absolute magnitude is  $H = 12.2$  (JPL, 2021). The WISE/NEOWISE satellite infrared radiometry survey (Masiero *et al.*, 2011) found a diameter  $D = 11.780 \pm 0.212$  km using an absolute magnitude  $H = 12.0$ .

Observations were conducted over four nights and collected 179 data points. The period analysis shows a bimodal solution for the rotational period of  $P = 8.089 \pm 0.001$  h with an amplitude  $A = 0.30 \pm 0.02$  mag. This result is in good agreement with the one recently published by Āurech *et al.* (2020) of  $P = 8.09346 \pm 0.00003$ .



3699 Milbourn (1984 UC2) was discovered on 1984 October 29 by E. Bowell at Flagstaff and named in honor of Stanley William Milbourn, editor of the circulars of the British Astronomical Association during 1969-1986, director of the comet section during 1968-1977 and later assistant director of the computing section. [Ref: Minor Planet Circ. 12809] It is a main-belt asteroid with a semi-major axis of 2.399 AU, eccentricity 0.187, inclination  $5.712^\circ$ , and an orbital period of 3.72 years. Its absolute magnitude is  $H = 12.96$  (JPL, 2021). The WISE/NEOWISE satellite infrared radiometry survey (Masiero et al., 2012) found a diameter  $D = 4.19 \pm 0.15$  km using an absolute magnitude  $H = 12.8$ .

Observations over three nights collected 174 data points. The period analysis shows a bimodal solution for the rotational period of  $P = 3.816 \pm 0.002$  h with an amplitude  $A = 0.20 \pm 0.02$  mag.

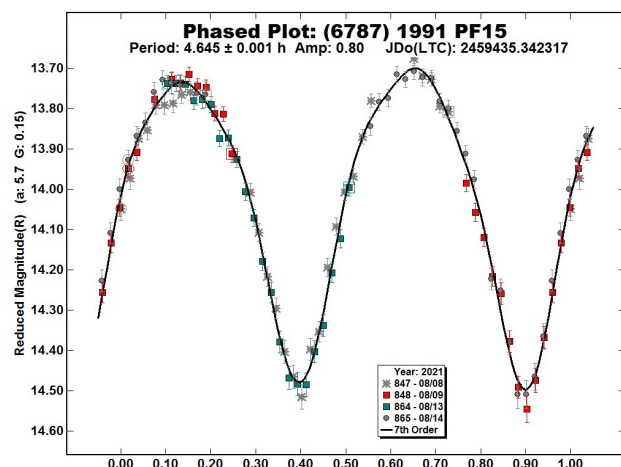
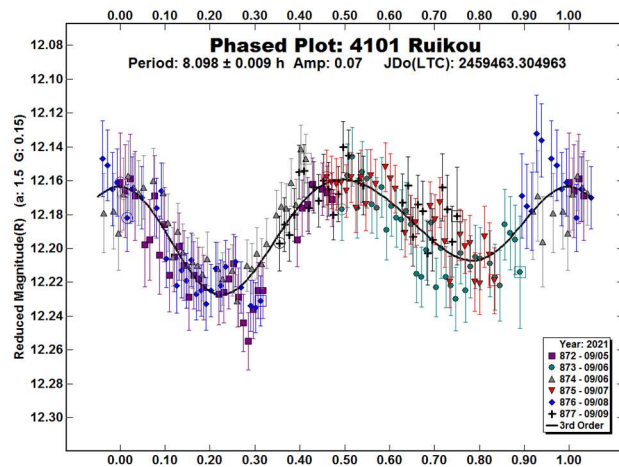
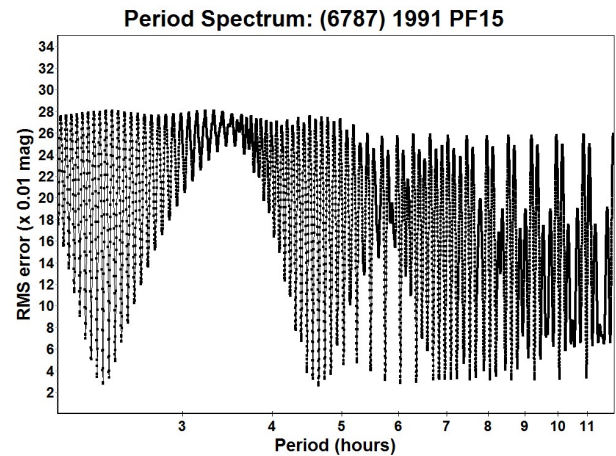
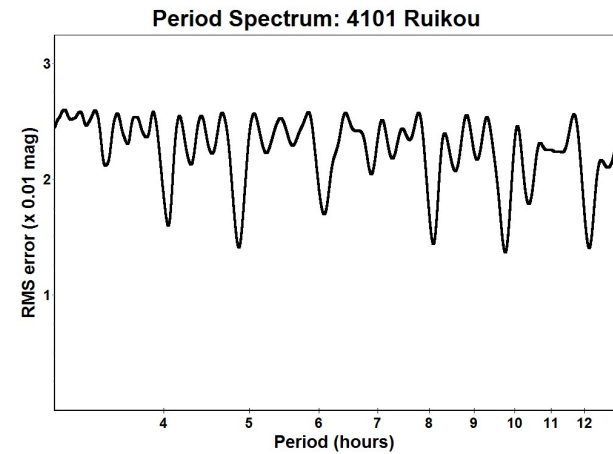
This target was observed within the Photometric Survey for Asynchronous Binary Asteroids under the leadership of Petr Pravec from Ondřejov Observatory, Czech Republic (Pravec et al., 2006; Pravec, 2021web) and their independent analysis confirmed our results.

4101 Ruikou (1988 CE) was discovered on 1988 February 8 by T. Seki at Geisei and named after Ruikou Kuroiwa (1862-1920), a great scholar, translator and commentator of the Meiji and Taisho eras; he was born in Aki city, on the western side of which the Geisei Station is situated. [Ref: Minor Planet Circ. 16247]. It is a main-belt asteroid with a semi-major axis of 2.699 AU, eccentricity 0.115, inclination  $8.749^\circ$ , and an orbital period of 4.43 years. Its absolute magnitude is  $H = 12.36$  (JPL, 2021). The WISE/NEOWISE satellite infrared radiometry survey (Masiero et al., 2012) found a diameter  $D = 13.63 \pm 0.80$  km using an absolute magnitude  $H = 12.2$ .

Observations were conducted over three nights and collected 197 data points. The period analysis shows a few possible solutions for the rotational period of this asteroid; we present here the one that has a full coverage of the folded curve without gaps, with a period  $P = 8.098 \pm 0.009$  h and with an amplitude  $A = 0.07 \pm 0.03$  mag, as the most likely bimodal solution. Due to its high uncertainty and the low amplitude of the lightcurve, further observations are strongly encouraged to nail down the actual period.

Number	Name	2021/mm/dd	Phase	$L_{PAB}$	$B_{PAB}$	Period(h)	P.E.	Amp	A.E.	Grp
2232	Altaj	07/14-07/21	8.6, 5.8	307	5	8.089	0.001	0.30	0.02	MB
3699	Milbourn	09/28-10/01	8.6, 7.6	16	-8	3.816	0.002	0.20	0.02	MB
4101	Ruikou	09/05-09/09	1.6, 0.8	346	1	8.098	0.009	0.07	0.03	MB
6787	1991 PF15	08/08-08/14	5.8, 3.5	323	4	4.645	0.001	0.80	0.01	MB
8416	Okada	08/30-09/05	2.1, 1.7	340	1	2.646	0.001	0.04	0.02	MB

Table I. Observing circumstances and results. The first line gives the results for the primary of a binary system. The second line gives the orbital period of the satellite and the maximum attenuation. The phase angle is given for the first and last date. If preceded by an asterisk, the phase angle reached an extrema during the period.  $L_{PAB}$  and  $B_{PAB}$  are the approximate phase angle bisector longitude/latitude at mid-date range (see Harris *et al.*, 1984). Grp is the asteroid family/group (Wamer *et al.*, 2009).



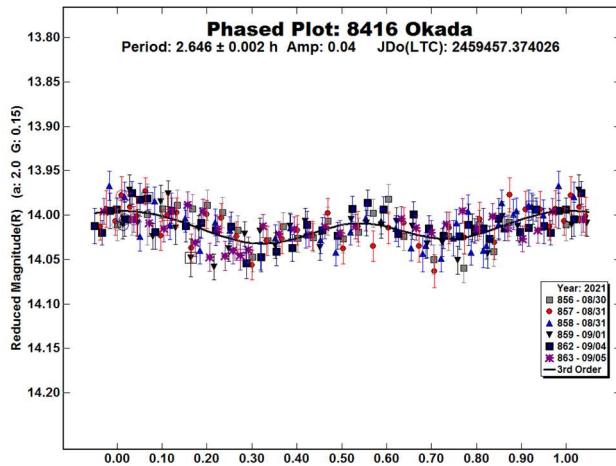
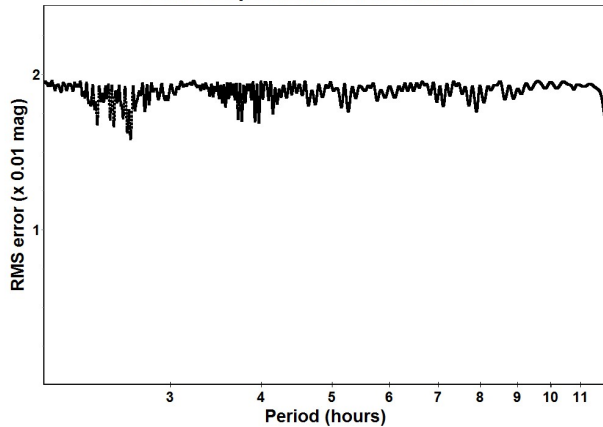
(6787) 1991 PF15 was discovered on 1991 August 7 by H. E. Holt at Palomar. It is a main-belt asteroid with a semi-major axis of 2.233 AU, eccentricity 0.148, inclination 3.290°, and an orbital period of 3.34 years. Its absolute magnitude is  $H = 13.57$  (JPL, 2021). The WISE/NEOWISE satellite infrared radiometry survey (Masiero *et al.*, 2011) found a diameter  $D = 4.865 \pm 0.117$  km using an absolute magnitude  $H = 13.5$ .

Observations over two nights collected 107 data points. The period analysis shows a solution for the rotational period of  $P = 4.645 \pm 0.001$  h with an amplitude  $A = 0.80 \pm 0.01$  mag, confirmed by the independent analysis performed by the already mentioned Photometric Survey for Asynchronous Binary Asteroids (Pravec *et al.*, 2006; Pravec, 2021web).

8416 Okada (1996 VB8) was discovered on 1996 November 3 by S. Ueda and H. Kaneda at Kushiro and named after Yoshiyuki Okada (b. 1947), a member of Shirakawa Observatory in Japan and Chiro Observatory in Australia, who is a talented amateur who played an important role in developing large portable telescopes. [Ref: Minor Planet Circ. 41936]. It is a main-belt asteroid with a semi-major axis of 2.153 AU, eccentricity 0.196, inclination 3.317°, and an orbital period of 3.16 years. Its absolute magnitude is  $H = 13.95$  (JPL, 2021). The WISE/NEOWISE satellite infrared radiometry survey (Masiero *et al.*, 2011) found a diameter  $D = 4.198 \pm 0.145$  km using an absolute magnitude  $H = 14.0$ .

Observations were conducted over three nights and collected 195 data points. Despite its very low amplitude, the period analysis shows a result for the rotational period of  $P = 2.646 \pm 0.001$  h with an amplitude  $A = 0.04 \pm 0.02$  mag as the most likely bimodal solution for this asteroid, confirmed by the independent analysis performed by the already mentioned Photometric Survey for Asynchronous Binary Asteroids (Pravec *et al.*, 2006; Pravec, 2021web).

### Period Spectrum: 8416 Okada



### Acknowledgements

Leonardo Cavaglioni and Chiara Angelica Privitera, students of the course in Physics and Advanced Technologies at the Department of Physical Sciences, Earth and Environment, actively participated to the observations and data analysis of some asteroids presented in this article during their internship activities at the Astronomical Observatory of the University of Siena, and appear deservedly as authors. Minor Planet Circulars (MPCs) are published by the International Astronomical Union's Minor Planet Center. [https://www.minorplanetcenter.net/iau/ECS/MPCArchive/MPCArchive\\_TBL.html](https://www.minorplanetcenter.net/iau/ECS/MPCArchive/MPCArchive_TBL.html)

### References

- DSFTA (2021). Dipartimento di Scienze Fisiche, della Terra e dell'Ambiente - Astronomical Observatory. <https://www.dsfta.unisi.it/en/research/labs/astronomical-observatory>
- Đurech, J.; Tonry, J.; Erasmus, N.; Denneau, L.; Heinze, A.N.; Flewelling, H.; Vančo, R. (2020). "Asteroid models reconstructed from ATLAS photometry." *Astronomy & Astrophysics* **643**, A59.
- Harris, A.W.; Young, J.W.; Scaltriti, F.; Zappala, V. (1984). "Lightcurves and phase relations of the asteroids 82 Alkmene and 444 Gytis." *Icarus* **57**, 251-258.
- JPL (2021). Small-Body Database Browser. <http://ssd.jpl.nasa.gov/sbdb.cgi#top>
- Masiero, J.R.; Mainzer, A.K.; Grav, T.; Bauer, J.M.; Cutri, R.M.; Dailey, J.; Eisenhardt, P.R.M.; McMillan, R.S.; Spahr, T.B.; Skrutskie, M.F.; Tholen, D.; Walker, R.G.; Wright, E.L.; DeBaun, E.; Elsbury, D.; Gautier IV, T.; Gomillion, S.; Wilkins, A. (2011). "Main Belt Asteroids with WISE/NEOWISE. I. Preliminary Albedos and Diameters." *Astrophys. J.* **741**, A68.
- Masiero, J.R.; Mainzer, A.K.; Grav, T.; Bauer, J.M.; Cutri, R.M.; Nugent, C.; Cabrera, M.S. (2012). "Preliminary Analysis of WISE/NEOWISE 3-Band Cryogenic and Post-cryogenic Observations of Main Belt Asteroids." *Astrophys. J. Letters* **759**.
- Pravec, P.; Scheirich, P.; Kušnirák, P.; Šarounová, L.; Mottola, S.; Hahn, G.; Brown, P.; Esquerdo, G.; Kaiser, N.; Krzeminski, Z.; Pray, D.P.; Warner, B.D.; Harris, A.W.; Nolan, M.C.; Howell, E.S.; Benner, L.A.M.; Margot, J.-L.; Galád, A.; Holliday, W.; Hicks, M.D. Krugly, Yu.N.; Tholen, D.; Whiteley, R.; Marchis, F.; DeGraff, D.R.; Grauer, A.; Larson, S.; Velichko, F.P.; Cooney, W.R.; Stephens, R.; Zhu, J.; Kirsch, K.; Dyvig, R.; Snyder, L.; Reddy, V.; Moore, S.; Gajdoš, Š.; Világi, J.; Masi, G.; Higgins, D.; Funkhouser, G.; Knight, B.; Slivan, S.; Behrend, R.; Grenon, M.; Burki, G.; Roy, R.; Demeautis, C.; Matter, D.; Waelchli, N.; Revaz, Y.; Klotz, A.; Rieugné, M.; Thierry, P.; Cotrez, V.; Brunetto, L.; Kober, G. (2006). "Photometric survey of binary near-Earth asteroids." *Icarus* **181**, 63-93.
- Pravec, P. (2021web). Photometric Survey for Asynchronous Binary Asteroids web site. <http://www.asu.cas.cz/~asteroid/binastphotosurvey.htm>
- Warner, B.D.; Harris, A.W.; Pravec, P. (2009). "The Asteroid Lightcurve Database." *Icarus* **202**, 134-146. Updated 2020 Oct. <http://www.minorplanet.info/lightcurvedatabase.html>
- Warner, B.D. (2018). MPO Software, MPO Canopus v10.7.7.0. Bdw Publishing. <http://minorplanetobserver.com>

## LIGHTCURVE ANALYSIS OF TWO POTENTIALLY HAZARDOUS ASTEROIDS AND THREE NEAR-EARTH ASTEROIDS

Ian Díaz-Vachier

Lunar & Planetary Laboratory, University of Arizona  
1629 E University Blvd, Tucson, AZ, 85721  
idiazvachier@arizona.edu

Desireé Cotto-Figueroa, Alexander Rivas-Díaz,  
Julian Abreu-Cintrón, Bryan Rivera-Rivera  
Dept. of Physics and Elec., University of Puerto Rico at Humacao  
Humacao, Puerto Rico, 00792

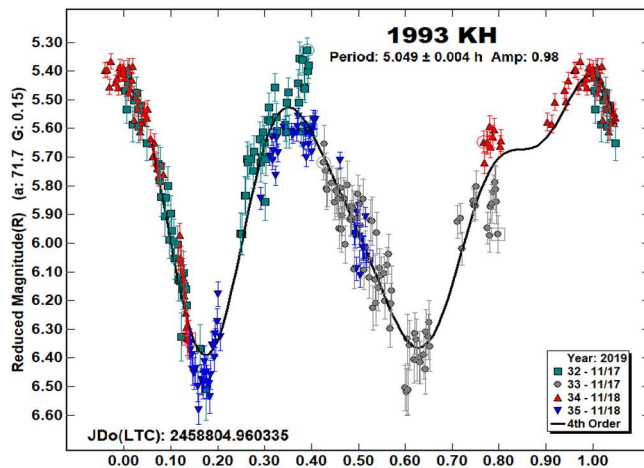
Peter Santana-Rodríguez, Felix Laurenó-La Puerta  
University of Puerto Rico at Mayagüez  
Mayagüez, Puerto Rico, 00681

(Received: 2021 Sep 7)

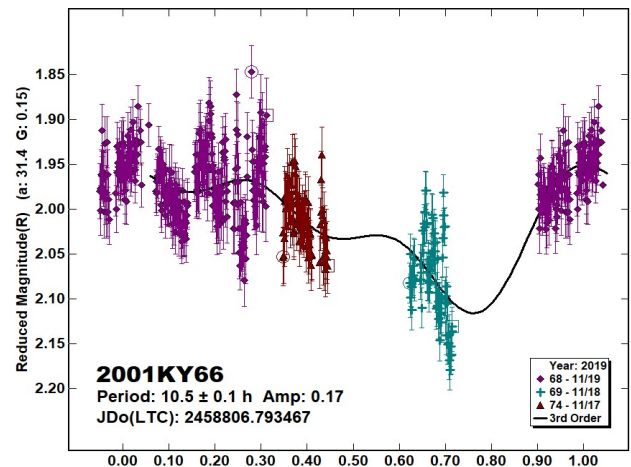
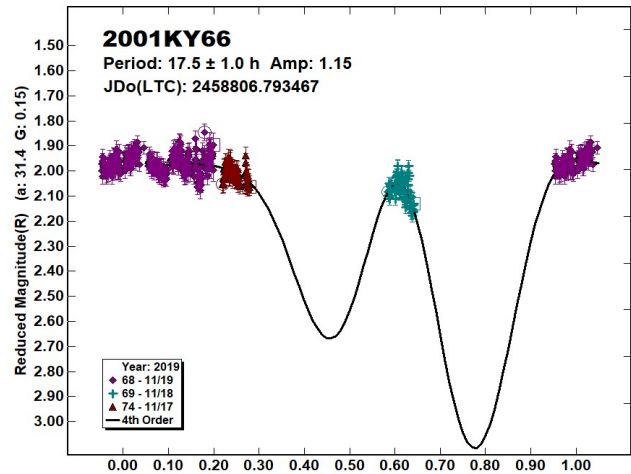
We report on rotation lightcurves of two potentially hazardous asteroids, 1993 KH and 2001 KY66, and three near-Earth asteroids, 2005 EC224, 2004 FM17, and 2013 OS3, performed by CCD photometric observation at the National Undergraduate Research Observatory telescope at the Lowell Observatory.

Photometric observations on five near-Earth asteroids (NEAs), two of which are listed as potentially hazardous asteroids (PHAs), were conducted at the Lowell Observatory in Flagstaff, Arizona. Data were acquired with the 31-inch National Undergraduate Research Observatory (NURO) telescope equipped with a 2K×2K thermoelectrically cooled CCD NASAcam camera. Exposures of 30 to 45 seconds were made using an R-band filter. Object images were bias and flat field corrected using *MPO Canopus* (version 10.8.1.1; Warner, 2019). Lightcurves and period analysis were performed with *MPO Canopus* as well.

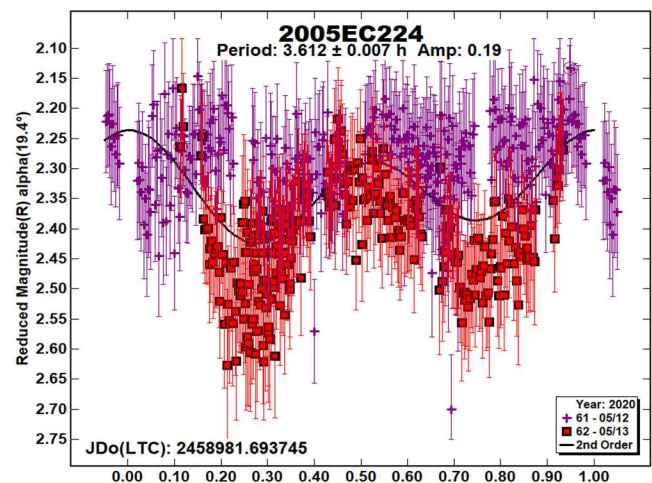
(85236) 1993 KH is a PHA Apollo-type ( $D \sim 490$  m) that was discovered by R.H. McNaught at Siding Spring Observatory on 1993 May 24. Observations were made on 2019 November 17-18 for a total of 7.58 hours, yielding 277 points. We found a period of  $P = 5.049 \pm 0.004$  h and amplitude of  $A = 0.98 \pm 0.10$  mag, the period is consistent with Warner and Stephens (2019a; 5.057 h).



(99248) 2001 KY66 is an Apollo-type 1.6 km diameter PHA. Warner (2015) found a rotation period of 19.7h, by experiencing some difficulties. In 2019, Warner and Stephens report a similar result of 19.9 h (Warner and Stephens, 2019b). In approximately 6 hours of observations, yielding 480 points, our results show a rotation period of  $P = 17.5 \pm 0.2$  h with  $A = 0.43 \pm 0.04$  mag. Another possible solution of  $10.5 \pm 0.1$  h with a 0.17 mag amplitude, which could be reported as half of the previously mentioned rotational periods.



(175189) 2005 EC224 is an Amor class NEA discovered at Mount Lemmon on 2005 March 11 by Mt. Lemmon Survey.

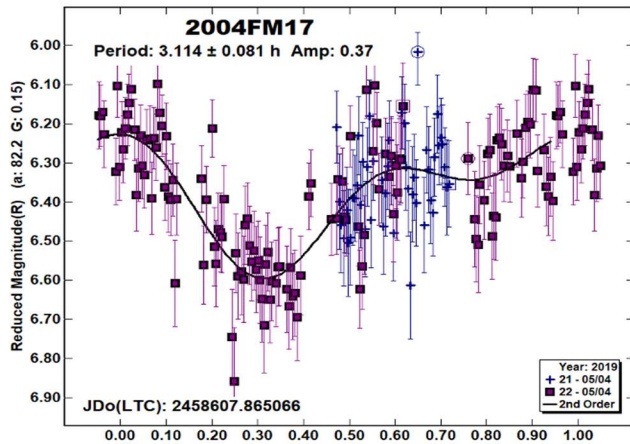


Number	Name	yyyy mm/dd	Phase	$L_{PAB}$	$B_{PAB}$	Period(h)	P.E.	Amp	A.E.	Grp
85236	1993 KH	2019 11/17-11/18	71.7	71	81	5.049	0.004	0.98	0.10	PHA
99248	2001 KY66	2019 11/17-11/19	31.4	72	19	17.5	1.0	1.15	0.04	PHA
175189	2005 EC224	2020 05/12-05/13	19.4	217	5	3.612	0.007	0.19	0.04	NEO
387816	2004 FM17	2019 05/04	82.2	261	34	3.114	0.081	0.37	0.01	NEO
437316	2013 OS3	2020 01/24-01/25	42.4	103	-10	5.46	0.01	0.76	0.10	NEO

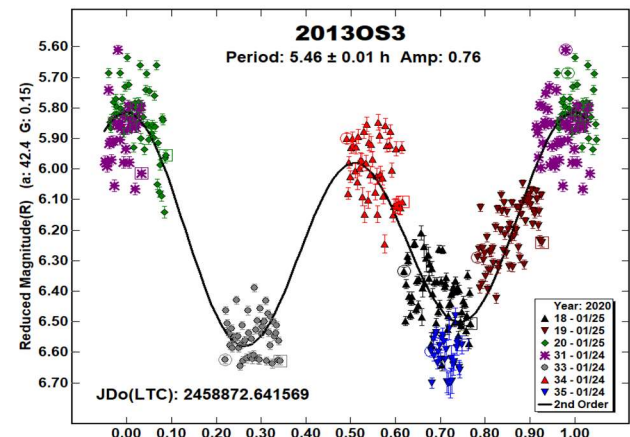
Table I. Observing circumstances and results. The phase angle is given for the first and last date. If preceded by an asterisk, the phase angle reached an extrema during the period.  $L_{PAB}$  and  $B_{PAB}$  are the approximate phase angle bisector longitude/latitude at mid-date range (see Harris et al., 1984). Grp is the asteroid family/group (Warner et al., 2009).

The photometric observations were made during two nights between May 12 and 13. During those nights, a total of 9.5 hours of observation produced 608 data points. The rotation period obtained in the analysis of the lightcurve was of  $P = 3.612 \pm 0.007$  h with an amplitude of  $A = 0.19 \pm 0.04$  mag. A search on the Asteroid Lightcurve Database (LCDB; Warner et al., 2009) found a previous reported period by Warner and Stephens (2020a), which has a period of 3.758 h and amplitude of 0.15 mag. The period and amplitude found are in full agreement with our solution.

(387816) 2004 FM17 is an Aten-type NEO discovered on 2004 March 26 by Linear at Socorro. A total of approximately 4 hours of observation produced 181 data points for analysis. Photometric observation was performed on 2019 May 4. The rotation period was found to be  $P = 3.114 \pm 0.081$  h with an amplitude of  $A = 0.37 \pm 0.01$  mag. A search of the Asteroid Lightcurve Database (LCDB; Warner et al., 2009) did not find any previously reported results.



(437316) 2013 OS3 is an Apollo-type NEO discovered by Pan-STARRS 1 on 2013 July 16. 2013 OS3 has an estimated diameter of 0.6 km. Photometric observations were performed on 2020 January 24-25.



We observed this asteroid for a total of 15.28 hours and 361 data points were obtained for analysis. Here we report a period of  $P = 5.46 \pm 0.01$  h and amplitude of  $A = 0.76 \pm 0.10$  mag, which is consistent with two previously reported periods on the lightcurve database (LCDB; Warner et al., 2009) of 5.593 h reported by Warner and Stephens (2020b) and 5.63 h reported by Benishek (2020).

#### Acknowledgements

The authors gratefully acknowledge the support of NASA Puerto Rico Space Grant Consortium grant NNX15AI11H and of the NASA MUREP Institutional Research Opportunity grant 80NSSC19M0197.

#### References

- Benishek, V. (2020). "Photometry of 39 Asteroids at Sopot Astronomical Observatory: 2019 September - 2020 March." *Minor Planet Bull.* **47**, 231-241.
- Harris, A.W.; Young, J.W.; Scaltriti, F.; Zappala, V. (1984). "Lightcurves and phase relations of the asteroids 82 Alkmene and 444 Ggyptis." *Icarus* **57**, 251-258.
- Warner, B.D.; Harris, A.W.; Pravec, P. (2009). "The Asteroid Lightcurve Database." *Icarus* **202**, 134-146. Updated 2016 Sep. <http://www.minorplanet.info/lightcurvedatabase.html>
- Warner, B.D. (2015). "Near-Earth Asteroid Lightcurve Analysis at CS3-Palmer Divide Station: 2015 January - March." *Minor Planet Bull.* **42**, 172-183.
- Warner, B.D. (2019). MPO Software, *MPO Canopus* v10.8.1.1. Bdw Publishing. <http://minorplanetobserver.com>
- Warner, B.D.; Stephens, R.D. (2019a). "Near-Earth Asteroid Lightcurve Analysis at the Center for Solar System Studies: 2019 March - July." *Minor Planet Bull.* **46**, 423-438.
- Warner, B.D.; Stephens, R.D. (2019b). "Near-Earth Asteroid Lightcurve Analysis at the Center for Solar System Studies: 2019 September - 2020 January." *Minor Planet Bull.* **47**, 105-120.
- Warner, B.D.; Stephens, R.D. (2020a). "Near-Earth Asteroid Lightcurve Analysis at the Center for Solar System Studies: 2020 April - June." *Minor Planet Bull.* **47**, 290-304.
- Warner, B.D.; Stephens, R.D. (2020b). "Near-Earth Asteroid Lightcurve Analysis at the Center for Solar System Studies: 2019 December - 2020 April." *Minor Planet Bull.* **47**, 200-213.

**NEAR-EARTH ASTEROID LIGHTCURVE ANALYSIS  
AT THE CENTER FOR SOLAR SYSTEM STUDIES:  
2021 AUGUST-OCTOBER**

Brian D. Warner  
Center for Solar System Studies / MoreData!  
446 Sycamore Ave.  
Eaton, CO 80615 USA  
brian@MinorPlanetObserver.com

Robert D. Stephens  
Center for Solar System Studies / MoreData!  
Rancho Cucamonga, CA

(Received: 2021 October 12)

Lightcurves of 12 near-Earth asteroids (NEAs) obtained at the Center for Solar System Studies (CS3) from 2021 July through early October were analyzed for rotation period, peak-to-peak amplitude, and signs of satellites or tumbling. We have good reason to believe that 2019 UD4 is in a tumbling state.

CCD photometric observations of 12 near-Earth asteroids (NEAs) were made at the Center for Solar System Studies (CS3) from 2021 August through early October. Table I lists the telescopes and CCD cameras that were available to make observations.

Up to nine telescopes can be used but seven is more common. All the cameras use CCD chips from the KAF blue-enhanced family and so have essentially the same response. The pixel scales ranged from 1.24-1.60 arcsec/pixel.

Telescopes	Cameras
0.30-m f/10 Schmidt-Cass	FLI Microline 1001E
0.35-m f/9.1 Schmidt-Cass	FLI Proline 1001E
0.40-m f/10 Schmidt-Cass	SBIG STL-1001E
0.40-m f/10 Schmidt-Cass	
0.50-m f/8.1 Ritchey-Chrétien	

Table I. List of available telescopes and CCD cameras at CS3. The exact combination for each telescope/camera pair can vary due to maintenance or specific needs.

All lightcurve observations were unfiltered since a clear filter can cause a 0.1-0.3 mag loss. The exposure duration varied depending on the asteroid's brightness and sky motion. Guiding on a field star sometimes resulted in a trailed image for the asteroid.

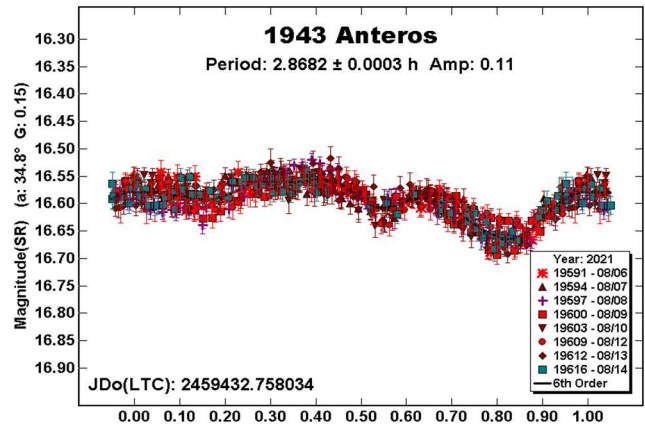
Measurements were made using *MPO Canopus*. The Comp Star Selector utility in *MPO Canopus* found up to five comparison stars of near solar-color for differential photometry. To reduce the number of times and amounts of adjusting nightly zero points, we use the ATLAS catalog  $r'$  (SR) magnitudes (Tonry et al., 2018). Those adjustments are usually  $|\Delta| \leq 0.03$  mag. The larger corrections, which are rare, may have been related in part to using unfiltered observations, poor centroiding of the reference stars, and not correcting for second-order extinction. Another cause may be selecting what appears to be a single star but is actually an unresolved pair.

The Y-axis values are ATLAS SR "sky" (catalog) magnitudes. The two values in the parentheses are the phase angle ( $a$ ) and the value of  $G$  used to normalize the data to the comparison stars used in the earliest session. This, in effect, corrected all the observations to seem to have been made at a single fixed date/time and phase angle, leaving any variations due only to the asteroid's rotation and/or

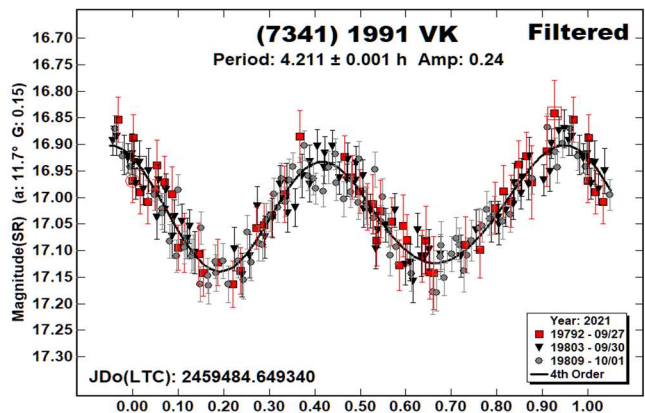
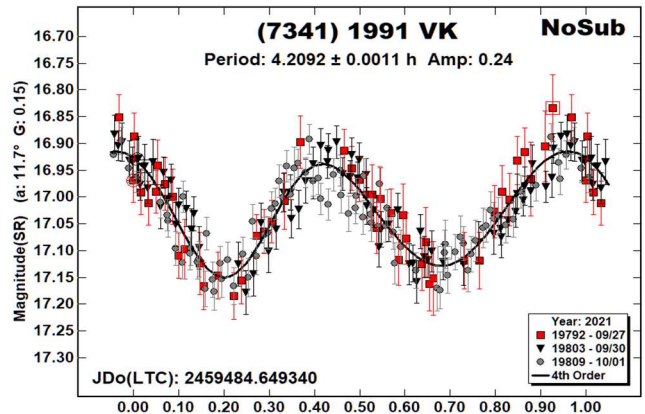
albedo changes. The X-axis shows rotational phase from  $-0.05$  to  $1.05$ . If the plot includes the amplitude, e.g., "Amp: 0.65", this is the amplitude of the Fourier model curve and *not necessarily the adopted amplitude for the lightcurve*.

"LCDB" substitutes for "Warner et al. (2009)" from here on.

**1943 Anteros.** Warner et al. (2017) reported this to be a suspected binary with an orbital period of 23.548 h. We (Warner and Stephens, 2019) found inconclusive results, finding a suspected secondary period of 19.7 h. The 2021 data showed no signs of a satellite. If nothing else, the negative results help constrain the pole solutions for the primary spin axis and satellite orbit.



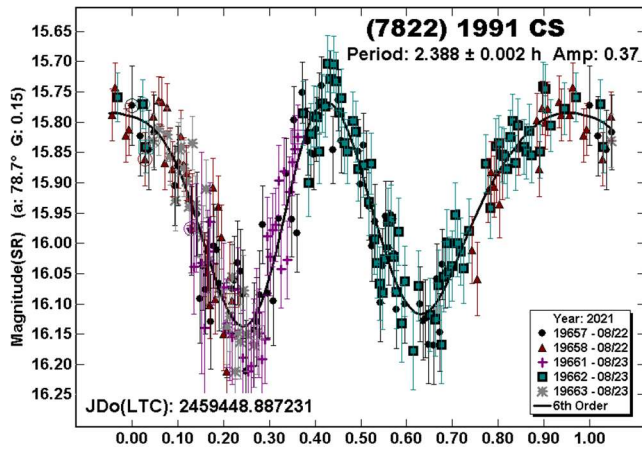
(7341) 1991 VK. Pravec et al. (1998) found a period of 4.2096 h. Our previous result of 4.211 h (Warner, 2017) is the same found with the most recent observations after applying a noise filter.



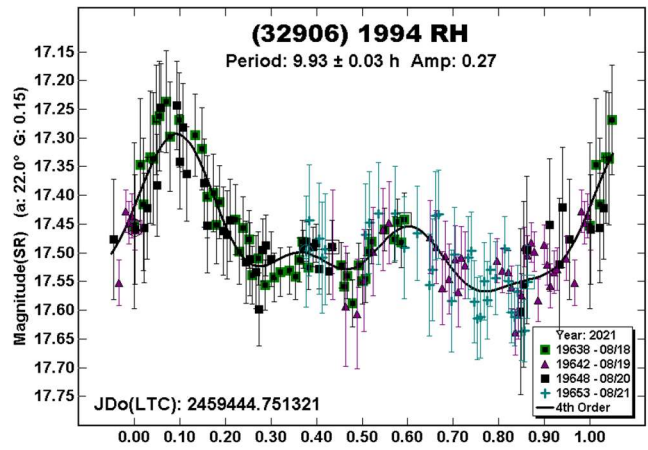
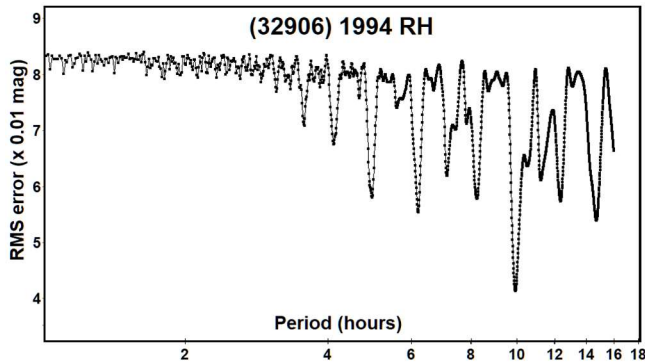
The “NoSub” plot shows the data phase to a single period but the scatter is a bit excessive. A dual-period search found several, low-amplitude possibilities but none of the phased plots showed indications of a satellite. Furthermore, the combination of period and estimated size (1 km), make it very unlikely that any of those secondary periods can be attributed to tumbling (Pravec et al., 2005; 2014). We applied the most dominant secondary solution to the original data to act as a *noise filter*. This produced a curve with less scatter (“Filtered” plot). The unfiltered data were submitted to ALCDEF (<https://alcdef.org>).

(7822) 1991 CS. The previously reported periods are all very close to 2.39 h, including our two previous results of 2.391 h (Warner, 2016a) and 2.392 h (Warner, 2016b), as well as Pravec et al. (1998; 2.389 h), Behrend (2016web; 2.3896 h), and KlingleSmith et al. (2016; 2.389 h). The amplitude has ranged from 0.26 to 0.46 mag.

It should be noted that the larger amplitudes were observed at more extreme phase angles,  $\alpha > 45^\circ$ , which exaggerates the amplitude due to shape alone that is seen at low phase angles (Zappala et al., 1990).

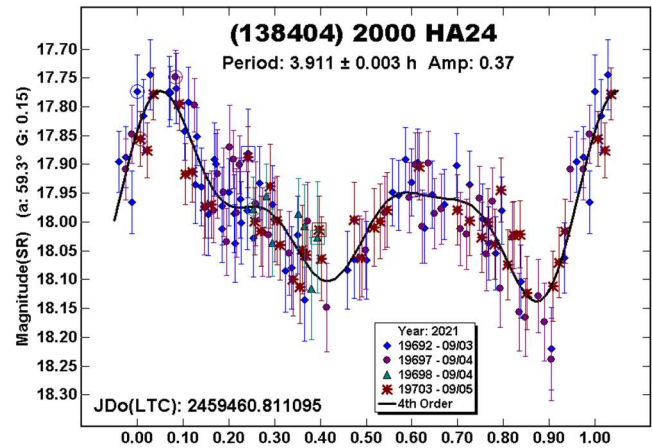


(32906) 1994 RH. Skiff (2012web) reported a period of 2.569 h, but no lightcurve is available. We could not get our data to fit anything close to that period, as seen in the period spectrum.



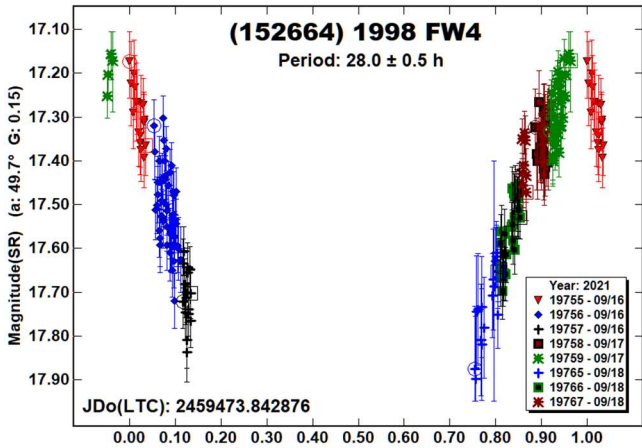
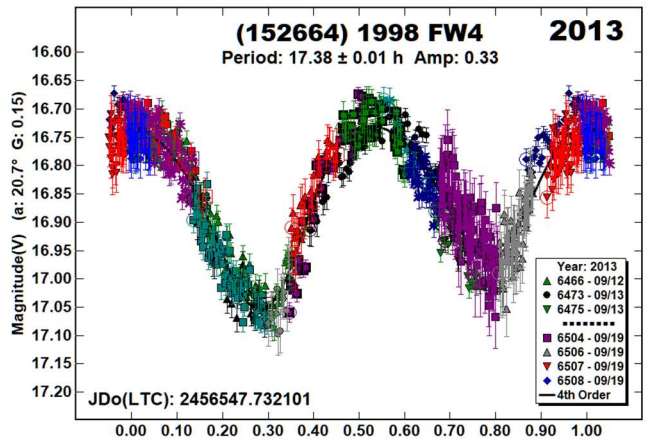
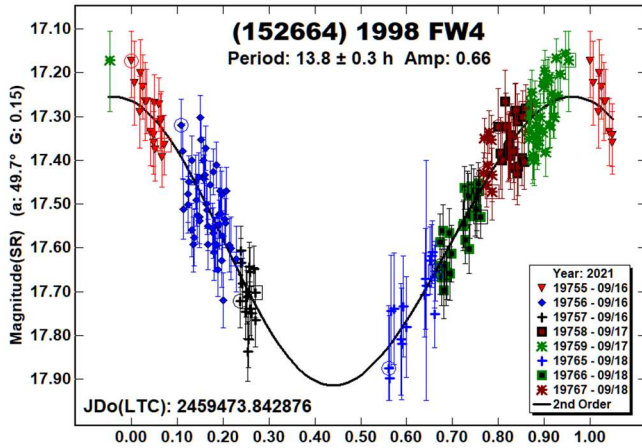
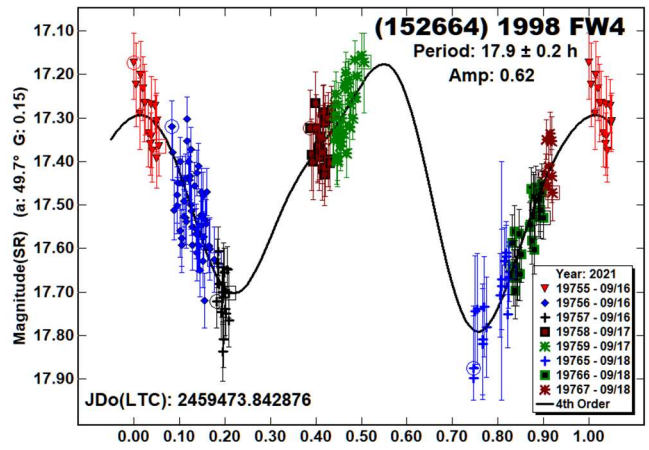
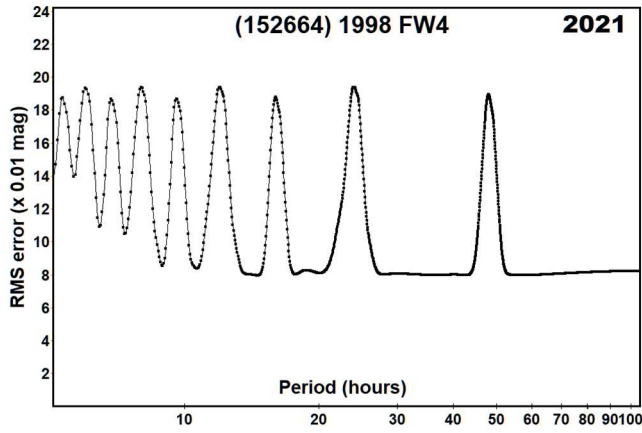
The odd shape of the lightcurve lends doubt to our period of 9.93 h despite its prominence in the period spectrum. Attempts to force a solution near some of the alternates in the period spectrum produced unsatisfactory results.

(138404) 2000 HA24. Hayes-Gehrke et al. (2017) reported a period of 3.7768 h but it is rated  $U = 2-$  in the LCDB, meaning that there is a good chance that the result is incorrect. It turned out that they were close. Monteiro et al. (2018) found  $P = 3.908$  h and Pravec et al. (2019web) found  $P = 3.9077$  h. Our result of 3.911 h is consistent with the longer periods.



(152664) 1998 FW4. Various circumstances did not allow observing the asteroid to where the lightcurve could be even mostly filled. Despite the high phase angle, which can distort the lightcurve shape (Harris et al., 2014), it’s very likely that the asteroid should produce a bimodal lightcurve.

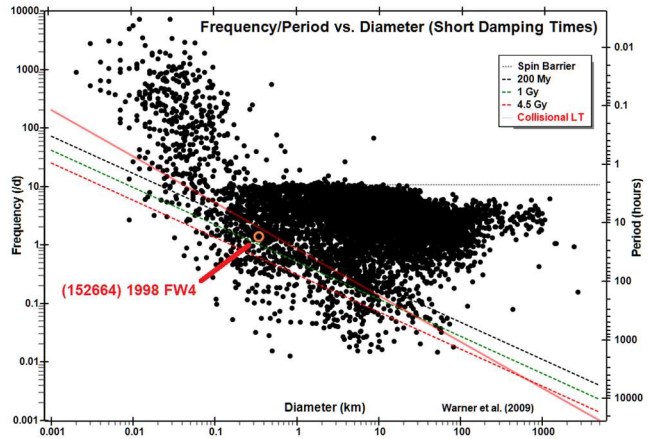
Proceeding on that assumption, we searched for a likely half-period. This would provide more coverage of the lightcurve and allow finding a good estimate for amplitude. That search found  $P = 13.8$  h and amplitude of  $A = 0.66$  mag. Based on this, we tried to find a solution near 28 h. The slopes of the lightcurve were far too steep to consider that possibility.



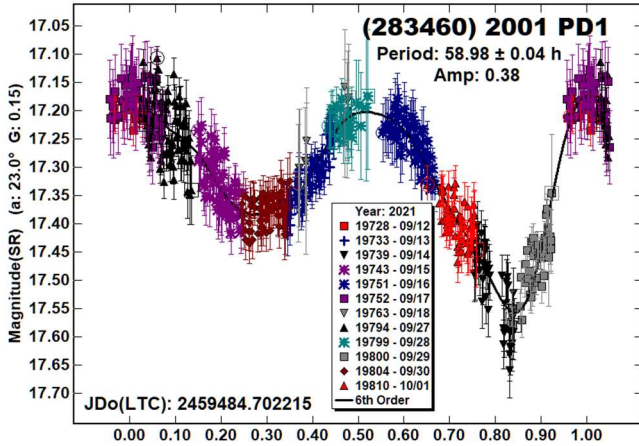
In the frequency-diameter plot from the LCDB, the asteroid is just below the 200 Myr damping and collisional life-time lines. By general rule of thumb (Pravec et al., 2005; 2014), there is a chance that the asteroid could be tumbling. There was no clear sign of such in 2013 nor, within the limits allowed by the sparse data set, in 2021.

However, “absence of evidence is not evidence of absence,” so future observations with low errors are encouraged to help confirm the rotational status of 1998 FW4.

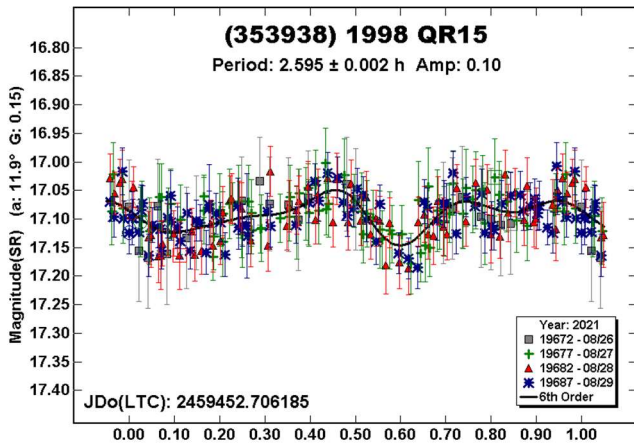
Using data from 2013 (Warner, 2014), we found a reliable solution of 17.38 h, but with an amplitude only half of what was suggested by the 2021 data (“2013” plot). We forced the latest data set to a period between 17-19 h and found one that is reasonably close to the earlier result when taking into account the gaps in the lightcurve.



(283460) 2001 PD1. Pravec et al. (2001web) found a period of 14.58 h, which is rated U = 2 in the LCDB. After the first few sessions, it seemed apparent that the correct period was much longer. It took several weeks of fighting weather and the moon to obtain what we consider a reliable period, despite the somewhat odd shape of the lightcurve. The period spectrum showed a very low likelihood that a period of about 14.5 h could be supported by the data.

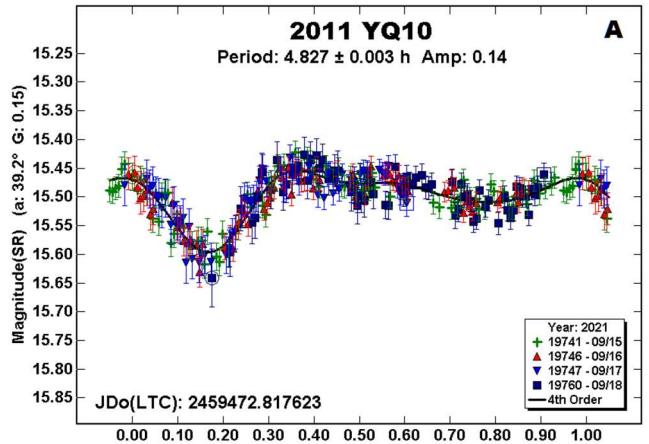
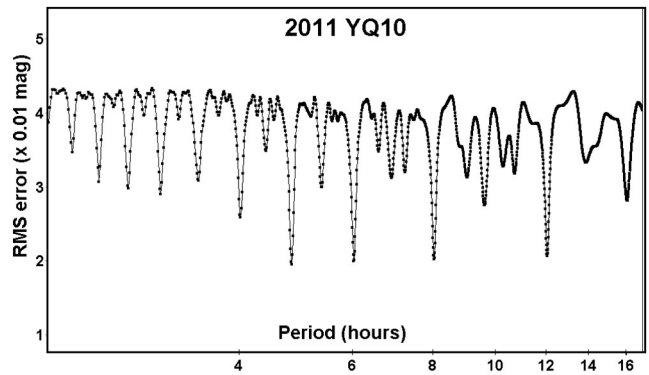


(353938) 1998 QR15. Pravec et al. (1998web) determined a rotation period of 2.454 hours, but this is rated U = 2- in the LCDB. Our data set allowed finding a more reliable period that was not too far removed from Pravec et al.

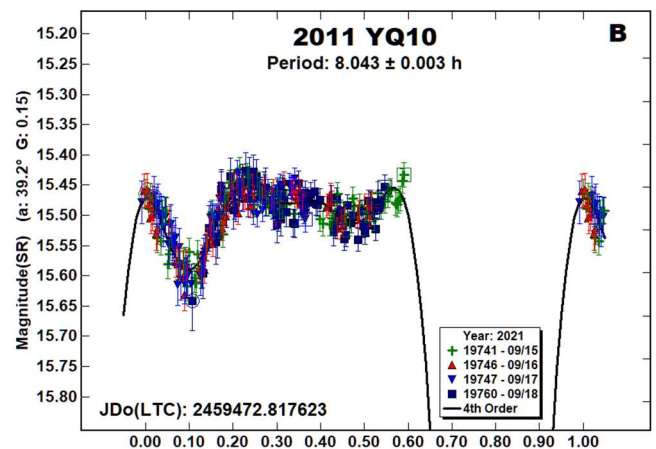


2011 YQ10. There were no previous results of any kind in the LCDB for this 0.5 km NEA. Some guidance from the past would have been helpful since our results are hardly conclusive.

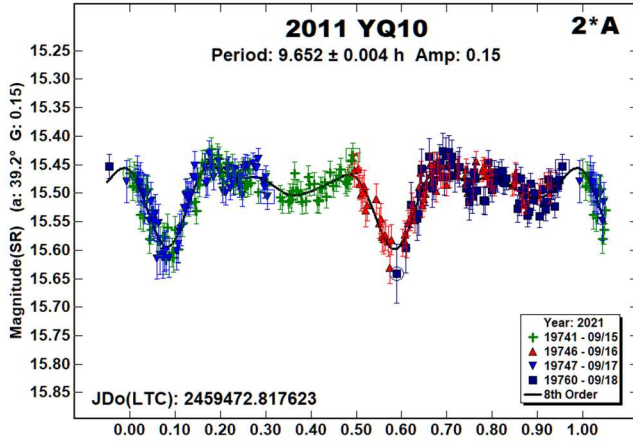
The period spectrum for the 2021 data shows four nearly equal solutions ranging from 5 to 12 h. The strongest one, at 4.827 h, produces an odd shape (“A”) but the observations were at phase angles near 40°, so shadowing may have come into play.



When assuming an alternate solution near 8.0 h, the Fourier curve reached unreasonable values (“B”). We clipped the curve, reduced the magnitude range, so that the data could still be seen to have a shape. For that solution to be given consideration, a minimum should be seen near 0.6 rotation phase. The data don’t cover that point, but those just before suggest but don’t confirm that that minimum would not exist even with more data.

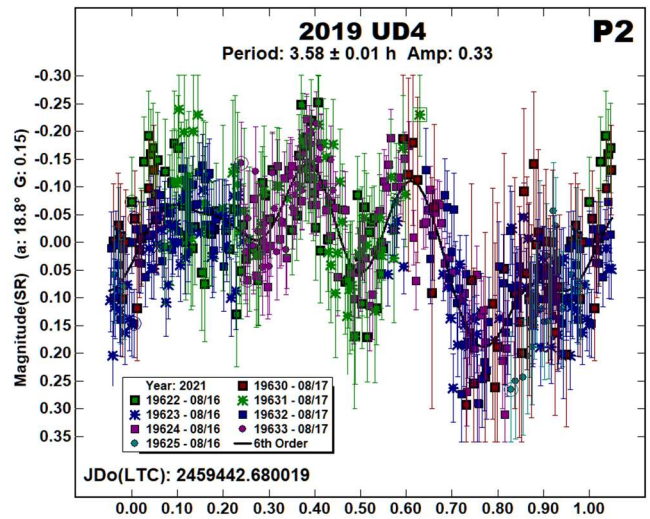
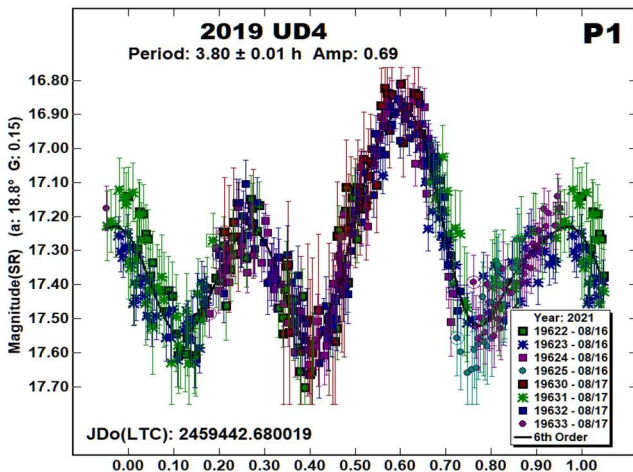
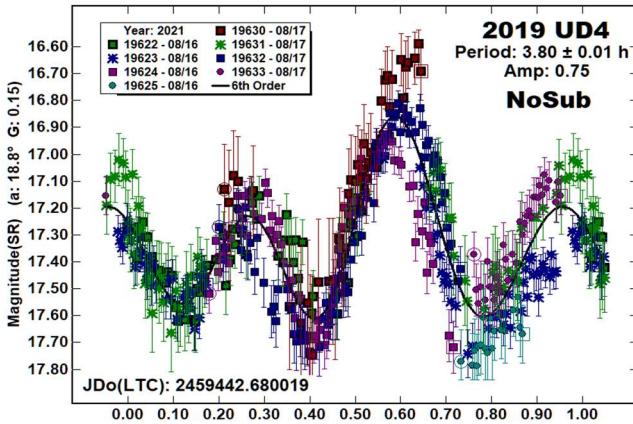


Plotting to the double-period of “A” (“2\*A”, 9.652 h) produced an intriguing lightcurve suggestive of a short period binary asteroid. However, the halves are identical in a split-halves plot (the second half superimposed on the first half). Such symmetry is unlikely. Even so, a search for a requisite short period due to the rotation of the primary or the satellite found nothing but a low-amplitude (flat) result. This further confirmed the unlikely symmetry.

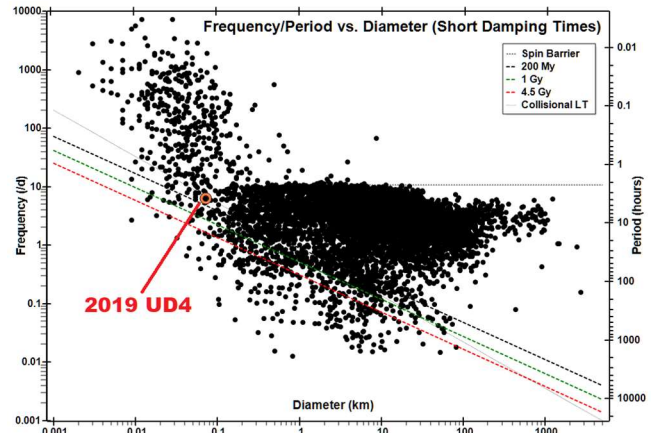


We adopt the period of 4.827 h as the best solution. We would suggest additional observations to confirm or refute that period but the 2021 apparition was the only one from 1995-2050 with  $V < 16$  and the brightest it will be through 2050 is  $V \sim 19.4$  in 2031.

**2019 UD4.** These appear to be the first results for this 70 m asteroid, which we suspect is in a tumbling state.



The “NoSub” plot, meaning a single-period solution, shows just enough deviations outside the noise to prompt a dual-period search. After several iterations, we found a second period of 3.80 h that, when subtracted from the raw data, produced a clean result of 3.80 h (“P1”). The lightcurve for 3.58 h (“P2”) is multimodal and very noisy, which is not unusual given that *MPO Canopus* does not implement an algorithm that properly analyzes tumbling asteroids.



If tumbling, there’s a good chance that one of true periods, precession or rotation, matches our 3.80 h, or that our result (taken as a frequency) is an integral fraction/multiple of the true period. The other period remains unresolved.

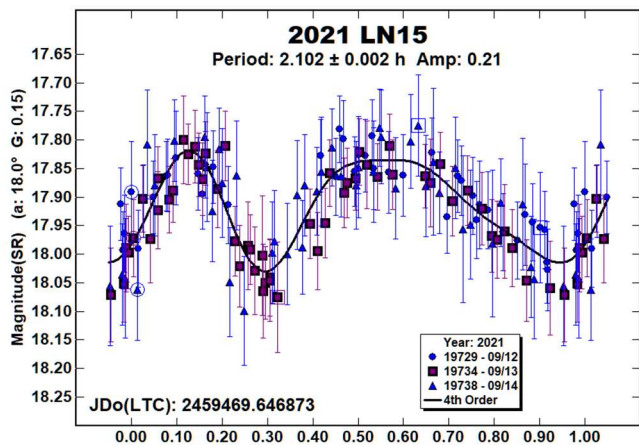
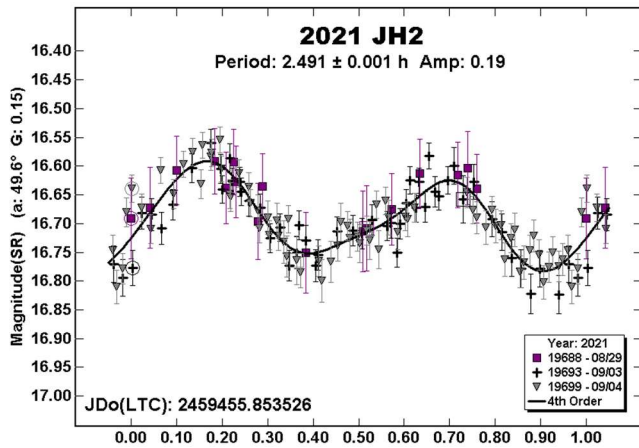
The LCDB frequency-diameter plot shows the asteroid’s location. While above the three tumbling damping lines (suggesting no tumbling), such small asteroids are much more likely to be involved in collisions that have a significant impact on their rotational characteristics.

**2021 JH2, 2021 LN15.** There were no previous results in the LCDB for either of these NEAs. 2021 JH2 has an estimated diameter of 400 m while the estimated diameter for 2021 LN15 is about 300 m. Referring to the frequency-diameter plot under 2019 UD4, they are both near that asteroid’s location. Despite that, there were no signs of tumbling in either data set, or at least none that came close to or above the noise level.

Number	Name	2021 mm/dd	Phase	$L_{PAB}$	$B_{PAB}$	Period(h)	P.E.	Amp	A.E.
1943	Anteros	08/06–08/14	34.8, 30.0	348	16	2.8682	0.0003	0.11	0.01
7341	1991 VK	09/27–10/01	11.7, 11.0	11	10	4.211	0.001	0.24	0.02
7822	1991 CS	08/22–08/23	78.6, 79.4	17	-4	2.388	0.002	0.37	0.04
32906	1994 RH	08/18–08/21	22.0, 20.9	353	6	9.93	0.03	0.27	0.03
138404	2000 HA24	09/03–09/05	59.2, 61.5	21	6	3.911	0.003	0.37	0.03
152664	1998 FW4	09/16–09/18	49.6, 56.2	27	2	17.9	0.2	0.62	0.05
283460	2001 PD1	09/12–10/01	23.1, 32.3	344	16	58.98	0.04	0.38	0.04
353938	1998 QR15	08/26–08/29	*11.9, 11.9	341	7	2.595	0.002	0.10	0.02
	2011 YQ10	09/15–09/18	39.1, 42.2	14	-13	4.827	0.002	0.14	0.01
	2019 UD4	08/16–08/17	19.0, 21.9	326	11	<sup>T</sup> 3.80	0.01	0.69	0.01
						3.58	0.01	0.33	0.04
	2021 JH2	08/29–09/04	49.7, 42.2	6	-7	2.491	0.001	0.19	0.02
	2021 LN15	09/12–09/14	18.0, 18.9	354	12	2.102	0.002	0.21	0.03

Table II. Observing circumstances and analysis results. <sup>T</sup>Tumbling asteroid. The phase angle ( $\alpha$ ) is given at the start and end of each date range. If there is an asterisk before the first phase value, the phase angle reached a maximum or minimum during the period.  $L_{PAB}$  and  $B_{PAB}$  are, respectively the average phase angle bisector longitude and latitude (see Harris et al., 1984).

Our calculations show that 2021 JH2 will be  $V \sim 19$  in 2037 and 2021 LN15 will be  $V \sim 19.4$  in 2038. Other than those apparitions, the two will be well below  $V = 20$  through 2050.



Acknowledgements

Funding work on the asteroid lightcurve database (Warner et al., 2009) and ALCDEF database (*alcdef.org*) were supported in part by NASA grant 80NSSC18K0851. The authors gratefully acknowledge Shoemaker NEO Grants from the Planetary Society (2007, 2013). These were used to purchase some of the telescopes and CCD cameras used in this research. This work includes data from the Asteroid Terrestrial-impact Last Alert System (ATLAS) project. ATLAS is primarily funded to search for near earth

asteroids through NASA grants NN12AR55G, 80NSSC18K0284, and 80NSSC18K1575; byproducts of the NEO search include images and catalogs from the survey area. The ATLAS science products have been made possible through the contributions of the University of Hawaii Institute for Astronomy, the Queen's University Belfast, the Space Telescope Science Institute, and the South African Astronomical Observatory. This paper made use of the services provided by the SAO/NASA Astrophysics Data System, which is operated by the Smithsonian Astrophysical Observatory under NASA Cooperative Agreement 80NSSC211M0056.

References

References from web sites should be considered transitory, unless from an agency with a long lifetime expectancy. Sites run by private individuals, even if on an institutional web site, do not necessarily fall into this category.

Behrend, R. (2016web). Observatoire de Geneve web site. [http://obswww.unige.ch/~behrend/page\\_cou.html](http://obswww.unige.ch/~behrend/page_cou.html)

Harris, A.W.; Young, J.W.; Scaltriti, F.; Zappala, V. (1984). "Lightcurves and phase relations of the asteroids 82 Alkmene and 444 Ggyptis." *Icarus* **57**, 251-258.

Harris, A.W.; Pravec, P.; Galad, A.; Skiff, B.A.; Warner, B.D.; Vilagi, J.; Gajdos, S.; Carbognani, A.; Hornoch, K.; Kusnirak, P.; Cooney, W.R.; Gross, J.; Terrell, D.; Higgins, D.; Bowell, E.; Koehn, B.W. (2014). "On the maximum amplitude of harmonics on an asteroid lightcurve." *Icarus* **235**, 55-59.

Hayes-Gehrke, M.; de La Beaujardiere, J.; Kotgire, P.; Piel, A.; King, M.; Tran, K.; Kenyon, J.; Hagen, D.; Fulling, L.; Walters, J.; Acuna, A. (2017). "Lightcurve Analysis for Near-Earth Asteroid (138404) 2000 HA24." *Minor Planet Bull.* **44**, 310.

Klinglesmith III, D.A.; Hendrickx, S.; Madden, K.; Montgomery, S. (2016). "Asteroid Lightcurves from Estcom Observatory." *Minor Planet Bull.* **43**, 234-239.

Monteiro, F.; Arcoverde, P.; Medeiros, H.; Rondon, E.; Souza, R.; Rodrigues, T.; Lazzaro, D. (2018). "Rotational Period Determination for 12 Near-Earth Asteroids." *Minor Planet Bull.* **45**, 221-224.

Pravec, P.; Wolf, M.; Sarounova, L. (1998web; 2001web; 2019web). <http://www.asu.cas.cz/~ppravec/neo.htm>

Pravec, P.; Wolf, M.; Sarounova, L. (1998). "Lightcurves of 26 Near-Earth Asteroids." *Icarus* **136**, 124-153.

Pravec, P.; Harris, A.W.; Scheirich, P.; Kušnirák, P.; Šarounová, L.; Hergenrother, C.W.; Mottola, S.; Hicks, M.D.; Masi, G.; Krugly, Yu.N.; Shevchenko, V.G.; Nolan, M.C.; Howell, E.S.; Kaasalainen, M.; Galád, A.; Brown, P.; Degraff, D.R.; Lambert, J.V.; Cooney, W.R.; Foglia, S. (2005). "Tumbling asteroids." *Icarus* **173**, 108-131.

Pravec, P.; Scheirich, P.; Durech, J.; Pollock, J.; Kusnirak, P.; Hornoch, K.; Galad, A.; Vokrouhlicky, D.; Harris, A.W.; Jehin, E.; Manfroid, J.; Opitom, C.; Gillon, M.; Colas, F.; Oey, J.; Vrstil, J.; Reichart, D.; Ivarsen, K.; Haislip, J.; LaCluyze, A. (2014). "The tumbling state of (99942) Apophis." *Icarus* **233**, 48-60.

Skiff, B.A. (2012web). Posting on CALL web site.  
<https://minorplanet.info/call.html>

Tonry, J.L.; Denneau, L.; Flewelling, H.; Heinze, A.N.; Onken, C.A.; Smartt, S.J.; Stalder, B.; Weiland, H.J.; Wolf, C. (2018). "The ATLAS All-Sky Stellar Reference Catalog." *Ap. J.* **867**, A105.

Warner, B.D.; Harris, A.W.; Pravec, P. (2009). "The Asteroid Lightcurve Database." *Icarus* **202**, 134-146. Updated 2021 June.  
<http://www.minorplanet.info/lightcurvedatabase.html>

Warner, B.D. (2014). "Near-Earth Asteroid Lightcurve Analysis at CS3-Palmer Divide Station: 2013 June-September." *Minor Planet Bull.* **41**, 41-47.

Warner, B.D. (2016a). "Near-Earth Asteroid Lightcurve Analysis at CS3-Palmer Divide Station: 2015 June-September." *Minor Planet Bull.* **43**, 66-79.

Warner, B.D. (2016b). "Near-Earth Asteroid Lightcurve Analysis at CS3-Palmer Divide Station: 2016 January-April." *Minor Planet Bull.* **43**, 240-250.

Warner, B.D. (2017). "Near-Earth Asteroid Lightcurve Analysis at CS3-Palmer Divide Station: 2016 July-September." *Minor Planet Bull.* **44**, 22-36.

Warner, B.D.; Benishek, V.; Harris, A.W. (2017). "1943 Anteros: A Possible Near-Earth Binary Asteroid." *Minor Planet Bull.* **44**, 186-188.

Warner, B.D.; Stephens, R.D. (2019). "Near-Earth Asteroid Lightcurve Analysis at the Center for Solar System Studies: 2018 September-December." *Minor Planet Bull.* **46**, 144-152.

Zappala, V.; Cellini, A.; Barucci, A.M.; Fulchignoni, M.; Lupishko, D.E. (1990). "An analysis of the amplitude-phase relationship among asteroids." *Astron. Astrophys.* **231**, 548-560.

## ON CONFIRMED AND SUSPECTED BINARY ASTEROIDS OBSERVED AT THE CENTER FOR SOLAR SYSTEM STUDIES

Brian D. Warner  
Center for Solar System Studies / MoreData!  
446 Sycamore Ave.  
Eaton, CO 80615 USA  
brian@MinorPlanetObserver.com

Robert D. Stephens  
Center for Solar System Studies / MoreData!  
Rancho Cucamonga, CA 91730

(Received: 2021 October 12)

Analysis of CCD photometric observations made at the Center for Solar System Studies from 2021 August through September suggested or confirmed that several asteroids were binary. The candidates are 5715 Ables, 7087 Lewotsky, 7173 Sepkoski, (16960) 1998 QS52, (68063) 2000 YJ66, (143649) 2003 QQ47, (159857) 2004 LJ1, and (326732) 2003 HB6,

Data from CCD photometric observations made at the Center for Solar System Studies in 2021 August through September were used to look for indications of an asteroid being binary. Confirmed binaries are those that show mutual events (occultations/eclipses) while suspected binaries include those with two periods, no obvious mutual events, and periods consistent with binary asteroids (Pravec et al., 2018, Figure 14).

Up to nine telescopes can be used but seven is more common. All the cameras use CCD chips from the KAF blue-enhanced family and so have essentially the same response. The pixel scales ranged from 1.24-1.60 arcsec/pixel.

Telescopes	Cameras
0.30-m f/10 Schmidt-Cass	FLI Microline 1001E
0.35-m f/9.1 Schmidt-Cass	FLI Proline 1001E
0.40-m f/10 Schmidt-Cass	SBIG STL-1001E
0.40-m f/10 Schmidt-Cass	
0.50-m f/8.1 Ritchey-Chrétien	

Table I. List of available telescopes and CCD cameras at CS3. The exact combination for each telescope/camera pair can vary due to maintenance or specific needs.

All lightcurve observations were unfiltered since a clear filter can cause a 0.1-0.3 mag loss. The exposure duration varied depending on the asteroid's brightness and sky motion. Guiding on a field star sometimes resulted in a trailed image for the asteroid.

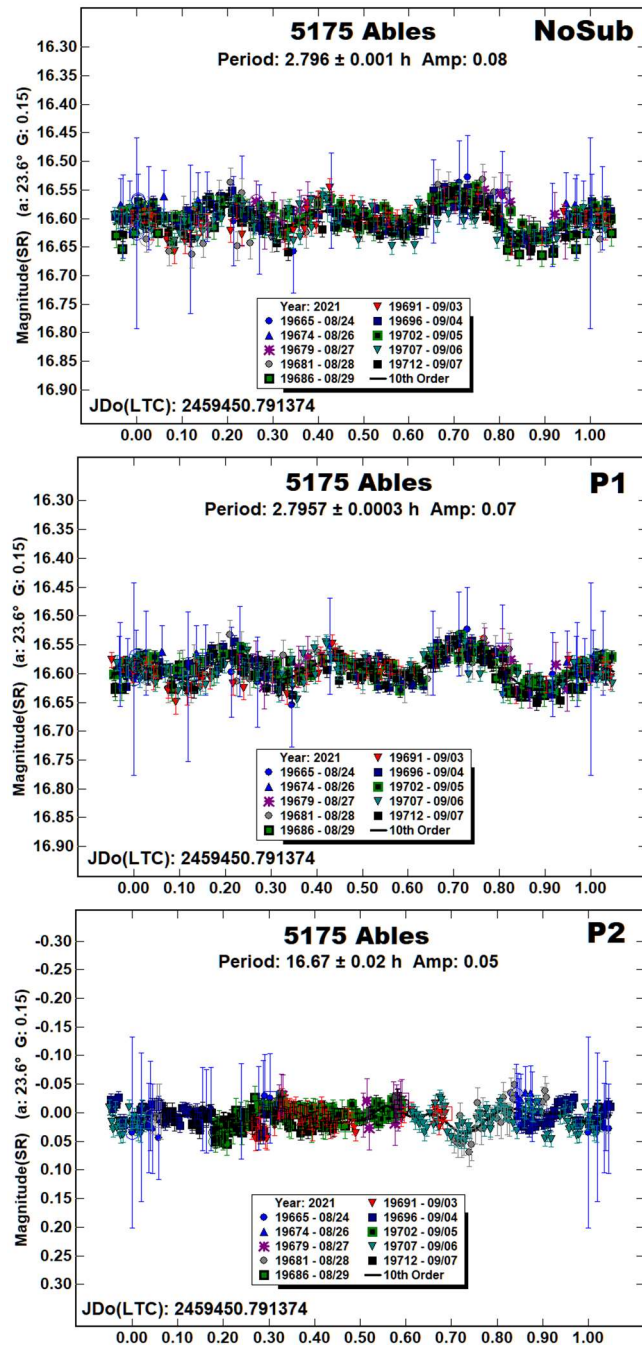
Measurements were made using *MPO Canopus*. The Comp Star Selector utility in *MPO Canopus* found up to five comparison stars of near solar-color for differential photometry. To reduce the number of adjusted nightly zero points and their amounts, the analysis of the 2021 data used the ATLAS catalog  $r'$  (SR) magnitudes (Tonry et al., 2018). The rare zero-point adjustments  $\geq \pm 0.03$  mag may be related in part to using unfiltered observations, poor centroiding of the reference stars, not correcting for second-order extinction, or selecting a star that is an unresolved pair.

The Y-axis values are ATLAS SR "sky" (catalog) magnitudes. The two values in the parentheses are the phase angle ( $\alpha$ ) and the value of  $G$  used to normalize the data to the comparison stars used in the earliest session. This, in effect, corrected all the observations to

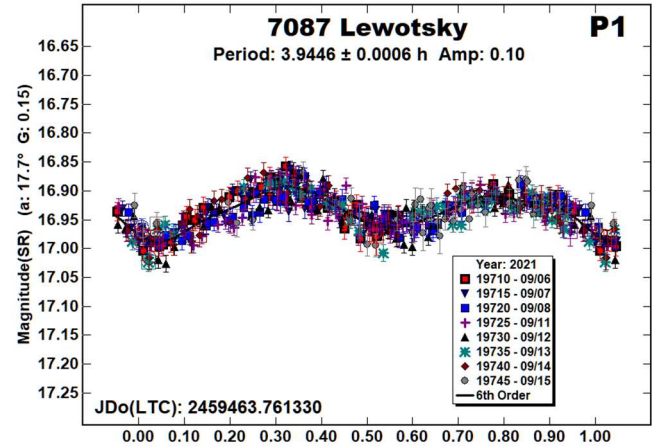
seem to have been made at a single fixed date/time and phase angle, leaving any variations due only to the asteroid's rotation and/or albedo changes. The X-axis shows rotational phase from  $-0.05$  to  $1.05$ . If the plot includes the amplitude, e.g., "Amp: 0.65", this is the amplitude of the Fourier model curve and *not necessarily the adopted amplitude for the lightcurve*.

"LCDB" substitutes for "Warner et al. (2009)" from here on.

5175 Ables. Warner (2014b) reported this as a suspected binary with a secondary period of 10.4 h but no mutual events to confirm a satellite. That solution was rejected in a follow-up analysis (Warner, 2019). The data from 2021 show some signs of mutual events and period of 16.67 h, but the events are near the noise level. Assuming there is a satellite, the estimated primary-to-satellite diameter ratio is  $D_s/D_p \geq 0.16 \pm 0.03$ .

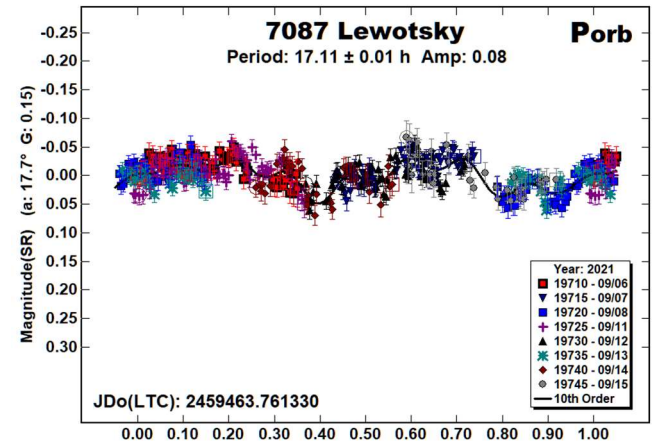
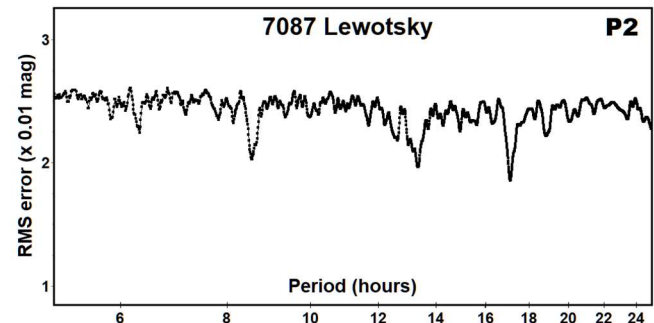


7087 Lewotsky. Being a Hungaria asteroid, which were targets of interest for many years at CS3, we've observed Lewotsky several times in the past (see Warner, 2014a, and references therein), all with final results of  $P = 3.941 \pm 0.005$  h, i.e., without indications of a satellite. The 2021 data finally showed what appear to be mutual events but with unusual shapes, not the typical smooth up/down change in the overall lightcurve.



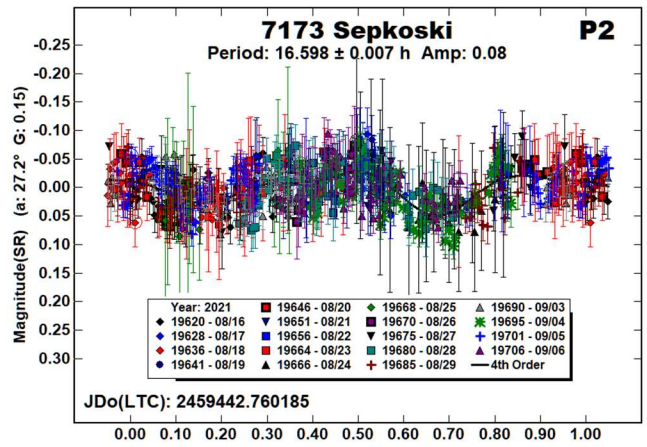
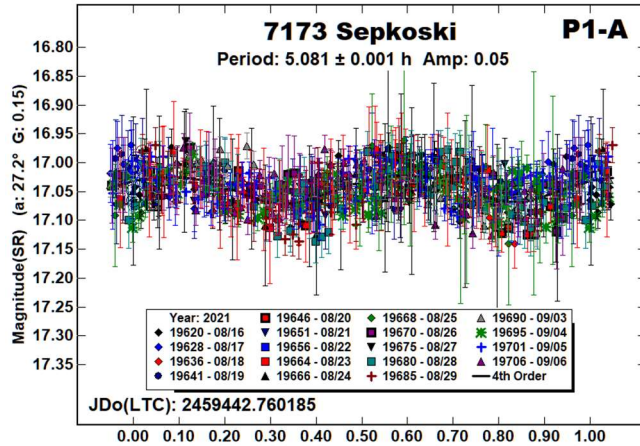
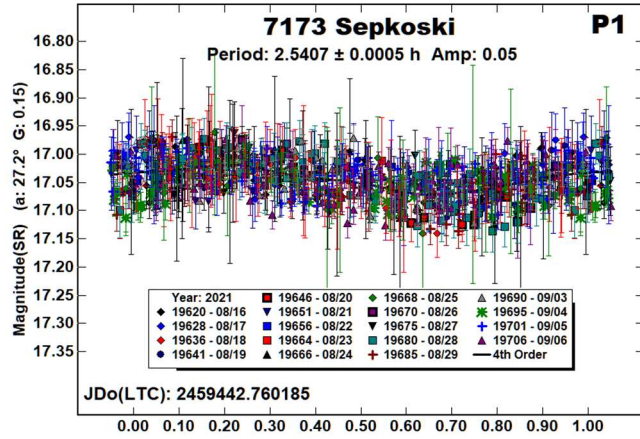
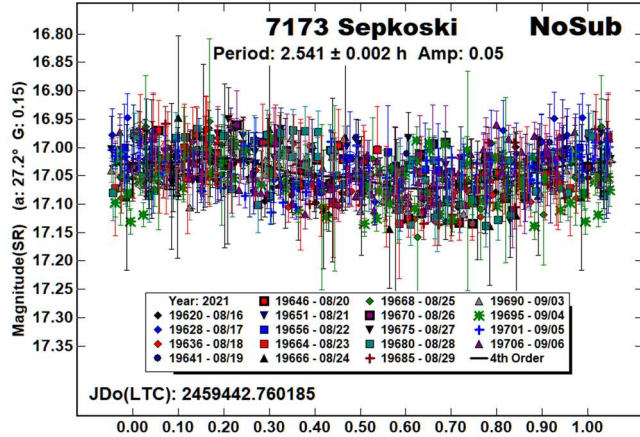
The period spectrum for the secondary period shows the adopted solution to be among a small group of candidates, all being nearly commensurate with an Earth day. Trying to fit the data to those other solutions produced unlikely lightcurves.

Given the odd-shape of the presumed events, it is difficult to give more than a rough estimate of the diameter ratio  $D_s/D_p$ . Assuming the shallower event is 0.06 mag deep, this gives  $D_s/D_p 0.23 \pm 0.04$ .

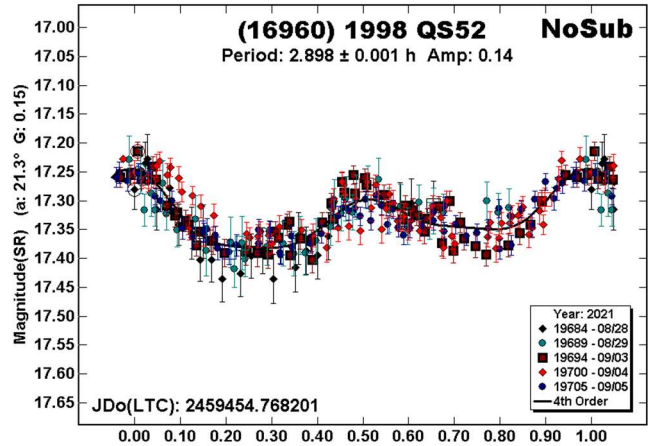


7173 Sepkoski. This asteroid was suspected of being binary using observations from 2013 (Warner, 2014a) but a secondary period could not be established. The 2021 data, hampered by a high noise level, provided a slightly better picture.

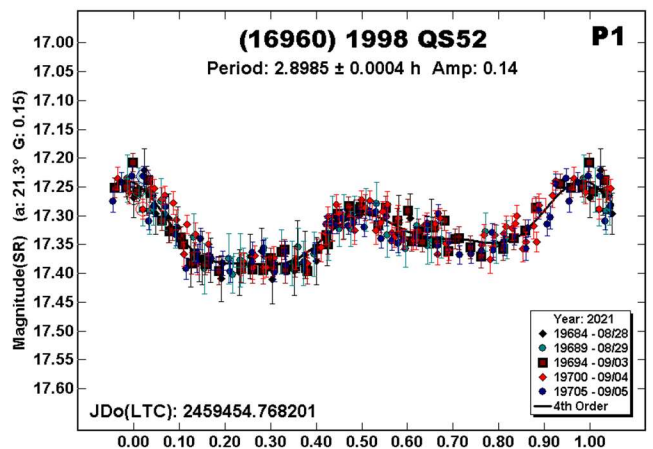
The earlier results had a primary period of about 2.5 h. Forcing to near that solution produced a monomodal lightcurve, which is not unexpected (see Harris et al., 2014). The bimodal lightcurve at the doubled-period of 5.081 h is very symmetrical but, because of the noise, cannot be formally excluded. It is worth noting that the 2021 result of 2.5407 h is 0.04 h longer than previous results, the difference being well beyond the reported errors. It may be that including a better secondary period altered the primary solution. The estimated satellite-to-primary diameter ratio is  $0.19 \pm 0.03$ .

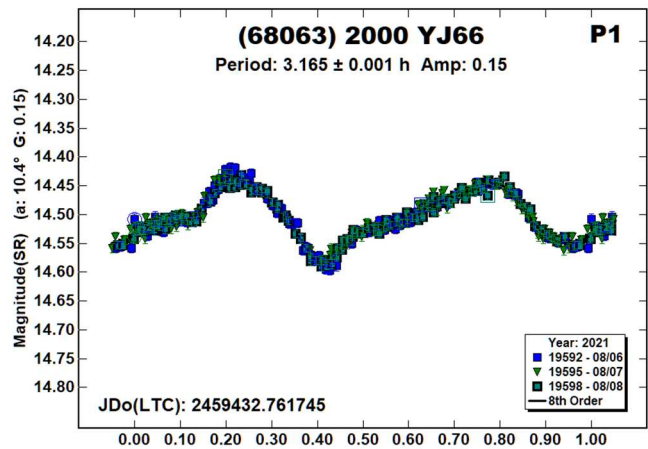
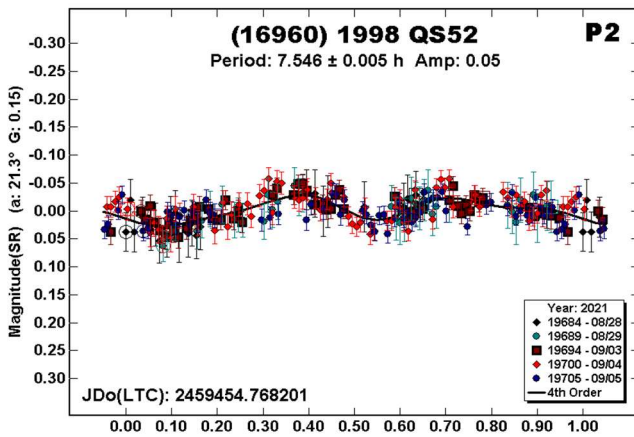


(16960) 1998 QS52. Warner (2009) found a period of 5.789 h for this near-Earth asteroid. Skiff (2019) reported 5.8 h and, more notable, an amplitude of  $1.5 \pm 0.2$  mag. Our data from 2021 showed a lightcurve amplitude that matched the results found by Warner.



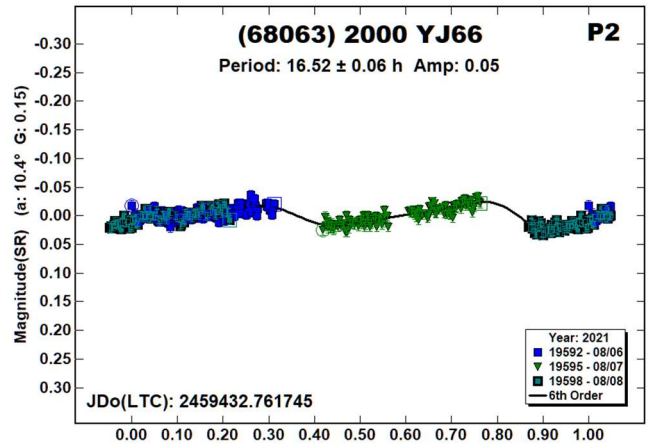
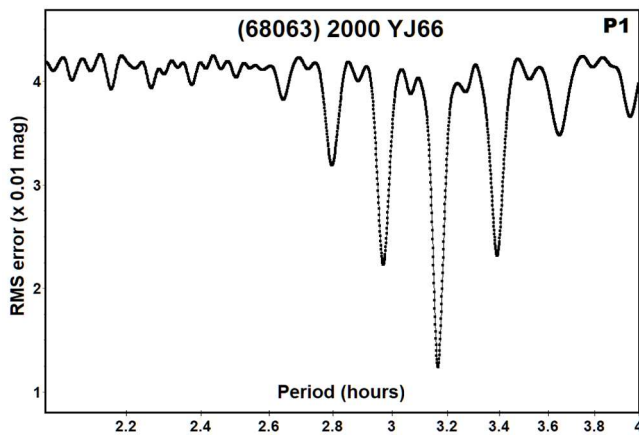
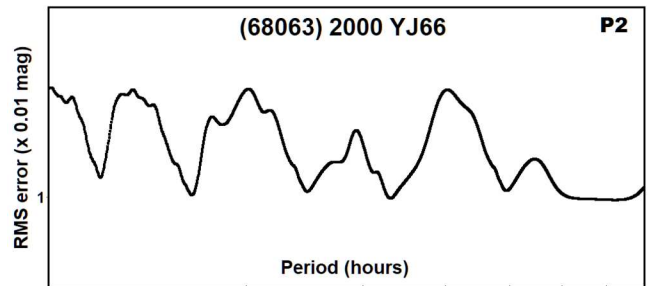
Neither observer reported signs of a satellite in those original results. Our 2021 data indicated a secondary period (NoSub plot) and so we ran a dual-period search in *MPO Canopus*. The end result was a secondary period of 7.548 h. If the true orbital period of a satellite, it would be among the shorter periods found in the LCDB for a typical small binary asteroid. Forcing the data to a more typical solution of the double-period (15.08 h) produced what appeared to be four evenly spaced mutual events. This was rejected.





(68063) 2000 YJ66. Warner et al. (2015) reported this to be a binary asteroid with a primary period of 2.11 h and orbital period of 15.69 h. The secondary lightcurve had an overall amplitude of 0.13 mag. Our most recent data gave much different results.

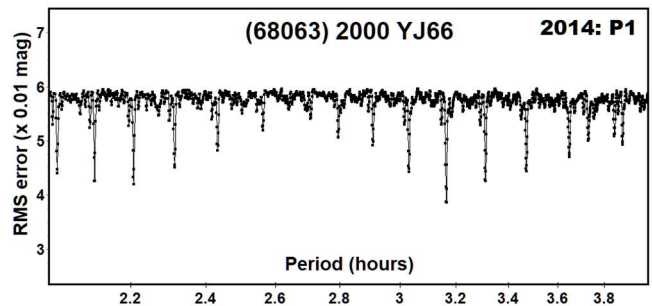
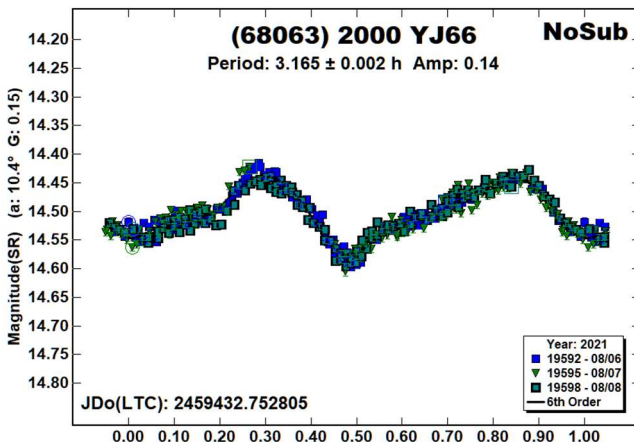
First was that a period of 2.11 h was not possible. The period spectrum shows only the slightest hint of a period near that value and is dominated by one of about 3.15 h.



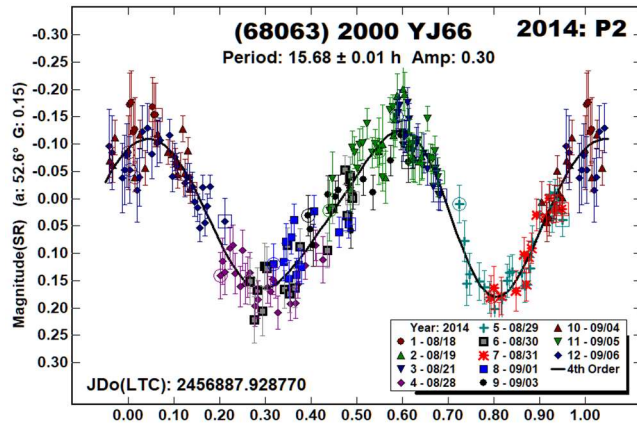
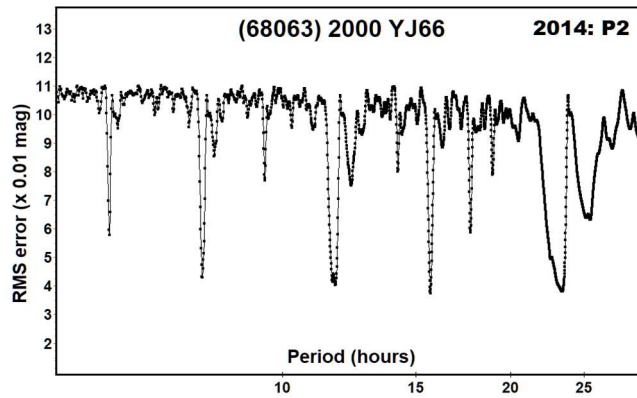
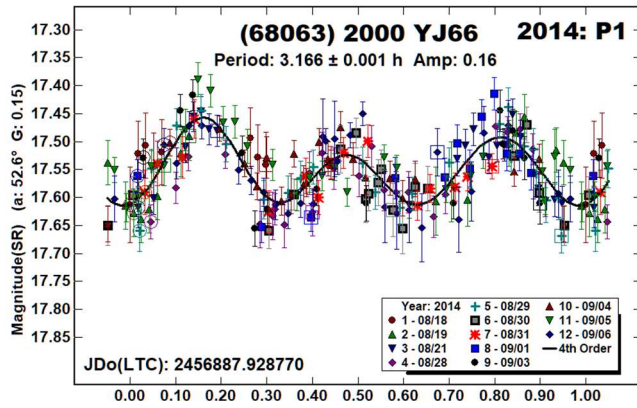
Looking at the single period solution lightcurve (NoSub), there seems little evidence of a secondary period. Since this was reported to be a binary, we ran the dual-period search of *MPO Canopus* to confirm whether or not there might be a second period present. The result is a highly-ambiguous set of solutions, all nearly commensurate with an Earth day. The one closest to that from Warner et al. (2015) was the only bimodal solution.

2014 Revisited

Given the new results, we returned to the data from 2014. Part of the revised analysis was to change the comparison star magnitudes to the SR (Sloan r') from the ATLAS catalog (Tonry et al, 2018). This removed almost all zero-point adjustments that might have altered the solution.

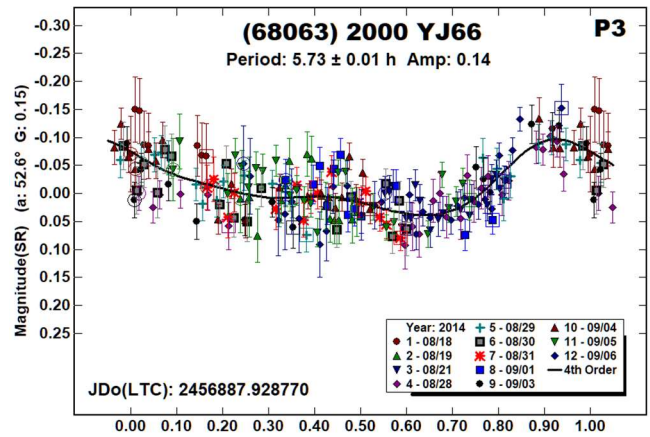


The period spectrum still shows a solution near 2.11 h being viable but one at 3.166 h a little more likely (the two periods have an almost integral ratio of 3:2). The trimodal lightcurve for the longer period is not unexpected (Harris et al., 2014) given the low amplitude. On the other hand, the large phase angle may have had an effect on the lightcurve shape.



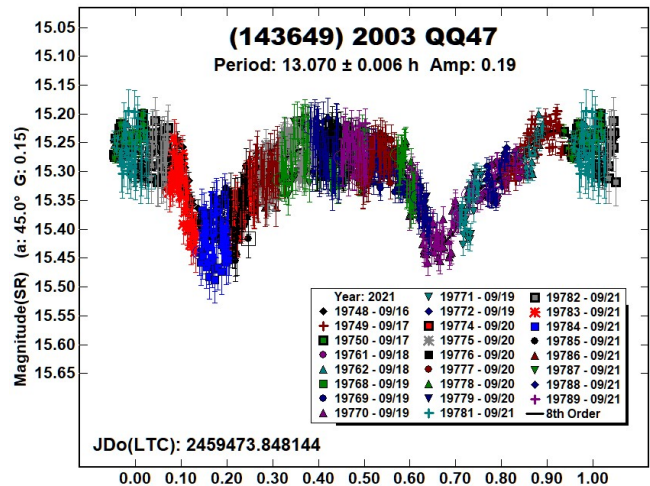
Subtracting the revised primary period from the data found a large amplitude (0.30 mag) secondary period of 15.68 h, which is close to the one derived from the 2021 data. Given the large amplitude of the 2014 solution, we consider it to be the more likely.

There remains no small amount of uncertainty. The P1 and P2 plots from 2014 are not the result of subtracting a single period from the data. Instead, a third period of about 5.7 h with an amplitude of 0.14 mag was found and factored into the analysis.



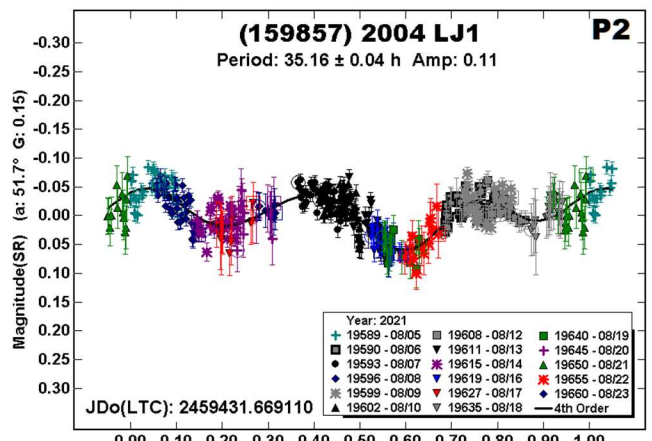
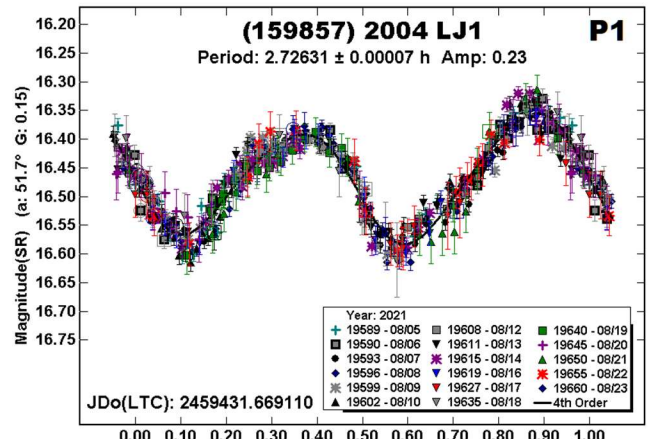
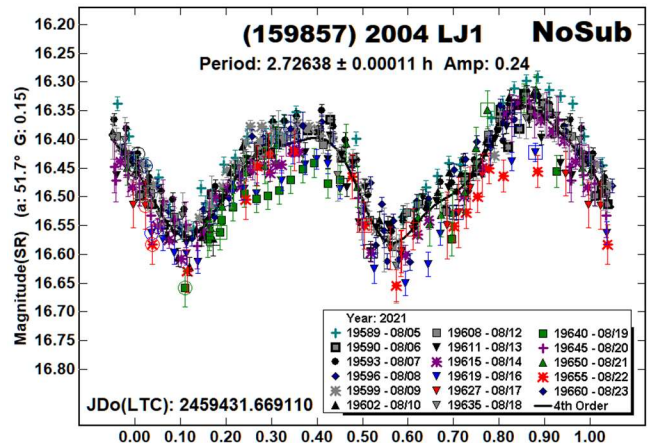
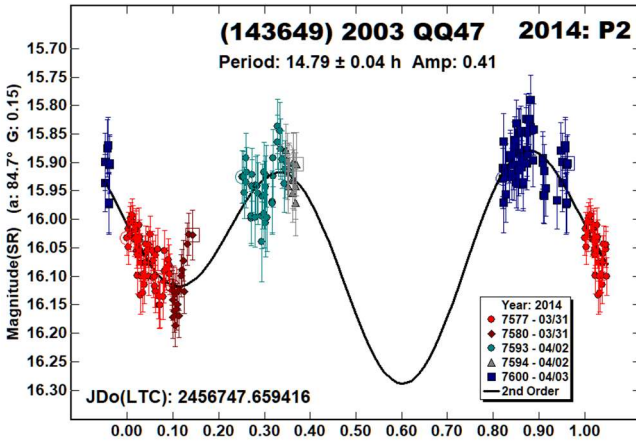
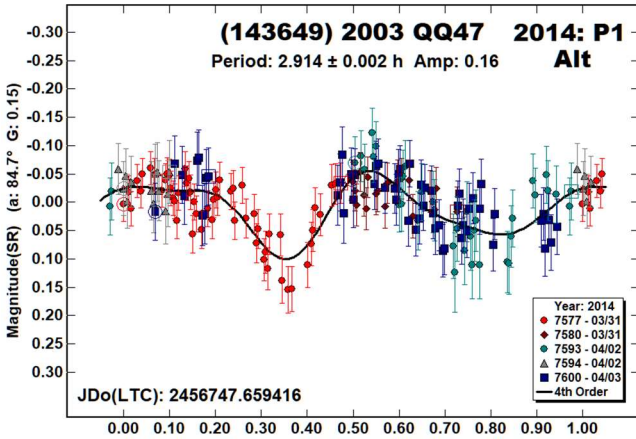
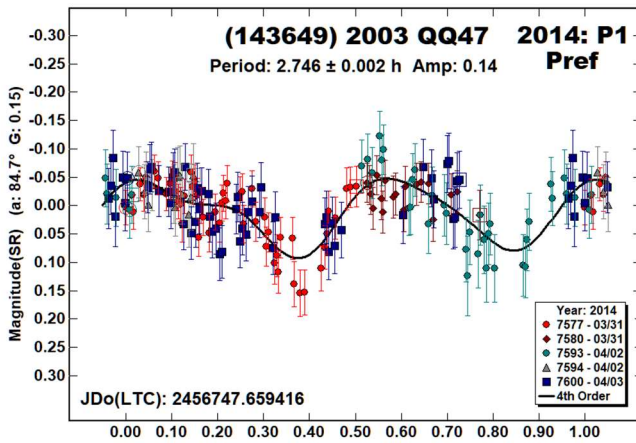
This period is close to being harmonically-related to the others and so may be an artifact of the Fourier analysis. We cannot give a plausible physical cause for the third period.

(143649) 2003 QQ47. The results from the data from 2021 thoroughly contradict our earlier findings (Warner, 2014c). The most recent data set produces a lightcurve that has all the signs of a highly-bifurcated body or, possibly, a binary with two similarly-sized bodies in a tight mutual orbit. There is no secondary period in this circumstance.



With such a definitive result, we returned to the data set obtained in 2014, which was considerably less dense and didn't cover as long a period. The best solution that could be obtained was a short period superimposed over a longer one. This is reminiscent of the *very wide binary* class (see Warner, 2016) but the 2021 data set dispels that possibility.

The raw data from 2014 clearly (or seemingly so) showed a long period. We could do only a second-order Fourier analysis because of the sparse data set and to avoid Fourier curves with amplitudes of hundreds to thousands of magnitudes. Once settling on a long period of 14.79 h, a search for the short primary period produced ambiguous results. The preference is for  $P_1 = 2.746$  h since it is more symmetrically shaped and is less of a *fit by exclusion*.



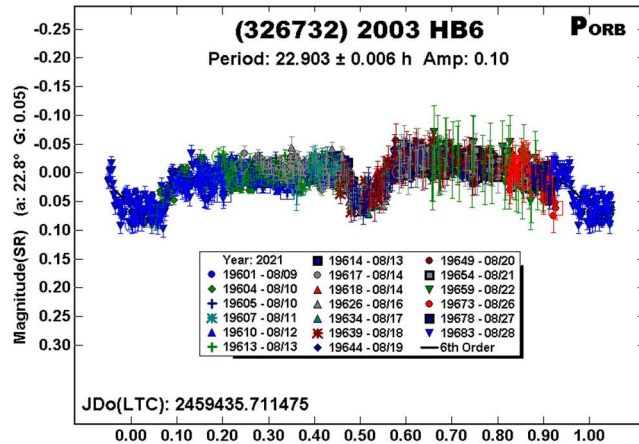
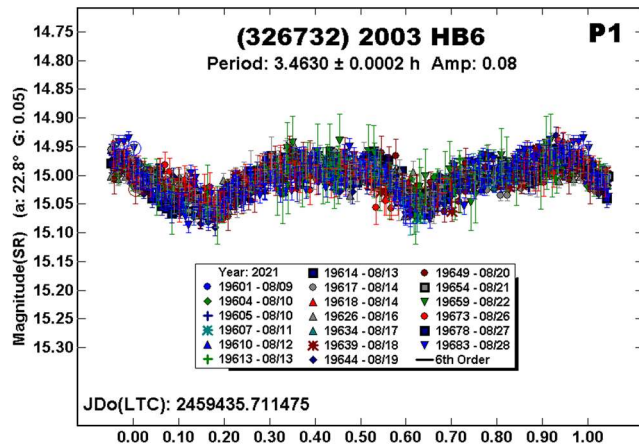
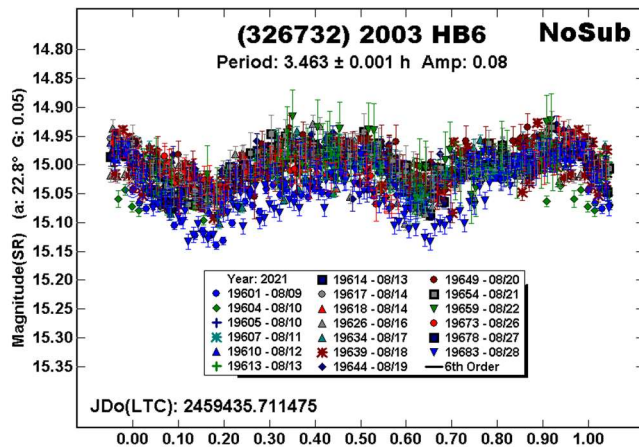
(159857) 2004 LJ1. Previous work on this NEA (Pravec et al., 2004web; Galad et al., 2005; and Warner (2015) produced periods between 2.661 and 2.7247 h. Those previous results did not include signs of the asteroid being a binary. Our 2021 data set seems to indicate otherwise.

The NoSub plot clearly shows deviations from a single period solution that are consistent with a satellite being present. The final dual-period search using *MPO Canopus* found a clean primary lightcurve with a period  $P_1 = 2.72631$  h. The secondary lightcurve ( $P_2 = 35.16$  h) is not ideal, but still leads to  $Ds/Dp \geq 0.22 \pm 0.02$ .

(326732) 2003 HB6. Our result from observations in 2012 (Warner, 2012) was  $P = 9.436$  h. This now seems highly unlikely even though Monteiro et al. (2018b) found a similar period.

The most recent data set, covering nearly 20 days in 2021 August, showed the usual signs of a secondary period. Dual-period analysis in *MPO Canopus* found  $P_1 = 3.4630$  h and  $P_{ORB} = 22.903$  h. Among all the targets in this work, this is the most secure solution.

The mutual events are about the same depth, 0.06 mag, with the one near orbital phase 0.0 coming close to being flat, which would imply a total eclipse/occultation. The estimated diameter ratio is  $D_s/D_p \geq 0.24 \pm 0.02$ . The secondary lightcurve shows a slight *bowing*. This indicates a modestly elongated satellite with its rotation period tidally-locked to its orbital period.



Acknowledgements

Funding work on the asteroid lightcurve database (Warner et al., 2009) and ALCDEF database (*alcdef.org*) were supported in part by NASA grant 80NSSC18K0851. The authors gratefully acknowledge Shoemaker NEO Grants from the Planetary Society (2007, 2013). These were used to purchase some of the telescopes and CCD cameras used in this research. This work includes data from the Asteroid Terrestrial-impact Last Alert System (ATLAS) project. ATLAS is primarily funded to search for near earth asteroids through NASA grants NN12AR55G, 80NSSC18K0284, and 80NSSC18K1575; byproducts of the NEO search include images and catalogs from the survey area. The ATLAS science products have been made possible through the contributions of the University of Hawaii Institute for Astronomy, the Queen's University Belfast, the Space Telescope Science Institute, and the South African Astronomical Observatory. This paper made use of the services provided by the SAO/NASA Astrophysics Data System, which is operated by the Smithsonian Astrophysical Observatory under NASA Cooperative Agreement 80NSSC211M0056.

References

References from web sites should be considered transitory, unless from an agency with a long lifetime expectancy. Sites run by private individuals, even if on an institutional web site, do not necessarily fall into this category.

Galád, A.; Pravec, P.; Kušnirák, P.; Gajdoš, Š.; Kornoš, L.; Világi, J. (2005). "Joint Lightcurve Observations of 10 Near-Earth Asteroids from Modra and ONDŘEJOV." *Earth, Moon, and Planets* **97**, 147-163.

Harris, A.W.; Young, J.W.; Scaltriti, F.; Zappala, V. (1984). "Lightcurves and phase relations of the asteroids 82 Alkmene and 444 Ggyptis." *Icarus* **57**, 251-258.

Harris, A.W.; Pravec, P.; Galad, A.; Skiff, B.A.; Warner, B.D.; Vilagi, J.; Gajdos, S.; Carbognani, A.; Hornoch, K.; Kusnirak, P.; Cooney, W.R.; Gross, J.; Terrell, D.; Higgins, D.; Bowell, E.; Koehn, B.W. (2014). "On the maximum amplitude of harmonics on an asteroid lightcurve." *Icarus* **235**, 55-59.

Monteiro, F.; Silva, J.S.; Lazzaro, D.; Arcoverde, P.; Medeiros, H.; Rodrigues, T.; Souza, R. (2018). "Rotational properties of near-earth objects obtained by the IMPACTON project." *Plan. Space Sci.* **164**, 54-74.

Pravec, P.; Wolf, M.; Sarounova, L. (2004web). <http://www.asu.cas.cz/~ppravec/neo.htm>

Pravec, P.; Fatka, P.; Vokrouhlicky, D.; Scheeres, D.J.; Kusnirak, P.; Hornoch, K.; Galad, A.; Vrstil, J.; Pray, D.P.; Krugly, Yu.N.; Gaftonyuk, N.M.; Inasaridze, R.Ya.; Ayvazian, V.R.; Kvaratskhelia, O.I.; Zhuzhunadze, V.T.; Husarik, M.; Cooney, W.R.; Gross, J.; Terrell, D.; Világi, J.; Kornos, L.; Gajdos, S.; Burkhonov, O.; Ehgamberdiev, Sh.A.; Donchev, Z.; Borisov, G.; Bonev, T.; Rumyantsev, V.V.; Molotov, I.E. (2018). "Asteroid clusters similar to asteroid pairs." *Icarus* **304**, 110-126.

Skiff, B.A.; McLelland, K.P.; Sanborn, J.J.; Pravec, P.; Koehn, B.W. (2019). "Lowell Observatory Near-Earth Asteroid Photometric Survey (NEAPS): Paper 3." *Minor Planet Bull.* **46**, 238-265.

Tonry, J.L.; Denneau, L.; Flewelling, H.; Heinze, A.N.; Onken, C.A.; Smartt, S.J.; Stalder, B.; Weiland, H.J.; Wolf, C. (2018). "The ATLAS All-Sky Stellar Reference Catalog." *Ap. J.* **867**, A105.

Warner, B.D. (2009). "Asteroid Lightcurve Analysis at the Palmer Divide Observatory: 2008 May - September." *Minor Planet Bull.* **36**, 7-13.

Warner, B.D.; Harris, A.W.; Pravec, P. (2009). "The Asteroid Lightcurve Database." *Icarus* **202**, 134-146. Updated 2021 May. <http://www.minorplanet.info/lightcurvedatabase.html>

Warner, B.D. (2012). "Asteroid Lightcurve Analysis at the Palmer Divide Observatory: 2012 March - June." *Minor Planet Bull.* **39**, 245-252.

Warner, B.D. (2014a). "Asteroid Lightcurve Analysis at CS3-Palmer Divide Station: 2013 September-December." *Minor Planet Bull.* **41**, 102-112.

Warner, B.D. (2014b). "Asteroid Lightcurve Analysis at CS3-Palmer Divide Station: 2014 January-March." *Minor Planet Bull.* **41**, 144-155.

Warner, B.D. (2014c). "Near-Earth Asteroid Lightcurve Analysis at CS3-Palmer Divide Station: 2014 March-June." *Minor Planet Bull.* **41**, 213-224.

Warner, B.D. (2015). "Near-Earth Asteroid Lightcurve Analysis at CS3-Palmer Divide Station: 2014 June-October." *Minor Planet Bull.* **42**, 41-53.

Warner, B.D.; Stephens, R.D.; Harris, A.W. (2015). "A Trio of Binary Asteroids." *Minor Planet Bull.* **42**, 31-34.

Warner, B.D. (2016). "Three Additional Candidates for the Group of Very Wide Binaries." *Minor Planet Bull.* **43**, 306-309.

Warner, B.D. (2019). "Asteroid Lightcurve Analysis at CS3-Palmer Divide Station: 2018 July-September." *Minor Planet Bull.* **46**, 46-51.

Number	Name	20yy mm/dd	Phase	$L_{PAB}$	$B_{PAB}$	Period(h)	P.E.	Amp	A.E.	Grp/Dr
5175	Ables	08/24-09/07	23.6,19.2	10	19	2.7957 16.67	0.0003 0.02	0.07 0.05	0.01 0.01	H
7087	Lewotsky	09/06-09/15	17.8,14.5	8	18	3.9446 17.11	0.0006 0.01	0.10 0.08	0.01 0.01	H
7173	Sepkoski	08/16-09/06	27.2,22.1	6	26	<sup>P</sup> 2.5407 5.081 16.598	0.0005 0.001 0.007	0.05 0.05 0.08	0.01 0.01 0.02	H
16960	1998 QS52	08/28-09/05	21.4,20.2	5	24	2.8985 7.546	0.0004 0.005	0.14 0.05	0.01 0.01	NEA
68063	2000 YJ66	08/06-08/08	10.4,9.4	323	2	3.165 16.52	0.002 0.06	0.14 0.05	0.01 0.01	NEA
68063	2000 YJ66	2014 08/18-09/06				3.166 15.68	0.001 0.01	0.16 0.30	0.02 0.03	
143649	2003 QQ47	09/16-09/21	45.2,25.9	17	-8	13.070	0.006	0.19	0.03	NEA
143649	2003 QQ47	2014 03/31-04/03				<sup>P</sup> 2.746 2.914 14.79	0.002 0.002 0.04	0.14 0.16 0.41	0.02 0.03 0.05	
159857	2004 LJ1	08/05-08/23	51.8,64.9	286	45	2.72631 35.16	0.00007 0.04	0.23 0.11	0.02 0.01	NEA
326732	2003 HB6	08/09-08/28	22.8,10.9	335	6	3.4630 22.903	0.0002 0.006	0.08 0.10	0.01 0.01	NEA

Table II. Observing circumstances. <sup>P</sup>Preferred period of ambiguous solution for the primary. The first line gives the primary period for the system. The second line gives the secondary period. The phase angle ( $\alpha$ ) is given at the start and end of each date range. An asterisk indicates that the phase angle reached a maximum or minimum during the period.  $L_{PAB}$  and  $B_{PAB}$  are, respectively the average phase angle bisector longitude and latitude (see Harris et al., 1984). For the Grp/Dr column, the first line gives the group/family based on Warner et al. (2009). FLOR Flora; HIL Hilda; MB-I Inner main-belt; NEA: Near-Earth asteroid. The Dr column on the second line indicates a confirmed binary and is the estimated diameter ratio of the secondary to primary ( $D_s/D_p$ ).

## LIGHTCURVES OF MAIN-BELT ASTEROID 7939 ASPHAUG AND NEAR-EARTH ASTEROID 2015 JD1

Ian Díaz-Vachier

Lunar & Planetary Laboratory, University of Arizona  
1629 E University Blvd, Tucson, AZ, 85721  
idiazvachier@arizona.edu

Desiree Cotto-Figueroa

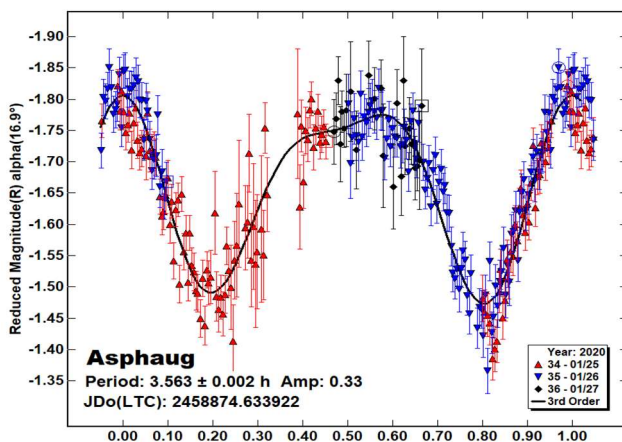
Dept. of Physics and Electronics  
University of Puerto Rico at Humacao  
Humacao, Puerto Rico, 00792

(Received: 2021 Sep 7)

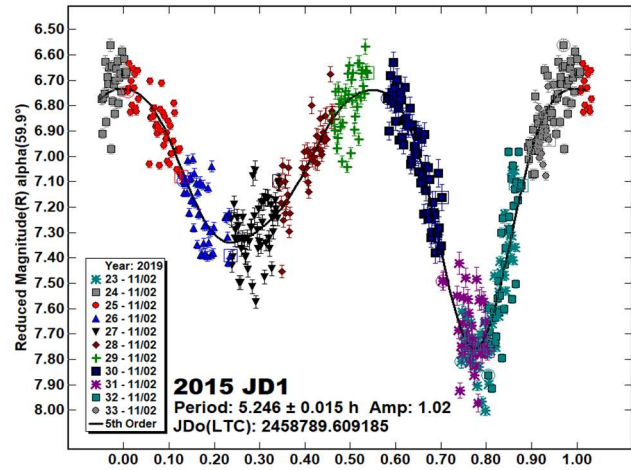
Photometric observations were conducted on main-belt asteroid 7939 Asphaug (1991 AP1) and potentially hazardous asteroid 2015 JD1. Results reveal rotation periods of  $P = 3.563 \pm 0.002$  h and  $P = 5.246 \pm 0.015$  h, respectively.

Photometric observations at the National Undergraduate Research Observatory (NURO) of the Lowell Observatory in Flagstaff, AZ, have been made. The observatory is equipped with a  $2K \times 2K$  thermoelectrically cooled CCD camera coupled to a 31-inch telescope. The data, collected using an R-band filter, was bias subtracted, and combined to bias-subtracted flat fields using the *Image Reduction and Analysis Facility* (IRAF) software package. Photometric measurements and lightcurves analysis were performed using *MPO Canopus* (v10.7.12.12; Warner, 2018).

**7939 Asphaug (1991 AP1).** First seen at Palomar Observatory on 1991 January 14 by E. F. Helin, Asphaug is a main-belt asteroid of  $D = 2.95$  km in diameter and an absolute magnitude of  $H = 14.61$  (JPL, 2021). The asteroid was studied for three nights from 2020 January 25-27. Observed for a total of 5 hours and with 45 second exposures, 275 data points were produced for analysis. The lightcurve shows a bimodal solution for the rotation period of  $P = 3.563 \pm 0.002$  h for an amplitude of  $A = 0.33 \pm 0.05$  mag. After a search on the lightcurve database (LCDB; Warner et al., 2009), it seems this is the first reported rotation period for Asphaug.



**2015 JD1** is an Apollo-class near-Earth and potentially hazardous asteroid of  $D = 260$  m, discovered in 2015 May. Its next visit is on 2023 May 5 at a nominal distance of 0.37 AU (JPL, 2021). The asteroid was studied on the night of 2019 November 2 for 6 hours. With 30 second exposures, 476 data points were produced for analysis. Here we see the bimodal solution for a rotation period of  $P = 5.246 \pm 0.015$  h for an amplitude of  $A = 1.02 \pm 0.18$  mag. This result is consistent with previous reported rotational periods: Pravec et al. (2019web;  $P = 5.20$  h,  $A = 0.58$ ), Skiff (2019web;  $P = 5.31$  h,  $A = 1.08$  mag) found on the *Collaborative Asteroid Lightcurve Link* (CALL), and Warner et al. (2020;  $P = 5.21$  h,  $A = 0.94$  mag).



### Acknowledgements

This research was made possible through funding by NASA Puerto Rico Space Grant Consortium.

### References

- Harris, A.W.; Young, J.W.; Scaltriti, F.; Zappala, V. (1984). "Lightcurves and phase relations of the asteroids 82 Alkmene and 444 Gyptis." *Icarus* **57**, 251-258.
- JPL (2021). Small Body Database Browser. <https://ssd.jpl.nasa.gov>
- Pravec, P.; Wolf, M.; Sarounova, L. (2019web). <http://www.asu.cas.cz/~ppravec/neo.htm> (Accessed 8/3/2020).
- Skiff, B.A. (2019web). 2015 JD1: Posting on CALL website. <http://www.minorplanet.info/call.html> (Accessed 8/3/2020)
- Warner, B.D.; Harris, A.W.; Pravec, P. (2009). "The Asteroid Lightcurve Database." *Icarus* **202**, 134-146. Updated 2020 Aug. <http://www.minorplanet.info/lightcurvedatabase.html>
- Warner, B.D. (2018). MPO Software, MPO Canopus v10.7.12.2. Bdw Publishing. <http://minorplanetobserver.com>
- Warner, B.D.; Stephens, R.D. (2020). "Near-Earth Asteroid Lightcurve Analysis at the Center for Solar System Studies: 2019 September - 2020 January." *Minor Planet Bull.* **47**, 105-120.

Number	Name	yyyy mm/dd	Phase	$L_{PAB}$	$B_{PAB}$	Period(h)	P.E.	Amp	A.E.	Grp
7939	Asphaug	2020 01/25-01/27	16.9	97	1	3.563	0.002	0.33	0.05	MBA
	2015 JD1	2019 11/02	59.9	185	-11	5.246	0.015	1.02	0.18	PHA

Table I. Observing circumstances and results. The phase angle is given for the first and last date. If preceded by an asterisk, the phase angle reached an extrema during the period.  $L_{PAB}$  and  $B_{PAB}$  are the approximate phase angle bisector longitude/latitude at mid-date range (see Harris et al., 1984). Grp is the asteroid family/group (Warner et al., 2009).

## MAIN-BELT ASTEROIDS OBSERVED FROM CS3: 2021 JULY-SEPTEMBER

Robert D. Stephens

Center for Solar System Studies (CS3) / MoreData!  
11355 Mount Johnson Ct., Rancho Cucamonga, CA 91737 USA  
rstephens@foxandstephens.com

Brian D. Warner

Center for Solar System Studies (CS3) / MoreData!  
Eaton, CO

(Received: 2021 October 8)

CCD photometric observations of 10 main-belt asteroids were obtained at the Center for Solar System Studies (CS3) from 2021 July-September.

The Center for Solar System Studies (CS3) has nine telescopes which are normally used in program asteroid family studies. The focus is on near-Earth asteroids, Jovian Trojans and Hildas. When a nearly full moon is too close to the family targets being studied, targets of opportunity amongst the main-belt families were selected.

Table I lists the telescopes and CCD cameras that were used to make the observations. Images were unbinned with no filter and had master flats and darks applied. The exposures depended upon various factors including magnitude of the target, sky motion, and Moon illumination.

Telescope	Camera
0.30-m f/6.3 Schmidt-Cass	SBIG 1001E
0.35-m f/9.1 Schmidt-Cass	FLI Microline 1001E
0.35-m f/9.1 Schmidt-Cass	FLI Microline 1001E
0.35-m f/9.1 Schmidt-Cass	FLI Microline 1001E
0.40-m f/10 Schmidt-Cass	FLI Proline 1001E
0.40-m f/10 Schmidt-Cass	FLI Proline 1001E
0.50-m F8.1 R-C	FLI Proline 1001E

Table I: List of CS3 telescope/CCD camera combinations.

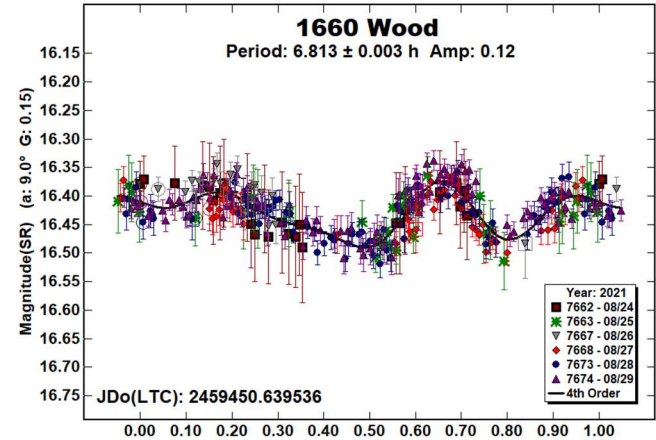
Image processing, measurement, and period analysis were done using *MPO Canopus* (Bdw Publishing), which incorporates the Fourier analysis algorithm (FALC) developed by Harris (Harris et al., 1989). The Comp Star Selector feature in *MPO Canopus* was used to limit the comparison stars to near solar color. Night-to-night calibration was done using field stars from the ATLAS catalog (Tonry et al., 2018), which has Sloan *griz* magnitudes that were derived from the GAIA and Pan-STARR catalogs and are “native” magnitudes of the catalog. Those adjustments are usually  $\leq \pm 0.03$  mag. The rare greater corrections may have been related in part to using unfiltered observations, poor centroiding of the reference stars, and not correcting for second-order extinction.

The Y-axis values are ATLAS SR “sky” magnitudes. The two values in the parentheses are the phase angle ( $\alpha$ ) and the value of  $G$  used to normalize the data to the comparison stars used in the earliest session. This, in effect, made all the observations seem to be made at a single fixed date/time and phase angle, leaving any variations due only to the asteroid’s rotation and/or albedo changes.

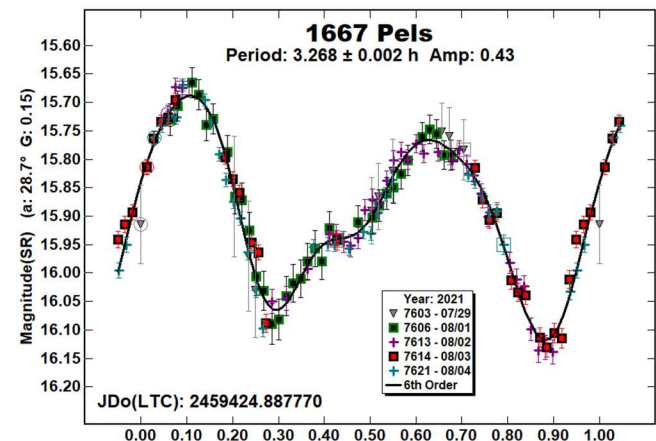
The X-axis shows rotational phase from  $-0.05$  to  $1.05$ . If the plot includes the amplitude, e.g., “Amp: 0.65”, this is the amplitude of the Fourier model curve and *not necessarily the adopted amplitude for the lightcurve*.

For brevity, only some of the previously reported rotational periods may be referenced. A complete list is available at the asteroid lightcurve database (LCDB; Warner et al., 2009).

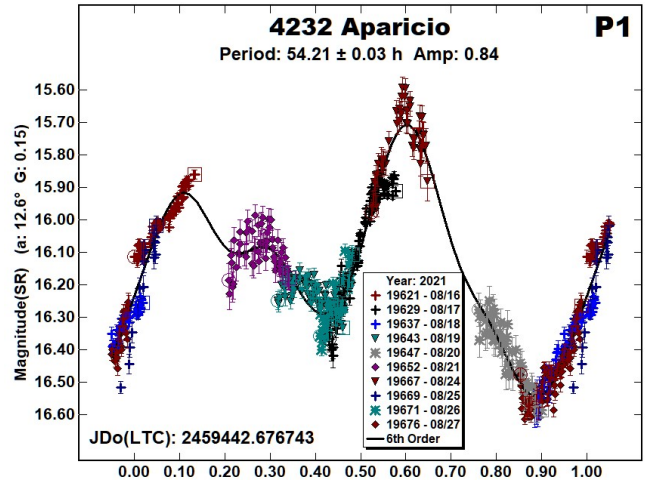
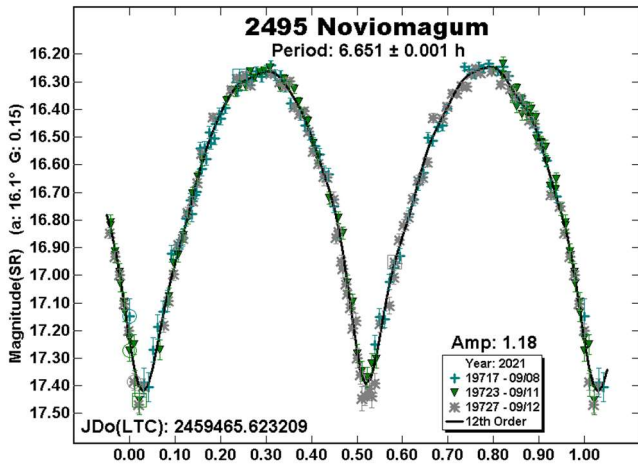
**1660 Wood.** This member of the Phocaea dynamical family has been observed three times in the past. Han et al. (2013), Hills (2012), and Oey & Alvarez (2012) all observed it in 2012 February finding periods near 6.809 h. Our results this year is in good agreement with those prior results.



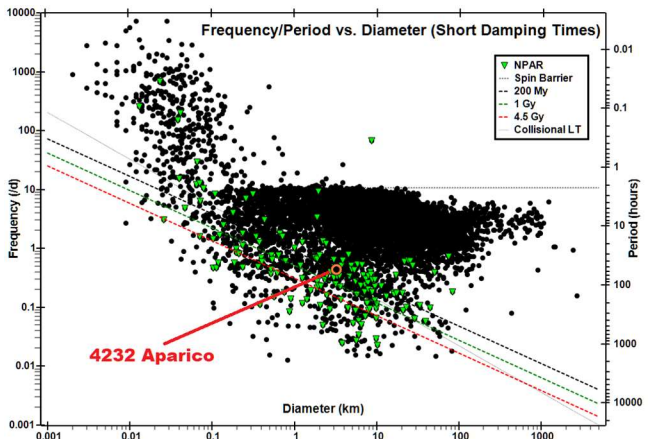
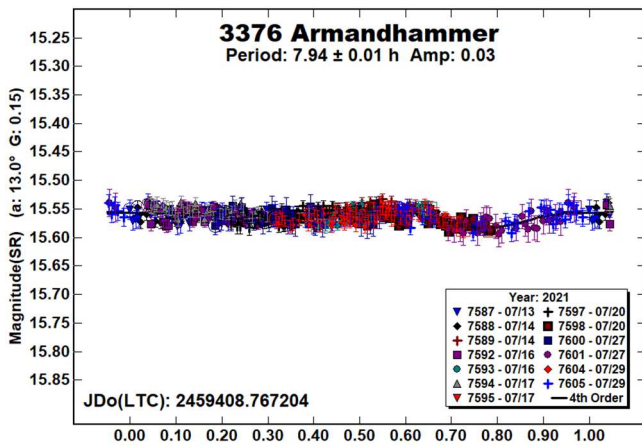
**1667 Pels.** This member of the Flora dynamical family has been observed several times in the past resulting in a pole/shape model (Stephens and Warner, 2020; and references therein). That model had a sidereal period of 3.268280 h and two possible pole positions ( $182^\circ, -53^\circ, 3.268280$  h) and ( $16^\circ, -63^\circ, 3.268280$  h). This year’s result is in good agreement with those prior findings.



**2495 Noviomagum.** Per the LCDB, this member of the Hungaria dynamical family has been observed once (Warner 2014), reporting a synodic period of 6.645 h. Hanuš et al. (2016) reported a spin axis model with  $(\lambda, \beta, P) = (15^\circ, -57^\circ)$  and a sidereal period of 6.65168 h. The result found this year is in good agreement with these prior periods.



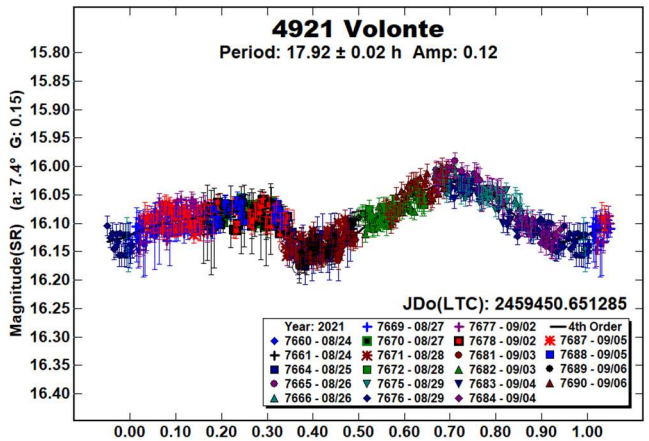
**3376 Armandhammer.** This member of the Flora dynamical family was observed by Pravec et al. (2009web) finding a period of 7.9184 h. and an amplitude of 0.04 mag. Using data from the Palomar Transient Factory, Waszczak et al. (2015) found a period of 9.480 h, which is a 5:6 alias of the Pravec period. Stephens (2016) found a period of 7.916 h and an amplitude of 0.27 mag. Even with the low amplitude of 0.03 mag., the result found this year is in good agreement with the prior Pravec and Stephens results.

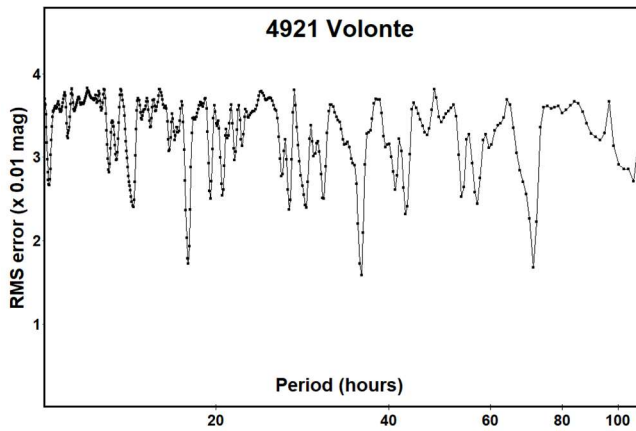


**4921 Volonte.** There are no previous results in the LCDB for this member of the Vestoid dynamical family. The Period Spectrum shows two plausible results for this year's data, 17.92 h and 35.78 h. We prefer the 17.92 h solution because it has an asymmetric bimodal lightcurve with maximums 0.5 phase apart. With this period being 2/3 commensurate with an Earth's day, the 35.78 h solution is fit-by-exclusion when viewed from a single longitude.

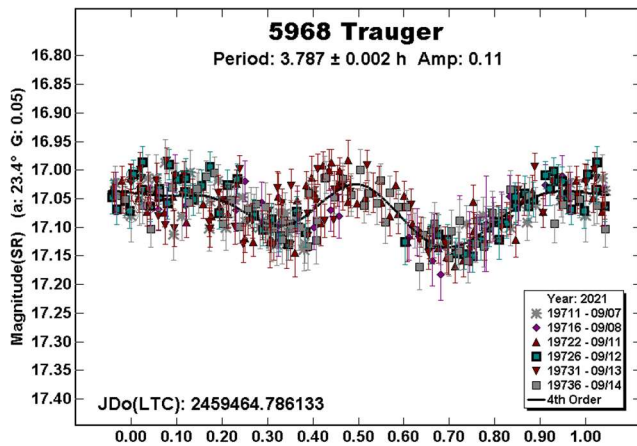
**4232 Aparicio.** This member of the Hungaria dynamical family is estimated to be 3.66 km in diameter. Warner (2006 and 2015) previously found a period near 54.3 h. Pravec et al. (2014) reported Aparicio to be in a tumbling state.

The data from 2021 also shows Aparicio to be tumbling. The tumbling frequencies cannot be confirmed from our data set alone, but we attempted to solve for the dominant period of the solution. The plot labeled "P1" is the dominant frequency, after subtracting one or more secondary frequencies, and is similar to dominant frequencies found in the past. The Frequency/Period vs. Diameter plot shows that Aparicio is near the 200 My damping line.

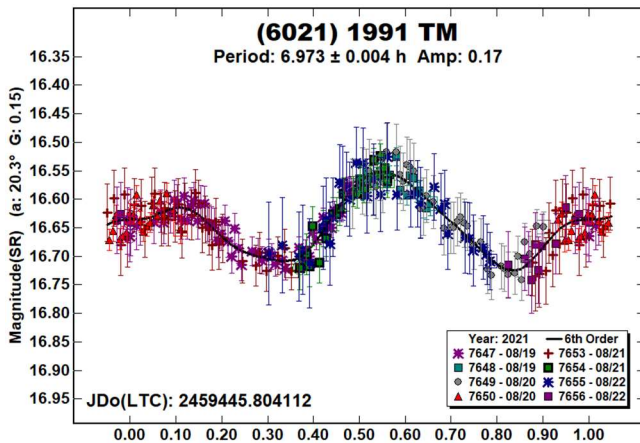




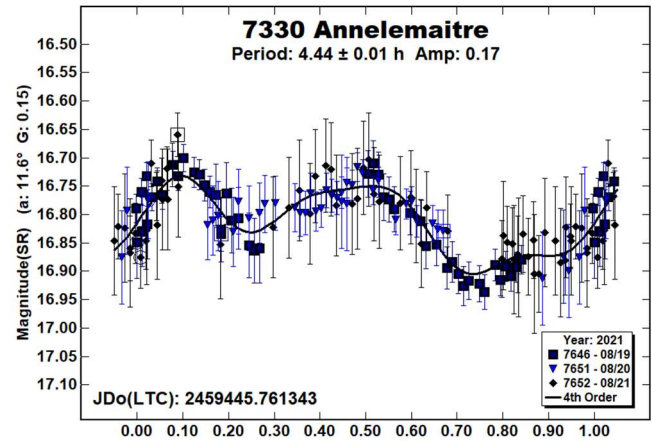
(5968) Trauger. The estimated diameter is 3.5 km for this member of the Hungaria dynamical family. It has been observed many times in the past (Warner, 2015; and references therein); most reporting a period near 3.748 h. The period found this year is in good agreement with those prior results.



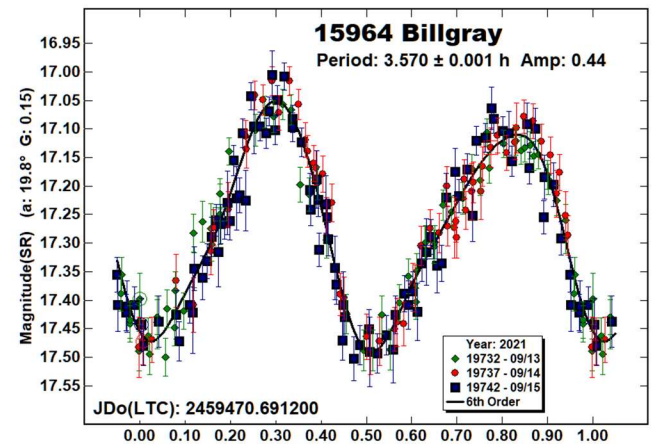
(6021) 1991 TM. Using data from the TESS spacecraft, Pál et al. (2020) found a period of 6.97081 h for this member of the Vestoid dynamical family. Our result this year is in good agreement with the Pál et al. result.



7330 Annelemaitre. This Mars-crosser has been observed three times in the past. Behrend (2014web) reported a period of 4.437 h. Stephens (2015) found a period of 4.438 h. Finally, using data from the TESS spacecraft, Pál et al. (2020) found a period of 4.43734 h. Our result this year is in good agreement with those prior results.



15964 Billgray. Periods for this member of the Hungaria dynamical family have been reported twice in the past. Warner (2011 and 2014) found periods near 3.57 h. Using data from the Palomar Transient Factory Survey, Waszczak et al. (2015) found a period of 3.570 h. The period found this year is in good agreement with the prior results.



Acknowledgements

This work includes data from the Asteroid Terrestrial-impact Last Alert System (ATLAS) project. ATLAS is primarily funded to search for near earth asteroids through NASA grants NN12AR55G, 80NSSC18K0284, and 80NSSC18K1575; byproducts of the NEO search include images and catalogs from the survey area. The ATLAS science products have been made possible through the contributions of the University of Hawaii Institute for Astronomy, the Queen's University Belfast, the Space Telescope Science Institute, and the South African Astronomical Observatory.

The authors gratefully acknowledge Shoemaker NEO Grants from the Planetary Society (2007, 2013). These were used to purchase some of the telescopes and CCD cameras used in this research.

Number	Name	2021/mm/dd	Phase	L <sub>PAB</sub>	B <sub>PAB</sub>	Period(h)	P.E.	Amp	A.E.
1660	Wood	08/24-08/29	9.0, 9.4	326	23	6.813	0.003	0.12	0.02
1667	Pels	07/29-08/04	28.7, 28.2	16	-5	3.268	0.002	0.43	0.02
2495	Noviomagum	09/08-09/12	16.1, 15.7	346	20	6.651	0.001	1.18	0.02
3376	Armandhammer	07/13-07/29	13.0, 6.4	315	7	7.94	0.01	0.03	0.01
4232	Aparicio	08/16-08/27	*12.6, 11.8	329	18	<sup>†</sup> 54.21	0.03	0.84	0.05
4921	Volonte	08/24-09/06	7.4, 13.3	321	7	17.92	0.02	0.12	0.01
5968	Trauger	09/07-09/14	23.5, 20.7	24	-2	3.787	0.002	0.11	0.02
6021	1991 TM	08/19-08/22	20.3, 19.3	6	-5	6.973	0.004	0.17	0.02
7330	Annelemaitre	08/19-08/21	11.6, 11.0	341	17	4.44	0.01	0.17	0.03
15964	Billgray	09/13-09/15	19.8, 19.3	9	22	3.570	0.001	0.44	0.03

Table II. Observing circumstances and results. <sup>†</sup>Dominant frequency for a tumbling asteroid. The phase angle is given for the first and last date. If preceded by an asterisk, the phase angle reached an extremum during the period. L<sub>PAB</sub> and B<sub>PAB</sub> are the approximate phase angle bisector longitude/latitude at mid-date range (see Harris et al., 1984).

## References

- Behrend, R. (2014web). Observatoire de Geneve web site. [http://obswww.unige.ch/~behrend/page\\_cou.html](http://obswww.unige.ch/~behrend/page_cou.html)
- Han, X.L.; Li, B.; Zhao, H. (2013). "Rotation Periods of 1660 Wood, 7173 Sepkoski, 12738 Satoshimiki and (23233) 2000 WM72." *Minor Planet Bull.* **40**, 14-15.
- Hanuš, J.; Ďurech, J.; Oszkiewicz, D.A.; Behrend, R.; Carry, B.; Delbo, M.; Adam, O.; Afonina, V.; Anquetin, R.; Antonini, P.; Arnold, L.; Audejean, M.; Aurard, P.; Bachschmidt, M.; Baduel, B.; Barbotin, E.; Barroy, P.; Baudouin, P.; Berard, L.; Berger, N. (2016). "New and updated convex shape models of asteroids based on optical data from a large collaboration network." *Astron. Astrophys.* **586**, A108.
- Harris, A.W.; Young, J.W.; Scaltriti, F.; Zappala, V. (1984). "Lightcurves and phase relations of the asteroids 82 Alkmene and 444 Ggyptis." *Icarus* **57**, 251-258.
- Harris, A.W.; Young, J.W.; Contreiras, L.; Dockweiler, T.; Belkora, L.; Salo, H.; Harris, W.D.; Bowell, E.; Poutanen, M.; Binzel, R.P.; Tholen, D.J.; Wang, S. (1989). "Phase relations of high albedo asteroids: The unusual opposition brightening of 44 Nysa and 64 Angelina." *Icarus* **81**, 365-374.
- Hills, K. (2012). "Asteroid Lightcurve Analysis at Riverland Dingo Observatory: 1394 Alga, 1660 Wood, 8882 Sakaetamura, and (15269) 1990 XF." *Minor Planet Bull.* **39**, 239-240.
- Oey, J.; Alvarez, E.M. (2012). "Period Determination for 1660 Wood." *Minor Planet Bull.* **39**, 147-148.
- Pál, A.; Szakáts, R.; Kiss, C.; Bódi, A.; Bognár, Z.; Kalup, C.; Kiss, L.L.; Marton, G.; Molnár, L.; Plachy, E.; Sárneczky, K.; Szabó, G.M.; Szabó, R. (2020). "Solar System Objects Observed with TESS - First Data Release: Bright Main-belt and Trojan Asteroids from the Southern Survey." *Ap. J.* **247**, A26.
- Pravec, P.; Wolf, M.; Sarounova, L. (2009web). <http://www.asu.cas.cz/~ppravec/neo.htm>
- Pravec, P.; Scheirich, P.; Ďurech, J.; Pollock, J.; Kusnirak, P.; Hornoch, K.; Galad, A.; Vokrouhlicky, D.; Harris, A.W.; Jehin, E.; Manfroid, J.; Opitom, C.; Gillon, M.; Colas, F.; Oey, J.; Vrastil, J.; Reichart, D.; Ivarsen, K.; Haislip, J.; LaCluyze, A. (2014). "The tumbling state of (99942) Apophis." *Icarus* **233**, 48-60.
- Stephens, R.D. (2015). "Asteroids Observed from CS3: 2014 July - September." *Minor Planet Bull.* **42**, 70-74.
- Stephens, R.D. (2016). "Asteroids Observed from CS3: 2016 January - March." *Minor Planet Bull.* **43**, 252-255.
- Stephens, R.D.; Warner, B.D. (2020). "Main-Belt Asteroids Observed from CS3: 2020 April to June." *Minor Planet Bull.* **47**, 275-284.
- Tonry, J.L.; Denneau, L.; Flewelling, H.; Heinze, A.N.; Onken, C.A.; Smartt, S.J.; Stalder, B.; Weiland, H.J.; Wolf, C. (2018). "The ATLAS All-Sky Stellar Reference Catalog." *Astrophys. J.* **867**, A105.
- Warner, B.D., (2006). "The lightcurve for the Hungaria asteroid 4232 Aparicio." *Minor Planet Bull.* **33**, 24-25.
- Warner, B.D. (2011). "Lightcurve Analysis at the Palmer Divide Observatory: 2010 June-September." *Minor Planet Bull.* **38**, 25-31
- Warner, B.D. (2014). "Asteroid Lightcurve Analysis at CS3-Palmer Divide Station: 2013 June - September." *Minor Planet Bull.* **41**, 27-32.
- Warner, B.D. (2015). "Asteroid Lightcurve Analysis at CS3-Palmer Divide Station: 2015 March-June." *Minor Planet Bull.* **42**, 267-276.
- Warner, B.D.; Harris, A.W.; Pravec, P. (2009). "The Asteroid Lightcurve Database." *Icarus* **202**, 134-146. Updated 2021 May. <http://www.minorplanet.info/lightcurvedatabase.html>
- Waszczak, A.; Chang, C.-K.; Ofek, E.O.; Laher, R.; Masci, F.; Levitan, D.; Surace, J.; Cheng, Y.-C.; Ip, W.-H.; Kinoshita, D.; Helou, G.; Prince, T.A.; Kulkarni, S. (2015). "Asteroid Light Curves from the Palomar Transient Factory Survey: Rotation Periods and Phase Functions from Sparse Photometry." *Astron. J.* **150**, A75.

## COLLABORATIVE ASTEROID PHOTOMETRY FROM UAI: 2021 JULY-SEPTEMBER

Lorenzo Franco  
Balzaretto Observatory (A81), Rome, ITALY  
lor\_franco@libero.it

Alessandro Marchini, Riccardo Papini  
Astronomical Observatory, DSFTA - University of Siena (K54)  
Via Roma 56, 53100 - Siena, ITALY

Giulio Scarfi  
Iota Scorpis Observatory (K78), La Spezia, ITALY

Paolo Bacci, Martina Maestripieri  
GAMP - San Marcello Pistoiese (104), Pistoia, ITALY

Pietro Aceti, Massimo Banfi  
Oss. Liceo Iris Versari, Felizzano, AL, ITALY  
Oss. Prealpi Orobitiche (A36), Ganda di Aviatice, BG, ITALY

Mauro Bachini  
BSCR Observatory (K47), Santa Maria a Monte, PI, ITALY

Giacomo Succi, Mauro Bachini  
Tavolaia Observatory (A29), Santa Maria a Monte, PI, ITALY

Gianni Galli  
GiaGa Observatory (203), Pogliano Milanese, ITALY

(Received: 2021 October 13)

Photometric observations of eight asteroids were made in order to acquire lightcurves for shape/spin axis modeling. The synodic period and lightcurve amplitude were found for 58 Concordia, 224 Oceana, 1046 Edwin, 2431 Skovoroda, 2824 Franke, (7822) 1991 CS, (143649) 2003 QQ47, and color index (V-R) for 790 Pretoria.

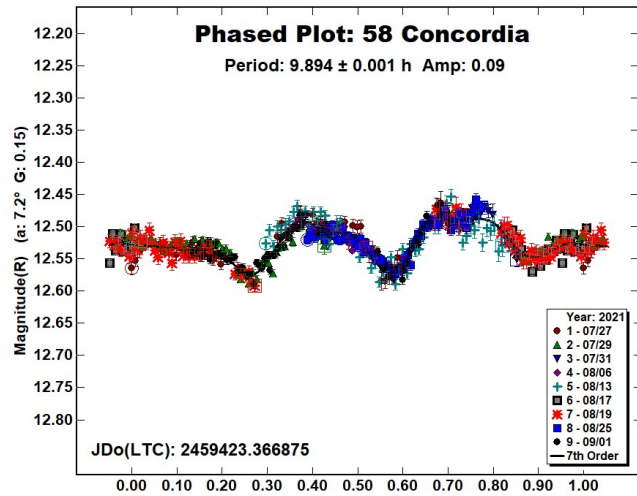
We report collaborative asteroid photometry performed by the Italian Amateur Astronomers Union (UAI; 2021). The targets were selected mainly in order to acquire lightcurves for shape/spin axis modeling. Table I shows the observing circumstances and results.

The CCD observations of eight asteroids were made in 2021 July-September using the instrumentation described in Table II. Lightcurve analysis was performed at the Balzaretto Observatory with *MPO Canopus* (Warner, 2021). All the images were calibrated with dark and flat frames and converted to R magnitudes using solar colored field stars from CMC15 catalogue, distributed with *MPO Canopus*. For brevity, the following citations to the asteroid lightcurve database (LCDB; Warner et al., 2009) will be summarized only as "LCDB".

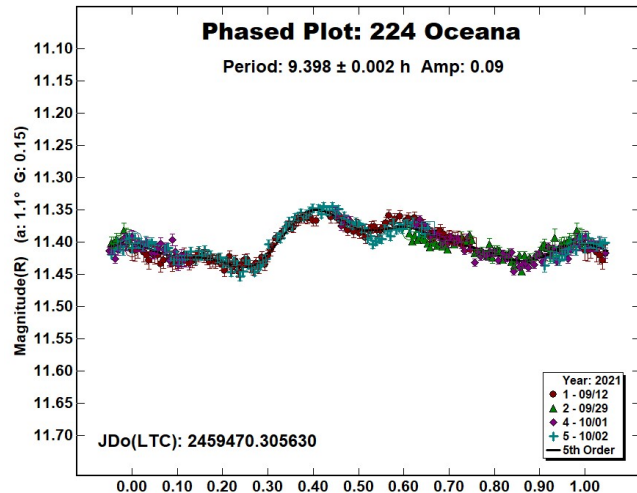
Number	Name	2021 mm/dd	Phase	$L_{PAB}$	$B_{PAB}$	Period(h)	P.E.	Amp	A.E.	Grp
58	Concordia	07/27-09/01	*7.2, 7.9	321	2	9.894	0.001	0.09	0.02	MB-M
224	Oceana	09/12-10/02	*1.0, 7.9	352	0	9.398	0.002	0.09	0.02	MB-M
790	Pretoria	07/29	8.6	307	21					MB-O
1046	Edwin	09/09-09/24	*1.6, 5.6	348	-4	5.291	0.001	0.33	0.03	MB-O
2431	Skovoroda	08/10-09/05	*5.6, 9.7	328	0	3.128	0.001	0.17	0.05	MB-M
2824	Franke	09/04-09/27	4.2, 17.1	338	3	3.380	0.001	0.07	0.03	MB-I
7822	1991 CS	08/18-08/20	76.1, 77.5	14	4	2.390	0.001	0.35	0.10	NEA
143649	2003 QQ47	09/24	28.3	6	16	3.74	0.06	0.26	0.04	NEA

Table I. Observing circumstances and results. The first line gives the results for the primary of a binary system. The second line gives the orbital period of the satellite and the maximum attenuation. The phase angle is given for the first and last date. If preceded by an asterisk, the phase angle reached an extrema during the period.  $L_{PAB}$  and  $B_{PAB}$  are the approximate phase angle bisector longitude/latitude at mid-date range (see Harris et al., 1984). Grp is the asteroid family/group (Warner et al., 2009).

58 Concordia is a Ch-type (Bus & Binzel, 2002) middle main-belt asteroid. Collaborative observations were made over nine nights. The period analysis shows a synodic period of  $P = 9.894 \pm 0.001$  h with an amplitude  $A = 0.09 \pm 0.02$  mag. The period is close to the previously published results in the LCDB.



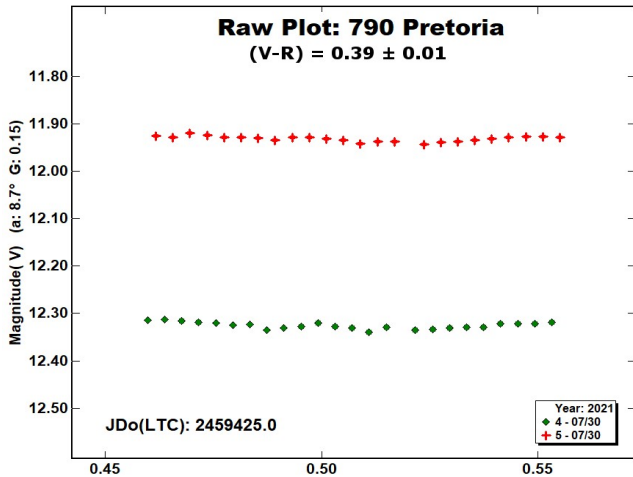
224 Oceana is an M-type (Tholen, 1984) middle main-belt asteroid. Collaborative observations were made over four nights. The period analysis shows a synodic period of  $P = 9.398 \pm 0.002$  h with an amplitude  $A = 0.09 \pm 0.02$  mag. The period is close to the previously published results in the LCDB.



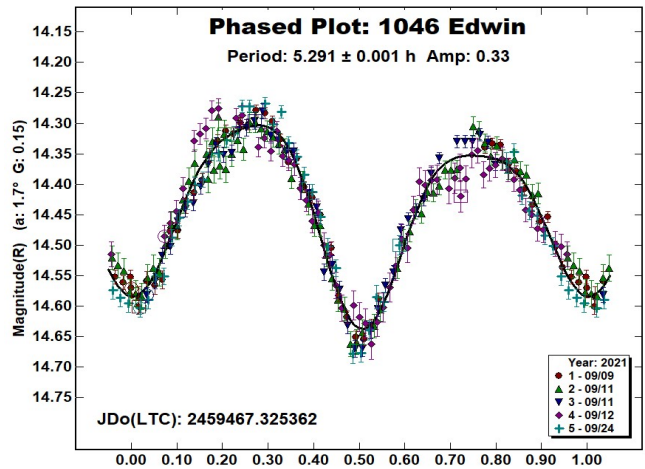
Observatory (MPC code)	Telescope	CCD	Filter	Observed Asteroids (#Sessions)
Astronomical Observatory of the University of Siena(K54)	0.30-m MCT f/5.6	SBIG STL-6303e (bin 2x2)	C, Rc	58 (6), 224 (3), 1046 (3), 2431 (3)
Iota Scorpii (K78)	0.40-m RCT f/8.0	SBIG STXL-6303e (bin 2x2)	Rc	224 (1), 790 (1), 1046 (2), 2824 (1), 7822 (3)
GAMP (104)	0.60-m NRT f/4.0	Apogee Alta	C	2431 (6), 2824 (3)
Oss. Liceo Iris Versari	0.20-m SCT f/6.3	Moravian G2-8300	Rc	58 (2), 2431 (3)
Oss. Prealpi Orobiche (A36)	0.50-m NRT f/5.0	Moravian G2-8300	Rc	58 (1), 2431 (2)
BSCR Observatory (K47)	0.25-m SCT f/7.0	DTA Discovery plus 1600	C	2431 (5)
Tavolaia Observatory (A29)	0.40-m NRT f/5.0	DTA Electra	C	2431 (2)
GiaGa Observatory (203)	0.36-m SCT f/5.8	Moravian G2-3200	C	143649 (1)

Table II. Observing Instrumentations. MCT: Maksutov-Cassegrain, NRT: Newtonian Reflector, RCT: Ritchey-Chretien, SCT: Schmidt-Cassegrain.

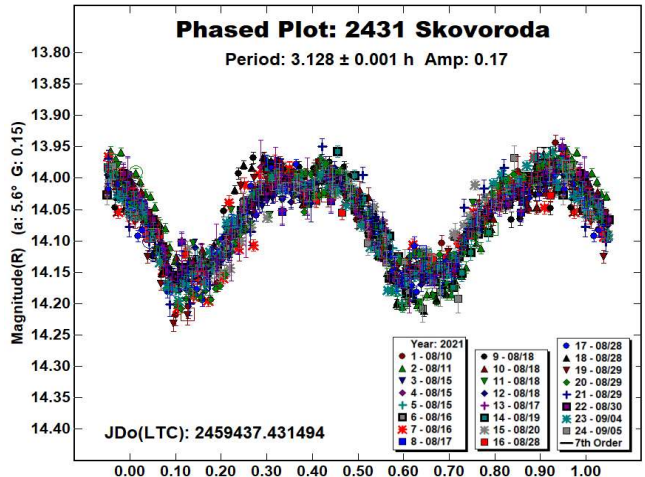
790 Pretoria is a P-type (Tholen, 1984) outer main-belt asteroid. Multiband photometry was made by G. Scarfi on 2021 July 29. We found a color index  $(V-R) = 0.39 \pm 0.01$ , consistent with a low albedo asteroid (Shevchenko and Lupishko, 1998).



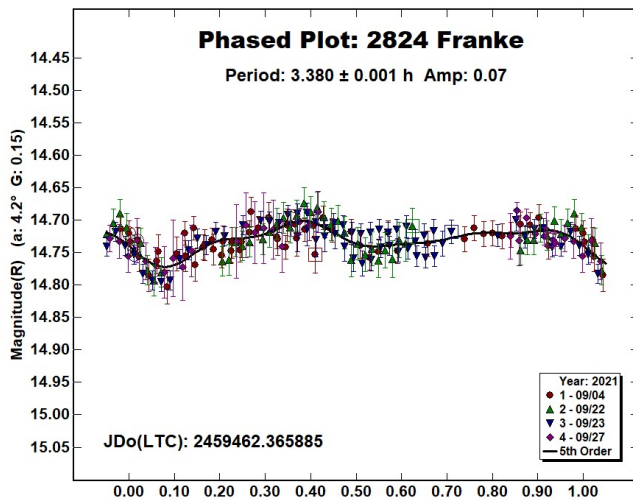
1046 Edwin is an Xe-type (Bus & Binzel, 2002) outer main-belt asteroid. Collaborative observations were made over four nights. We found a synodic period of  $P = 5.291 \pm 0.001$  h with an amplitude  $A = 0.33 \pm 0.03$  mag. The period is close to the previously published results in the LCDB.



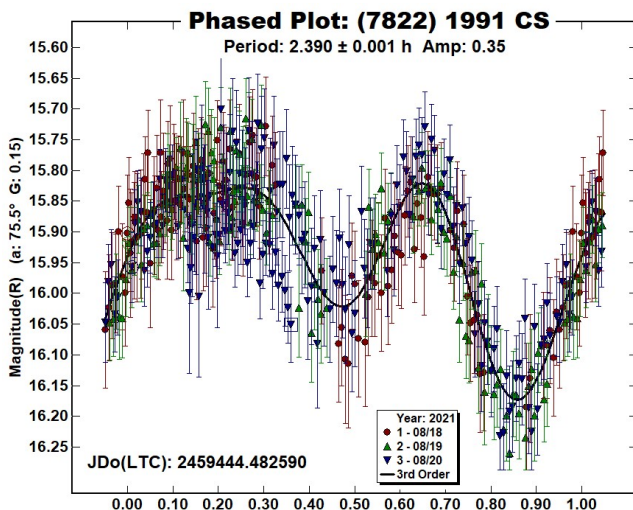
2431 Skovoroda is a medium albedo middle main-belt asteroid. Collaborative observations were made over thirteen nights. We found a synodic period of  $P = 3.128 \pm 0.001$  h with an amplitude  $A = 0.17 \pm 0.05$  mag. The period is close to the previously published results in the LCDB.



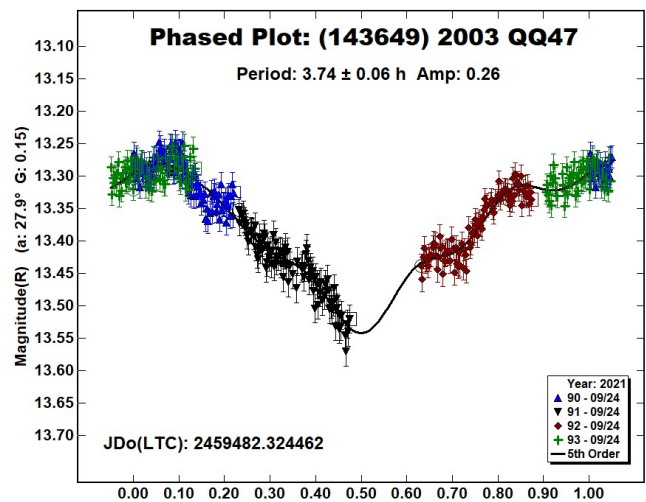
2824 Franke is an inner main-belt asteroid. Collaborative observations were made over four nights. We found a synodic period of  $P = 3.380 \pm 0.001$  h with an amplitude  $A = 0.07 \pm 0.03$  mag. The period is consistent with that previously published by Franco et. al. (2015).



(7822) 1991 CS is an S-type (Bus & Binzel, 2002) Amor Near-Earth asteroid classified as Potentially Hazardous Asteroid (PHA). Observations by G. Scarfi were made over three nights at Iota Scorpis Observatory. We found a synodic period of  $P = 2.390 \pm 0.001$  h with an amplitude  $A = 0.35 \pm 0.10$  mag. The period is close to the previously published results in the LCDB.



(143649) 2003 QQ47 is an Apollo Near-Earth asteroid classified as Potentially Hazardous Asteroid (PHA). Observations by G. Galli were made over one night at GiaGa Observatory. We found a synodic period of  $P = 3.74 \pm 0.06$  h with an amplitude  $A = 0.26 \pm 0.04$  mag. The period is close to the solution found by Warner (2014;  $3.679 \pm 0.005$  h) and differ from the solution found by Carbognani (2014;  $4.09 \pm 0.02$ ).



#### References

- Bus, S.J.; Binzel, R.P. (2002). "Phase II of the Small Main-Belt Asteroid Spectroscopic Survey - A Feature-Based Taxonomy." *Icarus* **158**, 146-177.
- Carbognani, A. (2014). "Asteroids Lightcurves at OAVdA: 2013 December - 2014 June." *Minor Planet Bulletin* **41**, 265-270.
- Franco, L.; Marchini, A.; Papini, R. (2015) "Lightcurve Analysis for 2824 Franke and 3883 Verbano." *Minor Planet Bulletin* **42**, 114.
- Harris, A.W.; Young, J.W.; Scaltriti, F.; Zappala, V. (1984). "Lightcurves and phase relations of the asteroids 82 Alkmene and 444 Gryptis." *Icarus* **57**, 251-258.
- Shevchenko, V.G.; Lupishko, D.F. (1998). "Optical properties of Asteroids from Photometric Data." *Solar System Research*, **32**, 220-232.
- Tholen, D.J. (1984). "Asteroid taxonomy from cluster analysis of Photometry." Doctoral Thesis. University Arizona, Tucson.
- UAI (2021). "Unione Astrofili Italiani" web site. <https://www.uai.it>
- Warner, B.D.; Harris, A.W.; Pravec, P. (2009) "The asteroid lightcurve database." *Icarus* **202**, 134-146. Updated 2021 Oct 11. <https://minplanobs.org/alcddef/index.php>
- Warner, B.D. (2014). "Near-Earth Asteroid Lightcurve Analysis at CS3-Palmer Divide Station: 2014 March-June." *Minor Planet Bulletin* **41**, 213-224.
- Warner, B.D. (2021). MPO Software, MPO Canopus v10.8.4.2. Bdw Publishing. <http://minorplanetobserver.com>

**CCD PHOTOMETRY OF 29 ASTEROIDS AT SOPOT  
ASTRONOMICAL OBSERVATORY:  
2020 JULY-2021 SEPTEMBER**

Vladimir Benishek  
Belgrade Astronomical Observatory  
Volgina 7, 11060 Belgrade 38, SERBIA  
vlaben@yahoo.com

(Received: 2021 October 15)

Lightcurves and synodic rotation periods for 29 asteroids determined from CCD photometric data obtained at Sopot Astronomical Observatory (SAO) over the time span 2020 July - 2021 September are presented in this paper.

Photometric observations of 29 asteroids were conducted at Sopot Astronomical Observatory (SAO) from 2020 July through 2021 September in order to determine the asteroids' synodic rotation periods. For this purpose, two 0.35-m  $f/6.3$  Meade LX200GPS Schmidt-Cassegrain telescopes were employed. The telescopes are equipped with a SBIG ST-8 XME and a SBIG ST-10 XME CCD cameras. The exposures were unfiltered and unguided for all targets. Both cameras were operated in  $2 \times 2$  binning mode, which produces image scales of 1.66 arcsec/pixel and 1.25 arcsec/pixel for ST-8 XME and ST-10 XME cameras, respectively. Prior to measurements, all images were corrected using dark and flat field frames.

Photometric reduction was conducted using *MPO Canopus* (Warner, 2018a). Differential photometry with up to five comparison stars of near solar color ( $0.5 \leq B-V \leq 0.9$ ) was performed using the Comparison Star Selector (CSS) utility. This helped ensure a satisfactory quality level of night-to-night zero-point calibrations and correlation of the measurements within the standard magnitude framework. Field comparison stars were calibrated using standard Cousins R magnitudes derived from the Carlsberg Meridian Catalog 15 (VizieR, 2021) Sloan r' magnitudes using the formula:  $R = r' - 0.22$  in all cases presented in this paper. In some instances, small zero-point adjustments were necessary in order to achieve the best match between individual data sets in terms of achieving the most favorable statistical indicators of Fourier fit goodness.

Lightcurve construction and period analysis was performed using *Perfindia* custom-made software developed in the R statistical programming language (R Core Team, 2020) by the author of this paper. The essence of its algorithm is reflected in finding the most favorable solution for rotational period by minimizing the *residual standard error* of the lightcurve Fourier fit.

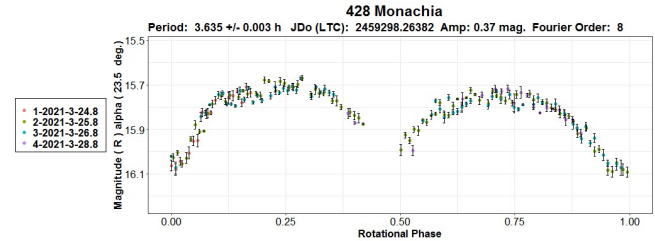
The lightcurve plots presented in this paper show so-called 2% error for rotational periods, i.e., an error that would cause the last data point in a combined data set by date order to be shifted by 2% (Warner, 2012) and represented by the following formula:  $\Delta P = (0.02 \cdot P^2) / T$ , where P and T are the rotational period and the total time span of observations, respectively. Both of these quantities must be expressed in the same units.

Some of the targets presented in this paper were observed within the Photometric Survey for Asynchronous Binary Asteroids (*BinAstPhot Survey*) under the leadership of Dr Petr Pravec from Ondřejov Observatory, Czech Republic.

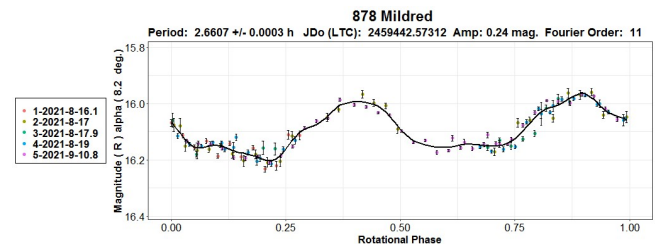
Table I gives the observing circumstances and results.

Observations and results

**428 Monachia.** Several previously determined synodic rotation periods (for example, Wisniewski et al. (3.63384 h, 1997), Warner (3.633 h, 2014), Behrend (3.6335 h, 2016web), a sidereal period by Durech et al. (3.63360 h, 2020), Pal et al. (3.6343 h, 2020)) are very well consistent with a value of  $P = 3.365 \pm 0.003$  h found from SAO data obtained over four nights in 2021 March.



**878 Mildred.** Stephens and French (2011) found a rotation period of 2.660 h. Period ( $P = 2.6607 \pm 0.0003$  h) found from the data obtained at SAO on five nights in 2021 August-September is in full agreement with the previously reported result.



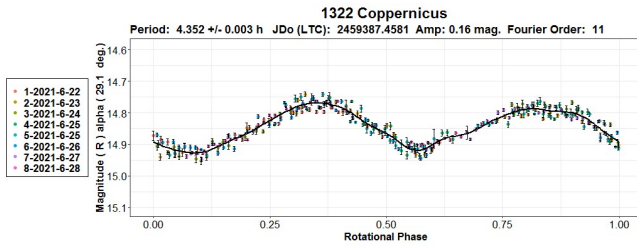
**894 Erda.** Although the rotational cycle corresponding to the found period value of  $P = 4.700 \pm 0.009$  h is not fully covered by the data obtained on three consecutive nights in 2021 August, the established period result fits quite well into the previously determined values by Behrend (4.69 h, 2001web), Stephens (4.69 h, 2002) and Higgins and Goncalves (4.6897, 2007).



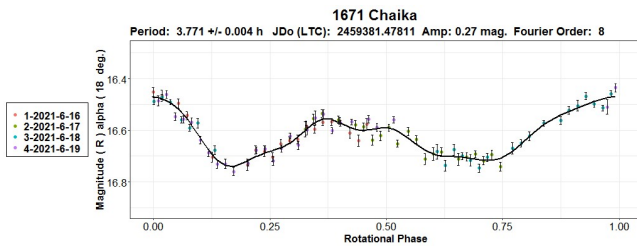
**1129 Neujmina.** Data from three consecutive nights in 2021 April resulted in a period of  $P = 5.06 \pm 0.02$  h. Carbo et al. (2009) and Ditteon and West (2011) previously found values of 5.089 h and 5.0844 h, respectively.



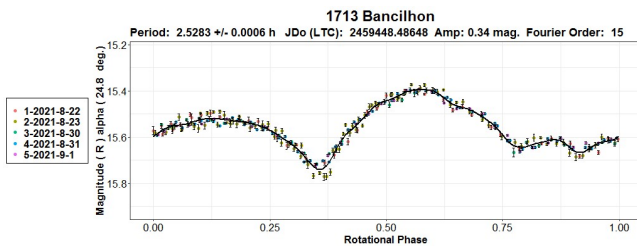
**1322 Copernicus.** Several period results have been reported previously of which only two of them determined more recently by Fauerbach and Brown (4.354 h, 2018) and Noschese et al. (4.354 h, 2018) are completely consistent with each other. A period of  $P = 4.352 \pm 0.003$  h derived from the late 2021 June SAO data is in very good agreement with the stated recent results.



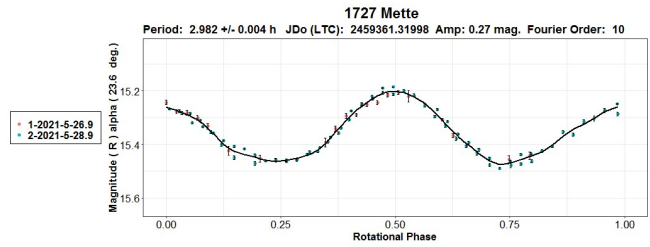
**1671 Chaika.** Two previously reported rotation period results by Behrend (3.7718 h, 2005web) and Menke et al. (3.774 h, 2008) are statistically identical with a period value of  $P = 3.771 \pm 0.004$  h obtained from the SAO data collected on four consecutive nights in 2021 June.



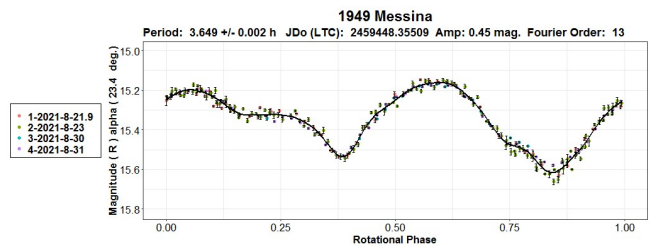
**1713 Bancelhon.** No reports on rotation period determinations were known previously on this asteroid. Period analysis upon photometric observations carried out over five nights in 2021 August-September led an unequivocal rotation period of  $P = 2.5283 \pm 0.0006$  h associated with a bimodal lightcurve showing a rather large amplitude of 0.34 mag.



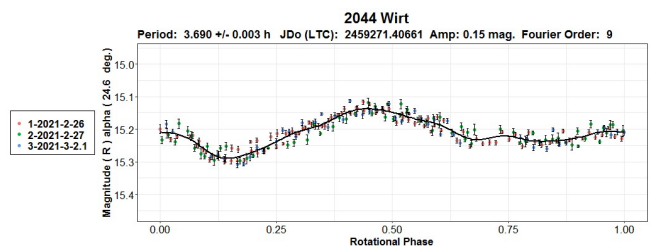
**1727 Mette.** A search of the LCDB database (Warner et al., 2009) finds multiple rotation period determinations on this Hungaria binary asteroid (Warner et al., 2013) over decades. Listed in chronological order, some of them are as follows: Wisniewski and McMillan (2.63 h, 1987), Prokof'eva et al. (2.637 h, 1992), Behrend (2.98125 h, 2006web), Gandolfi et al. (2.981 h, 2009), Warner et al. (2.98109 h, 2013), a sidereal value by Durech et al. (2.981174 h, 2020), Stephens and Warner (2.9804 h, 2020). Data from only two nights in late 2021 May obtained at SAO entirely cover the full rotational cycle corresponding to a period result of  $P = 2.982 \pm 0.004$  h found in the period analysis as the most favorable solution. This value matches many previously reported periods quite well.



**1949 Messina.** A *BinAstPhot Survey* program target. An LCDB database search indicates several quite consistent previously determined results for rotation period: Pravec (3.6491 h, 2014web), Waszczak et al. (3.649 h and 3.635 h, 2015), and a sidereal value by Durech et al. (3.649308 h, 2016). Data taken on four nights in 2021 August confirm the previously derived results indicating a bimodal solution for a rotation period of  $P = 3.649 \pm 0.002$  h with associated lightcurve showing a quite large amplitude of 0.45 magnitudes.



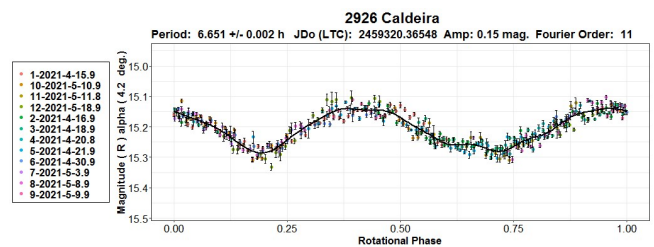
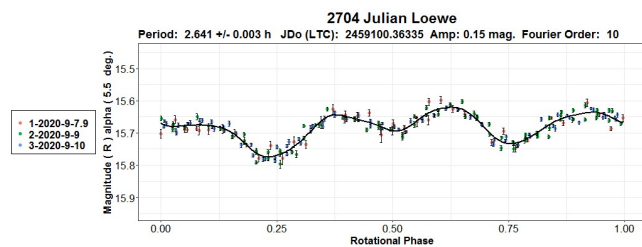
**2044 Wirt.** Another *BinAstPhot Survey* target and a confirmed Mars-crossing binary asteroid system. The companion was discovered photometrically by Donald Pray in 2006 within the *BinAstPhot Survey* (Pray et al., 2006). A number of fairly uniform rotation periods have been determined since 2005. For example, some of these are: Behrend (3.6900 h, 2005web), Pray et al. (3.6898 h, 2006), Waszczak et al. (3.690 h, 2015), Behrend (3.68989 h, 2016web). There are no satellite attenuation events in the SAO data collected in late February and early March 2021 over 3 nights only. Nevertheless, these data were sufficient to establish a secure rotation period result. A bimodal solution of  $P = 3.690 \pm 0.003$  h was found, which is in full accordance with the previously reported values.



**2704 Julian Loewe.** Recently processed backlog data on this spectroscopically confirmed V-type (Bus and Binzel, 2002) inner main-belt object obtained on three nights in 2020 September show a period of  $P = 2.641 \pm 0.003$  h, which is close to the value found by Oszkiewicz et al. (2.6385 h, 2020).

Number	Name	20yy/mm/dd	Phase	LPAB	BPAB	Period (h)	P.E.	Amp	A.E.	Grp
428	Monachia	21/03/24-20/03/28	23.5, 24.0	127	6	3.635	0.003	0.37	0.03	MB-I
878	Mildred	21/08/16-21/09/10	*8.2, 8.1	336	1	2.6607	0.0003	0.24	0.03	HER
894	Erda	21/04/23-21/04/25	16.8, 16.9	143	-9	4.700	0.009	0.11	0.02	MB-O
1129	Neujmina	21/04/23-21/04/25	18.9, 19.0	143	-8	5.06	0.02	0.11	0.03	EOS
1322	Copernicus	21/06/21-21/06/28	29.1, 28.1	316	25	4.352	0.003	0.16	0.02	MB-I
1671	Chaika	21/06/15-21/06/19	18.0, 17.5	314	4	3.771	0.004	0.27	0.03	ASTR
1713	Bancilhon	21/08/21-21/09/01	24.8, 20.6	8	-5	2.5283	0.0006	0.34	0.03	MB-I
1727	Mette	21/05/26-21/05/29	23.6, 23.9	220	32	2.982	0.004	0.27	0.02	HUN
1949	Messina	21/08/21-21/08/31	23.4, 19.5	4	7	3.649	0.002	0.45	0.03	MB-I
2044	Wirt	21/02/25-21/03/02	24.6, 23.2	182	30	3.690	0.003	0.15	0.02	MC
2704	Julian Loewe	20/09/07-20/09/10	5.5, 4.5	356	3	2.641	0.003	0.15	0.02	MB-I
2824	Franke	21/09/07-21/09/16	5.9, 10.8	337	2	3.382	0.002	0.07	0.02	MB-I
2926	Caldeira	21/04/15-21/05/18	4.2, 20.6	200	-1	6.651	0.002	0.15	0.03	FLOR
3760	Poutanen	21/06/07-21/07/04	17.2, 24.2	232	11	2.9558	0.0003	0.19	0.02	MB-I
3807	Pagels	21/05/08-21/05/11	4.8, 4.1	232	6	3.289	0.003	0.14	0.02	FLOR
3869	Norton	20/07/23-20/08/10	*6.9, 5.3	312	6	7.605	0.003	0.14	0.01	MB-I
5235	Jean-Loup	21/06/23-21/07/13	19.0, 9.8	303	4	2.4526	0.0003	0.11	0.02	MB-I
5402	Kejosmith	21/08/20-21/08/23	22.0, 21.2	346	25	2.694	0.002	0.14	0.03	MB-I
5682	Beresford	21/06/03-21/06/15	4.5, 9.0	251	7	3.774	0.002	0.08	0.03	MC
5972	Harryatkinson	21/06/20-21/07/14	*6.7, 10.6	271	15	3.3889	0.0004	0.12	0.03	MB-M
6307	Maiztegui	21/06/26-21/07/14	8.2, 14	260	10	5.290	0.002	0.27	0.03	MAR
6751	van Genderen	21/07/13-21/07/23	20.5, 16.9	326	6	3.143	0.001	0.57	0.03	MB-I
7784	Watterson	21/06/13-21/06/21	16.0, 17.9	261	24	5.080	0.003	0.12	0.02	MB-I
11452	1980 KE	21/08/03-21/08/07	13.7, 12.3	327	11	3.128	0.003	0.16	0.02	MB-I
14427	1991 VJ2	21/08/09-22/08/15	7.1, 5.5	323	7	6.250	0.007	0.25	0.03	MB-I
15317	1993 HW1	21/04/22-21/05/10	17.0, 7.8	236	9	2.6580	0.0004	0.26	0.03	MB-I
15989	1998 XK39	21/04/06-21/04/30	*9.4, 6.4	211	6	5.528	0.002	0.51	0.03	MB-I
19912	Aurapenenta	21/08/07-21/08/21	22.7, 16.6	348	4	2.7826	0.0005	0.13	0.02	MB-I
140158	2001 SX169	21/06/02-21/06/02	73.4, 45.7	289	11	3.143	0.002	0.62	0.05	NEA

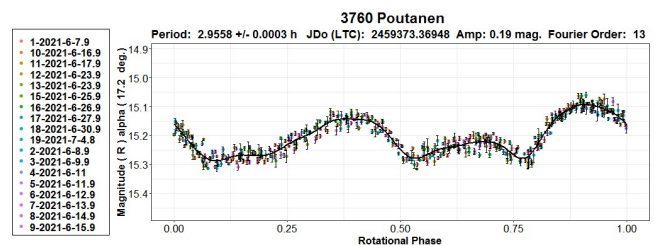
Table I. Observing circumstances and results. Phase is the solar phase angle given at the start and end of the date range. If preceded by an asterisk, the phase angle reached an extrema during the period. LPAB and BPAB are the average phase angle bisector longitude and latitude. Grp is the asteroid family/group (Warner et al., 2009): EOS = Eos, FLOR = Flora, MB-I/M/O = main-belt inner /middle/ outer, MC = Mars Crosser, NEA = near-Earth asteroid, MAR = Maria, HER = Hertha, ASTR = Astraea, HUN = Hungaria.



**2824 Franke.** Franco et al. (2015) found a value of 3.38 h for rotation period. The SAO data from 2021 September confirm this result yielding as secure result a period of  $P = 3.382 \pm 0.002$  h.

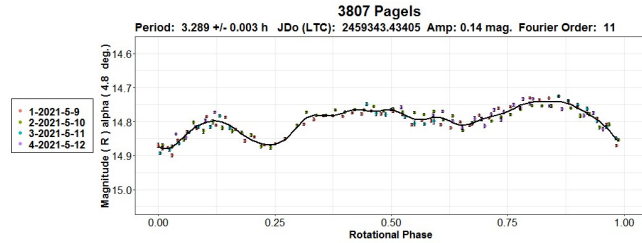


**3760 Poutanen.** A newly established rotation period result ( $P = 2.9558 \pm 0.0003$  h) from the SAO data taken in 2021 June-July is in good agreement with the previous results stated in the LCDB: Salvaggio et al. (2.956 h, 2017), Pal et al. (2.9558 h, 2020) and two previous ones found by Benishek (2.9554 h, 2018 and 2.957 h, 2021).

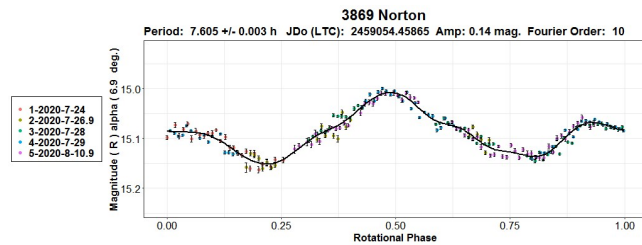


**2926 Caldeira.** The only prior rotation period result is the sidereal value reported more recently by Durech et al. (6.65099 h, 2020). A synodic period value obtained from the 2021 April-May SAO data is:  $P = 6.651 \pm 0.002$  h.

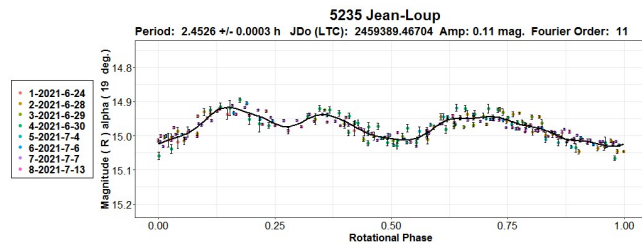
### 3807 Pagels.



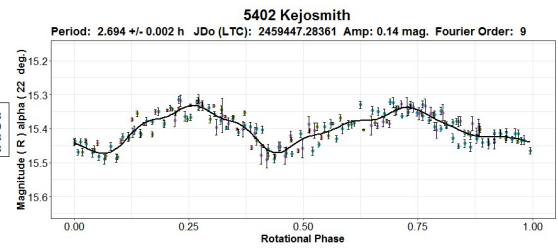
**3869 Norton.** Period analysis conducted over dense photometric data obtained at SAO in 2020 July-August over five nights implies a bimodal period solution of  $P = 7.605 \pm 0.003$  h as the most likely one. The only previous result from Pal et al. (17.0957 h, 2020) is in significant discrepancy with the result presented in this paper.



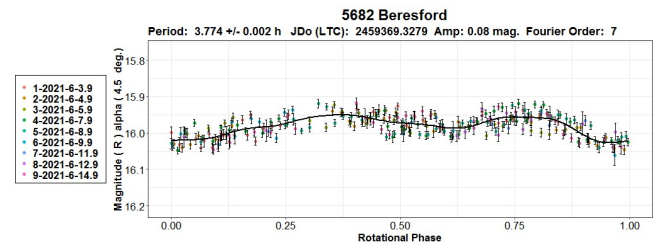
**5235 Jean-Loup.** Another V-type asteroid outside Vesta family. Oszkiewicz et al. (2020) found a period of 2.4524 h. The SAO data from 2021 June-July led to a virtually identical result:  $P = 2.4526 \pm 0.0003$  h.



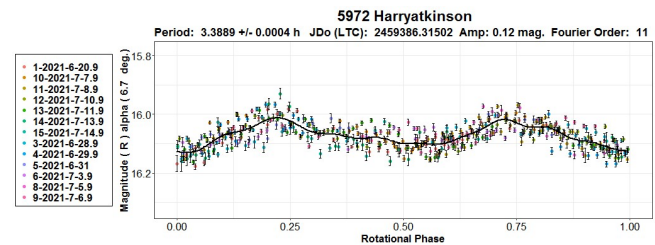
**5402 Kejosmith.** Benishek et al. (2018) photometrically detected a satellite around this inner main belt asteroid during its 2018 apparition. While a primary rotational period was established very well back then (2.69549 h), an ambiguity between the 16.31-hour and 32.62-hour satellite orbital period solutions remained to be resolved in the future. A new opportunity for photometric follow up of this binary target emerged again in 2021 August. Due to increased volume of work on other binary asteroids within the *BinAsterPhot Survey*, 5402 Kejosmith could have been observed to a limited extent and only on four bright Moon nights in the second half of August. Mutual events, which were very shallow in the 2018 apparition (0.03-0.07 mag.) were not observed this time. The cause of this could be somewhat increased noise due to the presence of the bright Moon in the sky, a quite limited amount of data obtained within relatively short observing runs, as well as the possibility that the system was outside the favorable mutual eclipse/occultation event geometry. Despite all the shortcomings of the newly obtained data, they served for a new rotation period determination, which resulted in a bimodal solution of  $P = 2.694 \pm 0.002$  h. This value is in full accordance with the 2018 apparition result.



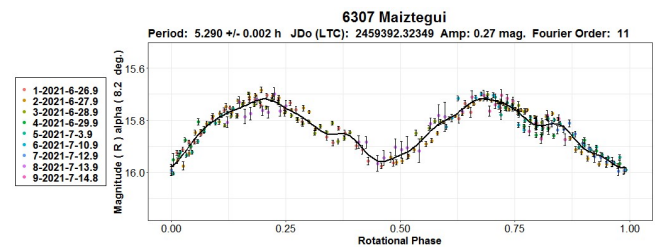
**5682 Beresford.** A rotation period result  $P = 3.774 \pm 0.002$  h found from the quite dense SAO data acquired on nine nights in 2021 June almost coincides with the result reported by Skiff (3.769 h, 2011web). Twice as much value was initially determined by Koff (7.536 h, 2005). Given the low lightcurve amplitude in the 2021 apparition of only 0.08 mag., there is still some uncertainty between the derived period  $P$  and twice the value  $2P$ , which could be resolved by further photometric observations in future apparitions.



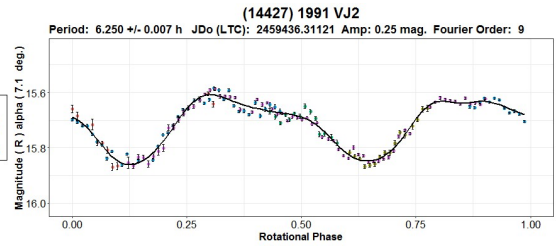
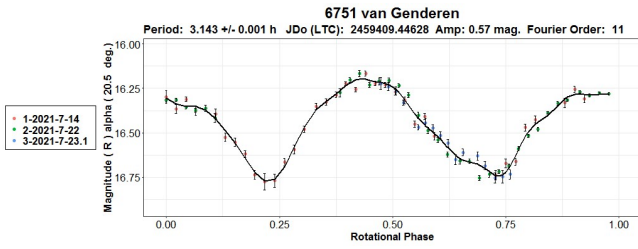
**5972 Harryatkinson.** Bonamico (3.376 h, 2020) and Pal et al. (3.38813 h, 2020) found fairly even period values. The result consistent with these values ( $P = 3.3889 \pm 0.0004$  h) was derived from dense photometric data obtained in 2021 June-July.



### 6307 Maiztegui.

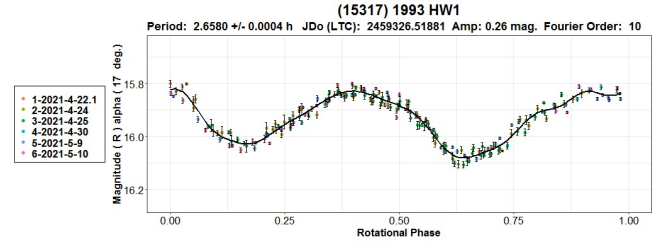


**6751 van Genderen.** The obtained period solution ( $P = 3.143 \pm 0.001$  h) is completely in line with almost all previously found results: Waszczak et al. (3.143 h, 2015), Pal et al. (3.14225 h, 2020) and a sidereal period by Durech et al. (3.142854 h, 2018).



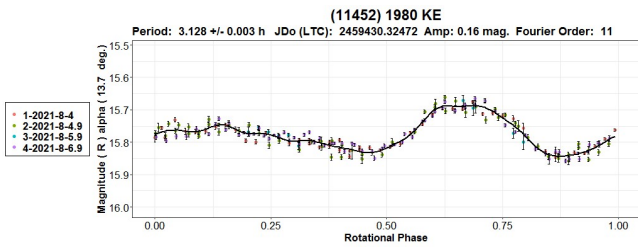
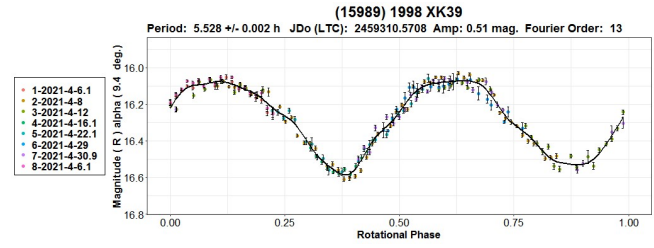
7784 Watterson. Skiff (2011) found a rotation period of 2.539 h. A dense combined photometric dataset was obtained on eight nights in 2021 June which show a value as twice as large as that found by Skiff, i.e.  $P = 5.080 \pm 0.003$  h. Lightcurve associated with this period shows four minima and four maxima per rotational cycle (a quadramodal solution) and a rather small amplitude of 0.12 mag. A split halves plot constructed for the 5.080-hour solution shows a clear difference between the two halves of the lightcurve, indicating its unambiguous plausibility over half the value.

(15317) 1993 HW1. A *BinAstPhot Survey* inner main belt target. The found period ( $P = 2.6580 \pm 0.0004$  h) is fully consistent with other reported results: Pravec (2.6580 h, 2007web), Hawkins and Ditteon (2.660 h, 2008), Pal et al. (2.65804 h, 2020).

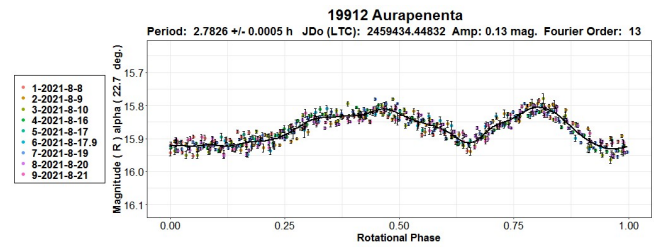


(15989) 1998 XK39. A *BinAstPhot Survey* inner main belt target with no prior rotation period results reported. Eight nights of observations in 2021 April at SAO resulted in a bimodal lightcurve phased to a period of  $P = 5.528 \pm 0.002$  h. Analyzing the same combined dataset Pravec finds a value of 5.52837 h (Pravec, 2021web).

(11452) 1980 KE. Sparse photometry by Waszczak et al. (2015) shows a rotation period of 4.239 h, characterized as likely wrong in the LCDB (an uncertainty flag of  $U = 1$ ). Period analysis of the combined dense photometry dataset obtained over four consecutive nights in 2021 August shows a different result as the most favorable solution:  $P = 3.128 \pm 0.003$  h.

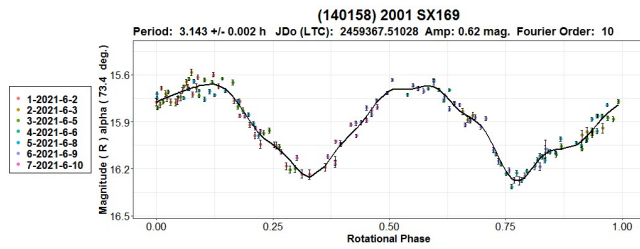


19912 Aurapenenta. Waszczak et al. (2015) derived a period of 2.340 h from sparse photometric dataset. Period analysis conducted over the dense SAO data obtained on nine nights in 2021 August shows a somewhat different bimodal period solution ( $P = 2.7826 \pm 0.0005$  h).



(14427) 191 VJ2. Five datasets obtained at SAO in 2021 August give an unambiguous bimodal solution for period of  $P = 6.250 \pm 0.007$  h. Prior period result by Pal et al. (22.8637 h, 2020) turned out to be incorrect.

(140158) 2001 SX169. This NEA target was observed on seven nights in the first half of 2021 June. The found bimodal period solution of  $P = 3.143 \pm 0.002$  h fully fits the previously reported values by Vecchione et al. (3.1409 h, 2018) and Warner (3.1430 h, 2018b).



### Acknowledgements

Observational work at Sopot Astronomical Observatory is supported by a 2018 Gene Shoemaker NEO Grant from The Planetary Society.

### References

- Behrend, R. (2001web, 2005web, 2006web, 2016web). Observatoire de Geneve web site.  
[http://obswww.unige.ch/~behrend/page\\_cou.html](http://obswww.unige.ch/~behrend/page_cou.html)
- Benishek, V. (2018). "Lightcurve and Rotation Period Determinations for 29 Asteroids." *Minor Planet Bull.* **45**, 82-91.
- Benishek, V.; Pravec, P.; Kucakova, H.; Hornoch, K.; Warner, B.; Oey, J.; Pilcher, F.; Chiorny, V. (2018). "(5402) Kejosmith." *CBET* **4561**.
- Benishek, V. (2021). "Lightcurve and Rotation Period Determinations for 25 Asteroids." *Minor Planet Bull.* **48**, 280-285.
- Bonamico, R. (2020). "Rotational Periods of Five Asteroids." *Minor Planet Bull.* **47**, 222-223.
- Bus, S.J.; Binzel, R.P. (2002). "Phase II of the Small Main-Belt Asteroid Spectroscopic Survey. The Observations." *Icarus* **158**, 106-145.
- Carbo, L.; Green, D.; Kragh, K.; Krotz, J.; Meiers, A.; Patino, B.; Pligge, Z.; Shaffer, N.; Getteon, R. (2009). "Asteroid Lightcurve Analysis at the Oakley Southern Sky Observatory: 2008 October thru 2009 March." *Minor Planet Bull.* **36**, 152-157.
- Ditteon, R.; West, J. (2011). "Asteroid Lightcurve Analysis at the Oakley Southern Observatory: 2011 January thru April." *Minor Planet Bull.* **38**, 214-217.
- Durech, J.; Hanuš, J.; Oszkiewicz, D.; Vančo, R. (2016). "Asteroid Models from the Lowell Photometric Database." *Astron. Astrophys.* **587**, A48.
- Durech, J.; Hanus, J.; Ali-Lagoa, V. (2018). "Asteroid models reconstructed from the Lowell Photometric Database and WISE data." *Astron. Astrophys.* **617**, A57.
- Durech, J.; Tonry, J.; Erasmus, N.; Denneau, L.; Heinze, A.N.; Flewelling, H.; Vanco, R. (2020). "Asteroid models reconstructed from ATLAS photometry." *Astron. Astrophys.* **643**, A59.
- Fauerbach, M.; Brown, A. (2018). "Lightcurve Analysis of Minor Planets 1132 Hollandia, 1184 Gaea, 1322 Copernicus, 1551 Argelander, and 3230 Vampilov." *Minor Planet Bull.* **45**, 240-241.
- Franco, L.; Marchini, A.; Papini, R. (2015). "Lightcurve Analysis for 2824 Franke and 3883 Verbano." *Minor Planet Bull.* **42**, 114.
- Gandolfi, D.; Cigna, M.; Fulvio, D.; Blanco, C. (2009). "CCD and Photon-Counting Photometric Observations of Asteroids Carried Out at Padova and Catania Observatories." *Planetary and Space Science* **57**, 1-9.
- Hawkins, S.; Ditteon, R. (2008). "Asteroid Lightcurve Analysis at the Oakley Observatory - May 2007." *Minor Planet Bull.* **35**, 1-4.
- Higgins, D.; Goncalves, R.M.D. (2007). "Asteroid Lightcurve Analysis at Hunters Hill Observatory and Collaborating Stations - June - September 2006." *Minor Planet Bull.* **34**, 16-18.
- Koff, R.A. (2005). "Lightcurve Photometry of Asteroids 212 Medea, 517 Edith, 3581 Alvarez, 5682 Beresford, and 5817 Robertfraser." *Minor Planet Bull.* **32**, 32-34.
- Menke, J.; Cooney, W.; Gross, J.; Terrell, D.; Higgins, D. (2008). "Asteroid Lightcurve Analysis at Menke Observatory." *Minor Planet Bull.* **35**, 155-160.
- Noschese, A.; Vecchione, A.; Ruocco, N.; Izzo, L. (2018). "Lightcurve Analysis for Minor Planets 1322 Copernicus and 9148 Boriszaitsev." *Minor Planet Bull.* **45**, 70-71.
- Oszkiewicz, D.; Troianskyi, V.; Föhring, D.; Galád, A.; Kwiatkowski, T.; Marciniak, A.; Skiff, B.A.; Geier, S.; Borczyk, W.; Moskovitz, N.A.; Kankiewicz, P.; Gajdoš, Š.; Világi, J.; Polčic, L.; Kluwak, T. and 5 colleagues. (2020). "Spin Rates of V-type Asteroids." *Astron. Astrophys.* **643**, A117.
- Pal, A.; Szakáts, R.; Kiss, C.; Bódi, A.; Bognár, Z.; Kalup, C.; Kiss, L.L.; Marton, G.; Molnár, L.; Plachy, E.; Sárneczky, K.; Szabó, G.M.; Szabó, R. (2020). "Solar System Objects Observed with TESS - First Data Release: Bright Main-belt and Trojan Asteroids from the Southern Survey." *Ap. J. Supl. Ser.* **247**, 26-34.
- Pravec, P. (2007web, 2014web, 2021web). Photometric Survey for Asynchronous Binary Asteroids web site.  
<http://www.asu.cas.cz/~ppravec/newres.txt>
- Pray, D.; Pravec P.; Kusnirak, P.; Cooney, W.; Gross, J.; Terrell, D.; Galad, A.; Gajdos, S.; Vilagi, J.; Durkee, R. (2006). "(2044) Wirt." *CBET* **353**.
- Prokof'eva, V.V.; Demchik, M.I.; Golub', A.I. (1992). "TV Photometry of Asteroids: Brightness Curve of Asteroid 1727 Mette." *Solar System Research* **26**, 373-375.
- R Core Team (2020). R: A language and environment for statistical computing. R Foundation for Statistical Computing, Vienna, Austria. <https://www.R-project.org/>
- Salvaggio, F.; Marchini, A.; Papini, R. (2017). "Rotation Period Determination for 3760 Poutanen and 14309 Defoy." *Minor Planet Bull.* **44**, 354-355.
- Skiff, B.A. (2011web). Posting on CALL web site.  
<https://minplanobs.org/MPInfo/php/call.php>
- Stephens, R.D. (2002). "Photometry of 866 Fatme, 894 Erda, 1108 Demeter, and 3443 Letsungdao." *Minor Planet Bull.* **29**, 2-3.
- Stephens, R.D.; French, L.M. (2011). "878 Mildred Revealed." *Minor Planet Bull.* **38**, 1-2.

Stephens, R.D.; Warner, B.D. (2020). “Main-belt Asteroids Observed from CS3: 2019 July to September.” *Minor Planet Bull.* **47**, 50-60.

Vecchione, A.; Noschese, A.; Catapano, A. (2018). “Lightcurve Analysis and Rotation Period for (140158) 2001 SX169.” *Minor Planet Bull.* **45**, 183-184.

VizieR (2021). <http://vizier.u-strasbg.fr/viz-bin/VizieR>

Warner, B.D.; Harris, A.W.; Pravec, P. (2009). “The Asteroid Lightcurve Database.” *Icarus* **202**, 134-146. Updated 2021 June. <http://www.minorplanet.info/lightcurvedatabase.html>

Warner, B.D. (2012). The MPO Users Guide: A Companion Guide to the MPO Canopus/PhotoRed Reference Manuals. BDW Publishing, Colorado Springs, CO.

Warner, B.D.; Stephens, R.D.; Harris, A.W. (2013). “(1727) Mette.” *CBET* **3402**.

Warner, B.D. (2014). “Asteroid Lightcurve Analysis at CS3-Palmer Divide Station: 2014 January-March.” *Minor Planet Bull.* **41**, 144-155.

Warner, B.D. (2018a). MPO Canopus software, version 10.7.11.3. <http://www.bdwpublishing.com>

Warner, B.D. (2018b). “Near-Earth Asteroid Lightcurve Analysis at CS3-Palmer Divide Station: 2017 October-December.” *Minor Planet Bull.* **45**, 138-147.

Waszczak, A.; Chang, C.-K.; Ofek, E.O.; Laher, R.; Masci, F.; Levitan, D.; Surace, J.; Cheng, Y.-C.; Ip, W.-H.; Kinoshita, D.; Helou, G.; Prince, T.A.; Kulkarni, S. (2015). “Asteroid Light Curves from the Palomar Transient Factory Survey: Rotation Periods and Phase Functions from Sparse Photometry.” *Astron. J.* **150**, A75.

Wisniewski, W.Z.; McMillan, R.S. (1987). “Differential CCD Photometry of Faint Asteroids in Crowded Star Fields and Nonphotometric Sky Conditions.” *Astron. J.* **93**, 1264.

Wisniewski, W.Z.; Michalowski, T.M.; Harris, A.W.; McMillan, R.S. (1997). “Photometric Observations of 125 Asteroids.” *Icarus* **126**, 395-449.

## LIGHTCURVES OF SEVEN ASTEROIDS

Eric V. Dose  
3167 San Mateo Blvd NE #329  
Albuquerque, NM 87110  
[mp@ericdose.com](mailto:mp@ericdose.com)

(Received: 2021 October 13)

We present lightcurves, synodic rotation periods, and G value (H-G) estimates for seven asteroids.

We present asteroid lightcurve photometry results obtained by following the workflow process described by Dose (2020a), with later improvements (Dose, 2020b). This workflow applies to each image an ensemble of typically 20-60 nearby ATLAS refcat2 catalog (Tonry et al, 2018) comparison (“comp”) stars as a basis for asteroid photometry. Diagnostic plots and numerous comp stars allow for effective identification and removal of outlier, variable, and poorly measured comp stars.

The custom workflow produces a time series of asteroid magnitude estimates on Sloan r’ (SR) catalog basis, unreduced and without H-G adjustment. These magnitudes are imported directly into *MPO Canopus* software (Warner, 2018, version 10.8.4.11) where they are adjusted for distances and phase-angle dependence, fit by Fourier analysis including identifying and ruling out of aliases, and plotted. Phase-angle dependence is corrected with a H-G model, using the G value that minimizes fit RMS error across all nights’ data.

No nightly zero-point adjustments (DeltaComps in *MPO Canopus* terminology) were made to any session herein, other than by adjusting the G value (H-G phase model). All lightcurve data herein have been submitted to ALCDEF.

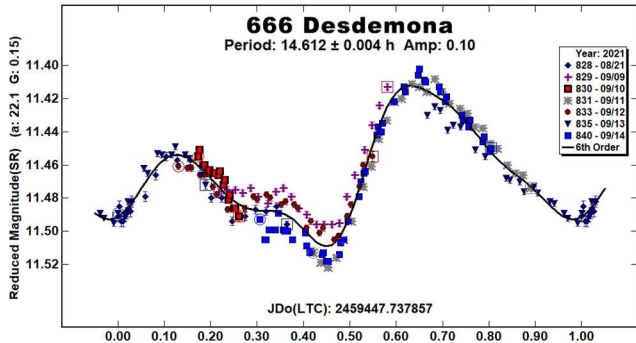
### Lightcurve Results

Seven asteroids were observed from Deep Sky West observatory (IAU V28) at 2210 meters elevation in northern New Mexico. Images were acquired with a 0.35-meter SCT reduced to f/7.7; a SBIG STXL-6303E camera cooled to -35 C and fitted with a Clear filter (Astrodon); and a PlaneWave L-500 mount. The equipment was operated remotely via ACP software (DC-3 Dreams, version 8.3), running plan files generated for each night by the author’s python scripts (Dose, 2020a). Observations often cycled among 2-4 asteroids. Exposure times targeted 5-8 millimagnitudes uncertainty in asteroid instrumental magnitude, subject to a minimum of 120 seconds to ensure suitable comp-star photometry, and to a maximum of 900 seconds. All exposures were autoguided.

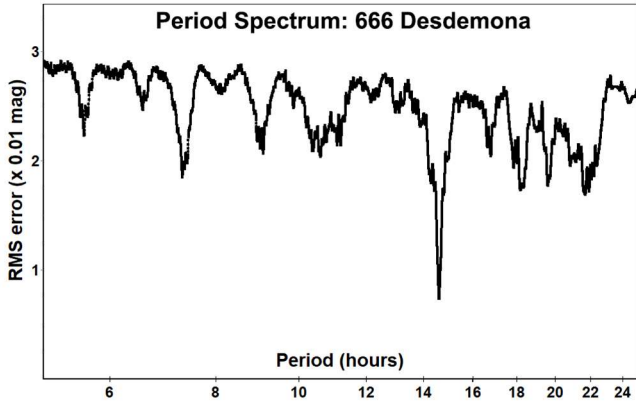
FITS images were plate-solved by *PinPoint* (DC-3 Dreams) or *TheSkyX* (Software Bisque) and were calibrated using temperature-matched, median-averaged dark images and recent flat images of a flux-adjustable flat panel. Every photometric image was visually inspected; all images with poor tracking, obvious interference by cloud or moon, or having stars or other light sources within 10 arcseconds of the target asteroid were excluded. Photometry-ready images that pass these screens were submitted to the workflow, which applies separately measured second-order transforms from Clear filter to deliver asteroid magnitudes in Sloan r’ passband.

In this work, “period” refers to an asteroid’s synodic rotation period, and “SR” denotes the Sloan r’ passband.

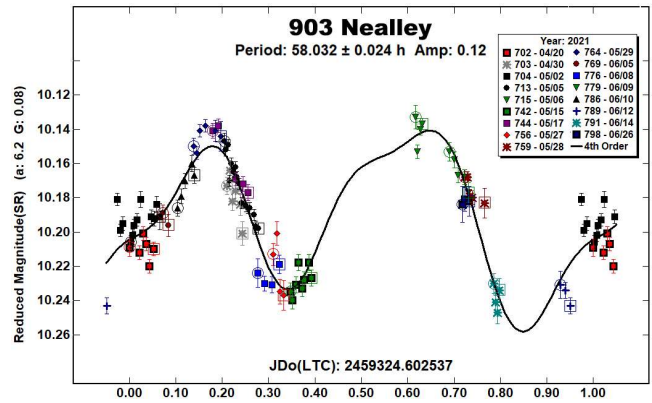
**666 Desdemona.** This relatively bright inner main-belt asteroid was found to have synodic rotation period  $14.612 \pm 0.004$  hours, in agreement with two previous reports (14.607 h, Marciniak et al, 2015; 14.5995 h, Pál et al, 2020), but differing from others (15.45 h, Stephens, 2001; 9.6 h, Behrend 2004web, Behrend 2005web, and Behrend 2006web).



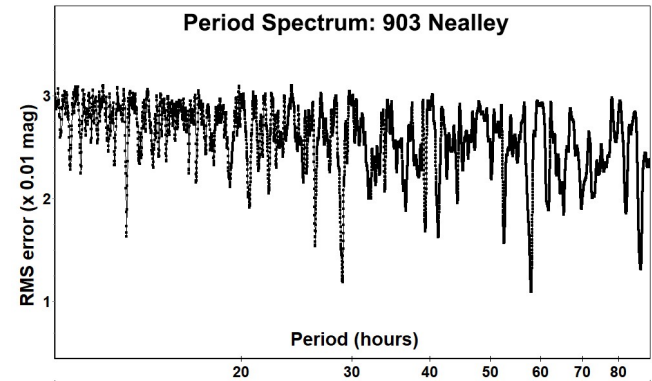
Fourier fit to the present data has RMS error of 7 millimagnitudes and indicates a G value (H-G phase model) close to 0.15. The period spectrum disfavors 15.45 h and 9.6 h candidate solutions, neither of which is an obvious alias of the present solution.



**903 Nealley.** This outer main-belt asteroid was found to have a rotational period of  $58.032 \pm 0.024$  h, at wide variance from previous reports (21.60 h, Warner, 2004; 19.72 h or 19.58 h, Warner, 2012; 16.2 h, Behrend, 2020web; 28.9882 h, Pál et al, 2020). Fourier fit to the present data has RMS error of 11 millimagnitudes and is optimized at G value of 0.08.



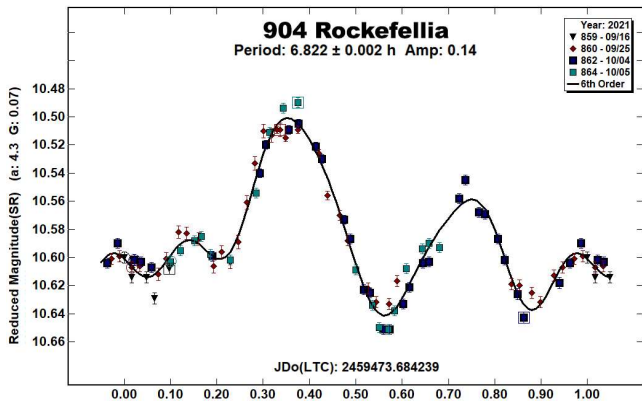
Even with 17 nights' observations, lightcurve phase coverage was incomplete. Even so, the period spectrum does not support periods shorter than about 26 hours. The coverage gap at present phases of 0.40 to 0.58 allows for a possible monomodal period of 29.016 h, which would agree with the result of Pál et al, but the present data slightly favor the 58.032 h bimodal period. The other previously reported periods are not readily explained as aliases of these monomodal or bimodal period candidates.



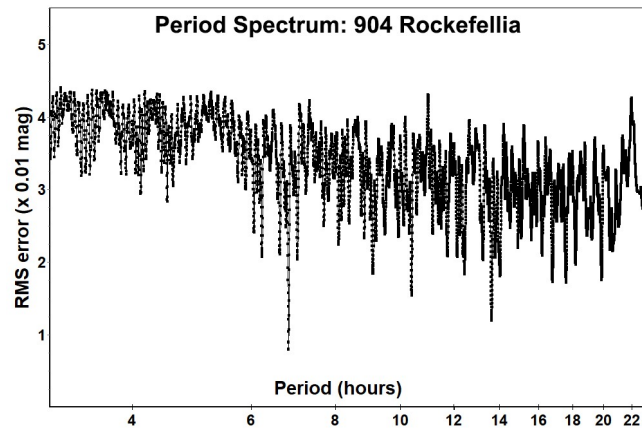
**904 Rockefelleria.** This outer main-belt asteroid was found to have rotation period of  $6.822 \pm 0.002$  h, in agreement with both determinations by Polakis (6.826 h, Polakis, 2018; 6.82 h, Polakis, 2020) but at variance with other previous reports (4.93 h, Koff, 2004web; 14.04 h, Behrend, 2009web; 5.823 h, Fauvaud and Fauvaud, 2013; 14.04 h, Behrend, 2014web; and 14.038 h, Behrend, 2020web). Our Fourier fit has RMS error of 8 millimagnitudes and suggests G of 0.08.

Number	Name	yyyy mm/dd	Phase	L <sub>PAB</sub>	B <sub>PAB</sub>	Period(h)	P.E.	Amp	A.E.	Grp
666	Desdemona	2021 08/21-09/14	21.9, 12.3	9	6	14.612	0.004	0.10	0.02	MB-I
903	Nealley	2021 04/20-06/26	6.5, 17.4	195	9	58.032	0.024	0.12	0.03	MB-O
904	Rockefelleria	2021 09/16-10/05	4.4, 9.9	348	9	6.822	0.002	0.14	0.02	MB-O
1990	Pilcher	2021 08/06-08/26	*7.3, 4.4	327	3	2.841	0.001	0.13	0.02	FLOR
3932	Edshay	2021 09/03-09/08	15.5, 13.7	10	12	3.431	0.001	0.33	0.02	EUN
4826	Wilhelms	2021 03/29-08/07	*21.7, 28.9	238	20	15.004	0.002	0.84	0.04	PHO
7328	Casanova	2021 08/21-09/11	20.5, 11.2	6	-1	9.122	0.002	0.46	0.03	EUN

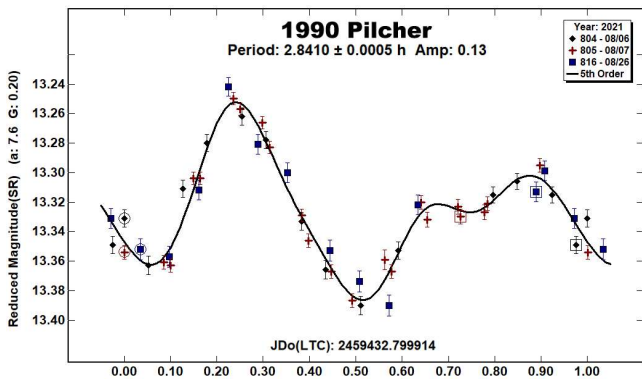
Table I. Observing circumstances and results. The phase angle is given for the first and last date. If preceded by an asterisk, the phase angle reached an extrema during the period. L<sub>PAB</sub> and B<sub>PAB</sub> are the approximate phase angle bisector longitude/latitude at mid-date range (see Harris et al., 1984). Grp is the asteroid family/group (Warner et al., 2009).



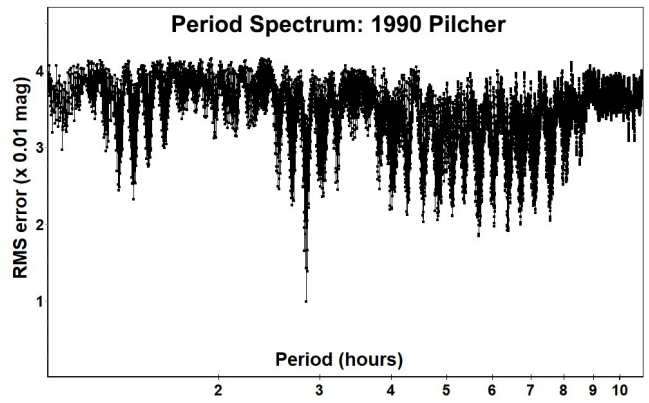
The other, previously reported period candidates are neither supported by the present period spectrum, nor readily explained as aliases of the present solution. The second-best solution in the period spectrum is simply twice the period proposed here.



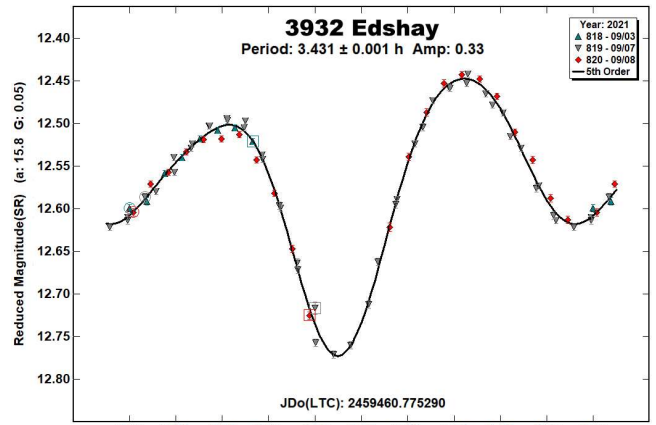
1990 Pilcher. Only one previous report exists of rotational period for this Flora asteroid; it is listed in the LCDB as ambiguous, between 3.895 h and 2.842 h (Brincat and Grech, 2017). We confirm the latter with a new report of period  $2.8410 \pm 0.0005$  h. Our Fourier fit has RMS error of 10 millimag and suggests G of 0.20.



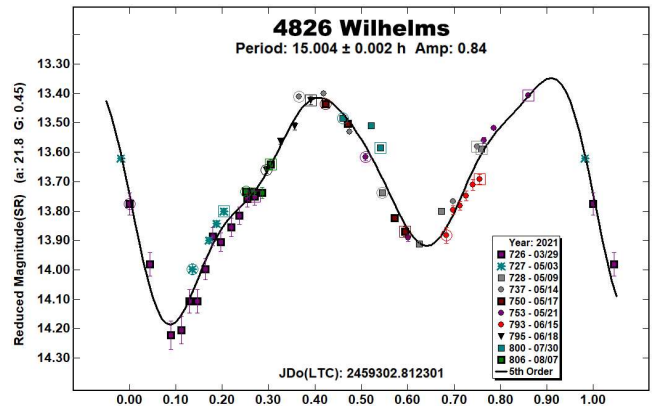
Our period spectrum benefited from two periods' coverage on the second night; it does not support the 3.895 h period candidate.



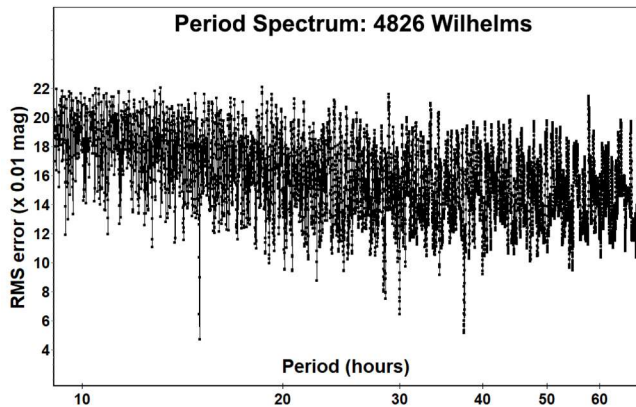
3932 Edshay. We report a rotational period of  $3.431 \pm 0.001$  h for this Eunomia asteroid, confirming both previous reports (3.432 h, Waszczak et al, 2015; 3.444 h, Behrend, 2017web). The lightcurve is clearly bimodal. Our Fourier fits yielded RMS error of 7 millimag and G value of 0.05.



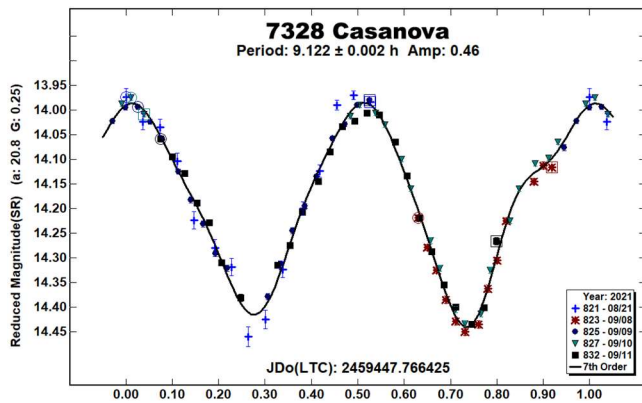
4826 Wilhelms. For this Phocaea asteroid, we find a rotational period of  $15.004 \pm 0.002$  h and a large amplitude of 0.84 magnitudes, in disagreement with the sole known previous report of 54 h (Pravec et al., 2012web). Our Fourier fit has RMS error of 47 millimag. G value is approximately 0.45.



Despite 10 nights' observations over 18 weeks, the period spectrum remains noisy - signals do appear for periods of 2 and 2.5 times our report of 15.004 h, and we cannot rule these out, although the lightcurve shape at our proposed period is entirely reasonable. Our spectrum does, however, strongly disfavor the candidate period of 54 hours.



**7328 Casanova.** For this Eunomia asteroid, we confirm the sole known previous period report of 9.122 h (Waszczak et al, 2015) with our own finding of  $9.122 \pm 0.002$  h. Our Fourier fits yielded RMS error of 18 millimagitudes and G of 0.25.



#### Acknowledgements

The author thanks all authors of the ATLAS paper (Tonry et al, 2018) and its numerous contributors for providing without cost the ATLAS refcat2 catalog release. This project makes extensive use of the python language interpreter and of several supporting packages (notably: pandas, ephem, matplotlib, requests, astropy, and statsmodels), all provided without cost.

#### References

- Behrend, R. (2004web, 2005web, 2006web, 2009web, 2014web, 2017web, 2020web). Observatoire de Genève web site. [http://obswww.unige.ch/~behrend/page\\_cou.html](http://obswww.unige.ch/~behrend/page_cou.html)
- Brincat, S.M.; Grech, W. (2017). "Photometric Observations of Main-Belt Asteroids 1990 Pilcher and 8443 Svecica." *Minor Planet Bull.* **44**, 287-288.
- Dose, E. (2020a). "A New Photometric Workflow and Lightcurves of Fifteen Asteroids." *Minor Planet Bull.* **47**, 324-330.
- Dose, E. (2020b). "Lightcurves of Nineteen Asteroids." *Minor Planet Bull.* **48**, 69-76.

Fauvaud, S.; Fauvaud, M. (2013). "Photometry of Minor Planets. I. Rotation Periods from Lightcurve Analysis for Seven Main-Belt Asteroids." *Minor Planet Bull.*, **40**, 224-229.

Harris, A.W.; Young, J.W.; Scaltriti, F.; Zappalà, V. (1984). "Lightcurves and phase relations of the asteroids 82 Alkmene and 444 Gyptis." *Icarus* **57**, 251-258.

Koff, R.A. (2004web). Posting on the CALL web site. <https://minplanobs.org/MPInfo/php/callsearch.php>

Marciniak, A. and 23 colleagues (2015). "Against the biases in spins and shapes of asteroids." *Planetary Space Sci.*, **118**, 256-266.

Pál, A.; Szakáts, R.; Kiss, C.; Bódi, A.; Bogárn, Z.; Kalup, C.; Kiss, L.L.; Marton, G.; Molnár, L.; Plachy, E.; Sárneczky, K.; Szabó, G. M.; Szabó, R. (2020). "Solar System Objects Observed with TESS - First Data Release: Bright Main-belt and Trojan Asteroids from the Southern Survey." *Astrophys. J. Suppl. Series* **247**, 26.

Polakis, T. (2018). "Lightcurve Analysis for Eleven Main-Belt Asteroids." *Minor Planet Bull.*, **45**, 199-203.

Polakis, T. (2020). "Photometric Observations of Twenty-Seven Minor Planets." *Minor Planet Bull.*, **47**, 314-321.

Pravec, P.; Wolf, M.; Sarounova, L. (2012). Ondrejov Asteroid Photometry Project. <http://www.asu.cas.cz/~ppravec/newres.txt>

Stephens, R.D. (2001). "Rotational Periods and Lightcurves of 1277 Dolores, 666 Desdemona, and (7505) 1997 AM2." *Minor Planet Bull.* **28**, 28-29.

Tonry, J.L.; Denneau, L.; Flewelling, H.; Heinze, A.N.; Onken, C.A.; Smartt, S.J.; Stalder, B.; Weiland, H.J.; Wolf, C. (2018). "The ATLAS All-Sky Stellar Reference Catalog." *Astrophys. J.* **867**, A105, 1-16.

Warner, B.D. (2004). "Lightcurve Analysis for Numbered Asteroids 863, 903, 907, 928, 977, 1386, 2841, and 75747." *Minor Planet Bull.* **31**, 85-88.

Warner, B.D.; Harris, A.W.; Pravec, P. (2009). "The asteroid lightcurve database." *Icarus*, **202**, 134-146. Updated 2020 August. <http://www.minorplanet.info/lightcurvedatabase.html>

Warner, B.D. (2012). "Asteroid Lightcurve Analysis at the Palmer Divide Observatory: 2011 June - September." *Minor Planet Bull.* **39**, 16-21.

Warner, B.D. (2018). MPO Canopus Software, version 10.8.4.11, BDW Publishing. <http://www.bdwpublishing.com>

Waszczak, A.; Chang, C.-K.; Ofek, E.O.; Laher, R.; Masci, F.; Levitan, D.; Surace, J.; Cheng, Y.-C.; Ip, W.-H.; Kinoshita, D.; Helou, G.; Prince, T.A.; Kulkarni, S. (2015). "Asteroid Light Curves from the Palomar Transient Factory Survey: Rotation Periods and Phase Functions from Sparse Photometry." *Astron. J.* **150**, 75.

## PHOTOMETRY AND LIGHT CURVE ANALYSIS OF EIGHT ASTEROIDS BY GORA'S OBSERVATORIES.

Milagros Colazo

Instituto de Astronomía Teórica y Experimental  
(IATE-CONICET), ARGENTINA

Facultad de Matemática, Astronomía y Física,  
Universidad Nacional de Córdoba, ARGENTINA

Grupo de Observadores de Rotaciones de Asteroides (GORA),  
ARGENTINA

[milirita.colazovinovo@gmail.com](mailto:milirita.colazovinovo@gmail.com)

Mario Morales, César Fornari, Andrés Chapman, Alberto García,  
Francisco Santos, Raúl Melia, Néstor Suárez, Ariel Stechina,  
Damián Scotta, Matías Martini, Marcos Santucho,  
Alejandro Moreschi, Aldo Wilberger, Aldo Mottino,  
Ezequiel Bellocchio, Cecilia Quiñones, Tiago Speranza,  
Ricardo Llanos, Leopoldo Altuna, Macarena Caballero,  
Fabricio Romero, Carlos Galarza, Carlos Colazo.

Grupo de Observadores de Rotaciones de Asteroides (GORA),  
ARGENTINA

Estación Astrofísica Bosque Alegre (MPC 821) -  
Bosque Alegre (Córdoba- ARGENTINA)

Observatorio Astronómico Giordano Bruno (MPC G05) -  
Piconcillo (Córdoba-ESPAÑA)

Observatorio Cruz del Sur (MPC I39)  
San Justo (Buenos Aires- ARGENTINA)

Observatorio de Sencelles (MPC K14)  
Sencelles (Mallorca-Islas Baleares-ESPAÑA)

Observatorio Los Cabezones (MPC X12)  
Santa Rosa (La Pampa- ARGENTINA)

Observatorio Orbis Tertius (MPC X14)  
Córdoba (Córdoba- ARGENTINA)

Observatorio Galileo Galilei (MPC X31)  
Oro Verde (Entre Ríos- ARGENTINA)

Observatorio Antares (MPC X39)  
Pilar (Buenos Aires- ARGENTINA)

Observatorio AstroPilar (GORA APB)  
Pilar (Buenos Aires- ARGENTINA)

Observatorio Astronómico Calchaquí (GORA OAC)  
El Bañado (Tucumán- ARGENTINA)

Observatorio de Aldo Mottino (GORA OAM)  
Rosario (Santa Fe- ARGENTINA)

Observatorio Astronómico Aficionado Omega (GORA OAO)  
Córdoba (Córdoba- ARGENTINA)

Observatorio de Ariel Stechina 1 (GORA OAS)  
Reconquista (Santa Fe- ARGENTINA)

Observatorio de Ariel Stechina 2 (GORA OA2)  
Reconquista (Santa Fe- ARGENTINA)

Observatorio de Damián Scotta 1 (GORA ODS)  
San Carlos Centro (Santa Fe- ARGENTINA)

Observatorio de Damián Scotta 2 (GORA OD2)  
San Carlos Centro (Santa Fe- ARGENTINA)

Observatorio Chopis (GORA OMI) -  
Alta Gracia (Córdoba- ARGENTINA)

Observatorio Astronómico Municipal Reconquista (GORA OMR)  
Reconquista (Santa Fe- ARGENTINA)

Observatorio Río Cofio (GORA ORC)  
Robledo de Chavela (Madrid-ESPAÑA)

Observatorio de Raúl Melia (GORA RMG)  
Gálvez (Santa Fe- ARGENTINA)

(Received: 2021 Sep 28)

Synodic rotation periods and amplitudes are reported for 128 Nemesis, 236 Honoria, 329 Svea, 1021 Flammario, 1026 Ingrid, 1034 Mozartia, 1938 Lausanna, and (285571) 2000 PQ9.

The periods and amplitudes of asteroid lightcurves presented here are the product of collaborative work by GORA (Grupo de Observadores de Rotaciones de Asteroides) group. In all the studies, we have applied relative photometry assigning V magnitudes to the calibration stars.

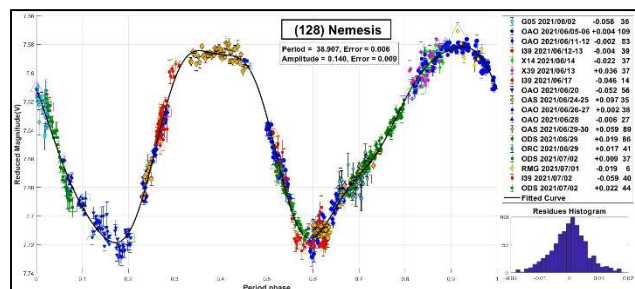
Image acquisition was performed without filters and with exposure times of a few minutes. All images used were corrected using dark frames and, in some cases, bias and flat-field were also used. Photometry measurements were performed using *FotoDif* software and, for the analysis, we employed *Periodos* software (Mazzone, 2012).

Below, we present the results for each asteroid under study. The lightcurve figures contain the following information: the estimated period and period error and the estimated amplitude and amplitude error. In the reference boxes, the columns represent, respectively, the marker, observatory MPC code, or - failing that - the GORA internal code, session date, session offset, and several data points.

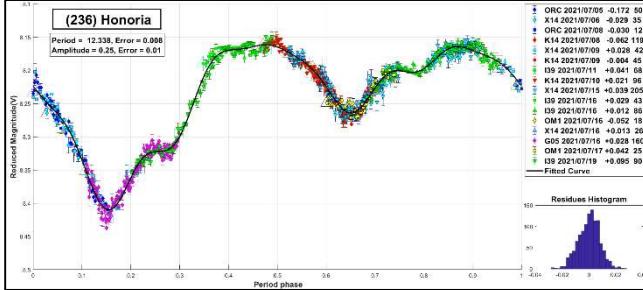
Targets were selected based on the following criteria: 1) those asteroids with magnitudes accessible to the equipment of all participants, 2) those with favorable observation conditions from Argentina or Spain, i.e., with negative or positive declinations  $\delta$ , respectively, and 3) objects with few periods reported in the literature and/or with Lightcurve Database (LCDB) (Warner et al., 2009) quality codes (U) of less than 3.

128 Nemesis is a C-type asteroid. It was discovered in 1872 by James Craig Watson. Our analysis yields a period  $P = 38.907 \pm 0.006$  h with  $\Delta m = 0.140 \pm 0.009$  mag. In previous observations, Scaltriti et al. (1979) reported a period  $P = 39$  h and Pilcher (2015) a period  $P = 77.81 \pm 0.01$  h.

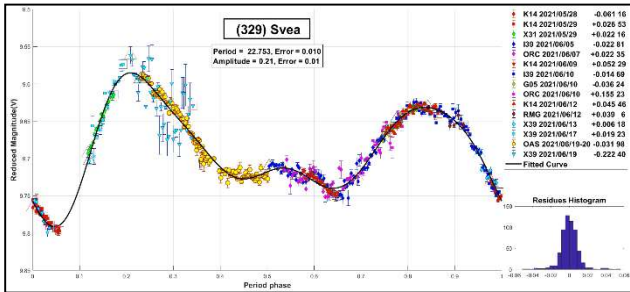
Note that our period is in good agreement with the one reported by Scaltriti et al. and is half the one measured by Pilcher. Irrespective of such dissimilarities, it is clear that this asteroid constitutes a long period example.



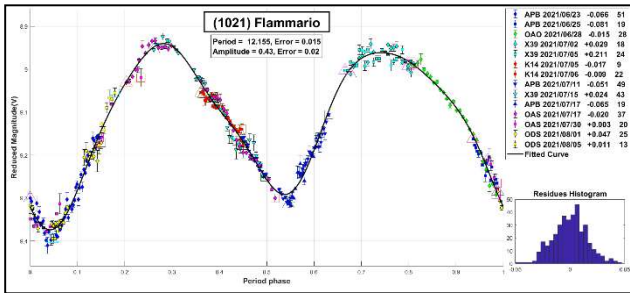
236 Honoria is an S-type asteroid. It was discovered in 1884 by Johann Palisa. We found in the literature two different periods calculated for this object:  $P = 12.338 \pm 0.002$  h with  $\Delta m = 0.27 \pm 0.02$  mag (Marciniak et al., 2014) and  $P = 16.8 \pm 0.1$  h with  $\Delta m = 0.05 \pm 0.01$  mag (Behrend, 2006web). The results we obtained are  $P = 12.338 \pm 0.008$  h and  $\Delta m = 0.25 \pm 0.01$  mag, with full coverage of the lightcurve. Our period agrees well with the one measured by Marciniak et al. (2014).



329 Svea is classified as type C in the Tholen taxonomy. It was discovered by Max Wolf in 1892. Two different periods were reported in the literature. Marciniak et al. (2017) found a period of  $22.778 \pm 0.006$  h, whereas Pray (2006) measured a period of  $P = 15.201 \pm 0.005$  h. We have determined a period of  $22.753 \pm 0.010$  h, which is consistent with the one proposed by Marciniak.

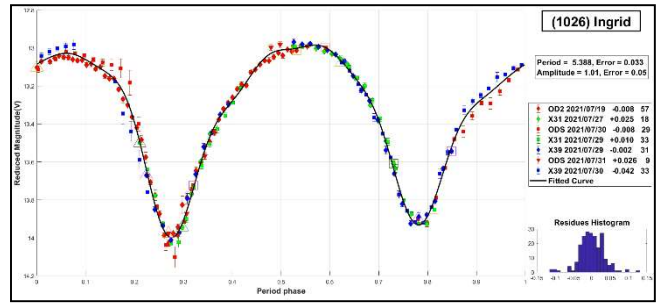


1021 Flammario is an F-type asteroid, discovered in 1924 by Max Wolf. The period more recently reported in the literature is  $P = 12.15186 \pm 0.00005$  h (Hanus et al., 2016).

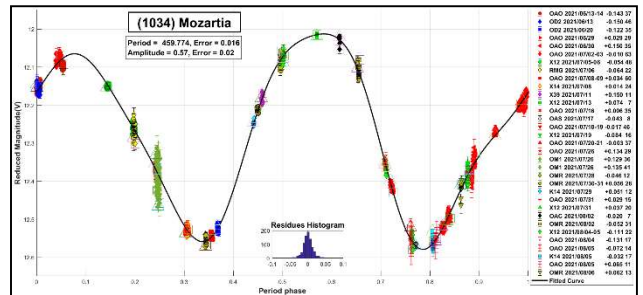


The results we obtained are  $P = 12.155 \pm 0.015$  h and  $\Delta m = 0.43 \pm 0.02$  mag. Our period agrees well with the one measured by Hanus et al. (2016).

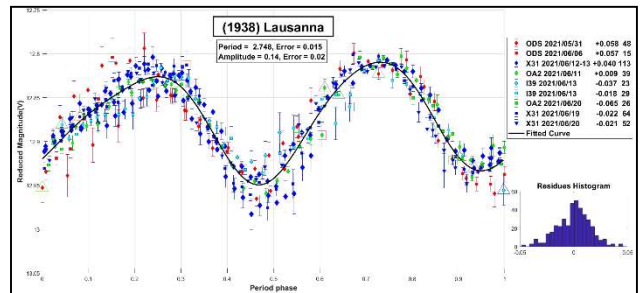
1026 Ingrid was discovered in 1923 by Karl Wilhelm Reinmuth. We measured a period of  $5.388 \pm 0.033$  h with  $\Delta m = 1.01 \pm 0.05$  mag. A similar period was previously reported by Székely et al. (2005), consisting of  $P = 5$  h. A large amplitude was also reported by these authors, resulting in  $\Delta m > 0.5$  mag.



1034 Mozartia is an S-type asteroid in the Bus-taxonomy, discovered in 1924 by Vladimír Albitski. Interestingly, we couldn't find a reported period for this object in the literature. According to our observations and after a thorough analysis, we propose a long-term period of  $P = 459.774 \pm 0.016$  h and  $\Delta m = 0.57 \pm 0.02$  mag. As can be seen, we have performed numerous observations on this object, with permanent generation of ephemeris to fill the gaps, which successfully allowed us to complete the curve. More important, we have observations on consecutive days, using same calibration stars, so that they were taken as a single observation. That way we were able to solve the puzzle related to this slow rotator.



1938 Lausanna is an S-type asteroid. It was discovered in 1974 by Paul Wild. The period reported in the literature is  $P = 2.748 \pm 0.001$  h with  $\Delta m = 0.12 \pm 0.02$  mag (Warell and Pappini, 2015). Our observations resulted in  $P = 2.748 \pm 0.015$  h with  $\Delta m = 0.14 \pm 0.02$  mag, consistent with a short-period asteroid, and in good agreement with the results from Warell & Pappini.



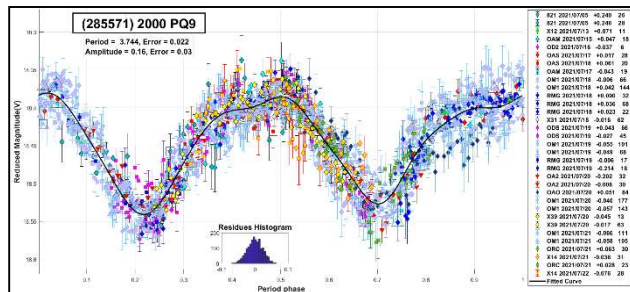
(285571) 2000 PQ9 was discovered in 2000 by LINEAR. It is a poorly studied object. Here we propose a candidate period of  $P = 3.744 \pm 0.022$  h and  $\Delta m = 0.16 \pm 0.03$  mag. This fast rotator hypothesis is consistent with its small estimated diameter of  $\sim 1$  km. Also, it is important to note that we have performed several observations on this object leading to a very good coverage of the lightcurve.

Number	Name	yy/mm/dd	Phase	$L_{PAB}$	$B_{PAB}$	Period(h)	P.E.	Amp	A.E.	Grp
128	Nemesis	21/06/02-21/07/02	2.6,13.2	245	1	38.907	0.006	0.14	0.01	MB-O
236	Honorina	21/07/05-21/07/19	9.9,5.4	301	10	12.338	0.008	0.25	0.01	MB-O
329	Svea	21/05/28-21/06/20	10.3,16.0	241	19	22.753	0.010	0.21	0.01	MB-I
1021	Flammario	21/06/23-21/08/05	*5.5,11.9	283	4	12.155	0.015	0.43	0.02	MB-O
1026	Ingrid	21/07/19-21/07/30	3.0,9.8	293	-2	5.388	0.033	1.01	0.05	FLOR
1034	Mozartia	21/06/13-21/08/06	*20.4,12.0	294	-2	459.774	0.016	0.57	0.02	MB-I
1938	Lausanna	21/05/31-21/06/20	*5.0,9.9	255	5	2.748	0.015	0.14	0.02	FLOR
285571	2000 PQ9	21/07/05-21/07/22	*35.3,6.7	287	-11	3.744	0.022	0.16	0.03	NEA

Table I. Observing circumstances and results. The phase angle is given for the first and last date. If preceded by an asterisk, the phase angle reached an extremum during the period.  $L_{PAB}$  and  $B_{PAB}$  are the approximate phase angle bisector longitude/latitude at mid-date range (see Harris et al., 1984). Grp is the asteroid family/group (Warner et al., 2009). MB-I/O: main-belt inner/outer.

Observatory	Telescope	Camera
821 Est.Astrof.Bosque Alegre	Telesc. Newtoniano (D=1540mm; f=4.9)	CCD APOGEE Alta U9
G05 Obs.Astr.Giordano Bruno	Telesc. SCT (D=203mm; f=6.0)	CCD Atik 420 m
I39 Obs.Astr.Cruz del Sur	Telesc. Newtoniano (D=254mm; f=4.7)	CMOS QHY174
K14 Obs.Astr.de Sencelles	Telesc. Newtoniano (D=250mm; f=4.0)	CCD SBIG ST-7XME
X12 Obs.Astr.Los Cabezones	Telesc. Newtoniano (D=200mm; f=5.0)	CMOS QHY174MGPS
X14 Obs.Astr.Orbis Tertius	Telesc. Newtoniano (D=200mm; f=5.0)	CCD QHY6 Mono
X31 Obs.Astr.Galileo Galilei	Telesc. RCT ap (D=405mm; f=8.0)	CCD SBIG STF8300M
X39 Obs.Astr.Antares	Telesc. Newtoniano (D=250mm; f=4.7)	CCD QHY9 Mono
APB Obs.Astr.AstroPilar	Telesc. Refractor (D=150mm; f=7.0)	CCD ZWO-ASI183
OAC Obs.Astr.Calchaquí	Telesc. GSO RC (D=203mm; f=8.0)	CCD QHY9S
OAM Obs.Astr.de Aldo Mottino	Telesc. Newtoniano (D=250mm; f=4.7)	CCD SBIG STF8300M
OA0 Obs.Astr.Aficionado Omega	Telesc. Newtoniano (D=150mm; f=5.0)	CMOS ZWO ASI178mm
OAS Obs.Astr.de Ariel Stechina 1	Telesc. Newtoniano (D=254mm; f=4.7)	CCD SBIG STF402
OA2 Obs.Astr.de Ariel Stechina 2	Telesc. Newtoniano (D=305mm; f=5.0)	CMOS QHY 174M
ODS Obs.Astr.de Damián Scotta 1	Telesc. Newtoniano (D=300mm; f=4.0)	CCD SBIG St-402 XME
OD2 Obs.Astr.de Damián Scotta 2	Telesc. Newtoniano (D=250mm; f=4.0)	CCD Atik 314L+
OM1 Obs.Astr.Chopis	Telesc. Newtoniano (D=200mm; f=4.5)	CMOS Nikon D5200
OMR Obs.Astr.Municipal Reconquista	Telesc. Newtoniano (D=254mm; f=4.0)	CMOS QHY5 Mono
ORC Obs.Astr.Río Cofio	Telesc. SCT (D=254mm; f=6.3)	CCD SBIG ST8-XME
RMG Obs.Astr.de Raúl Melia	Telesc. Newtoniano (D=254mm; f=4.7)	CCD Meade DSI Pro II

Table II. List of observatories and equipment.



#### Acknowledgements

We want to thank Julio Castellano as we use his *FotoDif* program for preliminary analyses, Fernando Mazzone for his *Periods* program, used in final analyses, and Matias Martini for his *CalculadorMDE\_v0.2* used for generating ephemeris used in the planning stage of the observations.

This research has made use of the Small Bodies Data Ferret (<http://sbn.psi.edu/ferret/>), supported by the NASA Planetary System. This research has made use of data and/or services provided by the International Astronomical Union's Minor Planet Center.

#### References

- Behrend, R. (2006web). Observatoire de Geneve web site. [http://obswww.unige.ch/~behrend/page\\_cou.html](http://obswww.unige.ch/~behrend/page_cou.html)
- Hanuš, J.; Ďurech, J.; Oszkiewicz, D.A.; Behrend, R.; Carry, B.; and 164 colleagues (2016). "New and updated convex shape models of asteroids based on optical data from a large collaboration network." *Astronomy & Astrophysics* **586**, A108.
- Harris, A.W.; Young, J.W.; Scaltriti, F.; Zappala, V. (1984). "Lightcurves and phase relations of the asteroids 82 Alkmene and 444 Gyptis." *Icarus* **57**, 251-258.
- Marciniak, A.; Pilcher, F.; Santana-Ros, T.; Oszkiewicz, D.; Kankiewicz, P. (2014). *ACM 2014*, Poster 57.
- Marciniak, A.; Pilcher, F.; Oszkiewicz, D.; Santana-Ros, T.; Urakawa, S.; and 19 colleagues (2017). "Against the biases in spins and shapes of asteroids." *Planetary and Space Science* **118**, 256-266.
- Mazzone, F.D. (2012). *Periodos* software, version 1.0. <http://www.astrosurf.com/salvador/Programas.html>
- Pilcher, F. (2015). "New Photometric Observations of 128 Nemesis, 249 Ise, and 279 Thule." *Minor Planet Bulletin* **42**, 190-192.

Pray, D.P. (2006). "Lightcurve analysis of asteroids 326, 329, 426, 619, 1829, 1967, 2453, 10518 and 42267." *Minor Planet Bulletin* **33**, 4-5.

Scaltriti, F.; Zappalà, V.; Schober, H.J. (1979). "The rotations of 128 Nemesis and 393 Lampetia: The longest known periods to date." *Icarus* **37**, 133-141.

Székely, P.; Kiss, L.L.; Szabó, Gy.M.; Sárneczky, K.; Csák, B.; Váradi, M.; Mészáros, Sz. (2005). "CCD photometry of 23 minor planets." *Planetary and Space Science* **53**, 925-936.

Warell, J.; Pappini, R. (2015). "Rotational Period of 1938 Lausanna." *Minor Planet Bulletin* **42**, 20-21.

Warner, B.D.; Harris, A.W.; Pravec, P. (2009). "The Asteroid Lightcurve Database." *Icarus* **202**, 134-146. Updated 2021 Oct. <http://www.minorplanet.info/lightcurvedatabase.html>

**LIGHTCURVE ANALYSIS OF L4 TROJAN ASTEROIDS  
AT THE CENTER FOR SOLAR SYSTEM STUDIES:  
2021 JULY TO SEPTEMBER**

Robert D. Stephens  
Center for Solar System Studies (CS3) / MoreData!  
11355 Mount Johnson Ct., Rancho Cucamonga, CA 91737 USA  
rstephens@foxandstephens.com

Brian D. Warner  
Center for Solar System Studies (CS3) / MoreData!  
Eaton, CO

(Received: 2021 October 8)

Lightcurves for 11 Jovian Trojan asteroids were obtained at the Center for Solar System Studies (CS3) from 2021 July to September.

For several years, the Center for Solar System Studies (CS3, MPC U81) has been conducting a study of Jovian Trojan asteroids. This paper reports CCD photometric observations of nine Trojan asteroids from the L<sub>4</sub> (Greek) Lagrange point and two from the L<sub>5</sub> (Trojan) Lagrange point from 2021 July to September.

All observations were made using a 0.4-m f/10 Schmidt-Cassegrain telescope and an FLI Proline 1001E CCD camera. Images were unbinned with no filter and had master flats and darks applied. The exposures were 180 seconds.

Image processing, measurement, and period analysis were done using *MPO Canopus* (Bdw Publishing), which incorporates the Fourier analysis algorithm (FALC) developed by Harris (Harris et al., 1989). The Comp Star Selector feature in *MPO Canopus* was used to limit the comparison stars to near solar color. Night-to-night calibration was done using field stars from the ATLAS catalog (Tonry et al., 2018), which has Sloan *griz* magnitudes that were derived from the GAIA and Pan-STARR catalogs and are the "native" magnitudes of the catalog.

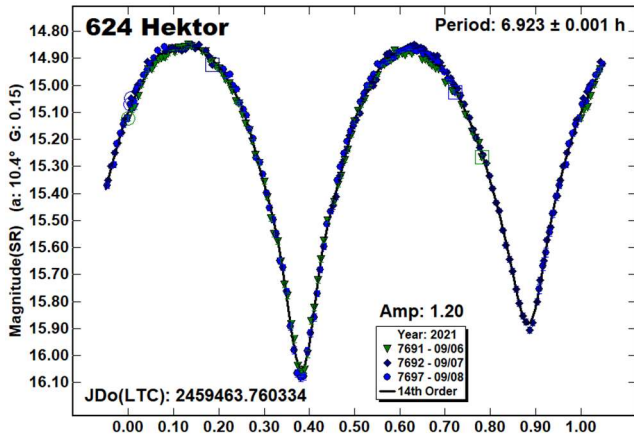
The Y-axis of lightcurves gives ATLAS SR "sky" (catalog) magnitudes. During period analysis, the magnitudes were normalized to the phase angle and value for *G* given in the parentheses. The X-axis rotational phase ranges from -0.05 to 1.05.

The amplitude indicated in the plots (e.g., Amp. 0.23) is the amplitude of the Fourier model curve and not necessarily the adopted amplitude of the lightcurve.

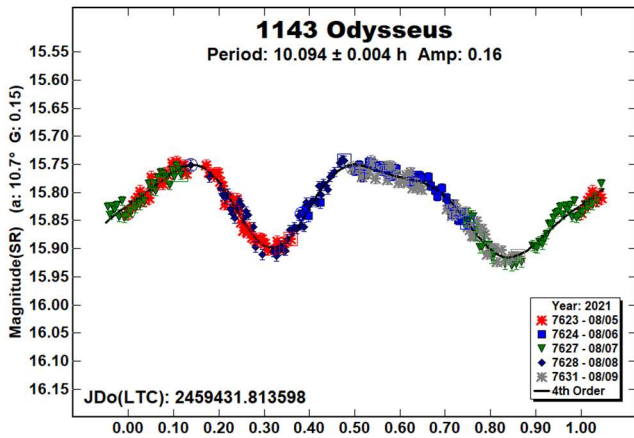
For brevity, only some of the previously reported rotational periods may be referenced. A complete list is available at the lightcurve database (LCDB; Warner et al., 2009).

624 Hektor. The LCDB shows that many synodic periods for Hektor were found in the past, all about 6.92 h. Hektor has also been previously found to be a binary asteroid (Marchis et al., 2006) with a primary that might have a bilobated shape approximately 350×210 km and a secondary estimated to be 15 km in size. Marchis et al. found a pole position with ecliptic coordinates of  $\lambda_1 = 332^\circ$  and  $\beta_1 = -32^\circ$ . Pole positions have also been independently found a number of times over the years, the latest by Hanuš et al. (2015), which is similar to the Marchis et al solution. Most of the pole solutions reported a sidereal period of 6.92051 h.

The synodic period found this year produced a classic bimodal lightcurve consistent with rotational periods found in previous years.

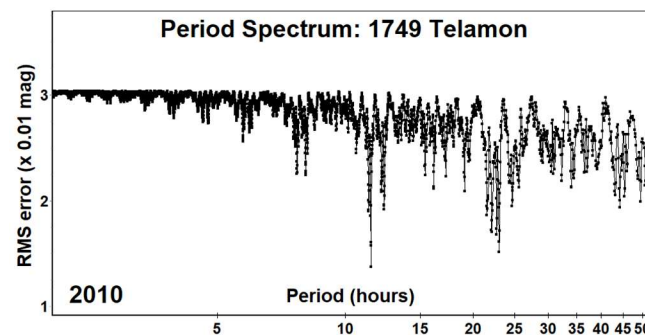
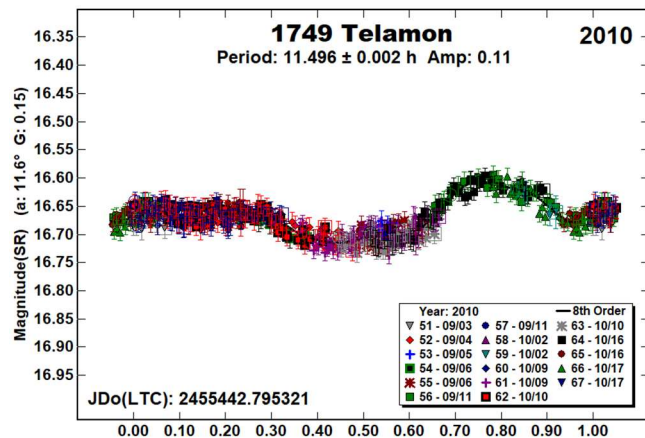
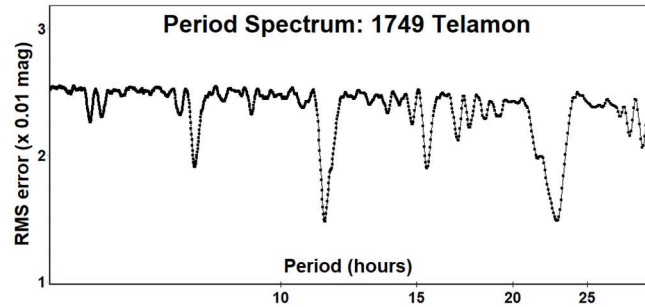
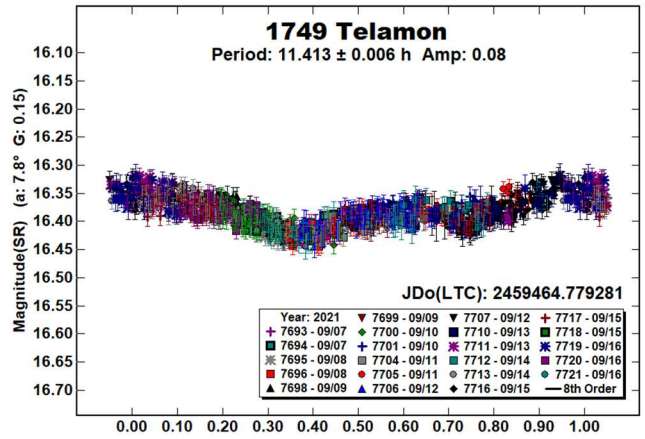


1143 Odysseus. Odysseus has been observed many times in the past. Molnar et al. (2008), Mottola et al. (2011), Shevchenko et al. (2012), Stephens et al. (2014), Waszczak et al. (2015), Ryan et al. (2017), and Szabó et al. (2017), and Stephens and Warner (2020b) each found a period near 10.11 h. The found this year is similar to those found in the past.

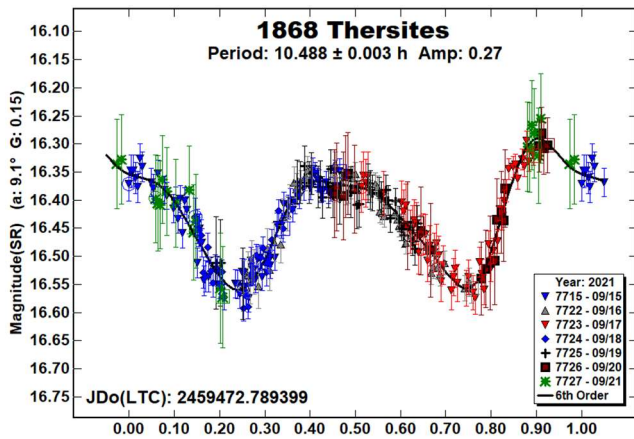


1749 Telamon. Because of its low amplitude, a period for this L4 Trojan has been difficult to resolve in the past (Mottola et al. 2011) reported a period of 11.187 h. French et al. (2011) found a result of 16.975 h. Using data from the K2 mission of the Kepler Space Telescope, Ryan et al. (2017) found a period of 22.613 h and Szabó et al. (2017) found a period of 11.331 h or a possible 22.662 h period.

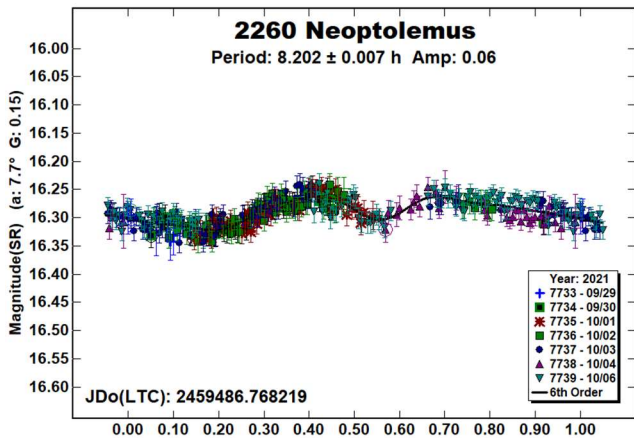
The results this year favored the 11 h period. The French et al. images obtained in 2010 were remeasured using field stars from the ATLAS catalog with careful attention to make sure that background stars were not in the measurement annulus. The remeasured 2010 data also showed a strong preference for the 11 h solution, given its asymmetric lightcurve.



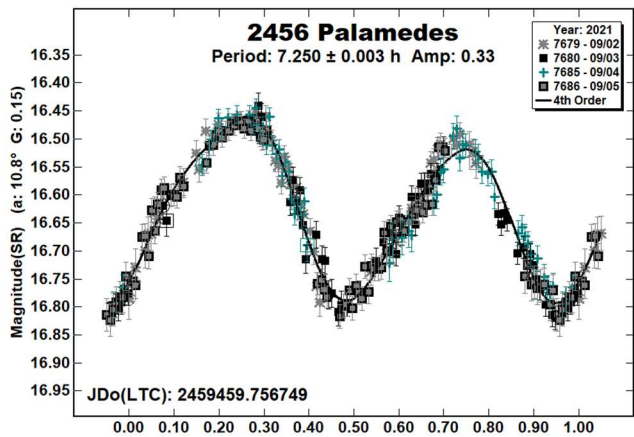
1868 Thersites. A period for this L4 Trojan has been reported four times in the past (Stephens and Warner, 2020a; and references therein), The result this year is in good agreement with past findings.



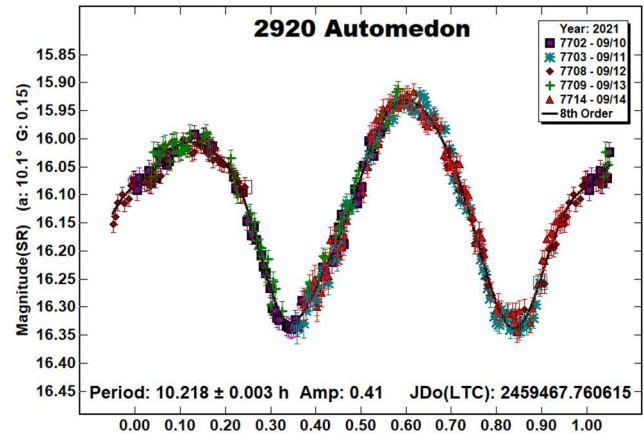
**2260 Neoptolemus.** A period for this L<sub>4</sub> Trojan has been reported four times in the past. Mottola et al. (2011) reported two periods of 8.180 h. Stephens et al. (2016a and 2016b) reported periods of 8.18 h and 8.199 h. The result this year is in good agreement with those prior findings.



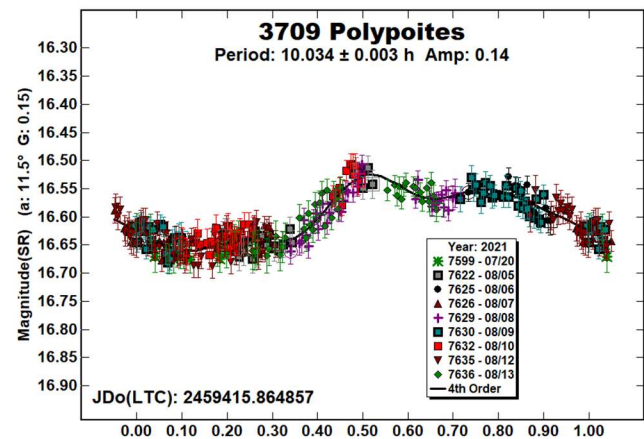
**2456 Palamedes.** This L<sub>4</sub> Trojan has been observed three times in the past (Stephens and Warner, 2021; and references therein), each time finding a rotational period near 7.25 h. Our period at this opposition is in good agreement with those previous results.



**2920 Automedon.** The synodic period found in 2021 agrees with previous synodic results (Stephens and Warner, 2019; and references within), all of which were near 10.21 h.

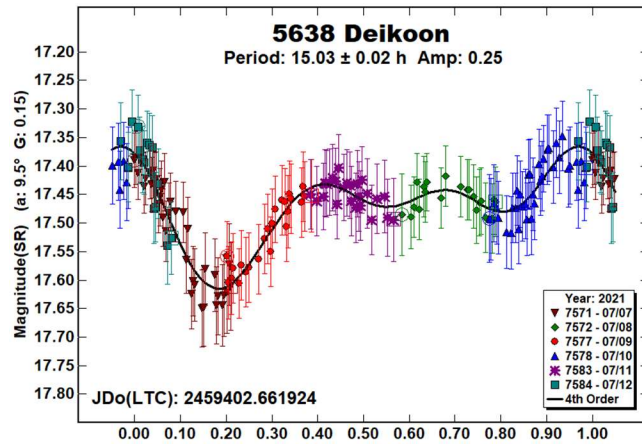
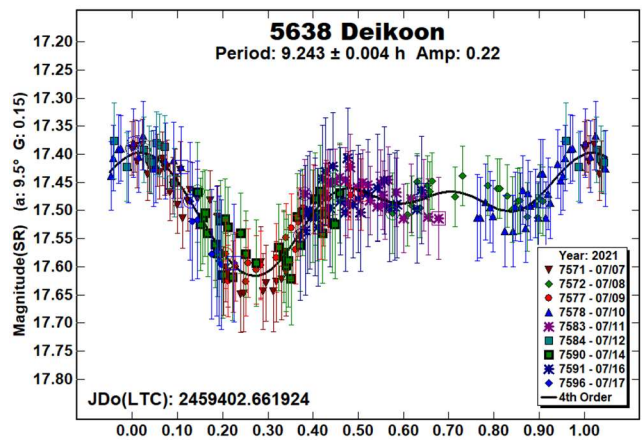
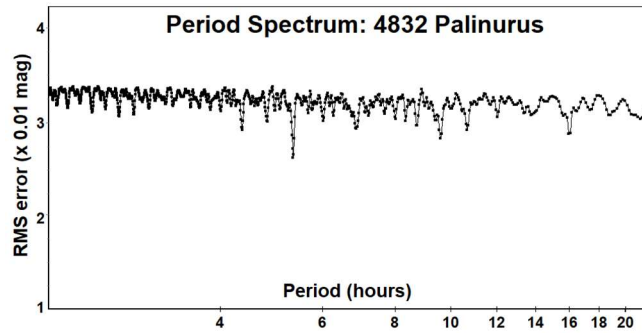
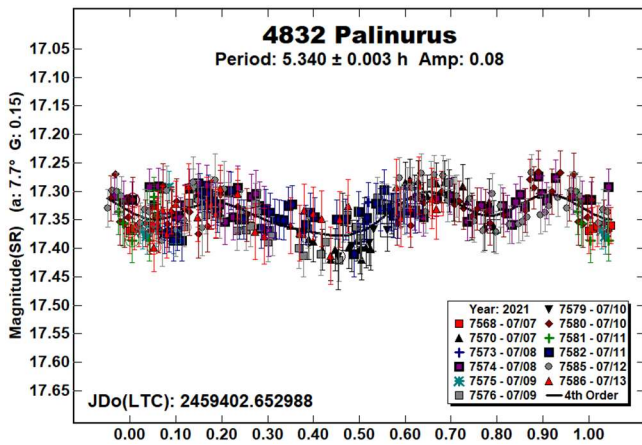


**3709 Polypoites.** This L<sub>4</sub> (Greek) Trojan has been observed seven times in the past (Stephens and Warner, 2021; and references within). The result from the 2021 data is in good agreement with those previous findings.

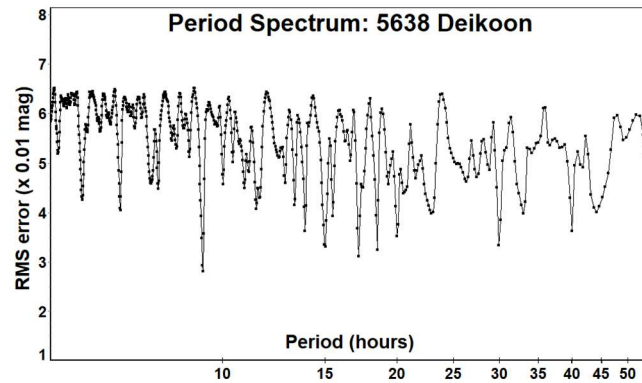
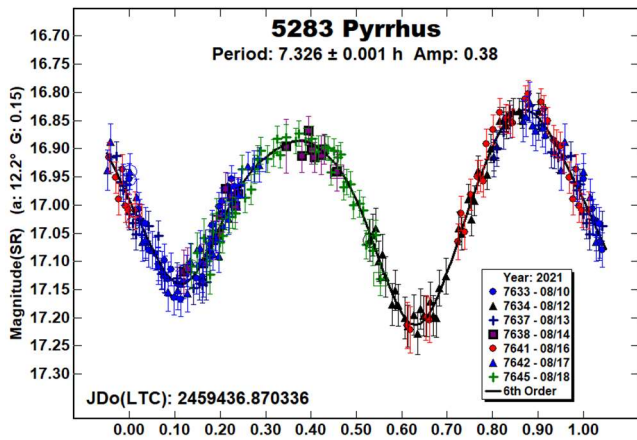


**4832 Palinurus.** This L<sub>5</sub> Trojan has been observed twice in the past. Mottola et al. (2011) found a period of 5.319 h with an amplitude of 0.09 mag from a sparse bimodal lightcurve they regarded as tentative. Stephens et al. (2015) found a period of 5.85 h. However, this period is rated U=1 and is considered unreliable. In those images from 2015, a bright field star cast internal reflections throughout the field of view.

The observations in 2021 are similar in longitude to the Mottola observations from 2010 and resulted in a period of 5.342 h. As expected from the similar longitude, the amplitude of our lightcurve of 0.08 mag is also near to the Mottola result. As noted by Harris et al. (2014), given the low amplitude, a bimodal solution cannot be assumed. Our observations in 2021 have three extrema in the lightcurve. The Period Spectrum shows another frequency near 10 h, which has an unlikely five extrema in the lightcurve. The next favorable opportunity to observe Palinurus is in 2022 July when the observing geometry should give a more certain solution.



5283 Pyrrhus. A period for this L<sub>5</sub> Trojan has been reported only once in the past by Mottola et al. (2011), who found it rotated every 7.323 h. The result this year is in good agreement with the Mottola finding.



5638 Deikoon. This L<sub>5</sub> Trojan was observed twice in the past. Molnar et al. (2008), using somewhat sparse data, found a period of 19.4 h resulting in a bimodal lightcurve. Mottola et al. (2011), also with sparse data, found a period of 9.137 h based on a trimodal lightcurve. Our Period Spectrum shows the 15 and 19 h periods to be possible, but they are fit-by-exclusion. Our most likely period of 9.243 h is in agreement with the Mottola finding.

Acknowledgements

This work includes data from the Asteroid Terrestrial-impact Last Alert System (ATLAS) project. ATLAS is primarily funded to search for near earth asteroids through NASA grants NN12AR55G, 80NSSC18K0284, and 80NSSC18K1575; byproducts of the NEO search include images and catalogs from the survey area. The ATLAS science products have been made possible through the contributions of the University of Hawaii Institute for Astronomy, the Queen's University Belfast, the Space Telescope Science Institute, and the South African Astronomical Observatory.

The purchase of a FLI-1001E CCD camera was made possible by a 2013 Gene Shoemaker NEO Grant from the Planetary Society.

Number	Name	2021/mm/dd	Phase	L <sub>PAB</sub>	B <sub>PAB</sub>	Period(h)	P.E.	Amp	A.E.
624	Hektor	09/06-09/08	10.4,10.3	49	17	6.923	0.001	1.20	0.01
1143	Odysseus	08/05-08/08	10.7,10.5	18	2	10.094	0.004	0.16	0.02
1749	Telamon	09/07-09/16	7.8,6.3	22	4	11.413	0.006	0.08	0.01
		2010/09/03-10/17	11.9,5.7	48	6	<sup>r</sup> 11.496	0.002	0.11	0.01
1868	Thersites	09/15-09/21	9.1,8.2	36	-5	10.488	0.003	0.27	0.02
2260	Neoptolemus	09/29-10/06	7.7,6.6	41	-15	8.202	0.007	0.06	0.01
2456	Palamedes	09/02-09/05	10.8,10.5	36	13	7.250	0.003	0.33	0.02
2920	Automedon	09/10-09/14	10.1,9.6	42	5	10.218	0.003	0.41	0.02
3709	Polypoites	07/20-08/13	11.5,10.2	17	-2	10.034	0.003	0.14	0.02
4832	Palinurus	07/07-07/13	7.8,8.5	249	18	5.340	0.003	0.08	0.02
5283	Pyrrhus	08/10-08/18	12.2,11.7	26	-15	7.326	0.001	0.38	0.02
5638	Deikoon	07/07-07/17	9.5,10.7	242	12	9.243	0.004	0.22	0.03
						<sup>a</sup> 15.03	0.02	0.25	0.03

Table I. Observing circumstances and results. <sup>r</sup>Restated previous period. <sup>a</sup>Alternative period. The phase angle is given for the first and last dates. If preceded by an asterisk, the phase angle reached an extremum during the period. L<sub>PAB</sub> and B<sub>PAB</sub> are the approximate phase angle bisector longitude/latitude at mid-date range (see Harris et al., 1984).

## References

- French, L.M.; Stephens, R.D.; Lederer, S.M.; Coley, D.R.; Rohl, D.A. (2011). "Preliminary Results from a Study of Trojan Asteroids." *Minor Planet Bull.* **38**, 116-120.
- Hanuš, J.; Delbò, M.; Ďurech, J.; Alí-Lagoa, V. (2015). "Thermophysical modeling of asteroids from WISE thermal infrared data - Significance of the shape model and the pole orientation uncertainties." *Icarus* **256**, 101-116.
- Harris, A.W.; Young, J.W.; Scaltriti, F.; Zappala, V. (1984). "Lightcurves and phase relations of the asteroids 82 Alkmene and 444 Gyptis." *Icarus* **57**, 251-258.
- Harris, A.W.; Young, J.W.; Bowell, E.; Martin, L.J.; Millis, R.L.; Poutanen, M.; Scaltriti, F.; Zappala, V.; Schober, H.J.; Debehogne, H.; Zeigler, K.W. (1989). "Photoelectric Observations of Asteroids 3, 24, 60, 261, and 863." *Icarus* **77**, 171-186.
- Harris, A.W.; Pravec, P.; Galad, A.; Skiff, B.A.; Warner, B.D.; Vilagi, J.; Gajdos, S.; Carbognani, A.; Hornoch, K.; Kusnirak, P.; Cooney, W.R.; Gross, J.; Terrell, D.; Higgins, D.; Bowell, E.; Koehn, B.W. (2014). "On the maximum amplitude of harmonics on an asteroid lightcurve." *Icarus* **235**, 55-59.
- Marchis, F.; Wong, M.H.; Berthier, J.; Descamps, P.; Hestroffer, D.; Vachier, F.; Le Mignant, D.; Keck Observatory, W.M.; de Pater, I. (2006). "S/2006 (624) 1". *IAU Circ.*, No. **8732**, #1.
- Molnar, L.A.; Haegert, M.J.; Hoogeboom, K.M. (2008). "Lightcurve Analysis of an Unbiased Sample of Trojan Asteroids." *Minor Planet Bull.* **35**, 82-84.
- Mottola, S.; Di Martino, M.; Erikson, A.; Gonano-Beurer, M.; Carbognani, A.; Carsenty, U.; Hahn, G.; Schober, H.; Lahulla, F.; Delbò, M.; Lagerkvist, C. (2011). "Rotational Properties of Jupiter Trojans. I. Light Curves of 80 Objects." *Astron. J.* **141**, A170.
- Ryan, E.L.; Sharkey, B.; Woodward, C.E. (2017). "Trojan Asteroids in the Kepler Campaign 6 Field." *Astron. J.* **153**, id 116.
- Shevchenko, V.G.; Belskaya, I.N.; Slyusarev, I.G.; Krugly, Yu.N.; Chiorny, V.G.; Gaftonyuk, N.M.; Donchev, Z.; Ivanova, V.; Ibrahimov, M.A.; Ehgamberdiev, Sh.A.; Molotov, I.E. (2012). "Opposition effect of Trojan asteroids." *Icarus* **217**, 202-208.
- Stephens, R.D., Coley, D.R., French, L.M., (2014). "Trojan Asteroids Observed from CS3: 2014 January-May." *Minor Planet Bull.* **41**, 210-212.
- Stephens, R.D.; Coley, D.R.; French, L.M. (2015). "Dispatches from the Trojan Camp - Jovian Trojan L5 Asteroids Observed from CS3: 2014 October - 2015 January." *Minor Planet Bull.* **42**, 216-224.
- Stephens, R.D.; Coley, D.R.; French, L.M. (2016a). "Large L5 Jovian Trojan Asteroid Lightcurves from the Center for Solar System Studies." *Minor Planet Bull.* **43**, 15-22.
- Stephens, R.D.; Coley, D.R.; Warner, B.D.; French, L.M. (2016b). "Lightcurves of Jovian Trojan Asteroids from the Center for Solar System Studies: L4 Greek Camp and Spies." *Minor Planet Bull.* **43**, 323-331.
- Stephens, R.D.; Warner, B.D. (2019). "Lightcurve Analysis of L4 Trojan Asteroids at the Center for Solar System Studies: 2018 July to September." *Minor Planet Bull.* **46**, 73-75.
- Stephens, R.D.; Warner, B.D. (2020a). "Lightcurve Analysis of L4 Trojan Asteroids at the Center for Solar System Studies: 2019 July to September." *Minor Planet Bull.* **47**, 43-47.
- Stephens, R.D.; Warner, B.D. (2020b). "Lightcurve Analysis of L4 Trojan Asteroids at the Center for Solar System Studies: 2020 July to September." *Minor Planet Bull.* **47**, 167-170.
- Stephens, R.D.; Warner, B.D. (2021). "Lightcurve Analysis of L4 Trojan Asteroids at the Center for Solar System Studies: 2020 October to December." *Minor Planet Bull.* **48**, 167-170.
- Szabó, Gy.M.; Pál, A.; Kiss, Cs.; Kiss, L.L.; Molnár, L.; Hanyecz, O.; Plachy, E.; Sárneczky, K.; Szabó, R. (2017). "The heart of the swarm: K2 photometry and rotational characteristics of 56 Jovian Trojan asteroids." *Astron. & Astrophys.* **599**, A44.
- Tonry, J.L.; Denneau, L.; Flewelling, H.; Heinze, A.N.; Onken, C.A.; Smartt, S.J.; Stalder, B.; Weiland, H.J.; Wolf, C. (2018). "The ATLAS All-Sky Stellar Reference Catalog." *Astrophys. J.* **867**, A105.
- Warner, B.D.; Harris, A.W.; Pravec, P. (2009). "The Asteroid Lightcurve Database." *Icarus* **202**, 134-146. Updated 2021 May. <http://www.minorplanet.info/lightcurvedatabase.html>
- Waszczak, A.; Chang, C.-K.; Ofek, E.O.; Laher, R.; Masci, F.; Levitan, D.; Surace, J.; Cheng, Y.-C.; Ip, W.-H.; Kinoshita, D.; Helou, G.; Prince, T.A.; Kulkarni, S. (2015). "Asteroid Light Curves from the Palomar Transient Factory Survey: Rotation Periods and Phase Functions from Sparse Photometry." *Astron. J.* **150**, A75.

## ASTEROID-DEEPSKY APPULSES IN 2022

Brian D. Warner  
Center for Solar System Studies  
446 Sycamore Ave.  
Eaton, CO 80615  
brian@MinorPlanetObserver.com

(Received: 2021 October 14)

The following list is a *very small* subset of the results of a search for asteroid-deepsky appulses for 2022, presenting only the highlights for the year based on close approaches of brighter asteroids to brighter DSOs. For the complete set visit

<https://minplanobs.org/MPInfo/php/dsoappulses.php>

For any event not covered, the Minor Planet Center's web site at <https://www.minorplanetcenter.net/cgi-bin/checkmp.cgi> allows you to enter the location of a suspected asteroid or supernova and check if there are any known targets in the area.

The table gives the following data:

Date/Time	Universal Date (MM DD) and Time of closest approach
#/Name	The number and name of the asteroid
RA/Dec	The J2000 position of the asteroid
AM	The approximate visual magnitude of the asteroid
Sep/PA	The separation in arcseconds and the position angle from the DSO to the asteroid
DSO	The DSO name or catalog designation
DM	The approximate total magnitude of the DSO
DT	DSO Type: OC = Open Cluster; GC = Globular Cluster; G = Galaxy
SE/ME	The elongation in degrees from the sun and moon, respectively
MP	The phase of the moon: 0 = New, 1.0 = Full. Positive = waxing; Negative = waning

Date	UT	#	Name	RA	Dec	AM	Sep	PA	DSO	DM	DT	SE	ME	MP
01 02	11:58	1584	Fuji	04:06.00	+52 33.8	13.9	897	102	NGC 1496	9.6	OC	137	142	0.00
01 27	17:06	15	Eunomia	13:40.06	-23 56.2	11.1	373	228	NGC 5260	12.9	G	95	36	-0.26
<b>01 31</b>	<b>13:29</b>	<b>135</b>	<b>Hertha</b>	<b>13:39.50</b>	<b>-11 29.0</b>	<b>13.2</b>	<b>1</b>	<b>23</b>	<b>NGC 5254</b>	<b>13.0</b>	<b>G</b>	<b>104</b>	<b>95</b>	<b>-0.01</b>
02 01	23:56	739	Mandeville	13:23.87	+09 42.4	12.8	34	317	NGC 5125	12.4	G	116	127	0.01
02 28	00:50	1816	Liberia	12:29.83	+14 00.8	14.0	650	80	NGC 4459	10.4	G	153	123	-0.09
02 28	04:00	1816	Liberia	12:29.79	+14 04.5	14.0	169	81	NGC 4468	12.8	G	153	124	-0.08
02 28	04:01	1816	Liberia	12:29.79	+14 04.5	14.0	185	261	NGC 4474	11.5	G	153	125	-0.08
03 03	11:44	747	Winchester	11:45.37	+19 23.6	12.6	34	220	NGC 3867	13.2	G	163	168	0.01
03 03	23:24	417	Suevia	09:55.66	+04 24.7	12.9	613	32	NGC 3055	12.1	G	164	148	0.02
03 04	06:08	747	Winchester	11:44.78	+19 30.4	12.6	431	218	NGC 3862	12.7	G	163	161	0.03
03 04	23:27	16	Psyche	10:55.70	+07 54.8	10.5	844	25	NGC 3462	12.2	G	178	150	0.06
03 05	06:35	471	Papagena	11:03.83	+28 57.2	11.3	271	21	NGC 3510	12.2	G	157	136	0.08
03 05	23:56	747	Winchester	11:43.44	+19 45.5	12.6	641	217	NGC 3837	13.3	G	163	141	0.12
03 06	01:01	747	Winchester	11:43.41	+19 45.9	12.6	835	217	NGC 3842	11.8	G	163	140	0.12
03 08	06:13	747	Winchester	11:41.67	+20 04.5	12.6	189	216	NGC 3816	12.5	G	163	113	0.30
03 09	05:47	1816	Liberia	12:26.27	+18 14.1	14.0	235	74	NGC 4394	10.9	G	158	111	0.39
<b>03 09</b>	<b>06:36</b>	<b>1816</b>	<b>Liberia</b>	<b>12:26.25</b>	<b>+18 15.0</b>	<b>14.0</b>	<b>663</b>	<b>75</b>	<b>M85</b>	<b>9.1</b>	<b>G</b>	<b>158</b>	<b>111</b>	<b>0.39</b>
03 09	17:44	747	Winchester	11:40.51	+20 16.5	12.6	411	216	NGC 3805	12.6	G	163	95	0.44
03 10	07:16	16	Psyche	10:51.59	+08 23.9	10.6	392	26	NGC 3427	13.2	G	172	83	0.49
04 03	21:35	739	Mandeville	13:19.78	+22 58.3	12.1	140	224	NGC 5092	13.3	G	151	135	0.07
04 04	05:18	70	Panopaea	18:11.81	-28 14.1	12.5	197	201	NGC 6565	13.0	PN	102	136	0.09
04 04	05:43	70	Panopaea	18:11.83	-28 14.2	12.5	505	21	PK 3-4.7	11.0	PN	102	136	0.09
<b>04 05</b>	<b>02:44</b>	<b>70</b>	<b>Panopaea</b>	<b>18:12.83</b>	<b>-28 19.1</b>	<b>12.5</b>	<b>56</b>	<b>22</b>	<b>PK 3-4.9</b>	<b>12.0</b>	<b>PN</b>	<b>102</b>	<b>147</b>	<b>0.15</b>
04 06	17:21	15	Eunomia	13:18.32	-26 41.9	10.1	629	16	NGC 5061	10.4	G	159	128	0.27
05 30	22:11	711	Marmulla	17:37.29	-36 02.1	13.6	886	341	Ru 127	8.8	OC	160	165	0.00
06 23	01:50	2035	Stearns	20:52.37	-48 46.9	14.0	218	88	NGC 6970	12.6	G	139	83	-0.30
06 25	00:01	786	Bredichina	18:31.15	-25 37.4	12.7	487	155	NGC 6638	9.2	GC	176	131	-0.14
06 28	19:23	786	Bredichina	18:27.72	-25 59.1	12.6	525	335	PK 7-6.2	13.1	PN	177	177	0.00
<b>07 01</b>	<b>14:20</b>	<b>606</b>	<b>Brangane</b>	<b>18:34.33</b>	<b>-32 29.6</b>	<b>13.7</b>	<b>521</b>	<b>186</b>	<b>M69</b>	<b>7.7</b>	<b>GC</b>	<b>171</b>	<b>150</b>	<b>0.06</b>
<b>07 03</b>	<b>06:27</b>	<b>135</b>	<b>Hertha</b>	<b>12:56.92</b>	<b>-08 30.0</b>	<b>12.9</b>	<b>62</b>	<b>20</b>	<b>NGC 4818</b>	<b>11.1</b>	<b>G</b>	<b>95</b>	<b>50</b>	<b>0.15</b>
07 06	20:01	2035	Stearns	20:50.32	-57 03.0	14.0	830	278	IC 5063	11.9	G	140	105	0.48
07 22	06:03	497	Iva	22:02.69	-19 07.9	12.9	755	161	NGC 7183	11.9	G	152	83	-0.34
07 24	07:07	372	Palma	00:23.40	+16 30.2	12.7	526	278	NGC 100	13.3	G	109	61	-0.17
07 29	09:46	70	Panopaea	17:42.64	-39 41.6	11.3	383	208	PK 350-5.1	13.2	PN	138	133	0.01
08 05	00:19	786	Bredichina	18:02.29	-28 38.0	13.6	859	147	PK 2-2.4	12.4	PN	138	54	0.45
08 20	09:51	71	Niobe	02:39.05	+41 29.4	13.0	403	113	NGC 995	13.4	G	96	30	-0.38
08 21	03:22	71	Niobe	02:39.31	+41 36.5	13.0	440	110	NGC 996	13.0	G	96	36	-0.31
08 21	06:23	71	Niobe	02:39.35	+41 37.7	13.0	397	110	NGC 999	13.5	G	96	37	-0.30
<b>08 28</b>	<b>19:08</b>	<b>71</b>	<b>Niobe</b>	<b>02:41.26</b>	<b>+42 48.8</b>	<b>12.9</b>	<b>500</b>	<b>282</b>	<b>M34</b>	<b>5.2</b>	<b>OC</b>	<b>102</b>	<b>115</b>	<b>0.02</b>
08 31	04:05	776	Berbericia	21:34.64	-40 50.9	11.8	117	168	NGC 7087	13.0	G	145	108	0.15
08 31	04:46	125	Liberatrix	00:29.95	+02 10.7	12.9	409	326	NGC 132	12.6	G	150	165	0.15
09 02	00:39	170	Maria	00:04.13	+20 51.1	13.3	442	14	NGC 7817	11.8	G	145	139	0.32
09 26	19:34	216	Kleopatra	22:43.32	+08 48.8	9.9	619	304	NGC 7362	12.7	G	157	146	0.01
09 29	12:44	1789	Dobrovolsky	23:39.12	-06 42.3	14.0	736	157	NGC 7721	11.6	G	166	121	0.15
10 31	01:42	1116	Catriona	06:58.04	+45 18.5	13.9	485	313	NGC 2308	13.2	G	114	160	0.37
11 18	00:23	497	Iva	22:00.70	-13 07.4	13.9	583	333	NGC 7171	12.2	G	92	165	-0.36
12 17	00:39	38	Leda	23:46.86	+07 01.8	13.6	658	349	NGC 7751	12.8	G	95	169	-0.43
12 21	02:28	1655	Comas Sola	07:08.09	+18 42.5	13.8	377	209	NGC 2339	11.8	G	162	131	-0.07

**Bold** indicates Messier objects and/or separations of 1 arcminute or less

**MINOR PLANETS AT UNUSUALLY FAVORABLE ELONGATIONS IN 2022**

Frederick Pilcher  
 4438 Organ Mesa Loop  
 Las Cruces, NM 88011 USA  
 fpilcher35@gmail.com

A list is presented of minor planets which are much brighter than usual at their 2022 apparitions.

The minor planets in the lists which follow will be much brighter at their 2022 apparitions than at their average distances at maximum elongation. Many years may pass before these planets will be again as bright as in 2022. Observers are encouraged to give special attention to those which lie near the limit of their equipment.

These lists have been prepared by an examination of the maximum elongation circumstances of minor planets computed by the author for all years through 2060 with a full perturbation program written by Dr. John Reed, and to whom he expresses his thanks. Elements are from EMP 1992, except that for all planets for which new or improved elements have been published subsequently in the Minor Planet Circulars or in electronic form, the newer elements have been used. Planetary positions are from the JPL DE-200 ephemeris, courtesy of Dr. E. Myles Standish.

Any planets whose brightest magnitudes near the time of maximum elongation vary by at least 2.0 in this interval and in 2022 will be within 0.3 of the brightest occurring, or vary by at least 3.0 and in 2022 will be within 0.5 of the brightest occurring; and which are visual magnitude 14.5 or brighter, are included. For planets brighter than visual magnitude 13.5, which are within the range of a large number of observers, these standards have been relaxed somewhat to include a larger number of planets. Magnitudes have been computed from the updated magnitude parameters published in MPC28104-28116, on 1996 Nov. 25, or more recently in the Minor Planet Circulars.

Oppositions may be in right ascension or in celestial longitude. Here we use still a third representation, maximum elongation from the Sun, instead of opposition. Though unconventional, it has the advantage that many close approaches do not involve actual opposition to the Sun near the time of minimum distance and greatest brightness and are missed by an opposition-based program. Other data are also provided according to the following tabular listings: Minor planet number, date of maximum elongation from the Sun in format yyyy/mm/dd, maximum elongation in degrees, right ascension on date of maximum elongation, declination on date of maximum elongation, both in J2000 coordinates, date of brightest magnitude in format yyyy/mm/dd, brightest magnitude, date of minimum distance in format yyyy/mm/dd, and minimum distance in AU.

Users should note that when the maximum elongation is about 177° or greater, the brightest magnitude is sharply peaked due to enhanced brightening near zero phase angle. Even as near as 10 days before or after minimum magnitude the magnitude is generally about 0.4 greater. This effect takes place in greater time interval for smaller maximum elongations. There is some interest in very small minimum phase angles. For maximum elongations E near 180° at Earth distance Δ, an approximate formula for the minimum phase angle φ is

$$\phi = (180^\circ - E) / (\Delta + 1)$$

A special list of asteroids approaching the Earth more closely than 0.3 AU is provided following the list of temporal sequence of favorable elongations.

Table I. Numerical Sequence of Favorable Elongations

Planet	Max	Elon	D	Max	E	RA	Dec	Br	Mag	D	Br	Mag	Min	Dist	D	Min	Dist
10	2022/04/29	174.6°	14h16m	-19°	2022/04/29	9.2	2022/05/01	1.799									
13	2022/05/04	179.5°	14h46m	-16°	2022/05/04	9.9	2022/05/02	1.590									
20	2022/02/05	178.7°	9h12m	+14°	2022/02/05	8.5	2022/02/02	1.119									
26	2022/05/21	178.4°	15h51m	-21°	2022/05/21	10.3	2022/05/22	1.406									
27	2022/11/12	177.8°	3h12m	+15°	2022/11/12	8.7	2022/11/16	1.026									
30	2022/11/29	176.5°	4h16m	+24°	2022/11/29	9.6	2022/11/25	1.114									
34	2022/02/21	175.0°	10h 9m	+ 6°	2022/02/21	11.4	2022/02/22	1.414									
46	2022/10/25	177.7°	2h 3m	+10°	2022/10/25	10.5	2022/10/20	1.146									
70	2022/06/23	164.8°	18h12m	-38°	2022/06/24	10.7	2022/06/27	1.190									
90	2022/07/31	176.9°	20h46m	-21°	2022/07/31	11.6	2022/08/01	1.610									
93	2022/07/15	165.9°	19h49m	-35°	2022/07/15	10.8	2022/07/14	1.381									
98	2022/02/16	166.8°	10h13m	+25°	2022/02/16	11.4	2022/02/18	1.212									
115	2022/11/19	157.7°	3h 5m	+40°	2022/11/18	9.6	2022/11/16	0.974									
128	2022/09/17	169.5°	23h56m	-11°	2022/09/17	10.6	2022/09/18	1.429									
156	2022/05/07	175.0°	14h49m	-21°	2022/05/07	10.7	2022/05/07	1.106									
164	2022/12/01	171.9°	4h25m	+13°	2022/11/29	10.8	2022/11/17	1.023									
166	2022/12/24	167.1°	6h 3m	+10°	2022/12/22	12.8	2022/12/16	1.330									
181	2022/02/21	174.7°	10h27m	+15°	2022/02/21	11.3	2022/02/16	1.660									
190	2022/01/19	172.7°	7h57m	+13°	2022/01/19	12.4	2022/01/16	2.418									
198	2022/08/04	166.8°	20h47m	- 4°	2022/08/06	10.3	2022/08/12	0.998									
204	2022/05/28	169.8°	16h28m	-11°	2022/05/28	11.4	2022/05/30	1.210									
222	2022/06/27	179.0°	18h21m	-24°	2022/06/27	12.6	2022/06/26	1.722									
232	2022/04/08	171.7°	13h19m	+ 0°	2022/04/08	12.5	2022/04/10	1.113									
264	2022/11/19	177.7°	3h35m	+21°	2022/11/19	11.3	2022/11/16	1.461									
269	2022/07/04	171.2°	18h49m	-14°	2022/07/04	11.6	2022/07/03	1.050									
275	2022/04/23	172.0°	14h14m	- 5°	2022/04/23	11.8	2022/04/20	1.395									
290	2022/01/31	136.9°	9h29m	+60°	2022/01/29	13.5	2022/01/28	0.885									
351	2022/01/12	176.5°	7h35m	+25°	2022/01/12	11.7	2022/01/14	1.369									
358	2022/08/04	176.5°	20h52m	-13°	2022/08/04	13.1	2022/08/09	1.971									
365	2022/10/23	170.5°	2h 7m	+ 2°	2022/10/23	12.1	2022/10/23	1.382									
382	2022/06/17	171.2°	17h38m	+32°	2022/06/16	12.4	2022/06/13	1.675									
384	2022/11/15	178.9°	3h23m	+19°	2022/11/16	12.1	2022/11/18	1.314									
394	2022/07/30	170.0°	20h50m	-28°	2022/07/31	12.1	2022/08/04	1.182									
397	2022/10/09	165.6°	0h26m	+18°	2022/10/08	11.3	2022/10/06	0.999									
416	2022/06/04	173.2°	16h49m	-29°	2022/06/04	10.2	2022/06/05	1.174									
455	2022/10/15	159.6°	1h41m	-11°	2022/10/11	10.9	2022/10/05	0.956									
465	2022/07/05	177.8°	18h58m	-24°	2022/07/05	13.1	2022/06/29	1.654									
479	2022/10/02	167.2°	0h56m	- 7°	2022/10/03	12.2	2022/10/07	1.210									
539	2022/09/04	168.4°	22h36m	+ 3°	2022/09/05	12.3	2022/09/08	1.203									
543	2022/10/26	166.5°	1h40m	+24°	2022/10/26	13.0	2022/10/26	1.625									
554	2022/01/02	178.6°	6h54m	+24°	2022/01/02	10.9	2021/12/29	1.090									
596	2022/05/28	178.4°	16h22m	-19°	2022/05/28	11.8	2022/05/29	1.439									
645	2022/12/15	169.1°	5h25m	+34°	2022/12/15	13.8	2022/12/15	1.795									
672	2022/07/25	166.1°	20h26m	-33°	2022/07/24	13.7	2022/07/23	1.215									
696	2022/10/06	159.1°	0h14m	+24°	2022/10/08	12.4	2022/10/10	1.483									
704	2022/08/17	160.4°	21h25m	+ 5°	2022/08/18	9.9	2022/08/21	1.728									
711	2022/06/13	166.7°	17h23m	-36°	2022/06/15	13.4	2022/06/20	0.848									
726	2022/11/19	177.2°	3h34m	+22°	2022/11/19	12.5	2022/11/08	1.068									
778	2022/01/15	169.2°	7h50m	+31°	2022/01/14	12.7	2022/01/12	1.413									
786	2022/06/28	177.3°	18h27m	-25°	2022/06/28	12.3	2022/06/23	1.805									
795	2022/04/09	178.9°	13h 8m	- 8°	2022/04/09	12.6	2022/04/10	1.470									
804	2022/09/21	174.9°	23h47m	+ 4°	2022/09/21	10.9	2022/09/18	1.467									
809	2022/09/01	178.8°	22h41m	- 9°	2022/09/01	12.9	2022/09/02	0.841									
852	2022/10/14	174.0°	1h21m	+ 2°	2022/10/13	11.7	2022/10/02	0.983									
854	2022/06/05	168.8°	16h58m	-11°	2022/06/05	14.0	2022/06/09	0.969									
925	2022/01/11	174.0°	7h29m	+27°	2022/01/11	11.5	2022/01/12	1.529									
941	2022/09/17	170.0°	23h54m	-11°	2022/09/18	14.3	2022/09/21	1.298									
956	2022/08/20	170.5°	21h43m	- 3°	2022/08/20	13.9	2022/08/18	0.824									
960	2022/09/09	173.5°	23h 1m	+ 0°	2022/09/09	14.3	2022/09/07	0.874									
972	2022/09/17	166.1°	23h19m	+10°	2022/09/18	12.5	2022/09/20	1.374									
986	2022/09/23	155.7°	0h39m	-22°	2022/09/22	13.0	2022/09/21	1.547									
987	2022/08/23	178.0°	22h 4m	- 9°	2022/08/23	12.1	2022/08/23	1.388									
990	2022/10/10	173.4°	0h51m	+12°	2022/10/09	13.6	2022/10/06	1.100									
1021	2022/12/28	170.0°	6h22m	+13°	2022/12/27	11.4	2022/12/19	1.164									
1052	2022/12/01	175.2°	4h32m	+17°	2022/12/01	13.6	2022/11/27	0.965									
1060	2022/07/26	166.5°	20h 9m	- 6°	2022/07/26	14.0	2022/07/26	0.782									
1077	2022/08/27	177.5°	22h24m	-12°	2022/08/27	13.7	2022/08/30	0.942									
1115	2022/01/06	165.7°	7h22m	+36°	2022/01/07	12.9	2022/01/08	1.621									
1116	2022/12/28	152.1°	6h34m	+51°	2022/12/27	12.9	2022/12/25	1.371									
1130	2022/07/27	175.1°	20h19m	-14°	2022/07/27	13.2	2022/07/31	0.802									
1131	2022/07/25	177.1°	20h21m	-22°	2022/07/25	13.6	2022/08/06	0.679									
1192	2022/03/19	176.6°	11h54m	+ 3°	2022/03/18	14.2	2022/03/12	0.862									
1239	2022/12/25	178.8°	6h16m	+24°	2022/12/25	13.7	2022/12/28	1.080									
1240	2022/10/08	166.4°	0h34m	+18°	2022/10/07	12.8	2022/10/03	1.419									
1277	2022/06/17	175.4°	17h46m	-18°	2022/06/18	13.1	2022/06/23	1.087									
1299	2022/12/20	166.6°	5h50m	+10°	2022/12/19	14.3	2022/12/17	1.340									
1319	2022/05/02	177.2°	14h31m	-17°	2022/05/02	13.8	2022/05/01	1.372									
1431	2022/08/28	163.5°	23h 0m	-24°	2022/08/28	14.0	2022/08/28	1.151									
1438	2022/10/14	177.8°	1h15m	+10°	2022/10/14	14.2	2022/10/11	1.423									
1448	2022/01/15	168.9°	7h56m	+32°	2022/01/15	14.4	2022/01/16	0.959									

Planet	Max	Elon	D	Max	E	RA	Dec	Br	Mag	D	Br	Mag	Min	Dist	D	Min	Dist
1476	2022/08/03	175.3°		20h59m	-21°			2022/08/04	14.1		2022/08/05	0.838					
1500	2022/11/13	171.5°		3h 6m	+26°			2022/11/13	14.4		2022/11/10	0.839					
1527	2022/10/04	179.0°		0h41m	+ 3°			2022/10/04	13.5		2022/09/25	0.888					
1543	2022/08/10	166.7°		21h13m	+ 3°			2022/08/10	13.4		2022/08/08	0.778					
1565	2022/12/07	173.8°		4h45m	+28°			2022/12/06	13.3		2022/11/23	0.755					
1573	2022/10/27	166.6°		2h37m	+ 1°			2022/10/26	13.8		2022/10/23	0.859					
1638	2022/08/02	179.5°		20h48m	-17°			2022/08/02	13.8		2022/07/29	1.244					
1657	2022/01/09	176.6°		7h25m	+25°			2022/01/09	14.3		2022/01/16	0.933					
1660	2022/12/06	148.6°		5h30m	- 7°			2022/12/13	13.9		2022/12/19	0.901					
1664	2022/02/24	167.5°		10h45m	+21°			2022/02/24	13.5		2022/02/24	0.832					
1683	2022/08/12	176.9°		21h29m	-18°			2022/08/12	14.0		2022/08/10	1.241					
1689	2022/09/03	172.3°		23h 1m	-14°			2022/09/04	13.8		2022/09/09	1.047					
1710	2022/07/24	163.6°		20h28m	-35°			2022/07/27	14.5		2022/08/02	0.749					
1718	2022/09/04	167.5°		22h28m	+ 3°			2022/09/03	14.5		2022/09/01	0.711					
1756	2022/10/09	169.7°		0h44m	+15°			2022/10/10	14.1		2022/10/11	0.979					
1792	2022/10/18	166.7°		1h48m	- 2°			2022/10/19	14.1		2022/10/20	1.030					
1836	2022/07/20	174.6°		19h55m	-15°			2022/07/20	13.8		2022/07/18	1.246					
1884	2022/01/10	138.1°		7h29m	+63°			2022/01/10	13.9		2022/01/10	0.934					
1994	2022/07/26	163.7°		20h 8m	- 3°			2022/07/27	14.2		2022/07/30	1.181					
2034	2022/11/30	166.2°		4h15m	+35°			2022/11/30	14.5		2022/12/01	0.879					
2100	2022/09/05	161.1°		21h58m	+ 5°			2022/09/03	13.7		2022/08/31	0.187					
2199	2022/08/25	178.4°		22h7m	-12°			2022/08/25	14.3		2022/08/17	0.854					
2212	2022/12/22	119.5°		10h42m	+39°			2023/01/11	13.5		2023/01/18	0.233					
2231	2022/09/08	179.1°		23h 4m	- 4°			2022/09/08	14.2		2022/09/11	1.057					
2235	2022/02/24	156.4°		9h47m	-11°			2022/02/22	14.5		2022/02/20	1.652					
2237	2022/09/18	176.6°		23h46m	- 5°			2022/09/18	14.4		2022/09/21	1.512					
2243	2022/10/23	178.1°		1h50m	+13°			2022/10/23	14.4		2022/10/10	0.985					
2316	2022/07/03	177.3°		18h49m	-20°			2022/07/03	14.5		2022/07/05	1.037					
2337	2022/10/22	176.1°		1h51m	+ 7°			2022/10/22	14.4		2022/10/25	1.225					
2341	2022/12/03	178.6°		4h36m	+23°			2022/12/03	13.8		2022/11/30	0.907					
2343	2022/09/11	176.9°		23h14m	- 1°			2022/09/12	14.3		2022/09/16	0.763					
2375	2022/07/13	179.9°		19h30m	-21°			2022/07/13	14.4		2022/07/06	1.895					
2583	2022/09/07	166.1°		23h23m	-19°			2022/09/08	14.3		2022/09/09	0.793					
2606	2022/04/19	174.6°		13h59m	- 6°			2022/04/19	13.3		2022/04/17	1.054					
2717	2022/08/04	175.7°		20h50m	-13°			2022/08/04	13.4		2022/08/07	0.730					
2751	2022/11/10	178.9°		3h 2m	+18°			2022/11/11	14.5		2022/11/14	1.071					
2757	2022/10/30	179.5°		2h16m	+14°			2022/10/30	14.4		2022/11/01	1.601					
2820	2022/10/10	177.8°		0h59m	+ 8°			2022/10/10	14.1		2022/10/09	0.870					
2870	2022/09/20	171.2°		0h 4m	- 9°			2022/09/20	14.3		2022/09/21	0.893					
3224	2022/04/16	177.2°		13h32m	-12°			2022/04/16	14.2		2022/04/20	1.347					
3284	2022/06/30	173.7°		18h43m	-29°			2022/07/02	14.5		2022/07/17	0.897					
3345	2022/01/09	171.1°		7h22m	+31°			2022/01/10	13.7		2022/01/14	1.067					
3382	2022/10/11	175.6°		0h58m	+10°			2022/10/10	14.5		2022/10/04	0.875					
3388	2022/01/04	173.9°		7h12m	+28°			2022/01/05	14.3		2022/01/06	0.914					
3728	2022/12/17	140.0°		5h40m	-16°			2022/12/17	14.5		2022/12/17	1.246					
3773	2022/10/16	178.1°		1h27m	+ 7°			2022/10/16	14.3		2022/10/10	0.810					
3901	2022/05/29	156.3°		16h15m	-45°			2022/05/28	14.4		2022/05/27	0.917					
3920	2022/07/12	177.7°		19h24m	-19°			2022/07/12	14.4		2022/07/25	0.832					
3925	2022/10/18	162.9°		1h59m	- 6°			2022/10/17	14.4		2022/10/15	1.589					
4080	2022/08/15	171.0°		21h27m	- 5°			2022/08/15	14.2		2022/08/13	0.724					
4135	2022/09/21	174.5°		23h44m	+ 4°			2022/09/21	14.4		2022/09/23	1.151					
4384	2022/08/11	179.0°		21h23m	-14°			2022/08/11	14.4		2022/08/16	1.219					
4451	2022/10/15	151.4°		23h49m	+27°			2022/10/08	13.7		2022/09/30	0.774					
4460	2022/08/09	170.6°		21h20m	-25°			2022/08/09	14.2		2022/08/13	1.478					
4512	2022/02/07	173.9°		9h31m	+21°			2022/02/06	14.4		2022/02/04	1.233					
4577	2022/12/02	176.0°		4h32m	+25°			2022/12/03	14.1		2022/12/11	1.052					
4724	2022/06/22	178.7°		18h 2m	-22°			2022/06/22	14.1		2022/06/26	0.792					
4768	2022/08/13	179.6°		21h30m	-14°			2022/08/13	14.1		2022/08/16	1.452					
4869	2022/08/08	175.0°		21h17m	-20°			2022/08/08	14.5		2022/08/07	0.833					
5216	2022/08/09	179.1°		21h15m	-14°			2022/08/09	13.8		2022/08/10	1.188					
5352	2022/11/25	177.7°		4h 0m	+22°			2022/11/25	14.5		2022/11/24	1.017					
5693	2022/05/08	136.6°		17h53m	- 6°			2022/05/24	14.0		2022/05/28	0.069					
6027	2022/07/04	179.0°		18h51m	-21°			2022/07/04	14.0		2022/07/03	0.845					
6146	2022/06/19	174.2°		17h53m	-29°			2022/06/20	13.9		2022/06/27	0.725					
6794	2022/10/23	174.3°		1h56m	+ 2°			2022/10/23	14.0		2022/10/22	1.438					
6906	2022/12/08	177.1°		4h59m	+25°			2022/12/08	14.5		2022/12/03	1.041					
7335	2022/05/20	152.0°		14h36m	+ 1°			2022/05/25	11.1		2022/05/27	0.027					
7482	2022/01/13	108.9°		6h26m	-47°			2022/01/18	10.4		2022/01/18	0.013					
7559	2022/07/03	173.6°		18h53m	-29°			2022/07/04	14.4		2022/07/09	0.871					
9117	2022/12/30	177.3°		6h38m	+25°			2022/12/30	14.4		2023/01/03	1.100					
9900	2022/06/02	172.1°		16h43m	-14°			2022/06/02	14.2		2022/06/04	0.680					
10449	2022/09/14	179.2°		23h29m	- 4°			2022/09/14	14.5		2022/09/11	1.042					
11650	2022/10/27	167.2°		1h45m	+24°			2022/10/25	14.4		2022/10/17	0.958					
13918	2022/08/06	178.8°		21h 2m	-15°			2022/08/06	14.4		2022/08/04	1.045					
23606	2022/07/19	179.6°		19h53m	-21°			2022/07/19	13.9		2022/07/18	0.102					
28017	2022/12/28	178.1°		6h26m	+21°			2022/12/27	14.3		2022/12/10	0.813					
52800	2022/01/10	170.4°		7h20m	+31°			2022/01/09	14.2		2021/12/31	0.728					
66875	2022/12/02	178.1°		4h32m	+23°			2022/12/02	14.0		2022/12/05	0.750					
85713	2022/10/29	134.4°		5h20m	+27°			2022/11/16	14.0		2022/11/21	0.141					
138971	2022/02/11	134.9°		12h45m	+25°			2022/02/28	14.0		2022/03/04	0.033					

Table II. Temporal Sequence of Favorable Elongations

Planet	Max	Elon	D	Max	E	RA	Dec	Br	Mag	D	Br	Mag	Min	Dist	D	Min	Dist
554	2022/01/02	178.6°		6h54m	+24°			2022/01/02	10.9		2022/01/29	1.090					
3388	2022/01/04	173.9°		7h12m	+28°			2022/01/05	14.3		2022/01/06	0.914					
1115	2022/01/06	165.7°		7h22m	+36°			2022/01/07	12.9		2022/01/08	1.621					
1657	2022/01/09																

Planet	Max	Elon	D	Max	E	RA	Dec	Br	Mag	D	Br	Mag	Min	Dist	D	Min	Dist
1683	2022/08/12	176.9°	21h29m	-18°		2022/08/12	14.0	2022/08/10	1.241								
4768	2022/08/13	179.6°	21h30m	-14°		2022/08/13	14.1	2022/08/16	1.452								
4080	2022/08/15	171.0°	21h27m	-5°		2022/08/15	14.2	2022/08/13	0.724								
704	2022/08/17	160.4°	21h25m	+5°		2022/08/18	9.9	2022/08/21	1.728								
956	2022/08/20	170.5°	21h43m	-3°		2022/08/20	13.9	2022/08/18	0.824								
987	2022/08/23	178.0°	22h 4m	-9°		2022/08/23	12.1	2022/08/23	1.388								
2199	2022/08/25	178.4°	22h17m	-12°		2022/08/25	14.3	2022/08/17	0.854								
1077	2022/08/27	177.5°	22h24m	-12°		2022/08/27	13.7	2022/08/30	0.942								
1431	2022/08/28	163.5°	23h 0m	-24°		2022/08/28	14.0	2022/08/28	1.151								
809	2022/09/01	178.8°	22h41m	-9°		2022/09/01	12.9	2022/09/02	0.841								
1689	2022/09/03	172.3°	23h 1m	-14°		2022/09/04	13.8	2022/09/09	1.047								
539	2022/09/04	168.4°	22h36m	+3°		2022/09/05	12.3	2022/09/08	1.203								
1718	2022/09/04	167.5°	22h28m	+3°		2022/09/03	14.5	2022/09/01	0.711								
2100	2022/09/05	161.1°	21h58m	+5°		2022/09/03	13.7	2022/08/31	0.187								
2583	2022/09/07	166.1°	23h23m	-19°		2022/09/08	14.3	2022/09/09	0.793								
2231	2022/09/08	179.1°	23h 4m	-4°		2022/09/08	14.2	2022/09/11	1.057								
960	2022/09/09	173.5°	23h 1m	+0°		2022/09/09	14.3	2022/09/07	0.874								
161989	2022/09/10	121.2°	2h49m	-37°		2022/09/03	13.3	2022/09/01	0.058								
2343	2022/09/11	176.9°	23h14m	-1°		2022/09/12	14.3	2022/09/16	0.763								
10449	2022/09/14	179.2°	23h29m	-4°		2022/09/14	14.5	2022/09/11	1.042								
128	2022/09/17	169.5°	23h56m	-11°		2022/09/17	10.6	2022/09/18	1.429								
941	2022/09/17	170.0°	23h54m	-11°		2022/09/18	14.3	2022/09/21	1.298								
972	2022/09/17	166.1°	23h19m	+10°		2022/09/18	12.5	2022/09/20	1.374								
2237	2022/09/18	176.6°	23h46m	-5°		2022/09/18	14.4	2022/09/21	1.512								
2870	2022/09/20	171.2°	0h 4m	-9°		2022/09/20	14.3	2022/09/21	0.893								
804	2022/09/21	174.9°	23h47m	+4°		2022/09/21	10.9	2022/09/18	1.467								
4135	2022/09/21	174.5°	23h44m	+4°		2022/09/21	14.4	2022/09/23	1.151								
986	2022/09/23	155.7°	0h39m	-22°		2022/09/22	13.0	2022/09/21	1.547								
479	2022/10/02	167.2°	0h56m	-7°		2022/10/03	12.2	2022/10/07	1.210								
1527	2022/10/04	179.0°	0h41m	+3°		2022/10/04	13.5	2022/09/25	0.888								
696	2022/10/06	159.1°	0h14m	+24°		2022/10/08	12.4	2022/10/10	1.483								
1240	2022/10/08	166.4°	0h34m	+18°		2022/10/07	12.8	2022/10/03	1.419								
397	2022/10/09	165.6°	0h26m	+18°		2022/10/08	11.3	2022/10/06	0.999								
1756	2022/10/09	169.7°	0h44m	+15°		2022/10/10	14.1	2022/10/11	0.979								
990	2022/10/10	173.4°	0h51m	+12°		2022/10/09	13.6	2022/10/06	1.100								
2820	2022/10/10	177.8°	0h59m	+8°		2022/10/10	14.1	2022/10/09	0.870								
3382	2022/10/11	175.6°	0h58m	+10°		2022/10/10	14.5	2022/10/04	0.875								
852	2022/10/14	174.0°	1h21m	+2°		2022/10/13	11.7	2022/10/02	0.983								
1438	2022/10/14	177.8°	1h15m	+10°		2022/10/14	14.2	2022/10/11	1.423								
455	2022/10/15	159.6°	1h41m	-11°		2022/10/11	10.9	2022/10/05	0.956								
4451	2022/10/15	151.4°	23h49m	+27°		2022/10/08	13.7	2022/09/30	0.774								
3773	2022/10/16	178.1°	1h27m	+7°		2022/10/16	14.3	2022/10/10	0.810								
1792	2022/10/18	166.7°	1h48m	-2°		2022/10/19	14.1	2022/10/20	1.030								
3925	2022/10/18	162.9°	1h15m	+6°		2022/10/17	14.4	2022/10/15	1.589								
2337	2022/10/22	176.1°	1h51m	+7°		2022/10/22	14.4	2022/10/25	1.225								
365	2022/10/23	170.5°	2h 7m	+2°		2022/10/23	12.1	2022/10/23	1.382								
2243	2022/10/23	178.1°	1h50m	+13°		2022/10/23	14.4	2022/10/14	0.985								
6794	2022/10/23	174.3°	1h56m	+5°		2022/10/23	14.0	2022/10/22	1.438								
46	2022/10/25	177.7°	2h 3m	+10°		2022/10/25	10.5	2022/10/20	1.146								
543	2022/10/26	166.5°	1h40m	+24°		2022/10/26	13.0	2022/10/26	1.625								
217628	2022/10/26	138.0°	4h53m	+10°		2022/11/14	14.4	2022/11/20	0.135								
1573	2022/10/27	166.6°	2h37m	+1°		2022/10/26	13.8	2022/10/23	0.859								
11650	2022/10/27	167.2°	1h45m	+24°		2022/10/25	14.4	2022/10/17	0.958								
85713	2022/10/29	134.4°	5h20m	+27°		2022/11/16	14.0	2022/11/21	0.141								
2757	2022/10/30	179.5°	2h16m	+14°		2022/10/30	14.4	2022/11/01	1.601								
2751	2022/11/10	178.9°	3h 2m	+18°		2022/11/11	14.5	2022/11/14	1.071								
27	2022/11/12	177.8°	3h12m	+15°		2022/11/12	8.7	2022/11/16	1.026								
1500	2022/11/13	171.5°	3h 6m	+26°		2022/11/13	14.4	2022/11/10	0.839								
384	2022/11/15	178.9°	3h23m	+19°		2022/11/16	12.1	2022/11/18	1.314								
115	2022/11/19	157.7°	3h 5m	+40°		2022/11/18	9.6	2022/11/16	0.974								
264	2022/11/19	177.7°	3h35m	+21°		2022/11/19	11.3	2022/11/16	1.461								
726	2022/11/19	177.2°	3h34m	+22°		2022/11/19	12.5	2022/11/08	1.068								
5352	2022/11/25	177.7°	4h 0m	+22°		2022/11/25	14.5	2022/11/24	1.017								
30	2022/11/29	176.5°	4h16m	+24°		2022/11/29	9.6	2022/11/25	1.114								
2034	2022/11/30	166.2°	4h15m	+35°		2022/11/30	14.5	2022/12/01	0.879								
164	2022/12/01	171.9°	4h25m	+13°		2022/11/29	10.8	2022/11/17	1.023								
1052	2022/12/01	175.2°	4h32m	+17°		2022/12/01	13.6	2022/11/27	0.965								
4577	2022/12/02	176.0°	4h32m	+25°		2022/12/03	14.1	2022/12/11	1.052								
66875	2022/12/02	178.1°	4h32m	+23°		2022/12/02	14.0	2022/12/05	0.750								
2341	2022/12/03	178.6°	4h36m	+23°		2022/12/03	13.8	2022/12/30	0.907								
1660	2022/12/06	148.6°	5h30m	-7°		2022/12/13	13.9	2022/12/19	0.901								
1565	2022/12/07	173.8°	4h45m	+28°		2022/12/06	13.3	2022/11/23	0.755								
6906	2022/12/08	177.1°	4h59m	+25°		2022/12/08	14.5	2022/12/03	1.041								
645	2022/12/15	169.1°	5h25m	+34°		2022/12/15	13.8	2022/12/15	1.795								
3728	2022/12/17	140.0°	5h40m	-16°		2022/12/17	14.5	2022/12/17	1.246								

Year	Time Range	Count
28.2. 2020	17:45:47 – 17:52:18	30
9.3.	19:49:25 – 20:03:16	40
	20:04:23 – 20:38:08	30
13.3.	18:42:00 – 19:02:14	30
14.3.	20:08:13 – 22:17:21	30
16.3.	18:55:45 – 19:13:41	30
18.3.	19:39:00 – 19:56:44	20
	19:58:06 – 20:01:32	15
22.3.	19:20:20 – 01:03:14	15
24.3.	19:19:44 – 01:16:44	15
27.3.	19:24:58 – 01:38:36	15
29.3.	19:16:47 – 20:15:46	15
30.3.	19:13:04 – 02:01:32	15
1.4.	19:14:16 – 02:04:22	30
10.4.	21:01:07 – 21:04:24	30
16.4.	19:23:34 – 19:32:45	30
7.5.	20:08:23 – 20:13:52	30

All frames have been corrected for the bias, flat, and dark-field frames. We have observed during clear sky nights only and with air humidity of around 50 percent. The mean statistical error for all our magnitudes from the individual frames was 0.047 magnitudes. The dispersion of our data is clearly seen in Figure 1. The comparison stars were selected individually from the Tycho-2 catalogue in the processing of the “fits” frames treatment in the standard way enabled within *AstroImageJ*. From our observations, taken on 16 nights, we obtained approximately 1800 values for Julian date, magnitude and magnitude error. On the foundation of these data, it was possible to Fourier analyze them with the goal of finding the period of rotation of the nucleus of the comet. Using the tool provided at the website

<https://exoplanetarchive.ipac.caltech.edu/cgi-bin/Pgram/nph-pgram> and, by using the *MPO Canopus* software package (Warner, 2015), we have been able to construct a periodogram of our data and what may represent the cometary core lightcurve. In our computations we have preferred the Lomb-Scargle algorithm. The obtained comet's lightcurve is presented in Figure 1. Two maxima and two minima within the obtained lightcurve are clearly seen as is typically the case of asteroids and comets.

While we propose that we have successfully measured and plotted the lightcurve of the nucleus of the comet C/2017 T2 (PanSTARRS), there remains the unknown possibility of changes in the cometary nucleus rotation period and shape owing to forced precession due to mass loss. It is important to note that the comet we observed was active at the time of our observations. With this in mind, of course, we suggest that the solid line in Figure 1 represents the rotation of the nucleus, because it has the character of a lightcurve of a rotation of an asteroid. Although the scatter of the data is at the level of the amplitude of the lightcurve, we have been working with 1,800 frames, therefore, the power of statistical averaging is the basis for the confidence of our measurement.

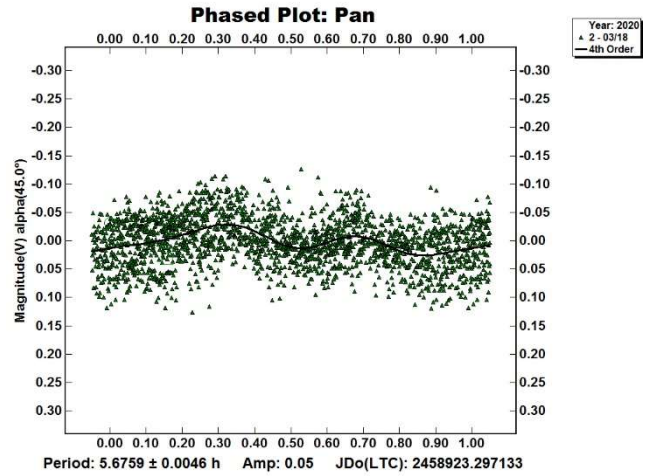


Figure 1. The lightcurve of the comet C/2017 T2 (PanSTARRS) composed from the individual frames of the observations. For better presentation, all data have been given in common so the date as shown on top right.

### Acknowledgements

This research has made use of the NASA Exoplanet Archive, which is operated by the California Institute of Technology, under contract with the National Aeronautics and Space Administration under the Exoplanet Exploration Program.

### References

Collins, K.A.; Kielkopf, J.F.; Stassun, K.G; Hessman, F.V. (2017). “ASTROIMAGEJ: Image processing and photometric extraction for ultra-precise astronomical light curves.” *Astron. J.* **153**:77, 13pp. <http://www.astro.louisville.edu/software/astroimagej/>

Moravian Instruments (2020). Cameras for Astronomers Main Page <http://www.gxccd.com>

Warner, B.D.; Harris, A.W.; Pravec, P. (2009). “The Asteroid Lightcurve Database.” *Icarus* **202**, 134-146. <http://www.minorplanet.info/lightcurvedatabase.html>

Warner, B. D. (2015) *MPO Canopus software* v10.7.06. Bdw Publishing <http://www.MinorPlanetObserver.com>

Yoshida, S. (2020). Seiichi Yoshida’s Homepage <http://www.aerith.net>

Zakajsek, J. (2020). COBS: Comet Observation Dataset <https://www.cobs.si/>

Number	Name	yyyy mm/dd	Phase	LPAB	BPAB	Period(h)	P.E.	Amp	A.E.	r
C/2020 T2	(PanSTARRS)	2020 02/28-07/05	31.9, 35.7	91	53	5.6759	0.0046	0.05	0.047	1.69

Table II. Observing circumstances and results. The phase angle is given for the first and last date. If preceded by an asterisk, the phase angle reached an extrema during the period. LPAB and BPAB are the approximate phase angle bisector longitude/latitude at mid-date range (see Harris et al., 1984). Grp is the asteroid family/group (Warner et al., 2009).

## LIGHTCURVE PHOTOMETRY OPPORTUNITIES: 2022 JANUARY-MARCH

Brian D. Warner  
Center for Solar System Studies / MoreData!  
446 Sycamore Ave.  
Eaton, CO 80615 USA  
brian@MinorPlanetObserver.com

Alan W. Harris  
MoreData!  
La Cañada, CA 91011-3364 USA

Josef Ďurech  
Astronomical Institute  
Charles University  
18000 Prague, CZECH REPUBLIC  
durech@sirrah.troja.mff.cuni.cz

Lance A.M. Benner  
Jet Propulsion Laboratory  
Pasadena, CA 91109-8099 USA  
lance.benner@jpl.nasa.gov

We present lists of asteroid photometry opportunities for objects reaching a favorable apparition and have no or poorly-defined lightcurve parameters. Additional data on these objects will help with shape and spin axis modeling using lightcurve inversion. We have changed the presentation of the “Radar-Optical Opportunities” section to include a list of potential radar targets as well as some that are in critical need of astrometric data and, if found, might also be targets for radar. These can have ephemeris errors on the order of tens to thousands of arcseconds and, despite the current surveys, have not been observed for several years. This makes them a double challenge: first to be found and, second, to determine astrometric positions and photometric properties.

We present several lists of asteroids that are prime targets for photometry and/or astrometry during the period 2022 January-March. The “Radar-Optical Opportunities” section has a new format that provides an expanded list of potential targets and no longer gives geocentric ephemerides.

In the first three sets of tables, “Dec” is the declination and “U” is the quality code of the lightcurve. See the latest asteroid lightcurve data base (LCDB from here on; Warner et al., 2009) documentation for an explanation of the U code:

<http://www.minorplanet.info/lightcurvedatabase.html>

The ephemeris generator on the CALL web site allows creating custom lists for objects reaching  $V \leq 18.0$  during any month in the current year and up to five years in the future, e.g., limiting the results by magnitude and declination, family, and more.

[http://www.minorplanet.info/PHP/call\\_OppLCDBQuery.php](http://www.minorplanet.info/PHP/call_OppLCDBQuery.php)

We refer you to past articles, e.g., Warner et al. (2021a) for more detailed discussions about the individual lists and points of advice regarding observations for objects in each list.

Once you’ve obtained and analyzed your data, it’s important to publish your results. Papers appearing in the *Minor Planet Bulletin* are indexed in the Astrophysical Data System (ADS) and so can be referenced by others in subsequent papers. It’s also important to make the data available at least on a personal website or upon request. We urge you to consider submitting your raw data to the ALCDEF database. This can be accessed for uploading and downloading data at

<http://www.alcdef.org>

The database contains more than 3.9 million observations for 15,000+ objects, making it one of the more useful sources for raw asteroid *time-series* lightcurve data.

### Lightcurve/Photometry Opportunities

Objects with  $U = 3-$  or 3 are excluded from this list since they will likely appear in the list for shape and spin axis modeling. Those asteroids rated  $U = 1$  should be given higher priority over those rated  $U = 2$  or  $2+$ , but not necessarily over those with no period. On the other hand, do *not* overlook asteroids with  $U = 2/2+$  on the assumption that the period is sufficiently established. Regardless, do not let the existing period influence your analysis since even highly-rated result have been proven wrong at times. Note that the lightcurve amplitude in the tables could be more or less than what’s given. Use the listing only as a guide.

An entry in bold italics is a near-Earth asteroid (NEA).

Number	Name	Brightest			Period	LCDB Data	
		Date	Mag	Dec		mp	U
2197	Shanghai	01 01.8	15.2	+26	5.99		0.16 2
4706	Dennisreuter	01 03.8	15.3	+6	2.578		0.07 1
5392	Parker	01 04.3	14.4	+60	87.15		0.60 2+
4719	Burnaby	01 05.4	15.2	+36	13.01	0.05	0.07 2
17966	1999 JS43	01 05.9	15.5	+24	78.116		0.58 2
2928	Epstein	01 08.8	15.4	+28	8.509		0.37 2
3872	Akirafujii	01 09.1	15.2	+28	10.635	0.23	0.35 2
1657	Roemera	01 09.6	14.3	+26	34	0.09	0.15 2
2808	Belgrano	01 14.4	15.2	+26	195.83		0.27 2
1854	Skvortsov	01 17.5	15.1	+12	78.5		0.56 2
2069	Hubble	01 22.3	14.9	+33	32.52		0.10 2
2563	Boyarchuk	01 25.3	15.2	+20	11.04		0.11 2
506459	2002 AL14	01 30.6	15.0	+25	2.309		0.35 2
2732	Witt	02 06.2	15.4	+14	12.622		0.50 2+
4512	Sinuhe	02 06.9	14.2	+21	18	0.23	0.80 2
5506	Artiglio	02 10.7	15.5	+23	9.406	0.76	1.01 2
6505	Muzzio	02 21.7	14.9	15	13.735		0.10 2+
1261	Legia	02 22.5	14.6	+14	8.693		0.13 2+
2265	Verbaandert	02 25.8	15.5	+22	2.99		0.12 2
138971	2001 CB21	02 28.6	14.0	+27	3.302		0.19 2
5641	McCleese	03 01.1	14.7	+16	418	0.06	1.3 2
4424	Arkhipova	03 02.9	15.1	+16	14.673		0.45 2
18243	Gunn	03 06.3	15.4	+10	6.637		0.27 2
4457	van Gogh	03 06.7	14.9	2	7.606		0.12 2
4528	Berg	03 06.7	14.7	+7	3.516	0.16	0.26 2
11512	1991 AB2	03 10.6	15.4	+3	2.933		0.20 2+
2696	Magion	03 11.5	15.1	8	480		0.31 2
1541	Estonia	03 11.6	14.6	+5	10.1		0.13 2
2802	Weisell	03 18.8	14.8	+11	14.683	0.25	0.37 2
3617	Eicher	03 20.0	15.2	1	10.305		0.07 2
	2013 BO76	03 22.1	15.4	54	5.03		0.26 2
1020	Arcadia	03 24.1	15.5	1	17.02		0.05 1
1859	Kovalevskaya	03 25.4	14.8	6	11.114	0.13	0.44 2+
9846	1990 OS1	03 31.0	15.2	6	18.546		0.09 1

### Low Phase Angle Opportunities

The Low Phase Angle list includes asteroids that reach very low phase angles ( $\alpha < 1^\circ$ ). The “ $\alpha$ ” column is the minimum solar phase angle for the asteroid. Getting accurate, calibrated measurements (usually V band) at or very near the day of opposition can provide important information for those studying the “opposition effect.” Use the on-line query form for the LCDB to get more details about a specific asteroid.

[http://www.minorplanet.info/PHP/call\\_OppLCDBQuery.php](http://www.minorplanet.info/PHP/call_OppLCDBQuery.php)

You will have the best chance of success working objects with low amplitude and periods that allow covering at least half a cycle every night. Objects with large amplitudes and/or long periods are much more difficult for phase angle studies since, for proper analysis, the data must be reduced to the average magnitude of the asteroid for each night. This reduction requires that you determine the period and the amplitude of the lightcurve; for long period objects that can be difficult. Refer to Harris et al. (1989) for the details of the analysis procedure.

As an aside, it is arguably better for physical interpretation (e.g.,  $G$  value versus albedo) to use the maximum light rather than mean level to find the phase slope parameter ( $G$ ). This better models the behavior of a spherical object of the same albedo, but it can produce significantly different values for both  $H$  and  $G$  versus using average light, which is the method used for values listed by the Minor Planet Center. Using and reporting the results of both methods can provide additional insights into the physical properties of an asteroid.

The International Astronomical Union (IAU) has adopted a new system, H-G<sub>12</sub>, introduced by Muinonen et al. (2010). It will be some years before H-G<sub>12</sub> becomes widely used, and hopefully not until a discontinuity flaw in the G<sub>12</sub> function has been fixed. This discontinuity results in false “clusters” or “holes” in the solution density and makes it impossible to draw accurate conclusions.

We strongly encourage obtaining data as close to 0° as possible, then every 1-2° out to 7°, below which the curve tends to be non-linear due to the opposition effect. From 7° out to about 30°, observations at 3-6° intervals should be sufficient. Coverage beyond about 50° is not generally helpful since the H-G system is best defined with data from 0-30°.

It's important to emphasize that all observations should (must) be made using high-quality catalogs to set the comparison star magnitudes. These include ATLAS, Pan-STARRS, SkyMapper, and GAIA2. Catalogs such as CMC-15, APASS, or the MPOSC from *MPO Canopus* should not be used due to significant systematic errors.

Also important is that there are sufficient data from each observing run such that their location can be found on a combined, phased lightcurve derived from two or more nights obtained *near the same phase angle*. This is so that the lightcurve amplitude isn't significantly different. If necessary, the magnitudes for the given run should be adjusted so that they correspond to mid-light of the combined lightcurve. This goes back to the H-G system being based on average, not maximum or minimum light.

For this table, the asteroid magnitudes are brighter than in others. This is because higher precision is required for this work and the asteroid may be a full magnitude or fainter when it reaches phase angles out to 20-30°.

Num	Name	Date	$\alpha$	V	Dec	Period	Amp	U
554	Peraga	01 03.0	0.61	11.0	+24	13.713	0.11 0.28	3
410	Chloris	01 03.4	0.47	12.9	+24	32.50	0.28 0.33	3
570	Kythera	01 07.5	0.69	13.3	+20	8.120	0.12 0.20	2
618	Elfriede	01 12.1	0.11	12.8	+22	14.791	0.11 0.17	3
851	Zeissia	01 16.2	0.95	13.4	+19	9.34	0.38 0.53	3
62	Erato	01 17.0	0.17	12.5	+20	9.221	0.12 0.22	3
268	Adorea	01 21.9	0.07	12.1	+20	7.80	0.15 0.20	3
49	Pales	01 24.2	0.53	11.6	+18	20.705	0.17 0.18	3
158	Koronis	01 28.1	0.28	12.8	+18	14.218	0.28 0.43	3
379	Huenna	01 29.2	0.45	13.7	+16	14.141	0.07 0.12	3
600	Musa	02 02.4	0.62	13.6	+15	5.886	0.26 0.28	3
1171	Rusthawelia	02 04.6	0.38	13.7	+17	10.98	0.26 0.31	3
20	Massalia	02 05.3	0.60	8.5	+15	8.098	0.17 0.27	3

Num	Name	Date	$\alpha$	V	Dec	Period	Amp	U
11	Parthenope	02 10.8	0.75	10.0	+16	13.720	0.05 0.12	3
924	Toni	02 11.0	0.59	13.8	+12	19.437	0.24 0.24	3
748	Simeisa	02 11.8	0.75	13.8	+11	11.919	0.22 0.36	2
215	Oenone	02 15.8	0.76	13.3	+15	27.937	0.1 0.20	3
19	Fortuna	02 22.5	0.83	10.5	+08	7.443	0.23 0.30	3
723	Hammonia	02 22.8	0.40	14.0	+09	5.436	0.08 0.18	3
201	Penelope	02 24.5	0.16	12.5	+09	3.747	0.15 0.73	3
1642	Hill	02 25.1	0.34	14.0	+10	6.056	0.21 0.25	3
200	Dynamene	02 26.8	0.89	12.1	+06	37.394	0.10	3
206	Hersilia	03 02.0	0.60	12.1	+09	11.122	0.13 0.20	3
16	Psyche	03 03.4	0.31	10.4	+08	4.196	0.03 0.34	3
74	Galatea	03 04.1	0.97	13.3	+04	17.268	0.08 0.16	3
177	Irma	03 05.5	0.15	13.9	+06	13.856	0.24 0.37	3
75	Eurydike	03 09.8	0.37	13.7	+06	5.357	0.10 0.15	3
150	Nuwa	03 11.0	0.55	13.0	+02	8.135	0.08 0.31	3
180	Garumna	03 13.1	0.41	12.8	+02	23.866	0.27 0.6	3
33	Polyhymnia	03 15.9	0.16	13.7	+03	18.608	0.13 0.20	3
243	Ida	03 18.0	0.33	13.6	+00	4.634	0.45 0.86	3
533	Sara	03 18.3	0.21	13.4	+01	11.654	0.19 0.30	3
178	Belisana	03 27.1	0.93	12.3	+00	12.323	0.08 0.18	3
203	Pompeja	03 27.5	0.56	12.5	-04	24.052	0.10	3
305	Gordonia	03 29.6	0.77	12.6	-05	12.893	0.16 0.23	3

### Shape/Spin Modeling Opportunities

Those doing work for modeling should contact Josef Āurech at the email address above. If looking to add lightcurves for objects with existing models, visit the Database of Asteroid Models from Inversion Techniques (DAMIT) web site

<https://astro.troja.mff.cuni.cz/projects/damit/>

Additional lightcurves could lead to the asteroid being added to or improving one in DAMIT, thus increasing the total number of asteroids with spin axis and shape models.

Included in the list below are objects that:

1. Are rated U = 3– or 3 in the LCDB.
2. Do not have reported pole in the LCDB Summary table.
3. Have at least three entries in the Details table of the LCDB where the lightcurve is rated U ≥ 2.

The caveat for condition #3 is that no check was made to see if the lightcurves are from the same apparition or if the phase angle bisector longitudes differ significantly from the upcoming apparition. The last check is often not possible because the LCDB does not list the approximate date of observations for all details records. Including that information is an on-going project.

Favorable apparitions are in bold text. NEAs are in italics.

Num	Name	Brightest			LCDB Data		
		Date	Mag	Dec	Period	Amp	U
<b>554</b>	<b>Peraga</b>	<b>01 02.9</b>	<b>11.0</b>	<b>+24</b>	<b>13.713</b>	<b>0.11 0.28</b>	<b>3</b>
410	Chloris	01 03.4	12.9	+24	32.5	0.19 0.33	3
<b>1090</b>	<b>Sumida</b>	<b>01 04.7</b>	<b>14.7</b>	<b>-9</b>	<b>2.719</b>	<b>0.10 0.34</b>	<b>3</b>
737	Arequipa	01 10.2	13.6	+5	7.026	0.08 0.26	3
284	Amalia	01 13.4	14.3	+11	8.545	0.13 0.16	3
1576	Fabiola	01 19.9	14.9	+19	6.889	0.2 0.26	3
2195	Tengstrom	01 23.0	14.7	+23	2.821	0.17 0.45	3
1405	Sibelius	01 23.7	14.7	+21	6.04	0.11 0.20	3
49	Pales	01 24.1	11.6	+18	20.705	0.17 0.19	3
194	Prokne	01 24.3	12.5	+4	15.679	0.08 0.27	3
1071	Brita	01 25.1	13.8	+27	5.817	0.12 0.23	3
605	Juvisia	01 25.9	14.8	+36	15.851	0.18 0.26	3
326	Tamara	01 26.8	13.5	+55	14.445	0.10 0.27	3
657	Gunlod	01 29.1	14.1	+15	15.665	0.19 0.20	3
379	Huenna	01 29.2	13.8	+16	14.141	0.07 0.22	3
1406	Komppa	01 30.2	14.8	+25	3.508	0.14 0.20	3
1120	Cannonia	01 30.6	14.6	+14	3.816	0.15 0.21	3
1587	Kahrstedt	02 01.8	14.0	+26	7.971	0.12 0.24	3
1234	Elyna	02 03.0	15.0	+15	5.422	0.14 0.37	3
1171	Rusthawelia	02 04.5	13.8	+17	10.98	0.26 0.31	3
1166	Sakuntala	02 06.0	14.8	+30	6.292	0.24 0.40	3
735	Marghanna	02 06.6	14.9	+37	20.625	0.11 0.13	3
522	Helga	02 07.9	14.4	+17	8.129	0.13 0.31	3
1578	Kirkwood	02 07.9	14.8	+16	17.885	0.05 0.22	3-

Num	Name	Brightest			Period	LCDB Data		U
		Date	Mag	Dec		Amplitude	Amplitude	
102	Miriam	02 09.5	13.7	+8	23.613	0.04	0.14	3
2463	Sterpin	02 14.8	14.9	+1	13.43	0.25	0.30	3-
<b>7341</b>	<b>1991 VK*</b>	<b>02 15.2</b>	<b>14.8</b>	<b>-46</b>	<b>4.21</b>	<b>0.21</b>	<b>0.70</b>	<b>3</b>
5407	1992 AX	02 16.1	14.7	+26	2.549	0.05	0.12	3
5598	Carl Murray	02 16.4	14.9	+6	2.923	0.19	0.32	3
200	Dynamene	02 26.7	12.1	+6	37.394	0.06	0.10	3
266	Aline	03 01.5	13.3	-10	13.018	0.07	0.10	3
206	Hersilia	03 02.0	12.2	+9	11.122	0.13	0.20	3
905	Universitas	03 03.4	14.7	+13	14.238	0.22	0.33	3
<b>143</b>	<b>Adria*</b>	<b>03 03.7</b>	<b>12.6</b>	<b>+4</b>	<b>22.005</b>	<b>0.07</b>	<b>0.10</b>	<b>3</b>
914	Palisana	03 05.2	13.7	-27	8.681	0.03	0.24	3-
177	Irma	03 05.4	13.9	+6	13.856	0.24	0.37	3
348	May	03 06.2	13.5	+19	7.381	0.14	0.16	3
975	Perseverantia	03 07.7	14.2	+8	7.267	0.17	0.23	3
142	Polana	03 10.2	12.6	+1	9.764	0.11	0.24	3
2008	Konstitutsiya	03 10.3	14.6	+18	11.269	0.06	0.11	3
1015	Christa	03 16.9	14.1	+12	11.23	0.12	0.20	3-
<b>533</b>	<b>Sara*</b>	<b>03 18.3</b>	<b>13.4</b>	<b>+1</b>	<b>11.654</b>	<b>0.19</b>	<b>0.30</b>	<b>3</b>
1186	Turnera	03 18.9	14.6	+11	12.085	0.22	0.36	3
952	Caia	03 19.1	14.5	+5	7.5	0.03	0.21	3
1644	Rafita	03 19.7	14.5	-11	3.344	0.13	0.38	3
504	Cora	03 23.7	14.9	+16	7.587	0.15	0.27	3
380	Fiducia	03 24.6	13.6	+7	13.69	0.04	0.32	3
947	Monterosa	03 26.7	14.6	+4	5.164	0.08	0.23	3-
305	Gordonia	03 29.4	12.6	-5	12.893	0.16	0.23	3
<b>137170</b>	<b>1999 HF1*</b>	<b>03 30.4</b>	<b>14.5</b>	<b>+81</b>	<b>2.319</b>	<b>0.12</b>	<b>0.26</b>	<b>3</b>

### Radar-Optical Opportunities

Table I below gives a list of near-Earth asteroids reaching maximum brightness for the current quarter-year based on calculations by Warner. We switched to this presentation in lieu of ephemerides for reasons outlined in the 2021 October-December opportunities paper (Warner et al., 2021b), which centered on the potential problems with ephemerides generated several months before publication.

The initial list of targets started using the planning tool at

[http://www.minorplanet.info/PHP/call\\_OppLCDBQuery.php](http://www.minorplanet.info/PHP/call_OppLCDBQuery.php)

where the search was limited to near-Earth asteroids only that were  $V \leq 18$  for at least part of the quarter.

The list was then filtered to include objects that might be targets for the Goldstone radar facility or, if it were still operational, the Arecibo radar. This was based on the calculated radar SNR using

<http://www.naic.edu/~eriverav/scripts/index.php>

and assuming a rotation period of 4 hours (2 hours if  $D \leq 200$  m) if a period was not given in the asteroid lightcurve database (LCDB; Warner et al., 2009a). The SNR values are estimates only and assume that the radar is fully functional.

If an asteroid was on the list but failed the SNR test, we checked if it might be a suitable target for radar and/or photometry sometime through 2050. If so, it was kept on the list to encourage physical and astrometric observations during the current apparition. In most of those cases, the SNR values in the “A” and “G” columns are not for the current quarter but the year given in the Notes column. If a better apparition is forthcoming through 2050, the Notes column in Table I contains SNR values for that time.

The final step was to cross-reference our list with that found on the Goldstone planned targets schedule at

[http://echo.jpl.nasa.gov/asteroids/goldstone\\_asteroid\\_schedule.html](http://echo.jpl.nasa.gov/asteroids/goldstone_asteroid_schedule.html)

It’s important to note that the final list in Table I is based on *known* targets and orbital elements when it was prepared. It is common for newly discovered objects to move in or out of the list. We recommend that you keep up with the latest discoveries by using the Minor Planet Center observing tools.

In particular, monitor NEAs and be flexible with your observing program. In some cases, you may have only 1-3 days when the asteroid is within reach of your equipment. Be sure to keep in touch with the radar team (through Benner’s email or their Facebook or Twitter accounts) if you get data. The team may not always be observing the target but your initial results may change their plans. In all cases, your efforts are greatly appreciated.

For observation planning, use these two sites

MPC: <http://www.minorplanetcenter.net/iau/MPEph/MPEph.html>

JPL: <http://ssd.jpl.nasa.gov/?horizons>

Cross-check the ephemerides from the two sites just in case there is discrepancy that might have you imaging an empty sky.

### About YORP Acceleration

Near-Earth asteroids are particularly sensitive to YORP acceleration. YORP (Yarkovsky–O’Keefe–Radzievskii–Paddack; Rubincam, 2000) is the asymmetric thermal re-radiation of sunlight that can cause an asteroid’s rotation period to increase or decrease. High precision lightcurves at multiple apparitions can be used to model the asteroid’s *sidereal* rotation period and see if it’s changing.

It usually takes four apparitions to have sufficient data to determine if the asteroid rotation rate is changing under the influence of YORP. This is why observing an asteroid that already has a well-known period remains a valuable use of telescope time. It is even more so when considering the BYORP (binary-YORP) effect among binary asteroids that has stabilized the spin so that acceleration of the primary body is not the same as if it would be if there were no satellite.

### The Quarterly Target List Table

The Table I columns are

Num	Asteroid number, if any.
Name	Name assigned by the MPC.
H	Absolute magnitude from MPCOrb.
Dkm	Diameter (km) assuming $p_V = 0.2$ .
Date	Date (mm dd.d) of brightest magnitude.
V	Approximate V magnitude at brightest.
Dec	Approximate declination at brightest.
Period	Synodic rotation period from summary line in the LCDB summary table.
Amp	Amplitude range (or single value) of reported lightcurves.
U	LCDB U (solution quality) from 1 (probably wrong) to 3 (secure).
A	Approximate SNR for Arecibo (if operational and at full power).
G	Approximate SNR for Goldstone radar at full power.
Notes	Comments about the object.

“PHA” is a potentially hazardous asteroid. For good measure, consider that astrometry and photometry have been requested to support Goldstone observations. Keep in mind that unnumbered objects may have been last observed several years ago and then only for a few days. The ephemerides uncertainties for these asteroids given by the MPC can be in the tens to thousands of arcseconds.

The sources for the rotation period are given in the Notes column. If none are qualified with a specific period, then the periods from multiple sources were in general agreement.

Higher priority should be given to those where the current apparition is the last one  $V \leq 18$  through 2050 or several years to come.

#### References

- Becker, T.M.; Howell, E.S.; Nolan, M.C.; Magri, C.; Pravec, P.; Taylor, P.A.; Oey, J.; Higgins, D.; Világi, J.; Kornoš, L.; Galád, A.; Gajdoš, Š.; Gaftonyuk, N.M.; Warner, B.D.; Vachier, F.; Marchis, F.; Pollock, J.T. (2015). “Physical modeling of triple near-Earth Asteroid (153591) 2001 SN263 from radar and optical light curve observations.” *Icarus* **248**, 499-515.
- Behrend, R. (2016web). Observatoire de Geneve web site. [http://obswww.unige.ch/~behrend/page\\_cou.html](http://obswww.unige.ch/~behrend/page_cou.html)
- Galád, A.; Pravec, P.; Kušnirák, P.; Gajdoš, Š.; Kornoš, L.; Világi, J. (2005). “Joint Lightcurve Observations of 10 Near-Earth Asteroids from Modra and ONDŘEJOV.” *Earth, Moon, and Planets* **97**, 147-163.
- Harris, A.W.; Young, J.W.; Bowell, E.; Martin, L.J.; Millis, R.L.; Poutanen, M.; Scaltriti, F.; Zappala, V.; Schober, H.J.; Debehogne, H.; Zeigler, K.W. (1989). “Photoelectric Observations of Asteroids 3, 24, 60, 261, and 863.” *Icarus* **77**, 171-186.
- Higgins, D.; Pravec, P.; Kusnirak, P.; Hornoch, K.; Brinsfield, J.W.; Allen, B.; Warner, B.D. (2008). “Asteroid Lightcurve Analysis at Hunters Hill Observatory and Collaborating Stations: November 2007 - March 2008.” *Minor Planet Bull.* **35**, 123-126.
- Muironen, K.; Belskaya, I.N.; Cellino, A.; Delbò, M.; Lvasseur-Regourd, A.-C.; Penttilä, A.; Tedesco, E.F. (2010). “A three-parameter magnitude phase function for asteroids.” *Icarus* **209**, 542-555.
- Pilcher, F.; Briggs, J.W.; Franco, L.; Inasaridze, R.Ya.; Krugly, Y.N.; Molotov, I.E.; KlingleSmith III, D.A.; Pollock, J.; Pravec, P. (2012a). “Rotation Period Determination for 5143 Heracles.” *Minor Planet Bull.* **39**, 148-151.
- Pilcher, F.; Benishek, V.; Briggs, J.W.; Ferrero, A.; KlingleSmith III, D.A.; Warren, C.A. (2012b). “Eight Months of Lightcurves of 1036 Ganymed.” *Minor Planet Bull.* **39**, 141-144.
- Pravec, P.; Wolf, M.; Sarounova, L. (1998). “Lightcurves of 26 Near-Earth Asteroids.” *Icarus* **136**, 124-153.
- Pravec, P.; Wolf, M.; Sarounova, L. (-2000web; -2002web; -2003web; -2021web). <http://www.asu.cas.cz/~ppravec/neo.htm>
- Pravec, P.; Scheirich, P.; Kusnirák, P.; Sarounová, L.; Mottola, S.; Hahn, G.; Brown, P.; Esquerdo, G.; Kaiser, N.; Krzeminski, Z.; and 47 coauthors (2006). “Photometric survey of binary near-Earth asteroids.” *Icarus* **181**, 63-93.
- Rubincam, D.P. (2000). “Radiative Spin-up and Spin-down of Small Asteroids.” *Icarus* **148**, 2-11.
- Warner, B.D., Harris, A.W., Pravec, P. (2009a). “The Asteroid Lightcurve Database.” *Icarus* **202**, 134-146. Updated 2021 June. <https://minplanobs.org/MPInfo/php/lcdb.php>
- Warner, B.D. (2009b). “Asteroid Lightcurve Analysis at the Palmer Divide Observatory: 2008 May - September.” *Minor Planet Bull.* **36**, 7-13.
- Warner, B.D. (2013). “Asteroid Lightcurve Analysis at the Palmer Divide Observatory: 2013 January - March.” *Minor Planet Bull.* **40**, 137-145.
- Warner, B.D. (2014a). “Near-Earth Asteroid Lightcurve Analysis at CS3-Palmer Divide Station: 2014 January-March.” *Minor Planet Bull.* **41**, 157-168.
- Warner, Brian D. (2014b). “Near-Earth Asteroid Lightcurve Analysis at CS3-Palmer Divide Station: 2014 March-June.” *Minor Planet Bull.* **41**, 213-224.
- Warner, B.D. (2015a). “Near-Earth Asteroid Lightcurve Analysis at CS3-Palmer Divide Station: 2014 October-December.” *Minor Planet Bull.* **42**, 115-127.
- Warner, B.D. (2015b). “Near-Earth Asteroid Lightcurve Analysis at CS3-Palmer Divide Station: 2015 March-June.” *Minor Planet Bull.* **42**, 256-266.
- Warner, B.D. (2016a). “Near-Earth Asteroid Lightcurve Analysis at CS3-Palmer Divide Station: 2016 January-April.” *Minor Planet Bull.* **43**, 240-250.
- Warner, B.D. (2016b). “Near-Earth Asteroid Lightcurve Analysis at CS3-Palmer Divide Station: 2016 April-July.” *Minor Planet Bull.* **43**, 311-319.
- Warner, B.D.; Stephens, R.D. (2020). “Near-Earth Asteroid Lightcurve Analysis at the Center for Solar System Studies: 2019 December - 2020 April.” *Minor Planet Bull.* **47**, 200-213.
- Warner, B.D.; Harris, A.W.; Pravec, P. (2009). “The asteroid lightcurve database.” *Icarus* **202**, 134-146.
- Warner, B.D.; Harris, A.W.; Durech, J.; Benner, L.A.M. (2021a). “Lightcurve Photometry Opportunities: 2021 January-March.” *Minor Planet Bull.* **48**, 89-97.
- Warner, B.D.; Harris, A.W.; Durech, J.; Benner, L.A.M. (2021b). “Lightcurve Photometry Opportunities: 2021 October-December.” *Minor Planet Bull.* **48**, 406-410.

Num	Name	H	D km	Date	V	Dec	Period (h)	Amp	U	A	G	Notes
5143	Heracles	13.9	4.840	01 04.5	14.6	-26	2.7063	0.05 0.22	3	5875	1680	PHA; Pilcher et al. (2012a) SNR: 2039 (0.058 au)
16960	1998 QS52	14.3	4.050	01 06.2	14.7	-29	5.789	0.24 1.4	2	1770	505	Warner (2009b). SNR: 2038 (0.081 au)
348314	2005 BC	18.0	0.780	01 17.4	17.8	-21				910	260	SNR: 2034 (0.047 au)
12711	Tukmit*	15.8	2.010	01 18.3	15.2	10	3.4848	0.7	3	75	20	Pravec et al. (2000web).
7482	1994 PC1*	16.5	1.440	01 18.5	10.2	-25	2.5999	0.29 0.38	3	72000	25000	Pravec et al. (1998)
162463	2000 JH5	17.7	0.850	01 21.8	17.9	50	3.024	0.21	2	15	-	Warner (2016b). SNR: 2048 (0.137 au)
524392	2002 AU5	17.8	0.900	01 27.1	16.4	64				15	-	SNR for 2045 (0.136 au)
1566	Icarus	16.3	1.600	01 28.0	17.2	-15	2.2726	0.05 0.22	3	940	270	Warner (2015b). SNR: 2043 (0.059 au)
137805	1999 YK5*	16.7	1.360	01 30.0	16.3	73	3.930	0.09 0.38	3-	70	20	Warner (2016a). SNR: 2050 (0.115 au)
506459	2002 AL14*	17.9	0.770	01 30.6	15.0	25	2.3088	0.35	2	35	10	Pravec et al. (2002web). SNR: 2039 (0.104 au)
277570	2005 YP180	19.2	0.430	02 06.7	18.0	12	3.689	0.27	3	28300	8100	Warner (2014a). SNR: 2039 (0.018 au)
3103	Eger	15.2	2.710	02 09.4	15.6	25	5.7059	0.49 1.18	3			Pravec et al. (1998). Easy Target
374158	2004 UL	18.8	0.520	02 09.5	16.7	-19	38.	1.2	2	85000	24400	Warner (2015a). SNR:2034 (0.0169 au)
388188	2006 DP14*	18.9	0.490	02 11.6	16.2	-14	5.77	0.9 1.05	3	15	5	Warner (2014a). Best through 2050
523590	2001 QC96*	20.9	0.200	02 11.7	16.3	14				15	-	Best through 2050
11405	1999 CV3	15.2	2.690	02 13.2	15.9	6	6.504	0.5 0.89	3	125	35	Warner (2013). SNR: 2043 (0.137 au)
7341	1991 VK*	16.8	1.270	02 15.2	14.8	-46	4.2096	0.21 0.7	3	670	190	Pravec et al. (1998). Best through 2050
1620	Geographos	15.3	2.600	02 16.4	16.5	-31	5.22204	0.95 2.03	3	220	60	Higgins et al. (2008). SNR: 2040 (0.114 au)
455176	1999 VF22	20.7	0.220	02 20.6	15.9	69				440	125	PHA; Best through 2050
322756	2001 CK32	18.9	0.480	02 22.1	16.9	59				30	10	SNR: 2030: 70/20 (0.078 au)
141851	2002 PM6	17.8	0.860	02 22.8	17.6	-19				70	20	SNR: 2040 (0.0960 au)
7822	1991 CS*	17.3	1.020	02 26.3	16.6	18	2.3896	0.26 0.39	3	350	100	Behrend (2016web). SNR: 2040 (0.064 au)
1036	Ganymed	9.2	41.970	02 27.1	15.4	-20	10.297	0.07 0.45	3			Pilcher et al. (2012b).
138971	2001 CB21	18.4	0.630	02 28.6	14.0	27	3.302	0.19	2	2740	785	PHA; Galád et al. (2005).
153591	2001 SN263	16.9	1.230	03 05.9	13.9	3	3.423	0.13 0.27	3	95	25	Multiple. Becker et al. (2015).
86667	2000 FO10	17.6	0.910	03 07.9	16.6	-2	53.756	1.01 1.30	3-	50	15	Pravec et al. (2021web). SNR: 2032 (0.135 au)
350751	2002 AW*	20.8	0.210	03 08.1	16.7	6				50	15	SNR: 2032: 155/45 (0.0423 au)
138127	2000 EE14	17.0	1.170	03 08.4	16.9	19	2.586	0.2 0.26	3	10	-	Warner (2014a). SNR: 2050 (0.163 au)
143649	2003 QQ47	17.4	0.980	03 12.4	17.6	-58	3.679	0.19	2-	125	35	Warner (2014b). SNR: 2031 (0.087 au)
8566	1996 EN	16.4	1.570	03 20.6	16.6	37				17100	4900	Warner & Stephens (2020). SNR: 2033 (0.030 au)
310842	2003 AK18	19.7	0.330	03 24.6	18.0	-76	5.3	0.19	2	60	15	Pravec et al. (2003web). SNR: 2034: (0.072 au)
317255	2002 DJ5*	19.8	0.330	03 27.3	15.8	-17				120	30	PHA; Best through 2050
137170	1999 HF1	14.6	3.640	03 30.4	14.5	81	2.3192	0.12 0.26	3	40	10	Pravec et al. (2006). Binary

Table I. A list of near-Earth asteroids reaching brightest in the fourth quarter of 2021. \* Favorable apparition. PHA: potentially hazardous asteroid. Diameters are based on  $p_v = 0.20$ . The Date, V, and Dec columns are the mm/dd.d, approximate magnitude, and declination when at brightest. Amp is the single or range of amplitudes. The A and G columns are the approximate SNRs for an assumed full-power Arecibo (not operational) and Goldstone radars. The references in the Notes column are those for the reported periods and amplitudes.

## IN THIS ISSUE

This list gives those asteroids in this issue for which physical observations (excluding astrometric only) were made. This includes lightcurves, color index, and H-G determinations, etc. In some cases, no specific results are reported due to a lack of or poor-quality data. The page number is for the first page of the paper mentioning the asteroid. EP is the "go to page" value in the electronic version.

Number	Name	EP	Page
57	Mnemosyne	9	9
58	Concordia	9	9
58	Concordia	35	35
128	Nemesis	48	48
224	Oceana	35	35
236	Honorina	48	48
329	Svea	48	48
428	Monachia	38	38
536	Merapi	6	6
624	Hektor	51	51
663	Gerlinde	5	5
666	Desdemona	44	44
790	Pretoria	35	35
878	Mildred	38	38
894	Erda	38	38
903	Nealley	44	44
904	Rockefellia	44	44
1021	Flammario	48	48
1026	Ingrid	48	48
1034	Mozartia	48	48
1046	Edwin	35	35
1129	Neujmina	38	38
1143	Odysseus	51	51
1322	Copernicus	38	38
1660	Wood	31	31

Number	Name	EP	Page	Number	Name	EP	Page
1667	Pels	31	31	5638	Deikoon	51	51
1671	Chaika	38	38	5682	Beresford	38	38
1713	Bancilhon	38	38	5968	Trauger	31	31
1727	Mette	38	38	5972	Harryatkinson	38	38
1749	Telamon	51	51	6021	1991 TM	31	31
1868	Thersites	51	51	6307	Maiztegui	38	38
1938	Lausanna	48	48	6751	van Genderen	38	38
1943	Anteros	16	16	6787	1991 PFl5	10	10
1949	Messina	38	38	7087	Lewotsky	22	22
1990	Pilcher	44	44	7173	Sepkoski	22	22
2044	Wirt	38	38	7328	Casanova	44	44
2229	Mezzarco	1	1	7330	Annelemaitre	31	31
2232	Altaj	10	10	7341	1991 VK	16	16
2260	Neoptolemus	51	51	7784	Watterson	38	38
2431	Skovoroda	35	35	7822	1991 CS	16	16
2456	Palamedes	51	51	7822	1991 CS	35	35
2495	Noviomagum	31	31	7939	Asphaug	30	30
2704	Julian Loewe	38	38	8416	Okada	10	10
2728	Yatskiv	7	7	11452	1980 KE	38	38
2824	Franke	35	35	14427	1991 VJ2	38	38
2824	Franke	38	38	15317	1993 HW1	38	38
2920	Automedon	51	51	15964	Billgray	31	31
2926	Caldeira	38	38	15989	1998 XK39	38	38
3376	Armandhammer	31	31	16960	1998 QS52	22	22
3648	Raffinetti	1	1	19912	Aurapenenta	38	38
3699	Milbourn	10	10	32906	1994 RH	16	16
3709	Polypoites	51	51	68063	2000 YJ66	22	22
3760	Poutanen	38	38	138404	2000 HA24	16	16
3807	Pagels	38	38	140158	2001 SX169	38	38
3869	Norton	38	38	143649	2003 QQ47	22	22
3919	Maryanning	1	1	143649	2003 QQ47	35	35
3932	Edshay	44	44	152664	1998 FW4	16	16
4101	Ruikou	10	10	159857	2004 LJ1	22	22
4232	Aparicio	31	31	283460	2001 PD1	16	16
4337	Arecibo	3	3	285571	2000 PQ9	48	48
4826	Wilhelms	44	44	326732	2003 HB6	22	22
4832	Palinurus	51	51	353938	1998 QR15	16	16
4921	Volonte	31	31		2001 KY66	14	14
5175	Ables	22	22		2005 EC224	14	14
5235	Jean-Loup	38	38		2011 YQ10	16	16
5283	Pyrrhus	51	51		2019 UD4	16	16
5402	Kejosmith	38	38		2021 JH2	16	16
					2021 LN15	16	16
					C/2017 T2 (PANNSTARRS)	59	59

**THE MINOR PLANET BULLETIN** (ISSN 1052-8091) is the quarterly journal of the Minor Planets Section of the Association of Lunar and Planetary Observers (ALPO, <http://www.alpo-astronomy.org>). Current and most recent issues of the *MPB* are available on line, free of charge from:

<https://mpbulletin.org/>

The Minor Planets Section is directed by its Coordinator, Prof. Frederick Pilcher, 4438 Organ Mesa Loop, Las Cruces, NM 88011 USA ([fpilcher35@gmail.com](mailto:fpilcher35@gmail.com)). Dr. Alan W. Harris (MoreData! Inc.; [harrisaw@colorado.edu](mailto:harrisaw@colorado.edu)), and Dr. Petr Pravec (Ondrejov Observatory; [ppravec@asu.cas.cz](mailto:ppravec@asu.cas.cz)) serve as Scientific Advisors. The Asteroid Photometry Coordinator is Brian D. Warner (Center for Solar System Studies), Palmer Divide Observatory, 446 Sycamore Ave., Eaton, CO 80615 USA ([brian@MinorPlanetObserver.com](mailto:brian@MinorPlanetObserver.com)).

The *Minor Planet Bulletin* is edited by Professor Richard P. Binzel, MIT 54-410, 77 Massachusetts Ave, Cambridge, MA 02139 USA ([rpb@mit.edu](mailto:rpb@mit.edu)). Brian D. Warner (address above) is Associate Editor, and Dr. David Polishook, Department of Earth and Planetary Sciences, Weizmann Institute of Science ([david.polishook@weizmann.ac.il](mailto:david.polishook@weizmann.ac.il)) is Assistant Editor. The *MPB* is produced by Dr. Pedro A. Valdés Sada ([psada2@ix.netcom.com](mailto:psada2@ix.netcom.com)). The *MPB* is distributed by Dr. Melissa Hayes-Gehrke. Direct all subscriptions, contributions, address changes, etc. to:

Dr. Melissa Hayes-Gehrke  
UMD Astronomy Department  
1113 PSC Bldg 415  
College Park, MD 20742 USA  
([mhayesge@umd.edu](mailto:mhayesge@umd.edu))

Effective with Volume 38, the *Minor Planet Bulletin* is a limited print journal, where print subscriptions are available only to libraries and major institutions for long-term archival purposes. Effective with Volume 50, January 1, 2023 and beyond, printed issues of the *Minor Planet Bulletin* will no longer be distributed. In addition to the free electronic download of the *MPB* noted above, electronic retrieval of all *Minor Planet Bulletin* articles (back to Volume 1, Issue Number 1) is available through the Astrophysical Data System:

<http://www.adsabs.harvard.edu/>

Authors should submit their manuscripts by electronic mail ([rpb@mit.edu](mailto:rpb@mit.edu)). Author instructions and a Microsoft Word template document are available at the web page given above. All materials must arrive by the deadline for each issue. Visual photometry observations, positional observations, any type of observation not covered above, and general information requests should be sent to the Coordinator.

\* \* \* \* \*

The deadline for the next issue (49-2) is January 15, 2022. The deadline for issue 49-3 is April 15, 2022.